Instytut Immunologii i Terapii Doświadczalnej im. Ludwika Hirszfelda
Polskiej Akademii Nauk

Agnieszka Barbara Szyposzyńska

Wpływ pęcherzyków zewnątrzkomórkowych pochodzących z mezenchymalnych komórek macierzystych na zahamowanie aktywności biologicznej nowotworowych komórek macierzystych raka jajnika

Rozprawa doktorska w dyscyplinie nauk biologicznych

Promotor:

prof. dr hab. Aleksandra Klimczak

Promotor pomocniczy:

dr Aleksandra Bielawska-Pohl

Samodzielne Laboratorium Biologii Komórek Macierzystych i Nowotworowych

Wrocław 2024

Hirszfeld Institute of Immunology and Experimental Therapy
Polish Academy of Sciences

Agnieszka Barbara Szyposzyńska

The effect of extracellular vesicles derived from mesenchymal stem cells on the suppression of biological activity of ovarian cancer stem cells

Doctoral Thesis in the scientific discipline biological sciences

Supervisor:

Professor Aleksandra Klimczak

Assistant supervisor:

PhD Aleksandra Bielawska-Pohl

Laboratory of Biology of Stem and Neoplastic Cells

Wrocław 2024

Chciałabym serdecznie podziękować

Prof. Aleksandrze Klimczak
za możliwość wykonania pracy doktorskiej, za zaangażowanie
oraz udzielone wsparcie na każdym etapie pracy

Dr Aleksandrze Bielawskiej-Pohl
za poświęcony czas oraz wprowadzenie mnie w świat
komórek nowotworowych

Koleżankom z Laboratorium
za przyjazną atmosferę i wszelką pomoc

Rodzicom i Dziadkom
za poświęcony czas na długie rozmowy
i wspieranie mnie w dążeniu do celu

Spis treści

Streszczenie

Wpływ pęcherzyków zewnątrzkomórkowych pochodzących z mezenchymalnych komórek macierzystych na zahamowanie aktywności biologicznej nowotworowych komórek macierzystych raka jajnika

Rak jajnika jest jednym z siedmiu najczęściej występujących nowotworów u kobiet na świecie. Ze względu na brak objawów w początkowych etapach choroby, pacjentki otrzymują diagnozę w zawansowanym stadium, często z przerzutami do innych narządów. Przy przerzutowaniu raka jajnika najczęściej dochodzi do gromadzenia się płynu puchlinowego w jamie otrzewnej. Wybór metody terapeutycznej jest uzależniony od kilku czynników, m.in. od typu histologicznego nowotworu, jego zaawansowania i stanu klinicznego pacjentki. Powszechnie stosowaną metodą jest chemioterapia oparta na lekach cytostatycznych na bazie platyny lub jej pochodnych z następowym chirurgicznym usunięciem guza. Niepowodzenia terapii są związane z obecnością w mikrośrodowisku nowotworu rzadkiej populacji nowotworowych komórek macierzystych (z ang. Cancer Stem Cells, CSCs), która jest oporna na powszechnie stosowane leki chemioterapeutyczne i radioterapię. Dlatego istnieje pilna potrzeba opracowania modeli komórkowych umożlwiających badania nad biologią CSCs oraz zidentyfikowanie czynników biologicznych lub farmakologicznych, które mogą zahamować aktywność biologiczną CSCs.

Mezenchymalne komórki macierzyste (z ang. Mesenchymal Stem Cells, MSCs) reprezentują heterogenną populację komórek multipotencjalnych, które rezydują w większości tkanek ludzkich i odpowiadają za utrzymanie homeostazy narządów. Badania nad biologią MSCs dokumentują, że mogą stać się obiecującymi narzędziami w zastosowaniach klinicznych w procesach regeneracji tkanek ze względu na ich wysoki potencjał proliferacyjny, właściwości przeciwzapalne i immunomodulujące. Ponadto MSCs uwalniają także różne cząsteczki bioaktywne w postaci czynników rozpuszczalnych, egzosomów i mikropęcherzyków (MVs), które działają w mikrośrodowisku tkanek jako mediatory komunikacji komórka-komórka, wywierając efekty parakrynne. W odniesieniu do nowotworów badania wykazały sprzeczne wyniki związane z przeciwnowotworową lub pronowotworową aktywnością MSC i ich pochodnych. Niniejsza rozprawa doktorska przedstawia badania aktywności przeciwnowotworowej MVs, pochodzących z unieśmiertelnionych MSC pozyskanych z tkanki tłuszczowej (HATMSC2-MVs), w odniesieniu do komórek raka jajnika.

Celami rozprawy były:

1) Charakterystyka MVs pochodzących z unieśmiertelnionych mezenchymalnych komórek macierzystych z tkanki tłuszczowej (HATMSC2-MVs); 2) Ocena wpływu HATMSC2-MVs na aktywność biologiczną komórek linii raka jajnika ES-2 i OAW-42; 3) Charakterystyka pierwotnych komórek raka jajnika pochodzących z tkanki pooperacyjnej raka jajnika i płynu puchlinowego; 4) Ocena wpływu HATMSC2-MVs na aktywność biologiczną pierwotnych komórek raka jajnik w modelu 2D i 3D; 5) Analiza obecności białek proapoptotycznych i antyapoptotycznych w komórkach HATMSC2 i w mikropęcherzykach HATMSC2-MVs; 6) Ocena fenotypu oraz właściwości biologicznych komórek pierwotnych raka jajnika izolowanych z płynu puchlinowego (OvCa3 A i OvCa7 A) i pochodzących z nich unieśmiertelnionych linii komórkowych OvCa3 A hTERT i OvCA7 A hTERT.

Rozprawa doktorska składa się z cyklu trzech powiązanych tematycznie prac oryginalnych opublikowanych w recenzowanym czasopiśmie z listy JCR.

W pierwszej publikacji (*IJMS 2020, 1;24(21):15862*) scharakteryzowano mikropęcherzyki pochodzące z unieśmiertelnionych MSC pozyskanych z tkanki tłuszczowej (HATMSC2-MVs). Otrzymano jednorodną populację HATMSC2-MVs o średniej wielkości koło 450 nm, co potwierdzono metodą dynamicznego rozpraszania światła (z ang. Dynamic Light Scattering, DLS) oraz metodą transmisyjnej mikroskopii elektronowej (z ang. Transmission Electron Microscopy, TEM). HATMSC2-MVs wykazywały ekspresję markerów CD73, CD90, CD105, HLA-ABC oraz brak ekspresji markerów CD45 oraz HLA-DR, porównywalną do fenotypu komórek rodzicielskich HATMSC2.

W dalszej części pracy oceniono wpływ HATMSC2-MVs na aktywność biologiczną komórek linii raka jajnika reprezentujących: raka jasnokomórkowego (ES-2) i torbielakogruczolaka (cystadenocarcinoma) (OAW-42). Zbadano wpływ HATMSC2-MVs na aktywność proliferacyjną, cykl komórkowy, przeżycie komórek, fenotyp oraz profil wydzielniczy komórek nowotworowych. Przed przystąpieniem do testów aktywności biologicznej potwierdzono internalizację HATMSC2-MVs do komórek linii raka jajnika ES-2 i OAW-42 z użyciem metod cytometrii przepływowej i mikroskopii fluorescencyjnej. W testach funkcjonalnych HATMSC2-MVs hamowały proliferację komórek (test MTT) oraz indukowały śmierć komórek nowotworowych na drodze apoptozy i/lub nekrozy co wykazano za pomocą cytometrii przepływowej. HATMSC2-MVs nie wypływały na zmianę fenotypu komórek ES-2 i OAW-42. Internalizacja HATMSC2-MVs do komórek ES-2 i OAW-42 prowadziła do wzrostu wydzielania przez komórki nowotworowe czynników przeciwnowotworowych (np. IL-2, IL-15, IFN-γ) oraz spadku wydzielania czynników

promujących wzrost nowotworu (np. VEGF, IL-8, GRO-alfa) co wykazano za pomocą analizy membran białkowych.

Druga publikacja (*IJMS 2023, 30;21(23):9143*) przedstawia wyniki charakterystyki pierwotnych komórek raka jajnika pochodzących z tkanki pooperacyjnej i płynu puchlinowego oraz ocenę wpływu HATMSC2-MVs na aktywność biologiczną pierwotnych komórek raka jajnika w modelu 2D i 3D. Zbadano również obecność czynników bioaktywnych regulujących apoptozę w komórkach HATMSC2 i HATMSC2-MVs, przy użyciu membran białkowych. Analiza fenotypu komórek została przeprowadzona z wykorzystaniem cytometrii przepływowej, obrazowania mikroskopowego i metody PCR w czasie rzeczywistym. Wykazano, że pierwotne komórki raka jajnika z tkanki pooperacyjnej i płynu puchlinowego są heterogenną populacją z ekspresją markerów MSCs (CD73, CD90, CD105), markerów CSCs (CD24, CD44, CD133, ALDH1, c-kit) na różnym poziomie. Ponadto, komórki nowotworowe wykazywały ekspresję markerów dla fibroblastów towarzyszących nowotworowi (z ang. Cancer-Associated Fibroblasts, CAFs) (PDGFRa, FAP), markerów przejścia nabłonkowo-mezenchymalnego (z ang. Epithelial to Mesenchymal Transition, EMT) (Snail, wimentyna) i markerów odpowiedzialnych za utrzymanie pluripotencji (Oct4, Sox2, Nanog) na poziomie ekspresji białka. Ponadto, pierwotne komórki raka jajnika wykazały ekspresję transkryptów odpowiedzialnych za pluripotencję (Oct4,Sox2) oraz transkryptów protoonkogennych p53, p21, c-myc na różnym poziomie ekspresji. W testach funkcjonalnych zaobserwowano wypływ HATMSC2-MVs na spadek aktywności metabolicznej oraz brak wpływu na aktywność migracyjną pierwotnych komórek. Podobnie jak w przypadku linii komórkowych ES-2 i OAW-42, traktowanie pierwotnych komórek nowotworowych przez HATMSC2-MVs indukowało proces apoptozy i/lub nekrozy. W ostatnim etapie pracy utworzono i scharakteryzowano sferoidy pochodzące z pierwotnych komórek raka jajnika na obecność markerów CSCs (CD133, CD44, CD24). Zaobserwowano różnice w ekspresji badanych markerów CSCs pomiędzy sferoidami utworzonymi z komórek izolowanych z tkanki pooperacyjnej i płynu puchlinowego. W sferoidach pochodzących z tkanki pooperacyjnej ekspresja markera CD133 była niższa w porównaniu do sferoidów z płynu puchlinowego. Z drugiej strony poziom CD24 był wyższy w sferoidach z tkanki pooperacyjnej w odniesieniu do sferoidów z płynu puchlinowego. Natomiast marker CD44 był obecny na podobnym poziomie dla obu typów sferoidów. Wykazano wypływ HATMSC2-MVs na spadek przeżycia komórek tworzących sferoidy. W pracy pokazano również różnice w ekspresji analizowanych czynników regulujących apoptozę pomiędzy mikropęcherzykami HATMSC2-MVs a komórkami rodzicielskimi HATMSC2. Spośród 43 badanych czynników bioaktywnych 15 czynników

proapoptotycznych było obecnych na wyższym poziomie w HATMSC2-MVs (np. bad, BID, BIM, kaspaza 3, cytochrom c, TRAIL-R1 i TRAIL-R2) niż w komórkach rodzicielskich HATMSC2.

W trzeciej pracy (*IJMS 2024, 25(10):5384*) porównano fenotyp oraz właściwości biologiczne komórek pierwotnych z płynu puchlinowego (OvCa3 A i OvCa7 A) i pochodzących z nich unieśmiertelnionych linii komórkowych OvCa3 A hTERT i OvCa7 A hTERT. Analiza fenotypu z wykorzystaniem cytometrii przepływowej i obrazowania mikroskopowego wykazała różnice w ekspresji markerów komórek nowotworowych (Pax8, p53), pochodzenia nabłonkowego (CA-125, cytokeratyna 8), fenotypu MSCs (CD73, CD90, CD105), CSCs (CD133, CD24, c-kit), CAFs (PDGFRa, FAP), EMT (Snail, wimentyna) oraz markerów komórek hematopoetycznych (CD34, CD45) i odpowiedzialnych za utrzymanie pluripotencji (Oct4, Sox2, Nanog), pomiędzy komórkami pierwotnymi a otrzymanymi z nich unieśmiertelnionymi liniami. Istotną jest obserwacja, że większość komórek OvCa7 A hTERT ma cechy CSCs z ekspresją CD133+ i była dodatnia pod względem obecności markerów Pax8, p53, CA-125, cytokeratyny 8. Z kolei linia komórkowa OvCa3 A hTERT nie ma ekspresji CD133 i wyróżnia się obecnością markera CD73, wyższą ekspresją CD105 oraz niższą ekspresją c-kit w odniesieniu do OvCa7 A hTERT)

Otrzymane linie komórkowe wykazywały ekspresję transkryptów odpowiedzialnych za utrzymanie pluripotencji (Oct4, Sox2) i protoonkogennych (p53,p21 i c-myc) na różnym poziomie ekspresji co analizowano za pomocą metody RT-PCR w czasie rzeczywistym. W testach funkcjonalnych wykazano, że aktywność metaboliczna (test MTT) oraz aktywność migracyjna (test zarastania rysy) była wyższa w obu unieśmiertelnionych liniach komórkowych, OvCa3 A hTERT i OvCa7 A hTERT, w porównaniu do komórek pierwotnych. Aktywność dehydrogenazy aldehydowej 1 (ALDH1) była niższa w komórkach pierwotnych w porównaniu do odpowiednich linii unieśmiertelnionych. Ponadto, aktywność ALDH1 w komórkach OvCa7 A hTERT była ponad 3-krotnie wyższa w porównaniu z komórkami OvCa3 A hTERT. Aby ocenić obecność CSCs w powstałych sferoidach analizowano ekspresję markerów CD133, CD44 za pomocą cytometrii przepływowej. W sferoidach z komórek OvCa3 A i OvCa3 A hTERT nie stwierdzono obecności komórek CD133. Dla sferoidów utworzonych z komórek OvCa7 A hTERT populacja komórek CD133-pozytywna była większa w porównaniu do komórek pierwotnych OvCa7 A (12% vs. 2%) . Nie stwierdzono różnic w ekspresji markera CD44 dla sferoidów utworzonych z komórek pierwotnych i unieśmiertelnionych.

Badania wykonane w ramach rozprawy doktorskiej wykazały, że traktowanie komórek linii raka jajnika ES-2 i OAW-42 przez HATMSC2-MVs prowadzi do spadku aktywności proliferacyjnej, indukuje śmierć komórek na drodze apoptozy i/lub nekrozy oraz zwiększa wydzielanie czynników przeciwnowotworowych a zmniejsza wydzielanie czynników promujących nowotwór. Wyniki uzyskane na liniach komórkowych zostały potwierdzone w badaniach pierwotnych komórek raka jajnika pozyskanych z tkanki pooperacyjnej i płynu puchlinowego, gdzie zaobserwowano spadek aktywności metabolicznej, obniżenie przeżycia komórek, indukcję apoptozy i/lub nekrozy w modelu 2D oraz spadek przeżycia komórek w modelu 3D po traktowaniu HATMSC2-MVs. Wykazano również obecność populacji komórek z ekspresją markerów CSCs (CD133, CD24, CD44, c-kit (CD117) i ALDH1) oraz markerów odpowiedzialnych za utrzymanie pluripotencji (Oct4, Sox2, Nanog) w pierwotnych komórkach raka jajnika izolowanych z tkanki pooperacyjnej i płynu puchlinowego. W ostatnim etapie badań wykazano, że plazmid niosący gen hTERT może być wykorzystany do unieśmiertelnienia pierwotnych komórek raka jajnika. Otrzymana unieśmiertelniona linia komórkowa OvCa7 A hTERT CD133-pozytywna, z ekspresją markerów Pax8 i p53 oraz wysoką aktywnością ALDH1 może być użytecznym narzędziem w badaniach nad biologią CSCs i opracowaniem nowych strategii terapeutycznych ukierunkowanych na CSCs.

Summary

The effect of extracellular vesicles derived from mesenchymal stem cells on the suppression of biological activity of ovarian cancer stem cells

Ovarian cancer is one of the seven most common cancers in women in the world. Due to the lack of symptoms in the initial stages of the disease, patients are diagnosed in an advanced stage, usually with metastases to other organs. Metastasis of ovarian cancer are commonly associated with ascitic fluid accumulation in the peritoneal cavity. The choice of therapeutic method depends on several factors, including the histological type of cancer, its advancement, and the patient's clinical condition. A commonly used method is chemotherapy based on cytostatic drugs (platinum or its derivatives) followed by surgical removal of the tumor. Therapy failures are related to the presence of a rare population of cancer stem cells (CSCs) in the tumor microenvironment, which are resistant to commonly used chemotherapy drugs and radiotherapy. Therefore, there is an urgent need to develop cellular models enabling research on the biology of CSCs and the identification of biological or pharmacological factors that can inhibit the biological activity of CSCs.

Mesenchymal stem cells (MSCs) represent a heterogeneous population of multipotent cells that reside in most human tissues and are responsible for maintaining organ homeostasis. Research on the biology of MSCs documents that they may become promising tools in clinical applications in tissue regeneration processes due to their high proliferative potential, anti-inflammatory and immunomodulatory properties. Moreover, MSCs also release various bioactive molecules in the form of soluble factors, exosomes and microvesicles (MVs), which act in the tissue microenvironment as mediators of cell-cell communication, exerting paracrine effects. Numerous studies on cancer have shown conflicting results related to the anti-tumor or pro-tumorigenic activity of MSCs and their derivatives (exosomes and microvesicles).

This doctoral dissertation presents research on the anticancer activity of MVs, derived from immortalized MSCs obtained from adipose tissue (HATMSC2-MVs), in ovarian cancer cells.

The objectives of the dissertation:

1) Characterization of MVs derived from immortalized adipose tissue mesenchymal stem cells (HATMSC2-MVs); 2) Assessment of the impact of HATMSC2-MVs on the biological activity of ES-2 and OAW-42 ovarian cancer cells; 3) Characterization of primary ovarian cancer cells derived from postoperative ovarian cancer tissue and ascitic fluid; 4) Assessment of the impact of HATMSC2-MVs on the biological activity of primary ovarian cancer cells using a 2D and

3D model; 5) Analysis of pro-apoptotic and anti-apoptotic proteins in HATMSC2 cells and HATMSC2-MVs; 6) Assessment of the phenotype and biological properties of primary cells from ascites fluid (OvCa3 A and OvCa7 A) and the immortalized cell lines OvCa3 A hTERT and OvCA7 A hTERT derived from primary cells.

The doctoral dissertation consists of a series of three thematically related works, published in a peer-reviewed journal from the JCR list.

The first publication (*IJMS 2020, 1;24(21):15862*) characterized microvesicles derived from immortalized MSCs obtained from adipose tissue (HATMSC2-MVs). A homogeneous population of HATMSC2-MVs with an average size of approximately 450 nm was obtained, which was confirmed by Dynamic Light Scattering (DLS) and Transmission Electron Microscopy (TEM). HATMSC2-MVs expressed CD73, CD90, CD105, HLA-ABC markers and lack of expression of CD45 and HLA-DR markers, comparable to the phenotype of parental HATMSC2 cells.

Further in the study, the influence of HATMSC2-MVs on the biological activity of ovarian cancer cells representing: clear cell carcinoma (ES-2) and cystadenocarcinoma (OAW-42) was assessed. The effect of HATMSC2-MVs on the proliferative activity, cell cycle, cell survival, phenotype and secretory profile of cancer cells was investigated. Before biological activity tests, the internalization of HATMSC2-MVs into cells of the ES-2 and OAW-42 ovarian cancer lines was confirmed using flow cytometry and fluorescence microscopy methods. In functional tests, HATMSC2-MVs inhibited cell proliferation (MTT test) and induced cancer cell death by apoptosis and/or necrosis, as demonstrated by flow cytometry. HATMSC2-MVs did not change the phenotype of ES-2 and OAW-42 cells. Internalization of HATMSC2-MVs into ES-2 and OAW-42 cells led to an increase in the secretion of antitumor factors (e.g., IL-2, IL-15, IFN-γ) by tumor cells and a decrease in the secretion of tumor growth-promoting factors (e.g., VEGF, IL -8, GRO-alpha) as demonstrated by analysis of protein membranes.

The second publication (*IJMS 2023, 30;21(23):9143*) presents the results of the characterization of primary ovarian cancer cells derived from postoperative tissue and ascitic fluid and the assessment of the impact of HATMSC2-MVs on the biological activity of primary ovarian cancer cells in a 2D and 3D model. The presence of bioactive factors regulating apoptosis in HATMSC2 and HATMSC2-MVs cells was also examined using protein membranes. Cell phenotype analysis was performed using flow cytometry, microscopic imaging and real-time PCR. It has been shown that primary ovarian cancer cells from postoperative tissue and ascitic fluid are a heterogeneous population expressing MSCs markers (CD73, CD90, CD105) and CSCs markers (CD24, CD44, CD133, ALDH1, c-kit) at various

levels. Moreover, cancer cells expressed markers for Cancer-Associated Fibroblasts (CAFs) (PDGFRa, FAP), markers of Epithelial to Mesenchymal Transition (EMT) (Snail, vimentin) and markers responsible for maintaining pluripotency (Oct4, Sox2, Nanog) at protein level. Moreover, primary ovarian cancer cells expressed transcripts responsible for pluripotency (Oct4,Sox2) and proto-oncogenic transcripts p53, p21, c-myc at various levels of expression. In functional tests, HATMSC2-MVs influenced the decrease in metabolic activity and had no effect on the migratory activity of primary cells. As in the case of ES-2 and OAW-42 cell lines, treatment of primary tumor cells with HATMSC2-MVs induced apoptosis and/or necrosis. In the last stage of the work, spheroids derived from primary ovarian cancer cells were created and characterized for the presence of CSCs markers (CD133, CD44, CD24). Differences in the expression of the tested CSC markers were observed between spheroids from postoperative tissue and ascitic fluid. In spheroids from postoperative tissue, the expression of the CD133 marker was lower compared to spheroids from ascitic fluid. On the other hand, CD24 levels were higher in spheroids from postoperative tissue compared to spheroids from ascites. However, the CD44 marker was present at similar levels for both types of spheroids. The influence of HATMSC2-MVs on the decrease in the survival of cells forming spheroids was demonstrated. The study also shows differences in the expression of the analyzed factors regulating apoptosis between HATMSC2-MVs microvesicles and HATMSC2 parental cells. Out of the 43 bioactive factors tested, 15 pro-apoptotic factors were present at higher levels in HATMSC2-MVs (e.g. bad, BID, BIM, caspase 3, cytochrome c, TRAIL-R1, and TRAIL-R2) than in parental HATMSC2 cells.

In the third paper (*IJMS 2024, 25(10):5384*), the phenotype and biological properties of primary cells from ascites fluid (OvCa3 A and OvCa7 A) and the immortalized cell lines OvCa3 A hTERT and OvCa7 A hTERT derived from them were compared. Phenotype analysis using flow cytometry and microscopic imaging showed differences between primary cells and the immortalized lines obtained from them, in the expression of markers of ovarian tumor cells (Pax8, p53), of epithelial origin (CA-125, cytokeratin 8), MSCs phenotype (CD73, CD90, CD105), CSCs (CD133, CD24, c-kit), CAFs (PDGFRa, FAP), EMT (Snail, vimentin) and markers of hematopoietic cells (CD34, CD45) and those responsible for maintaining pluripotency (Oct4, Sox2, Nanog). An important observation is that the majority of OvCa7 A hTERT cells have the characteristics of CSCs expressing CD133 + and were positive in terms of the presence of the ovarian cancer markers Pax8, p53, CA-125, and cytokeratin 8. In turn, the OvCa3 A hTERT cell line does not express CD133 and is distinguished by the presence of

the marker CD73, higher CD105 expression and lower c-kit expression compared to OvCa7 A hTERT)

The obtained cell lines expressed transcripts responsible for maintaining pluripotency (Oct4, Sox2) and proto-oncogenic ones (p53, p21 and c-myc) at various expression levels, which were analyzed using the real-time RT-PCR method. Functional tests showed that metabolic activity (MTT test) and migratory activity (crack closure test) were higher in both immortalized cell lines, OvCa3 A hTERT and OvCa7 A hTERT, compared to primary cells. Aldehyde dehydrogenase 1 (ALDH1) activity was lower in primary cells compared to the corresponding immortalized lines. Moreover, ALDH1 activity in OvCa7 A hTERT cells was more than 3-fold higher compared to OvCa3 A hTERT cells. To assess the presence of CSCs in the spheroids, the expression of CD133 and CD44 markers was analyzed using flow cytometry. No CD133 cells were detected in spheroids from OvCa3 A and OvCa3 A hTERT cells. For spheroids created from OvCa7 A hTERT cells, the CD133-positive cell population was higher compared to primary OvCa7 A cells (12% vs. 2%, respectively). There were no differences in the expression of the CD44 marker for spheroids created from primary and immortalized cells..

Research carried out as part of the doctoral dissertation showed that the treatment of ES-2 and OAW-42 ovarian cancer cells with HATMSC2-MVs leads to decrease in proliferative activity, induces cell death by apoptosis and/or necrosis, and increases the secretion of anticancer factors and reduces the secretion of factors promoting cancer growth. The results obtained on cell lines were confirmed in studies on primary ovarian cancer cells obtained from postoperative tissue and ascites fluid, where a decrease in metabolic activity, decreased cell survival, induction of apoptosis and/or necrosis in the 2D model and a decrease in cell survival in the 3D model after HATMSC2-MVs treatment were observed. The presence of the population of cells expressing CSCs markers (CD133, CD24, CD44, c-kit (CD117) and ALDH1), and markers responsible for maintaining pluripotency (Oct4, Sox2, Nanog) was also showed in primary ovarian cancer cells isolated from postoperative tissue and ascites fluid. The last stage of research showed that a plasmid carrying the hTERT gene can be used to immortalize primary ovarian cancer cells. The immortalized OvCa7 A hTERT CD133-positive cell line, expressing Pax8 and p53 markers and high ALDH1 activity, may be a useful tool in research on the biology of CSCs and the development of new therapeutic strategies targeting CSCs.

Lista publikacji wchodzących w skład rozprawy doktorskiej

1. **Szyposzynska A**, Bielawska-Pohl A, Krawczenko A, Doszyn O, Paprocka M, Klimczak A. Suppression of Ovarian Cancer Cell Growth by AT-MSC Microvesicles. *International Journal of Molecular Sciences*. 2020 Nov 30;21(23):9143. doi: 10.3390/ijms21239143.
   Impact Factor = 5.6
2. **Szyposzynska A**, Bielawska-Pohl A, Murawski M, Sozanski R, Chodaczek G, Klimczak A. Mesenchymal Stem Cell Microvesicles from Adipose Tissue: Unraveling Their Impact on Primary Ovarian Cancer Cells and Their Therapeutic Opportunities. *International Journal of Molecular Sciences*. 2023 Nov 1;24(21):15862. doi: 10.3390/ijms242115862.
   Impact Factor = 5.6
3. **Szyposzynska A**, Bielawska-Pohl A, Paprocka M, Bar J, Murawski M, Klimczak A. Comparative Analysis of Primary Ovarian Cancer Cells and Established Cell Lines as a New Tool for Studies on Ovarian Cancer Cell Complexity. *International Journal of Molecular Sciences*. 2024; 25(10):5384. doi: 10.3390/ijms25105384.
   Impact Factor = 5.6

Oświadczenia współautorów

Mgr Agnieszka Szyposzyńska

Samodzielne Laboratorium Biologii Komórek

Macierzystych i Nowotworowych,

Instytut Immunologii i Terapii Doświadczalnej,

Polskiej Akademii Nauk, 53-114 Wrocław, Polska

15.05.2024

Oświadczenie

Oświadczam, że mój udział w następującej pracy:

Szyposzynska A, Bielawska-Pohl A, Krawczenko A, Doszyn O, Paprocka M, Klimczak A. Suppression of Ovarian Cancer Cell Growth by AT-MSC Microvesicles. Int J Mol Sci. 2020 Nov 30;21(23):9143. doi: 10.3390/ijms21239143,

jest prawidłowo scharakteryzowany w poniższej tabeli.

Autor	Opis udziału własnego
Agnieszka Szyposzyńska	koncepcja badań, prowadzenie hodowli komórkowych, izolacja MVs pochodzących z HATMSC2, prowadzenie analizy z wykorzystaniem cytometrii przepływowej (fenotyp komórek HATMSC2, ES-2 i OAW-42), przygotowanie próbek do analizy przeżycia komórek i cyklu komórkowego, wykonanie testu MTT i barwienia kalceiną, analiza wyników oraz przygotowanie rycin do publikacji, analiza formalna, gromadzenie i przechowywanie danych, przygotowanie pierwotnej wersji manuskryptu
Aleksandra Bielawska-Pohl	prowadzenie analizy z wykorzystaniem cytometrii przepływowej (przeżycie komórek, internalizacja HATMSC2-MVs), charakterystyka HATMSC2-MVs, analiza formalna, gromadzenie i przechowywanie danych, przygotowanie pierwotnej wersji manuskryptu
Agnieszka Krawczenko	analiza z wykorzystaniem membran białkowych
Olga Doszyń	analiza internalizacji z wykorzystaniem mikroskopii fluorescencyjnej, przygotowanie zdjęć mikroskopowych z internalizacji
Maria Paprocka	pomiar cyklu komórkowego z wykorzystaniem cytometrii przepływowej
Aleksandra Klimczak	koncepcja badań, wybór metod badawczych, analiza formalna, archiwizacja danych, opieka merytoryczna nad badaniami, pozyskanie funduszy na badania, korekta i akceptacja końcowej wersji manuskryptu, odpowiedzi na recenzje, korekta i akceptacja wersji do druku

Agnieszka Szyposzyńska

(Podpis współautora)

Dr Aleksandra Bielawska-Pohl
Samodzielne Laboratorium Biologii Komórek
Macierzystych i Nowotworowych,
Instytut Immunologii i Terapii Doświadczalnej,
Polskiej Akademii Nauk, 53-114 Wrocław, Polska

15.05.2024

Oświadczenie

Oświadczam, że mój udział w następującej pracy:

Szyposzynska A, Bielawska-Pohl A, Krawczenko A, Doszyn O, Paprocka M, Klimczak A. Suppression of Ovarian Cancer Cell Growth by AT-MSC Microvesicles. Int J Mol Sci. 2020 Nov 30;21(23):9143. doi: 10.3390/ijms21239143,

jest prawidłowo scharakteryzowany w poniższej tabeli.

Autor	Opis udziału własnego
Agnieszka Szyposzyńska	koncepcja badań, prowadzenie hodowli komórkowych, izolacja MVs pochodzących z HATMSC2, prowadzenie analizy z wykorzystaniem cytometrii przepływowej (fenotyp komórek HATMSC2, ES-2 i OAW-42), przygotowanie próbek do analizy przeżycia komórek i cyklu komórkowego, wykonanie testu MTT i barwienia kalceiną, analiza wyników oraz przygotowanie rycin do publikacji, analiza formalna, gromadzenie i przechowywanie danych, przygotowanie pierwotnej wersji manuskryptu
Aleksandra Bielawska-Pohl	prowadzenie analizy z wykorzystaniem cytometrii przepływowej (przeżycie komórek, internalizacja HATMSC2-MVs), charakterystyka HATMSC2-MVs, analiza formalna, gromadzenie i przechowywanie danych, przygotowanie pierwotnej wersji manuskryptu
Agnieszka Krawczenko	analiza z wykorzystaniem membran białkowych
Olga Doszyń	analiza internalizacji z wykorzystaniem mikroskopii fluorescencyjnej, przygotowanie zdjęć mikroskopowych z internalizacji
Maria Paprocka	pomiar cyklu komórkowego z wykorzystaniem cytometrii przepływowej
Aleksandra Klimczak	koncepcja badań, wybór metod badawczych, analiza formalna, archiwizacja danych, opieka merytoryczna nad badaniami, pozyskanie funduszy na badania, korekta i akceptacja końcowej wersji manuskryptu, odpowiedzi na recenzje, korekta i akceptacja wersji do druku

A. Bielawska-Pohl

(Podpis współautora)

Dr Agnieszka Krawczenko
Samodzielne Laboratorium Biologii Komórek
Macierzystych i Nowotworowych,
Instytut Immunologii i Terapii Doświadczalnej,
Polskiej Akademii Nauk, 53-114 Wrocław, Polska

15.05.2024

Oświadczenie

Oświadczam, że mój udział w następującej pracy:

Szyposzynska A, Bielawska-Pohl A, Krawczenko A, Doszyn O, Paprocka M, Klimczak A. Suppression of Ovarian Cancer Cell Growth by AT-MSC Microvesicles. Int J Mol Sci. 2020 Nov 30;21(23):9143. doi: 10.3390/ijms21239143,

jest prawidłowo scharakteryzowany w poniższej tabeli.

Autor	Opis udziału własnego
Agnieszka Szyposzyńska	koncepcja badań, prowadzenie hodowli komórkowych, izolacja MVs pochodzących z HATMSC2, prowadzenie analizy z wykorzystaniem cytometrii przepływowej (fenotyp komórek HATMSC2, ES-2 i OAW-42), przygotowanie próbek do analizy przeżycia komórek i cyklu komórkowego, wykonanie testu MTT i barwienia kalceiną, analiza wyników oraz przygotowanie rycin do publikacji, analiza formalna, gromadzenie i przechowywanie danych, przygotowanie pierwotnej wersji manuskryptu
Aleksandra Bielawska-Pohl	prowadzenie analizy z wykorzystaniem cytometrii przepływowej (przeżycie komórek, internalizacja HATMSC2-MVs), charakterystyka HATMSC2-MVs, analiza formalna, gromadzenie i przechowywanie danych, przygotowanie pierwotnej wersji manuskryptu
Agnieszka Krawczenko	analiza z wykorzystaniem membran białkowych
Olga Doszyń	analiza internalizacji z wykorzystaniem mikroskopii fluorescencyjnej, przygotowanie zdjęć mikroskopowych z internalizacji
Maria Paprocka	pomiar cyklu komórkowego z wykorzystaniem cytometrii przepływowej
Aleksandra Klimczak	koncepcja badań, wybór metod badawczych, analiza formalna, archiwizacja danych, opieka merytoryczna nad badaniami, pozyskanie funduszy na badania, korekta i akceptacja końcowej wersji manuskryptu, odpowiedzi na recenzje, korekta i akceptacja wersji do druku

A. Krawczenko
.....
(Podpis współautora)

Mgr Olga Doszyń

Samodzielne Laboratorium Biologii Komórek

Macierzystych i Nowotworowych,

Instytut Immunologii i Terapii Doświadczalnej,

Polskiej Akademii Nauk, 53-114 Wrocław, Polska

15.05.2024

Oświadczenie

Oświadczam, że mój udział w następującej pracy:

Szyposzynska A, Bielawska-Pohl A, Krawczenko A, Doszyn O, Paprocka M, Klimczak A. Suppression of Ovarian Cancer Cell Growth by AT-MSC Microvesicles. Int J Mol Sci. 2020 Nov 30;21(23):9143. doi: 10.3390/ijms21239143,

jest prawidłowo scharakteryzowany w poniższej tabeli.

Autor	Opis udziału własnego
Agnieszka Szyposzyńska	koncepcja badań, prowadzenie hodowli komórkowych, izolacja MVs pochodzących z HATMSC2, prowadzenie analizy z wykorzystaniem cytometrii przepływowej (fenotyp komórek HATMSC2, ES-2 i OAW-42), przygotowanie próbek do analizy przeżycia komórek i cyklu komórkowego, wykonanie testu MTT i barwienia kalceiną, analiza wyników oraz przygotowanie rycin do publikacji, analiza formalna, gromadzenie i przechowywanie danych, przygotowanie pierwotnej wersji manuskryptu
Aleksandra Bielawska-Pohl	prowadzenie analizy z wykorzystaniem cytometrii przepływowej (przeżycie komórek, internalizacja HATMSC2-MVs), charakterystyka HATMSC2-MVs, analiza formalna, gromadzenie i przechowywanie danych, przygotowanie pierwotnej wersji manuskryptu
Agnieszka Krawczenko	analiza z wykorzystaniem membran białkowych
Olga Doszyń	analiza internalizacji z wykorzystaniem mikroskopii fluorescencyjnej, przygotowanie zdjęć mikroskopowych z internalizacji
Maria Paprocka	pomiar cyklu komórkowego z wykorzystaniem cytometrii przepływowej
Aleksandra Klimczak	koncepcja badań, wybór metod badawczych, analiza formalna, archiwizacja danych, opieka merytoryczna nad badaniami, pozyskanie funduszy na badania, korekta i akceptacja końcowej wersji manuskryptu, odpowiedzi na recenzje, korekta i akceptacja wersji do druku

.....

(Podpis współautora)

Dr Maria Paprocka

Samodzielne Laboratorium Biologii Komórek

Macierzystych i Nowotworowych,

Instytut Immunologii i Terapii Doświadczalnej,

Polskiej Akademii Nauk, 53-114 Wrocław, Polska

15.05.2024

Oświadczenie

Oświadczam, że mój udział w następującej pracy:

Szyposzynska A, Bielawska-Pohl A, Krawczenko A, Doszyn O, Paprocka M, Klimczak A. Suppression of Ovarian Cancer Cell Growth by AT-MSC Microvesicles. Int J Mol Sci. 2020 Nov 30;21(23):9143. doi: 10.3390/ijms21239143,

jest prawidłowo scharakteryzowany w poniższej tabeli.

Autor	Opis udziału własnego
Agnieszka Szyposzyńska	koncepcja badań, prowadzenie hodowli komórkowych, izolacja MVs pochodzących z HATMSC2, prowadzenie analizy z wykorzystaniem cytometrii przepływowej (fenotyp komórek HATMSC2, ES-2 i OAW-42), przygotowanie próbek do analizy przeżycia komórek i cyklu komórkowego, wykonanie testu MTT i barwienia kalceiną, analiza wyników oraz przygotowanie rycin do publikacji, analiza formalna, gromadzenie i przechowywanie danych, przygotowanie pierwotnej wersji manuskryptu
Aleksandra Bielawska-Pohl	prowadzenie analizy z wykorzystaniem cytometrii przepływowej (przeżycie komórek, internalizacja HATMSC2-MVs), charakterystyka HATMSC2-MVs, analiza formalna, gromadzenie i przechowywanie danych, przygotowanie pierwotnej wersji manuskryptu
Agnieszka Krawczenko	analiza z wykorzystaniem membran białkowych
Olga Doszyń	analiza internalizacji z wykorzystaniem mikroskopii fluorescencyjnej, przygotowanie zdjęć mikroskopowych z internalizacji
Maria Paprocka	pomiar cyklu komórkowego z wykorzystaniem cytometrii przepływowej
Aleksandra Klimczak	koncepcja badań, wybór metod badawczych, analiza formalna, archiwizacja danych, opieka merytoryczna nad badaniami, pozyskanie funduszy na badania, korekta i akceptacja końcowej wersji manuskryptu, odpowiedzi na recenzje, korekta i akceptacja wersji do druku

Paprocka

.....

(Podpis współautora)

Prof. dr hab. Aleksandra Klimczak

Samodzielne Laboratorium Biologii Komórek

Macierzystych i Nowotworowych,

Instytut Immunologii i Terapii Doświadczalnej,

Polskiej Akademii Nauk, 53-114 Wrocław, Polska

15.05.2024

Oświadczenie

Oświadczam, że mój udział w następującej pracy:

Szyposzynska A, Bielawska-Pohl A, Krawczenko A, Doszyn O, Paprocka M, Klimczak A. Suppression of Ovarian Cancer Cell Growth by AT-MSC Microvesicles. Int J Mol Sci. 2020 Nov 30;21(23):9143. doi: 10.3390/ijms21239143,

jest prawidłowo scharakteryzowany w poniższej tabeli.

Autor	Opis udziału własnego
Agnieszka Szyposzyńska	koncepcja badań, prowadzenie hodowli komórkowych, izolacja MVs pochodzących z HATMSC2, prowadzenie analizy z wykorzystaniem cytometrii przepływowej (fenotyp komórek HATMSC2, ES-2 i OAW-42), przygotowanie próbek do analizy przeżycia komórek i cyklu komórkowego, wykonanie testu MTT i barwienia kalceiną, analiza wyników oraz przygotowanie rycin do publikacji, analiza formalna, gromadzenie i przechowywanie danych, przygotowanie pierwotnej wersji manuskryptu
Aleksandra Bielawska-Pohl	prowadzenie analizy z wykorzystaniem cytometrii przepływowej (przeżycie komórek, internalizacja HATMSC2-MVs), charakterystyka HATMSC2-MVs, analiza formalna, gromadzenie i przechowywanie danych, przygotowanie pierwotnej wersji manuskryptu
Agnieszka Krawczenko	analiza z wykorzystaniem membran białkowych
Olga Doszyń	analiza internalizacji z wykorzystaniem mikroskopii fluorescencyjnej, przygotowanie zdjęć mikroskopowych z internalizacji
Maria Paprocka	pomiar cyklu komórkowego z wykorzystaniem cytometrii przepływowej
Aleksandra Klimczak	koncepcja badań, wybór metod badawczych, analiza formalna, archiwizacja danych, opieka merytoryczna nad badaniami, pozyskanie funduszy na badania, korekta i akceptacja końcowej wersji manuskryptu, odpowiedzi na recenzje, korekta i akceptacja wersji do druku

.....

(Podpis współautora)

Mgr Agnieszka Szyposzyńska

Samodzielne Laboratorium Biologii Komórek

Macierzystych i Nowotworowych,

Instytut Immunologii i Terapii Doświadczalnej,

Polskiej Akademii Nauk, 53-114 Wrocław, Polska

15.05.2024

Oświadczenie

Oświadczam, że mój udział w następującej pracy:

Szyposzynska A, Bielawska-Pohl A, Murawski M, Sozanski R, Chodaczek G, Klimczak A. Mesenchymal Stem Cell Microvesicles from Adipose Tissue: Unraveling Their Impact on Primary Ovarian Cancer Cells and Their Therapeutic Opportunities. Int J Mol Sci. 2023 Nov 1;24(21):15862. doi: 10.3390/ijms242115862

jest prawidłowo scharakteryzowany w poniższej tabeli.

Autor	Opis udziału własnego
Agnieszka Szyposzyńska	koncepcja badań, izolacja MVs pochodzących z HATMSC2, izolacja, hodowla i charakterystyka pierwotnych komórek raka jajnika z wykorzystaniem cytometrii przepływowej, metody RT-PCR w czasie rzeczywistym, barwień immunofluorescencyjnych i obrazowania mikroskopowego, wykonanie testu MTT i zarastania rysy, analiza przeżycia komórek w modelu 2D i 3D, tworzenie sferoidów, analiza wyników oraz przygotowanie rycin do publikacji, analiza formalna; gromadzenie i przechowywanie danych, przygotowanie pierwotnej wersji manuskryptu
Aleksandra Bielawska-Pohl	prowadzenie analizy z wykorzystaniem cytometrii przepływowej (przeżycie komórek, fenotyp sferoidów), oraz membran białkowych, analiza formalna, gromadzenie i przechowywanie danych, przygotowanie pierwotnej wersji manuskryptu
Marek Murawski	pozyskanie i opis materiału klinicznego
Rafał Sozański	pozyskanie i opis materiału klinicznego
Grzegorz Chodaczek	obrazowanie przeżycia komórek w modelu 2D i 3D z wykorzystaniem mikroskopii konfokalnej, przygotowanie i analiza obrazów z mikroskopii konfokalnej
Aleksandra Klimczak	koncepcja badań, wybór metod badawczych, analiza formalna, archiwizacja danych, sprawowanie opieki merytorycznej nad badaniami, pozyskanie funduszy na badania, udział w przygotowaniu pierwotnej wersji manuskryptu oraz korekta i akceptacja końcowej wersji manuskryptu, odpowiedzi na recenzje, korekta i akceptacja wersji do druku

Agnieszka Szyposzyńska

(Podpis współautora)

Dr Aleksandra Bielawska-Pohl
Samodzielne Laboratorium Biologii Komórek
Macierzystych i Nowotworowych,
Instytut Immunologii i Terapii Doświadczalnej,
Polskiej Akademii Nauk, 53-114 Wrocław, Polska

15.05.2024

Oświadczenie

Oświadczam, że mój udział w następującej pracy:

Szyposzynska A, Bielawska-Pohl A, Murawski M, Sozanski R, Chodaczek G, Klimczak A. Mesenchymal Stem Cell Microvesicles from Adipose Tissue: Unraveling Their Impact on Primary Ovarian Cancer Cells and Their Therapeutic Opportunities. Int J Mol Sci. 2023 Nov 1;24(21):15862. doi: 10.3390/ijms242115862

jest prawidłowo scharakteryzowany w poniższej tabeli.

Autor	Opis udziału własnego
Agnieszka Szyposzyńska	koncepcja badań, izolacja MVs pochodzących z HATMSC2, izolacja, hodowla i charakterystyka pierwotnych komórek raka jajnika z wykorzystaniem cytometrii przepływowej, metody RT-PCR w czasie rzeczywistym, barwień immunofluorescencyjnych i obrazowania mikroskopowego, wykonanie testu MTT i zarastania rysy, analiza przeżycia komórek w modelu 2D i 3D, tworzenie sferoidów, analiza wyników oraz przygotowanie rycin do publikacji, analiza formalna; gromadzenie i przechowywanie danych, przygotowanie pierwotnej wersji manuskryptu
Aleksandra Bielawska-Pohl	prowadzenie analizy z wykorzystaniem cytometrii przepływowej (przeżycie komórek, fenotyp sferoidów), oraz membran białkowych, analiza formalna, gromadzenie i przechowywanie danych, przygotowanie pierwotnej wersji manuskryptu
Marek Murawski	pozyskanie i opis materiału klinicznego
Rafał Sozański	pozyskanie i opis materiału klinicznego
Grzegorz Chodaczek	obrazowanie przeżycia komórek w modelu 2D i 3D z wykorzystaniem mikroskopii konfokalnej, przygotowanie i analiza obrazów z mikroskopii konfokalnej
Aleksandra Klimczak	koncepcja badań, wybór metod badawczych, analiza formalna, archiwizacja danych, sprawowanie opieki merytorycznej nad badaniami, pozyskanie funduszy na badania, udział w przygotowaniu pierwotnej wersji manuskryptu oraz korekta i akceptacja końcowej wersji manuskryptu, odpowiedzi na recenzje, korekta i akceptacja wersji do druku

A. Bielawska-Pohl

(Podpis współautora)

Dr hab. Marek Murawski

I Katedra i Klinika Ginekologii i Położnictwa

Uniwersytet Medyczny we Wrocławiu

50-599 Wrocław, Polska

15.05.2024

Oświadczenie

Oświadczam, że mój udział w następującej pracy:

Szyposzynska A, Bielawska-Pohl A, Murawski M, Sozanski R, Chodaczek G, Klimczak A. Mesenchymal Stem Cell Microvesicles from Adipose Tissue: Unraveling Their Impact on Primary Ovarian Cancer Cells and Their Therapeutic Opportunities. Int J Mol Sci. 2023 Nov 1;24(21):15862. doi: 10.3390/ijms242115862

jest prawidłowo scharakteryzowany w poniższej tabeli.

Autor	Opis udziału własnego
Agnieszka Szyposzyńska	koncepcja badań, izolacja MVs pochodzących z HATMSC2, izolacja, hodowla i charakterystyka pierwotnych komórek raka jajnika z wykorzystaniem cytometrii przepływowej, metody RT-PCR w czasie rzeczywistym, barwień immunofluorescencyjnych i obrazowania mikroskopowego, wykonanie testu MTT i zarastania rysy, analiza przeżycia komórek w modelu 2D i 3D, tworzenie sferoidów, analiza wyników oraz przygotowanie rycin do publikacji, analiza formalna; gromadzenie i przechowywanie danych, przygotowanie pierwotnej wersji manuskryptu
Aleksandra Bielawska-Pohl	prowadzenie analizy z wykorzystaniem cytometrii przepływowej (przeżycie komórek, fenotyp sferoidów), oraz membran białkowych, analiza formalna, gromadzenie i przechowywanie danych, przygotowanie pierwotnej wersji manuskryptu
Marek Murawski	pozyskanie i opis materiału klinicznego
Rafał Sozański	pozyskanie i opis materiału klinicznego
Grzegorz Chodaczek	obrazowanie przeżycia komórek w modelu 2D i 3D z wykorzystaniem mikroskopii konfokalnej, przygotowanie i analiza obrazów z mikroskopii konfokalnej
Aleksandra Klimczak	koncepcja badań, wybór metod badawczych, analiza formalna, archiwizacja danych, sprawowanie opieki merytorycznej nad badaniami, pozyskanie funduszy na badania, udział w przygotowaniu pierwotnej wersji manuskryptu oraz korekta i akceptacja końcowej wersji manuskryptu, odpowiedzi na recenzje, korekta i akceptacja wersji do druku

.....

(Podpis współautora)

Dr Rafał Sozański

I Katedra i Klinika Ginekologii i Położnictwa

Uniwersytet Medyczny we Wrocławiu

50-599 Wrocław, Polska

15.05.2024

Oświadczenie

Oświadczam, że mój udział w następującej pracy:

Szyposzynska A, Bielawska-Pohl A, Murawski M, Sozanski R, Chodaczek G, Klimczak A. Mesenchymal Stem Cell Microvesicles from Adipose Tissue: Unraveling Their Impact on Primary Ovarian Cancer Cells and Their Therapeutic Opportunities. Int J Mol Sci. 2023 Nov 1;24(21):15862. doi: 10.3390/ijms242115862

jest prawidłowo scharakteryzowany w poniższej tabeli.

Autor	Opis udziału własnego
Agnieszka Szyposzyńska	koncepcja badań, izolacja MVs pochodzących z HATMSC2, izolacja, hodowla i charakterystyka pierwotnych komórek raka jajnika z wykorzystaniem cytometrii przepływowej, metody RT-PCR w czasie rzeczywistym, barwień immunofluorescencyjnych i obrazowania mikroskopowego, wykonanie testu MTT i zarastania rysy, analiza przeżycia komórek w modelu 2D i 3D, tworzenie sferoidów, analiza wyników oraz przygotowanie rycin do publikacji, analiza formalna; gromadzenie i przechowywanie danych, przygotowanie pierwotnej wersji manuskryptu
Aleksandra Bielawska-Pohl	prowadzenie analizy z wykorzystaniem cytometrii przepływowej (przeżycie komórek, fenotyp sferoidów), oraz membran białkowych, analiza formalna, gromadzenie i przechowywanie danych, przygotowanie pierwotnej wersji manuskryptu
Marek Murawski	pozyskanie i opis materiału klinicznego
Rafał Sozański	pozyskanie i opis materiału klinicznego
Grzegorz Chodaczek	obrazowanie przeżycia komórek w modelu 2D i 3D z wykorzystaniem mikroskopii konfokalnej, przygotowanie i analiza obrazów z mikroskopii konfokalnej
Aleksandra Klimczak	koncepcja badań, wybór metod badawczych, analiza formalna, archiwizacja danych, sprawowanie opieki merytorycznej nad badaniami, pozyskanie funduszy na badania, udział w przygotowaniu pierwotnej wersji manuskryptu oraz korekta i akceptacja końcowej wersji manuskryptu, odpowiedzi na recenzje, korekta i akceptacja wersji do druku

dr n. med. Rafał Sozański
specjalista
położnictwa i ginekologii
ginekologia onkologiczna
Wrocław, ul. Grunwaldzki 16/68
tel. 602395[illegible] 4714216

.....

(Podpis współautora)

Dr hab. Grzegorz Chodaczek

Laboratorium Bioobrazowania

Sieć Badawcza Łukasiewicz – PORT Polski Ośrodek Rozwoju Technologii

54-066 Wrocław, Polska

15.05.2024

Oświadczenie

Oświadczam, że mój udział w następującej pracy:

Szyposzynska A, Bielawska-Pohl A, Murawski M, Sozanski R, Chodaczek G, Klimczak A. Mesenchymal Stem Cell Microvesicles from Adipose Tissue: Unraveling Their Impact on Primary Ovarian Cancer Cells and Their Therapeutic Opportunities. Int J Mol Sci. 2023 Nov 1;24(21):15862. doi: 10.3390/ijms242115862

jest prawidłowo scharakteryzowany w poniższej tabeli.

Autor	Opis udziału własnego
Agnieszka Szyposzyńska	koncepcja badań, izolacja MVs pochodzących z HATMSC2, izolacja, hodowla i charakterystyka pierwotnych komórek raka jajnika z wykorzystaniem cytometrii przepływowej, metody RT-PCR w czasie rzeczywistym, barwień immunofluorescencyjnych i obrazowania mikroskopowego, wykonanie testu MTT i zarastania rysy, analiza przeżycia komórek w modelu 2D i 3D, tworzenie sferoidów, analiza wyników oraz przygotowanie rycin do publikacji, analiza formalna; gromadzenie i przechowywanie danych, przygotowanie pierwotnej wersji manuskryptu
Aleksandra Bielawska-Pohl	prowadzenie analizy z wykorzystaniem cytometrii przepływowej (przeżycie komórek, fenotyp sferoidów), oraz membran białkowych, analiza formalna, gromadzenie i przechowywanie danych, przygotowanie pierwotnej wersji manuskryptu
Marek Murawski	pozyskanie i opis materiału klinicznego
Rafał Sozański	pozyskanie i opis materiału klinicznego
Grzegorz Chodaczek	obrazowanie przeżycia komórek w modelu 2D i 3D z wykorzystaniem mikroskopii konfokalnej, przygotowanie i analiza obrazów z mikroskopii konfokalnej
Aleksandra Klimczak	koncepcja badań, wybór metod badawczych, analiza formalna, archiwizacja danych, sprawowanie opieki merytorycznej nad badaniami, pozyskanie funduszy na badania, udział w przygotowaniu pierwotnej wersji manuskryptu oraz korekta i akceptacja końcowej wersji manuskryptu, odpowiedzi na recenzje, korekta i akceptacja wersji do druku

Grzegorz Chodaczek

(Podpis współautora)

Prof. dr hab. Aleksandra Klimczak

Samodzielne Laboratorium Biologii Komórek

Macierzystych i Nowotworowych,

Instytut Immunologii i Terapii Doświadczalnej,

Polskiej Akademii Nauk, 53-114 Wrocław, Polska

15.05.2024

Oświadczenie

Oświadczam, że mój udział w następującej pracy:

Szyposzynska A, Bielawska-Pohl A, Murawski M, Sozanski R, Chodaczek G, Klimczak A. Mesenchymal Stem Cell Microvesicles from Adipose Tissue: Unraveling Their Impact on Primary Ovarian Cancer Cells and Their Therapeutic Opportunities. Int J Mol Sci. 2023 Nov 1;24(21):15862. doi: 10.3390/ijms242115862

jest prawidłowo scharakteryzowany w poniższej tabeli.

Autor	Opis udziału własnego
Agnieszka Szyposzyńska	koncepcja badań, izolacja MVs pochodzących z HATMSC2, izolacja, hodowla i charakterystyka pierwotnych komórek raka jajnika z wykorzystaniem cytometrii przepływowej, metody RT-PCR w czasie rzeczywistym, barwień immunofluorescencyjnych i obrazowania mikroskopowego, wykonanie testu MTT i zarastania rysy, analiza przeżycia komórek w modelu 2D i 3D, tworzenie sferoidów, analiza wyników oraz przygotowanie rycin do publikacji, analiza formalna; gromadzenie i przechowywanie danych, przygotowanie pierwotnej wersji manuskryptu
Aleksandra Bielawska-Pohl	prowadzenie analizy z wykorzystaniem cytometrii przepływowej (przeżycie komórek, fenotyp sferoidów), oraz membran białkowych, analiza formalna, gromadzenie i przechowywanie danych, przygotowanie pierwotnej wersji manuskryptu
Marek Murawski	pozyskanie i opis materiału klinicznego
Rafał Sozański	pozyskanie i opis materiału klinicznego
Grzegorz Chodaczek	obrazowanie przeżycia komórek w modelu 2D i 3D z wykorzystaniem mikroskopii konfokalnej, przygotowanie i analiza obrazów z mikroskopii konfokalnej
Aleksandra Klimczak	koncepcja badań, wybór metod badawczych, analiza formalna, archiwizacja danych, sprawowanie opieki merytorycznej nad badaniami, pozyskanie funduszy na badania, udział w przygotowaniu pierwotnej wersji manuskryptu oraz korekta i akceptacja końcowej wersji manuskryptu, odpowiedzi na recenzje, korekta i akceptacja wersji do druku

.....

(Podpis współautora)

Mgr Agnieszka Szyposzyńska

Samodzielne Laboratorium Biologii Komórek

Macierzystych i Nowotworowych,

Instytut Immunologii i Terapii Doświadczalnej,

Polskiej Akademii Nauk, 53-114 Wrocław, Polska

15.05.2024

Oświadczenie

Oświadczam, że mój udział w następującej pracy:

Szyposzynska A, Bielawska-Pohl A, Paprocka M, Bar J, Murawski M, Klimczak A. Comparative Analysis of Primary Ovarian Cancer Cells and Established Cell Lines as a New Tool for Studies on Ovarian Cancer Cell Complexity Int. J. Mol. Sci. 2024, 25, 5384. https://doi.org/10.3390/ijms25105384

jest prawidłowo scharakteryzowany w poniższej tabeli.

Autor	Opis udziału własnego
Agnieszka Szyposzyńska	koncepcja badań, hodowla oraz charakterystyka pierwotnych i unieśmiertelnionych komórek raka jajnika z wykorzystaniem cytometrii przepływowej, metody RT-PCR w czasie rzeczywistym, barwień immunofluorescencyjnych i obrazowania mikroskopowego, wykonanie testu MTT, testu zarastania rysy i aktywności ALDH1, tworzenie sferoidów; analiza wyników oraz przygotowanie rycin do publikacji, analiza formalna, gromadzenie i przechowywanie danych, przygotowanie pierwotnej wersji manuskryptu
Aleksandra Bielawska-Pohl	analiza z wykorzystaniem cytometrii przepływowej (fenotyp sferoidów) oraz Western blot, analiza formalna, gromadzenie i przechowywanie danych, przygotowanie pierwotnej wersji manuskryptu
Maria Paprocka	unieśmiertelnienie pierwotnych komórek z płynu puchlinowego
Julia Bar	wykonanie barwień immunocytochemicznych i H&E, analiza i opis badań cytologicznych i immunocytochemicznych, przygotowanie obrazów mikroskopowych
Marek Murawski	pozyskanie i opis materiału klinicznego
Aleksandra Klimczak	koncepcja badań, wybór metod badawczych, analiza formalna, archiwizacja danych, sprawowanie opieki merytorycznej nad badaniami, pozyskanie funduszy na badania, udział w przygotowaniu pierwotnej wersji manuskryptu, korekta i akceptacja końcowej wersji manuskryptu, odpowiedzi na recenzje, korekta i akceptacja wersji do druku

Agnieszka Szyposzyńska

(Podpis współautora)

Dr Aleksandra Bielawska-Pohl
Samodzielne Laboratorium Biologii Komórek
Macierzystych i Nowotworowych,
Instytut Immunologii i Terapii Doświadczalnej,
Polskiej Akademii Nauk, 53-114 Wrocław, Polska

15.05.2024

Oświadczenie

Oświadczam, że mój udział w następującej pracy:

Szyposzynska A, Bielawska-Pohl A, Paprocka M, Bar J, Murawski M, Klimczak A. Comparative Analysis of Primary Ovarian Cancer Cells and Established Cell Lines as a New Tool for Studies on Ovarian Cancer Cell Complexity Int. J. Mol. Sci. 2024, 25, 5384. https://doi.org/10.3390/ijms25105384

jest prawidłowo scharakteryzowany w poniższej tabeli.

Autor	Opis udziału własnego
Agnieszka Szyposzyńska	koncepcja badań, hodowla oraz charakterystyka pierwotnych i unieśmiertelnionych komórek raka jajnika z wykorzystaniem cytometrii przepływowej, metody RT-PCR w czasie rzeczywistym, barwień immunofluorescencyjnych i obrazowania mikroskopowego, wykonanie testu MTT, testu zarastania rysy i aktywności ALDH1, tworzenie sferoidów; analiza wyników oraz przygotowanie rycin do publikacji, analiza formalna, gromadzenie i przechowywanie danych, przygotowanie pierwotnej wersji manuskryptu
Aleksandra Bielawska-Pohl	analiza z wykorzystaniem cytometrii przepływowej (fenotyp sferoidów) oraz Western blot, analiza formalna, gromadzenie i przechowywanie danych, przygotowanie pierwotnej wersji manuskryptu
Maria Paprocka	unieśmiertelnienie pierwotnych komórek z płynu puchlinowego
Julia Bar	wykonanie barwień immunocytochemicznych i H&E, analiza i opis badań cytologicznych i immunocytochemicznych, przygotowanie obrazów mikroskopowych
Marek Murawski	pozyskanie i opis materiału klinicznego
Aleksandra Klimczak	koncepcja badań, wybór metod badawczych, analiza formalna, archiwizacja danych, sprawowanie opieki merytorycznej nad badaniami, pozyskanie funduszy na badania, udział w przygotowaniu pierwotnej wersji manuskryptu, korekta i akceptacja końcowej wersji manuskryptu, odpowiedzi na recenzje, korekta i akceptacja wersji do druku

A. Bielawska-Pohl

(Podpis współautora)

Dr Maria Paprocka

Samodzielne Laboratorium Biologii Komórek

Macierzystych i Nowotworowych,

Instytut Immunologii i Terapii Doświadczalnej,

Polskiej Akademii Nauk, 53-114 Wrocław, Polska

15.05.2024

Oświadczenie

Oświadczam, że mój udział w następującej pracy:

Szyposzynska A, Bielawska-Pohl A, Paprocka M, Bar J, Murawski M, Klimczak A. Comparative Analysis of Primary Ovarian Cancer Cells and Established Cell Lines as a New Tool for Studies on Ovarian Cancer Cell Complexity Int. J. Mol. Sci. 2024, 25, 5384. https://doi.org/10.3390/ijms25105384

jest prawidłowo scharakteryzowany w poniższej tabeli.

Autor	Opis udziału własnego
Agnieszka Szyposzyńska	koncepcja badań, hodowla oraz charakterystyka pierwotnych i unieśmiertelnionych komórek raka jajnika z wykorzystaniem cytometrii przepływowej, metody RT-PCR w czasie rzeczywistym, barwień immunofluorescencyjnych i obrazowania mikroskopowego, wykonanie testu MTT, testu zarastania rysy i aktywności ALDH1, tworzenie sferoidów; analiza wyników oraz przygotowanie rycin do publikacji, analiza formalna, gromadzenie i przechowywanie danych, przygotowanie pierwotnej wersji manuskryptu
Aleksandra Bielawska-Pohl	analiza z wykorzystaniem cytometrii przepływowej (fenotyp sferoidów) oraz Western blot, analiza formalna, gromadzenie i przechowywanie danych, przygotowanie pierwotnej wersji manuskryptu
Maria Paprocka	unieśmiertelnienie pierwotnych komórek z płynu puchlinowego
Julia Bar	wykonanie barwień immunocytochemicznych i H&E, analiza i opis badań cytologicznych i immunocytochemicznych, przygotowanie obrazów mikroskopowych
Marek Murawski	pozyskanie i opis materiału klinicznego
Aleksandra Klimczak	koncepcja badań, wybór metod badawczych, analiza formalna, archiwizacja danych, sprawowanie opieki merytorycznej nad badaniami, pozyskanie funduszy na badania, udział w przygotowaniu pierwotnej wersji manuskryptu, korekta i akceptacja końcowej wersji manuskryptu, odpowiedzi na recenzje, korekta i akceptacja wersji do druku

.....

(Podpis współautora)

Prof. dr. hab. Julia Bar

Zakład Immunopatologii i Biologii Molekularnej

Uniwersytet Medyczny we Wrocławiu

50-599 Wrocław, Polska

15.05.2024

Oświadczenie

Oświadczam, że mój udział w następującej pracy:

Szyposzynska A, Bielawska-Pohl A, Paprocka M, Bar J, Murawski M, Klimczak A. Comparative Analysis of Primary Ovarian Cancer Cells and Established Cell Lines as a New Tool for Studies on Ovarian Cancer Cell Complexity Int. J. Mol. Sci. 2024, 25, 5384. https://doi.org/10.3390/ijms25105384

jest prawidłowo scharakteryzowany w poniższej tabeli.

Autor	Opis udziału własnego
Agnieszka Szyposzyńska	koncepcja badań, hodowla oraz charakterystyka pierwotnych i unieśmiertelnionych komórek raka jajnika z wykorzystaniem cytometrii przepływowej, metody RT-PCR w czasie rzeczywistym, barwień immunofluorescencyjnych i obrazowania mikroskopowego, wykonanie testu MTT, testu zarastania rysy i aktywności ALDH1, tworzenie sferoidów; analiza wyników oraz przygotowanie rycin do publikacji, analiza formalna, gromadzenie i przechowywanie danych, przygotowanie pierwotnej wersji manuskryptu
Aleksandra Bielawska-Pohl	analiza z wykorzystaniem cytometrii przepływowej (fenotyp sferoidów) oraz Western blot, analiza formalna, gromadzenie i przechowywanie danych, przygotowanie pierwotnej wersji manuskryptu
Maria Paprocka	unieśmiertelnienie pierwotnych komórek z płynu puchlinowego
Julia Bar	wykonanie barwień immunocytochemicznych i H&E, analiza i opis badań cytologicznych i immunocytochemicznych, przygotowanie obrazów mikroskopowych
Marek Murawski	pozyskanie i opis materiału klinicznego
Aleksandra Klimczak	koncepcja badań, wybór metod badawczych, analiza formalna, archiwizacja danych, sprawowanie opieki merytorycznej nad badaniami, pozyskanie funduszy na badania, udział w przygotowaniu pierwotnej wersji manuskryptu, korekta i akceptacja końcowej wersji manuskryptu, odpowiedzi na recenzje, korekta i akceptacja wersji do druku

Julia Bar

.....

(Podpis współautora)

Dr hab. Marek Murawski

I Katedra i Klinika Ginekologii i Położnictwa

Uniwersytet Medyczny we Wrocławiu

50-599 Wrocław, Polska

15.05.2024

Oświadczenie

Oświadczam, że mój udział w następującej pracy:

Szyposzynska A, Bielawska-Pohl A, Paprocka M, Bar J, Murawski M, Klimczak A. Comparative Analysis of Primary Ovarian Cancer Cells and Established Cell Lines as a New Tool for Studies on Ovarian Cancer Cell Complexity Int. J. Mol. Sci. 2024, 25, 5384. https://doi.org/10.3390/ijms25105384

jest prawidłowo scharakteryzowany w poniższej tabeli.

Autor	Opis udziału własnego
Agnieszka Szyposzyńska	koncepcja badań, hodowla oraz charakterystyka pierwotnych i unieśmiertelnionych komórek raka jajnika z wykorzystaniem cytometrii przepływowej, metody RT-PCR w czasie rzeczywistym, barwień immunofluorescencyjnych i obrazowania mikroskopowego, wykonanie testu MTT, testu zarastania rysy i aktywności ALDH1, tworzenie sferoidów; analiza wyników oraz przygotowanie rycin do publikacji, analiza formalna, gromadzenie i przechowywanie danych, przygotowanie pierwotnej wersji manuskryptu
Aleksandra Bielawska-Pohl	analiza z wykorzystaniem cytometrii przepływowej (fenotyp sferoidów) oraz Western blot, analiza formalna, gromadzenie i przechowywanie danych, przygotowanie pierwotnej wersji manuskryptu
Maria Paprocka	unieśmiertelnienie pierwotnych komórek z płynu puchlinowego
Julia Bar	wykonanie barwień immunocytochemicznych i H&E, analiza i opis badań cytologicznych i immunocytochemicznych, przygotowanie obrazów mikroskopowych
Marek Murawski	pozyskanie i opis materiału klinicznego
Aleksandra Klimczak	koncepcja badań, wybór metod badawczych, analiza formalna, archiwizacja danych, sprawowanie opieki merytorycznej nad badaniami, pozyskanie funduszy na badania, udział w przygotowaniu pierwotnej wersji manuskryptu, korekta i akceptacja końcowej wersji manuskryptu, odpowiedzi na recenzje, korekta i akceptacja wersji do druku

.....

(Podpis współautora)

Prof. dr. hab. Aleksandra Klimczak

Samodzielne Laboratorium Biologii Komórek

Macierzystych i Nowotworowych,

Instytut Immunologii i Terapii Doświadczalnej,

Polskiej Akademii Nauk, 53-114 Wrocław, Polska

15.05.2024

Oświadczenie

Oświadczam, że mój udział w następującej pracy:

Szyposzynska A, Bielawska-Pohl A, Paprocka M, Bar J, Murawski M, Klimczak A. Comparative Analysis of Primary Ovarian Cancer Cells and Established Cell Lines as a New Tool for Studies on Ovarian Cancer Cell Complexity Int. J. Mol. Sci. 2024, 25, 5384. https://doi.org/10.3390/ijms25105384

jest prawidłowo scharakteryzowany w poniższej tabeli.

Autor	Opis udziału własnego
Agnieszka Szyposzyńska	koncepcja badań, hodowla oraz charakterystyka pierwotnych i unieśmiertelnionych komórek raka jajnika z wykorzystaniem cytometrii przepływowej, metody RT-PCR w czasie rzeczywistym, barwień immunofluorescencyjnych i obrazowania mikroskopowego, wykonanie testu MTT, testu zarastania rysy i aktywności ALDH1, tworzenie sferoidów; analiza wyników oraz przygotowanie rycin do publikacji, analiza formalna, gromadzenie i przechowywanie danych, przygotowanie pierwotnej wersji manuskryptu
Aleksandra Bielawska-Pohl	analiza z wykorzystaniem cytometrii przepływowej (fenotyp sferoidów) oraz Western blot, analiza formalna, gromadzenie i przechowywanie danych, przygotowanie pierwotnej wersji manuskryptu
Maria Paprocka	unieśmiertelnienie pierwotnych komórek z płynu puchlinowego
Julia Bar	wykonanie barwień immunocytochemicznych i H&E, analiza i opis badań cytologicznych i immunocytochemicznych, przygotowanie obrazów mikroskopowych
Marek Murawski	pozyskanie i opis materiału klinicznego
Aleksandra Klimczak	koncepcja badań, wybór metod badawczych, analiza formalna, archiwizacja danych, sprawowanie opieki merytorycznej nad badaniami, pozyskanie funduszy na badania, udział w przygotowaniu pierwotnej wersji manuskryptu, korekta i akceptacja końcowej wersji manuskryptu, odpowiedzi na recenzje, korekta i akceptacja wersji do druku

.....

(Podpis współautora)

Publikacje wchodzące w skład rozprawy doktorskiej

International Journal of
Molecular Sciences

MDPI

Article

Suppression of Ovarian Cancer Cell Growth by AT-MSC Microvesicles

Agnieszka Szyposzynska, Aleksandra Bielawska-Pohl, Agnieszka Krawczenko, Olga Doszyn, Maria Paprocka and Aleksandra Klimczak *

Laboratory of Biology of Stem and Neoplastic Cells, Hirszfeld Institute of Immunology and Experimental Therapy, Polish Academy of Sciences, R. Weigla 12, 53-114 Wroclaw, Poland; agnieszka.szyposzynska@hirszfeld.pl (A.S.); aleksandra.bielawska-pohl@hirszfeld.pl (A.B.-P.); agnieszka.krawczenko@hirszfeld.pl (A.K.); olga.doszyn@hirszfeld.pl (O.D.); maria.paprocka@hirszfeld.pl (M.P.)
* Correspondence: aleksandra.klimczak@hirszfeld.pl; Tel.: +48-71-3371-172 (ext. 118)

Received: 20 November 2020; Accepted: 27 November 2020; Published: 30 November 2020

Abstract: Transport of bioactive cargo of microvesicles (MVs) into target cells can affect their fate and behavior and change their microenvironment. We assessed the effect of MVs derived from human immortalized mesenchymal stem cells of adipose tissue-origin (HATMSC2-MVs) on the biological activity of the ovarian cancer cell lines ES-2 (clear cell carcinoma) and OAW-42 (cystadenocarcinoma). The HATMSC2-MVs were characterized using dynamic light scattering (DLS), transmission electron microscopy, and flow cytometry. The anti-tumor properties of HATMSC2-MVs were assessed using MTT for metabolic activity and flow cytometry for cell survival, cell cycle progression, and phenotype. The secretion profile of ovarian cancer cells was evaluated with a protein antibody array. Both cell lines internalized HATMSC2-MVs, which was associated with a decreased metabolic activity of cancer cells. HATMSC2-MVs exerted a pro-apoptotic and/or necrotic effect on ES-2 and OAW-42 cells and increased the expression of anti-tumor factors in both cell lines compared to control. In conclusion, we confirmed an effective transfer of HATMSC2-MVs into ovarian cancer cells that resulted in the inhibition of cell proliferation via different pathways, apoptosis and/or necrosis, which, with high likelihood, is related to the presence of different anti-tumor factors secreted by the ES-2 and OAW-42 cells.

Keywords: ovarian cancer cells; ES-2; OAW-42; microvesicles; adipose tissue origin mesenchymal stem cells

1. Introduction

Today, ovarian cancer is one of the most dangerous types of cancer in women. This is associated with a lack of screening tests and late diagnosis. Moreover, the disease has no symptoms in the early stages. Currently, various ovarian cancer therapies are used depending on the histological type of ovarian cancer, its stage, and the patient's predisposition. Standard treatment is a surgery combined with platinum-based chemotherapy [1]. Clinical trials focus primarily on an anti-angiogenic strategy [Vascular endothelial growth factor (VEGF) inhibition] or on modulating the immune system [2]. An extremely important field in oncology is research focused on cancer stem cells (CSCs). Cancer stem cells constitute a small population of tumor cells and play an important role in metastasis. Moreover, these cells are resistant to widely used drugs, which often leads to tumor recurrence [3]. Thus, a search for effective factors is needed that inhibit the biological activity of CSCs.

Mesenchymal stem/stromal cells (MSCs) are multipotent cells that reside in the majority of human tissues and organs, and in steady-state conditions, are responsible for the maintenance of tissue homeostasis [4,5]. Cells with MSC characteristics can be isolated from various source tissues, such as bone marrow, adipose tissue, dental pulp, skin, skeletal muscle, or perinatal tissues, including the

umbilical cord, cord blood, Warton's jelly, and amniotic fluid. The tissue source of MSCs affects their cellular phenotype and biological properties [6]. MSCs and their derivates are a promising tool in clinical applications thanks to their high proliferative potential, longevity, and immunomodulatory properties [7,8].

Extracellular vesicles (EVs), such as exosomes and microvesicles (MVs), play an important role as mediators of cell-to-cell communication [9]. EVs are released by all normal, apoptotic, and neoplastic cells [10]. The transport of bioactive cargo, such as proteins, lipids, or nucleic acids, into the recipient cells may affect their phenotype and biological activity [11].

The tumor microenvironment consist not only of tumor cells, but also fibroblasts, smooth muscle cells, immune cells, endothelial cells, and mesenchymal stem cells [12]. Cell-to-cell communication in tumor niches takes place through direct contact between the surrounding cells and gap junctions or through the paracrine activity of the cells (e.g., the release of soluble factors or EVs).

The effect of EVs derived from MSCs of different tissue origin on cancer cells is not well understood. Different studies have confirmed the pro-tumorigenic [13] or anti-tumorigenic activity [14] of EVs derived from MSCs on ovarian cancer cells. This effect depends on the origin of the MSCs, methods of EV isolation, and tumor type [15].

The aim of this study was to examine the effect of MVs derived from immortalized human MSCs of adipose tissue origin (HATMSC2-MVs) on the biological activity of two ovarian cancer cell lines: ES-2, representing poorly differentiated ovarian clear cell carcinoma, and OAW-42, representing ovarian cystadenocarcinoma, with different genetic backgrounds and therapeutic responses. These two cell lines were characterized according to their phenotype and the secretion profile of cytokines and trophic factors released in response to MV treatment. Moreover, we investigated the proliferation and cell death processes/pathways (apoptosis and necrosis) of ovarian cancer cells in the presence of different ratios of HATMSC2-MVs and target cells.

2. Results

2.1. Characterization of HATMSC2-Derived MVs

Size distribution of MVs was analyzed using dynamic light scattering (DLS). In the histogram, a single distinct peak characteristic for MVs was observed, confirming the presence of a homogenous population of MVs. The average size of MVs, assessed using DLS, was 456 nm (Figure 1a). The size of individual MVs was confirmed using transmission electron microscopy (TEM) imaging (Figure 1b).

Isolation efficiency, using the flow cytometry method, revealed that the average number of MVs was 172×10^6 MVs/mL (Figure 1c). A Bradford assay was performed to estimate the protein concentration within the MVs, and the average protein concentration was assessed at 169.8 μg/mL.

2.2. Surface Marker Analysis of HATMSC2 Cells and HATMSC2-MVs

The HATMSC2 cells and HATMSC2-MVs were tested for the presence of MSC markers CD73, CD90, CD105, the HLA ABC and HLA DR antigens, and the leukocyte marker CD45. The analysis confirmed the presence of CD73, CD90, and CD105 on the surface of HATMSC2 cells. The cells were also positive for the HLA ABC antigen and negative for the HLA DR antigen and for the pan-leukocyte antigen CD45 [16]. Importantly, HATMSC2-MVs expressed surface markers typical for MSCs, including CD73 (50.50 ± 2.18% of the population), CD90 (90.67 ± 5.36% of the population), CD105 (45.32 ± 3.24% of the population), and HLA ABC (88.20 ± 4.61% of the population). HATMSC2-MVs did not express HLA DR or CD45 (Figure 2).

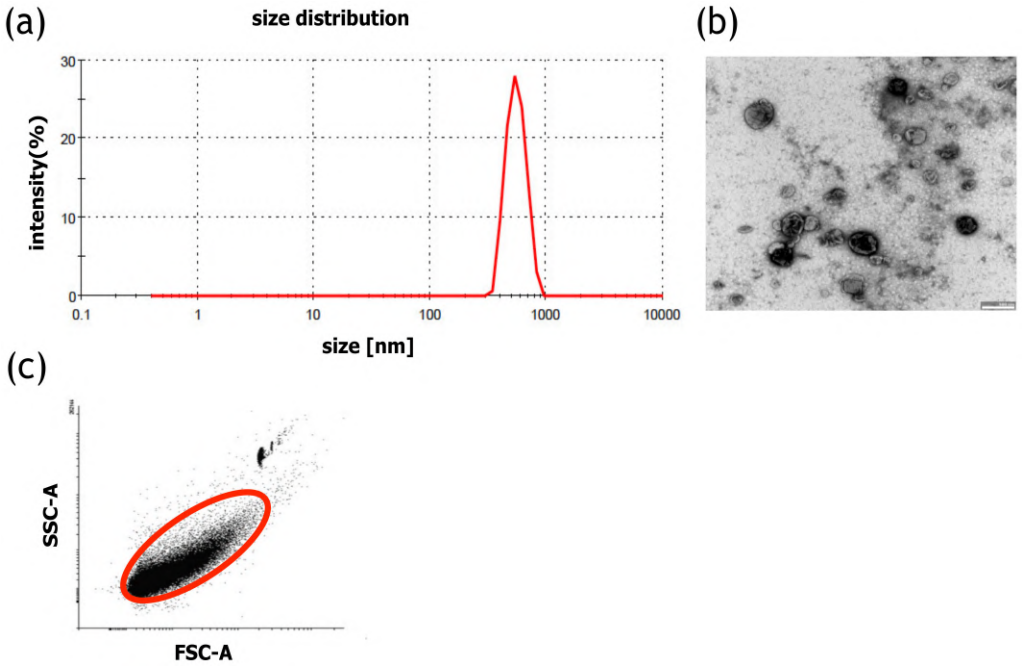

Figure 1. Characteristics of HATMSC2-MVs (**a**) Representative HATMSC2-MV size distribution histogram obtained using dynamic light scattering analysis. (**b**) Representative transmission electron microscopy image of HATMSC2-MVs, bars represent 500 nm. (**c**) Representative dot plot showing forward scatter (FSC) vs. side scatter (SSC). Gate R-1 shows the population of HATMSC2-MVs, and gate R-2 represents the counting beads. HATMSC2-MVs—microvesicles derived from immortalized human mesenchymal stem cells of adipose tissue origin.

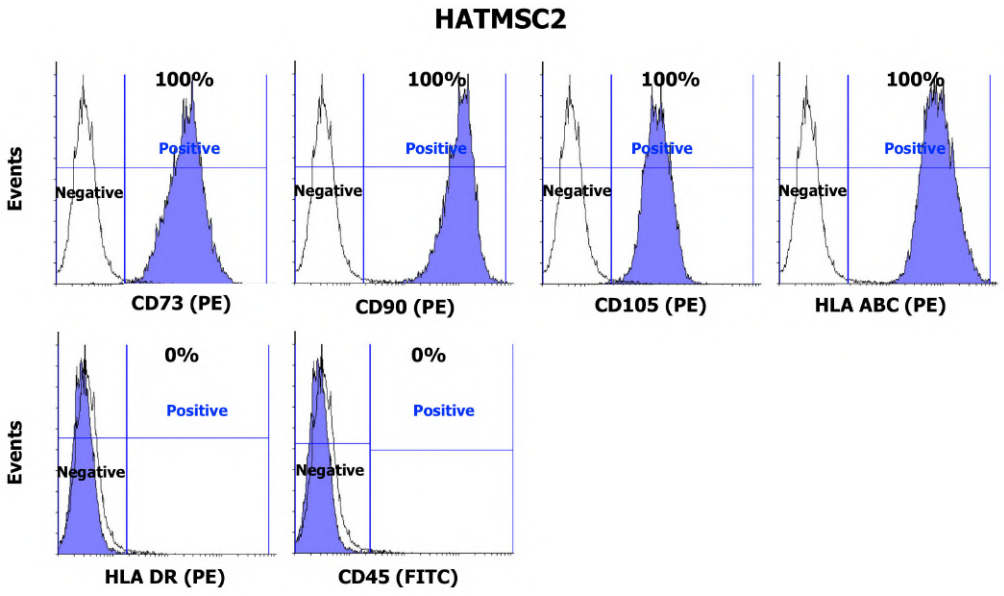

Figure 2. *Cont.*

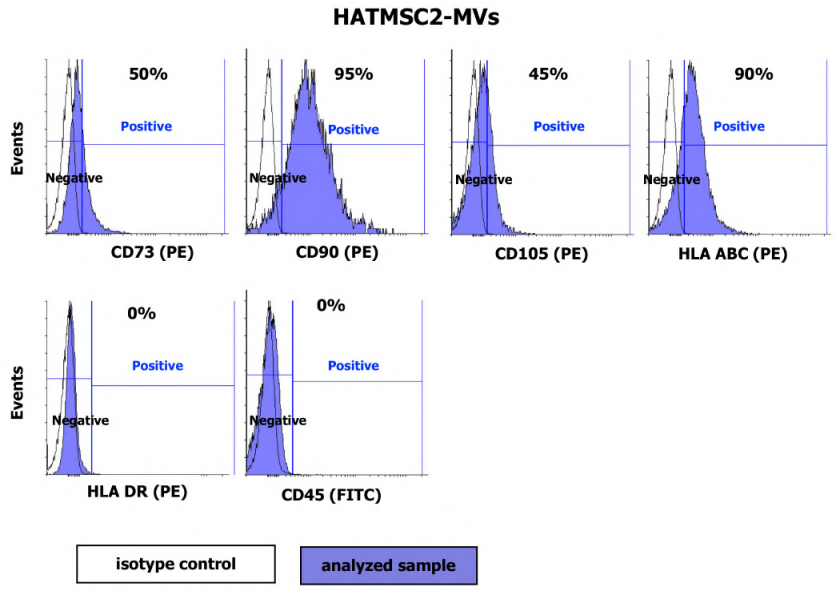

Figure 2. Representative flow cytometry histograms of flow cytometry analysis of mesenchymal stem cells markers (CD73, CD90, CD105, HLA ABC, HLA DR, and CD45) on HATMSC2 cells and HATMSC2-MVs from three independent experiments. Cells and MVs were stained with selected antibodies conjugated with fluorochromes. Blue filled histograms correspond to HATMSC2 cells and HATMSC2-MVs labeled with defined antibodies, and empty histograms represent the isotype controls. HATMSC2-MVs—microvesicles derived from immortalized human mesenchymal stem cells of adipose tissue origin.

2.3. Internalization of HATMSC2-MVs into Ovarian Cancer Cells

The internalization of fluorescently-labeled HATMSC2-MVs into ovarian cancer cell lines was analyzed using three-dimensional microscopic imaging. HATMSC2-MV co-culture with target cells (ES-2 and OAW-42 cell lines) for 24 h resulted in the incorporation of the MVs into ES-2 and OAW-42 cells, as shown by green fluorescence (DiO) expression in the cytoplasm of the target cells across the Z-stack slices (Figure 3a).

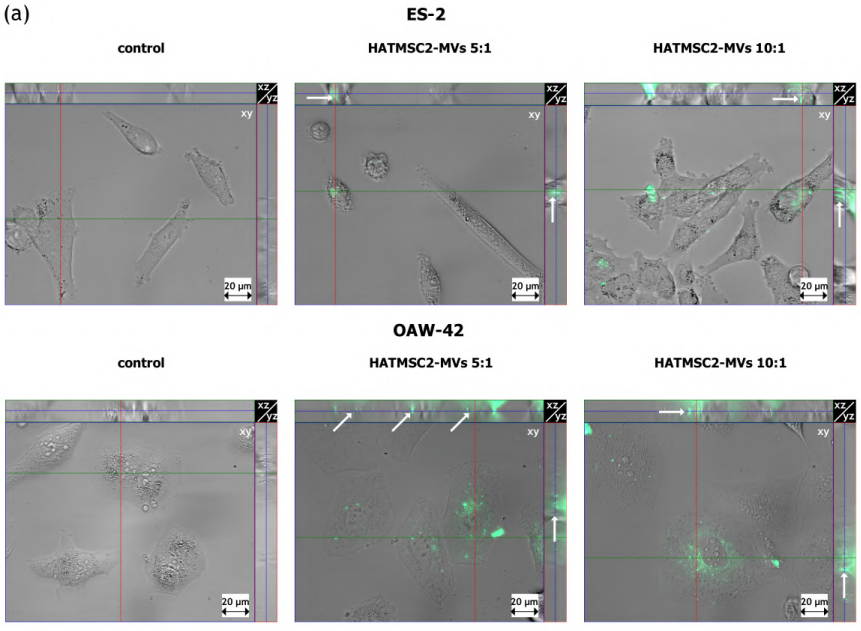

Figure 3. *Cont.*

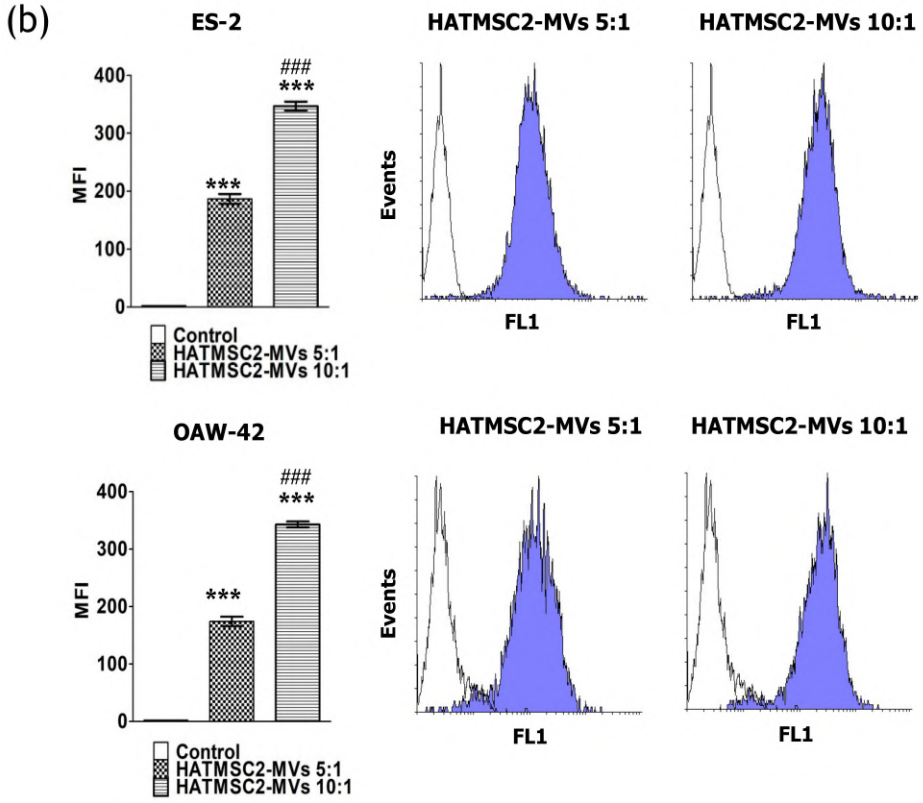

Figure 3. Internalization of HATMSC2-MVs into ovarian cancer cells. (**a**) Images from three-dimensional microscopic analysis of HATMSC2-MV internalization into ES-2 and OAW-42 cells at different ratios. The images were taken using an inverted microscope after 24 h of incubation with fluorescently-labeled HATMSC2-MVs (scale bar: 20 µm). A set of representative orthogonal slices is shown. Each image in a group consists of a large middle segment that represents the midpoint of the Z-stack in the *xy* plane; a narrow top segment that represents the *xz* plane; and a narrow segment on the right that represents the *yz* plane. The arrows point to MVs that have been taken up into the cell. (**b**) Bottom left panel, the bar graph represents the mean fluorescence intensity (MFI) of ES-2 cells treated with fluorescently labeled HATMSC2-MVs at different ratios. Untreated cells without MVs served as a control. Right panel, flow cytometry analysis of HATMSC2-MV internalization. Empty histograms represent the control for untreated cells, and blue filled histograms show the green fluorescence of ovarian cancer cells ES-2 and OAW-42 after HATMSC2-MV internalization at different ratios. The data represent mean ± SEM values from three independent experiments performed in duplicate. *** $p < 0.001$ calculated vs. control, ### $p < 0.001$ calculated vs. The HATMSC2-MVs 5:1 treatment. HATMSC2-MVs—microvesicles derived from immortalized human mesenchymal stem cells of adipose tissue origin.

Furthermore, the uptake of HATMSC2-MVs by ovarian cancer cells was confirmed by an increase in mean fluorescence intensity (MFI), as analyzed using flow cytometry. The results showed a significant increase in MFI in the ES-2 and OAW-42 cell lines treated with HATMSC2-MVs for both the ratios of 5:1 and 10:1 (the number of MVs to one target cell) compared to the control groups ($p < 0.001$). Moreover, this effect was dose-dependent, and significant differences between the ratios 5:1 and 10:1 ($p < 0.001$) were observed (Figure 3b).

2.4. Anti-Proliferative Activity of HATMSC2-MVs

The anti-proliferative activity of HATMSC2-MVs was analyzed using the MTT assay. ES-2 and OAW-42 cells were treated with MVs at four different ratios: 1:1, 5:1, 10:1, and 100:1. The HATMSC-MV treatment caused a significant decrease in OAW-42 cell proliferation on day 3 ($p < 0.01$) at a ratio of 100:1 (Figure 4a). The anti-proliferative activity of the MVs used at a ratio of 100:1 in OAW-42 cells on day 3 was also shown on a microscopic images of calcein-stained ovarian cancer cells (Figure 4b).

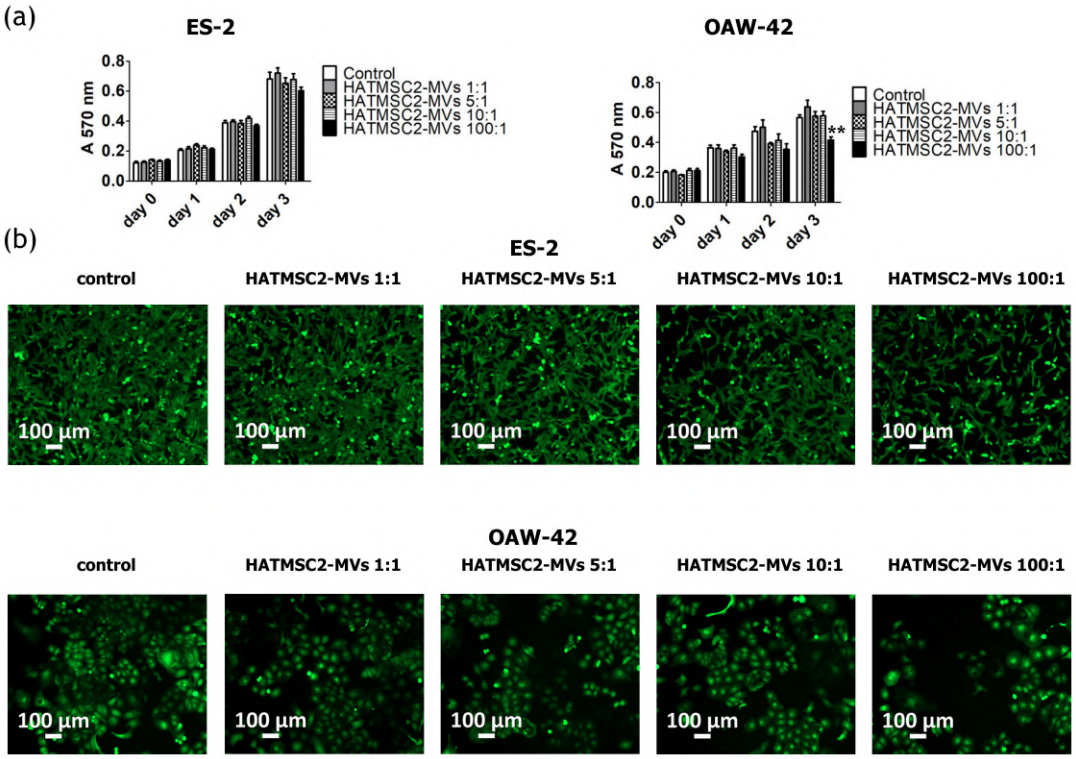

Figure 4. Effect of HATMSC2-MVs on the proliferation activity of ovarian cancer cells. (**a**) Proliferation activity of ES-2 and OAW-42 cells cultured in standard conditions was measured using an MTT assay on day 0, 1, 2, and 3 following treatment with HATMSC2-MVs at different ratios. Untreated cells without MVs served as a control. The data represent mean ± SEM values from four independent experiments performed in triplicate. ** $p < 0.01$ calculated vs. control on a given day. (**b**) Representative images from microscopic analysis of the morphology of ovarian cancer cells treated with HATMSC2-MVs at different ratios. ES-2 and OAW-42 cells were co-incubated with HATMSC2-MVs for 72 h. Afterwards, the cells were stained with Calcein AM and images were taken using an inverted microscope (scale bar: 100 µm). HATMSC2-MVs—microvesicles derived from immortalized human mesenchymal stem cells of adipose tissue origin.

2.5. Effect of HATMSC2-MVs on Cell Cycle Progression

The effect of HATMSC2-MVs on cell cycle progression was tested using flow cytometry analysis of ES-2 and OAW-42 cells stained with propidium iodide. We observed an increase in the percentage of cells in the sub-G1 phase (dead cells) in the samples treated with the MV ratio of 100:1 in ES-2 cells, compared to the control group (mean 2.57 ± 0.54% vs. 0.79 ± 0.05%; $p < 0.01$). Similarly, in OAW-42 cells treated with the MVs ratio of 100:1, the percentage of cells in the sub-G1 phase increased to 15.66 ± 2.86% compared to 2.74 ± 0.48% in control group ($p < 0.001$). Moreover, in OAW-42 cells treated with an MVs ratio of 100:1, the percentage of cells in the G0/G1 phase decreased from 63.06 ± 1.49% in the control group to 55.87 ± 1.37% in the test group ($p < 0.01$), (Figure 5).

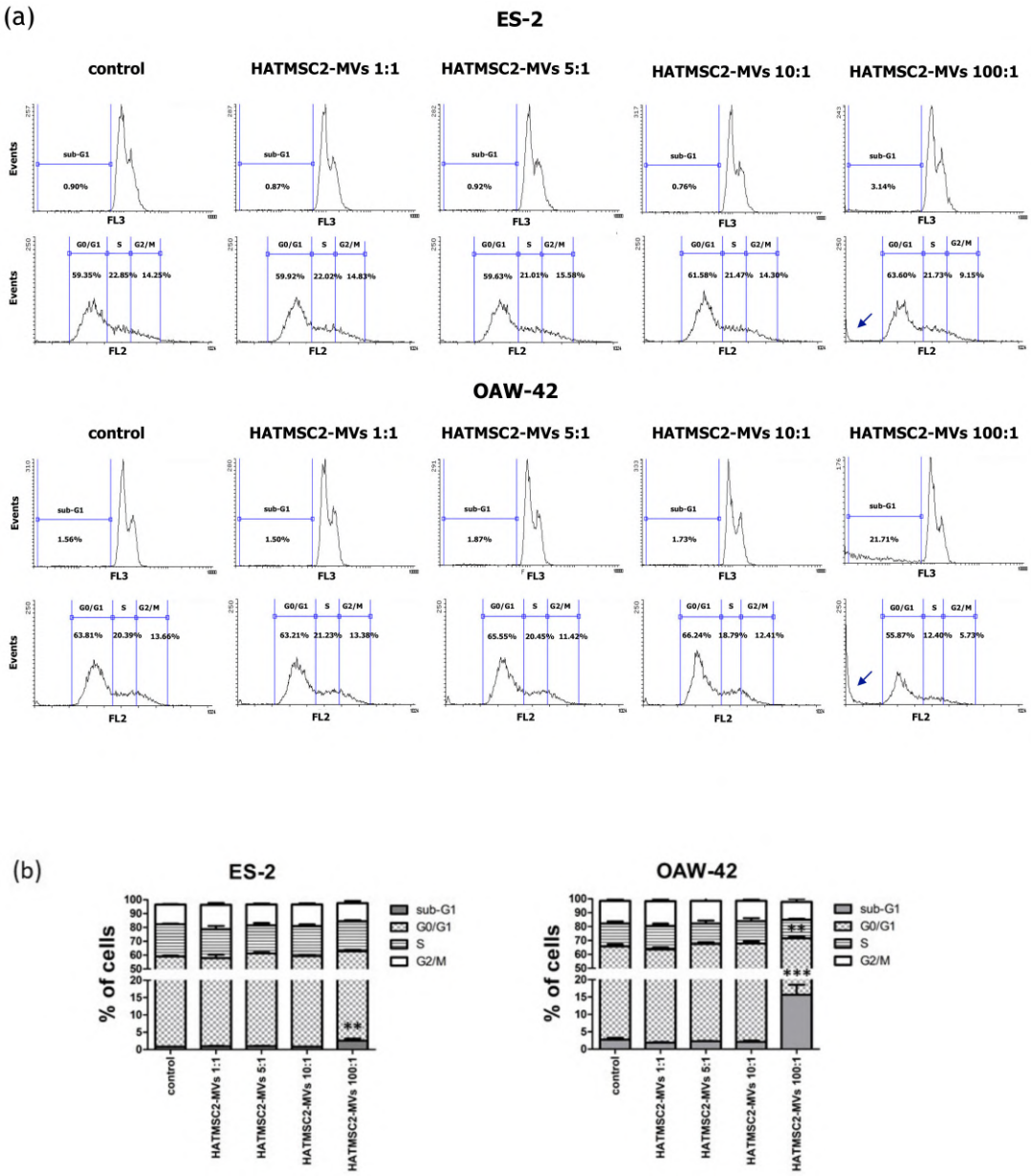

Figure 5. Effect of HATMSC2-MVs on the cell cycle progression of ovarian cancer cells. (**a**) Representative flow cytometry histograms showing cell cycle progression in ES-2 and OAW-42 cells treated with HATMSC2-MVs at different ratios. Untreated cells without MVs served as a control. Arrows represent the increased peaks in the sub-G1 phase of the cell cycle. (**b**) Percentages of cells in the sub-G1, G0/G1, S, and G2/M phases were determined using Flowing Software 2. The data represent mean ± SEM values from three independent experiments performed in duplicate. *** $p < 0.001$, ** $p < 0.01$ calculated vs. control. HATMSC2-MVs—microvesicles derived from immortalized human mesenchymal stem cells of adipose tissue origin

2.6. Proapoptotic Activity of HATMSC2-MVs

We examined the impact of HATMSC2-MVs on ovarian cancer cell survival. Cell death processes, such as apoptosis and necrosis, were assessed using flow cytometry after 72 h of co-culture of HATMSC2-MVs with ES-2 and OAW-42 cells at the ratios of 1:1, 5:1, 10:1, and 100:1. Untreated cells served as a control. The obtained results revealed that the HATMSC2-MVs treatment affected cell viability depending on the ratio of HATMSC2-MVs and cancer cells. The ratio of MVs 100:1 had the greatest impact on cell viability, both in the ES-2 and OAW-42 cells (Figure 6).

In ES-2 cells, the percentage of live cells treated with HATMSC2-MVs decreased to 61.23 ± 7.71% for the ratio of 100:1 vs. control (89.65 ± 0.99%; $p < 0.001$). The average percentage of early apoptotic cells increased to 8.22 ± 1.32% vs. control 1.95 ± 0.41%, ($p < 0.001$), whereas the average percentage of late apoptotic cells increased to 11.75 ± 3.22% vs. control 2.79 ± 0.32%, ($p < 0.01$). The average percentage of ES-2 necrotic cells increased to 18.81 ± 4.79% vs. control 5.72 ± 0.81%, ($p < 0.01$).

In OAW-42 cells, the percentage of live cells treated with HATMSC2-MVs decreased to 47.78 ± 10.11% for the ratio of 100:1 vs. control (86.17 ± 2.12%, $p < 0.001$). The average percentage of late apoptotic cells increased to 18.53 ± 5.17% vs. control 1.57 ± 0.34%, ($p < 0.001$). The average percentage of OAW-42 necrotic cells increased to 27.51 ± 5.04% vs. control 10.70 ± 2.02%, ($p < 0.001$).

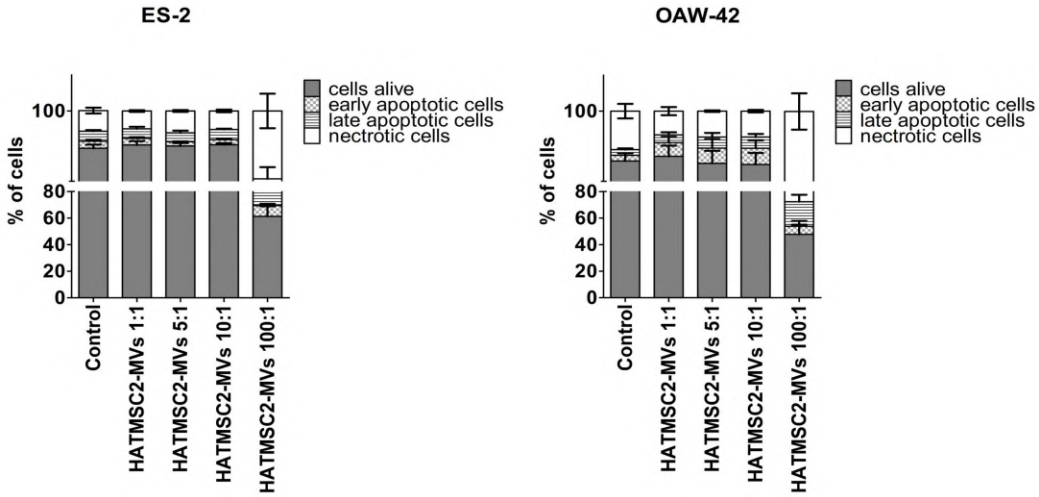

ES-2	HATMSC2-MVs 100:1
cells alive	***
early apoptotic cells	***
late apoptotic cells	**
necrotic cells	**

OAW-42	HATMSC2-MVs 100:1
cells alive	***
early apoptotic cells	ns
late apoptotic cells	***
necrotic cells	***

Figure 6. Quantification of cell viability after treatment with HATMSC2-MVs for 72 h at different ratios, determined using flow cytometric analysis of the apoptotic and necrotic cells via the double-staining of ES-2 and OAW-42 cells with propidium iodide and Annexin V. The percentages of alive, early apoptotic, late apoptotic, and necrotic cells were determined using Flowing Software 2. The data represent mean ± SEM values from five independent experiments performed in duplicate. *** $p < 0.001$, ** $p < 0.01$ calculated vs. control, ns: non-significant results. HATMSC2-MVs—microvesicles derived from immortalized human mesenchymal stem cells of adipose tissue origin.

2.7. Effect of HATMSC2-MVs on the Phenotype of Ovarian Cancer Cell Lines

To determine the effect of HATMSC2 -MVs on the phenotype of ovarian cancer cell lines treated at the ratios of 10:1 and 100:1, we tested the presence of the CD34, CD44, CD133, SSEA4, CD73, CD90, and CD105 markers using flow cytometry. The results showed that both cell lines, ES-2 and OAW-42, were positive for the adhesion molecule CD44 (Figure 7). However, the expression of the CD44 marker was higher (97.80% ± 2.20% of the population) for the ES-2 cells compared to OAW-42 cells (78.36% ± 3.20% of the population). Both ES-2 and OAW-42 cell lines were negative for CD34 and CD133 and for the pluripotency-related marker SSEA4. An analysis of the expression of MSC markers showed that both ES-2 and OAW-42 were positive for CD73 and CD90, whereas the CD105 marker

was detected in ES-2 cells (98.20% ± 1.79% of the population), but not in OAW-42 cells (Figure 7a). The HATMSC2-MVs treatment did not affect the phenotype of ES-2 and OAW-42 cells (Figure 7b).

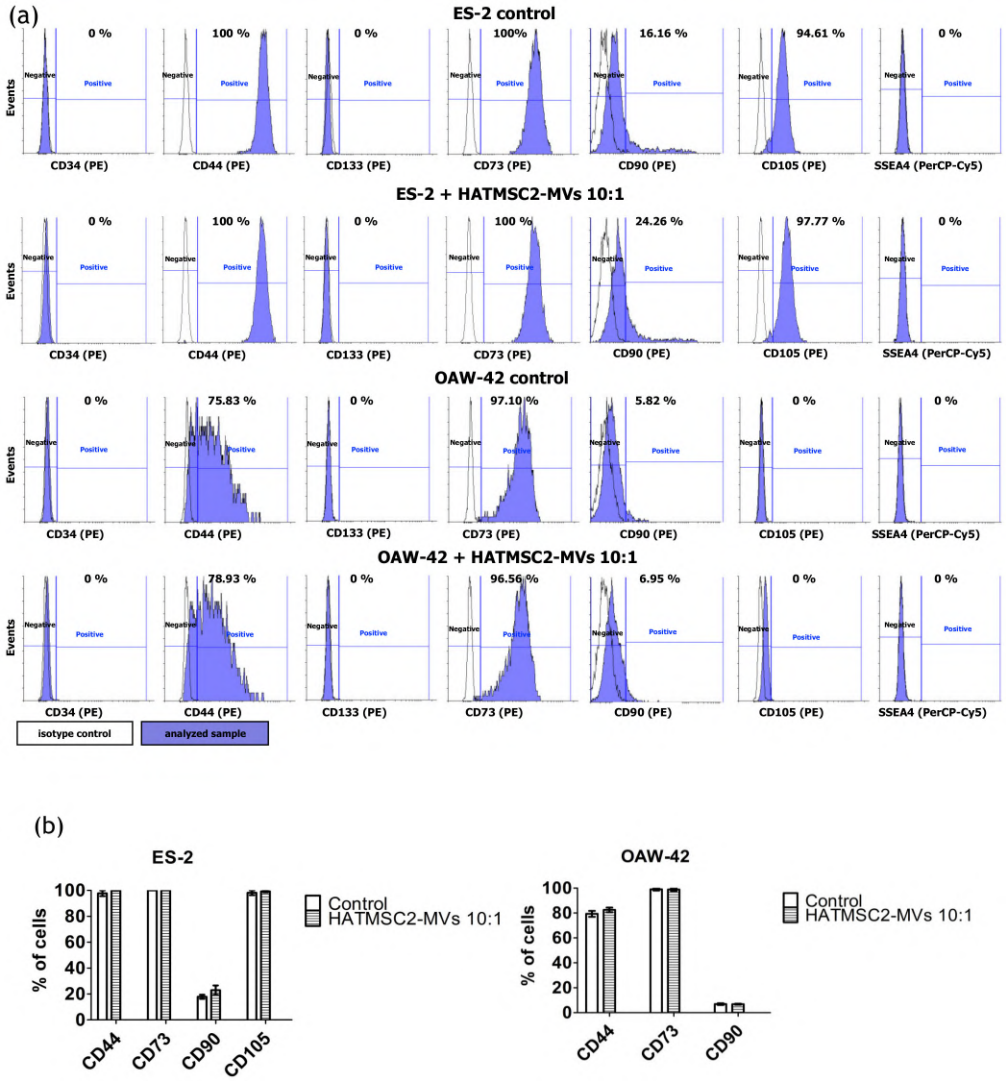

Figure 7. Characteristics of human ovarian cancer cell lines before and after HATMSC2-MV treatment at different ratios. (**a**) Representative histograms of flow cytometry analysis for surface markers (CD34, CD44, CD133, SSEA4, CD73, CD90, and CD105) on the ES-2 and OAW-42 cell lines. The cells were stained with selected antibodies conjugated with fluorochromes. Blue filled histograms correspond to ES-2 and OAW-42 cells, labeled with defined antibodies, and empty histograms represent the isotype controls. (**b**) The percentages of cells positive for selected markers were determined using Flowing Software 2. The data represent mean ± SEM values from three independent experiments. HATMSC2-MVs—microvesicles derived from immortalized human mesenchymal stem cells of adipose tissue origin.

2.8. Effect of HATMSC2-MVs on the Secretion Profile of Ovarian Cancer Cell Lines

The effect of HATMSC2-MVs on the biological properties of ovarian cancer cells was determined in all experiments at different ratios of MVs to cancer cells (1:1, 5:1, 10:1 and 100:1). However, the best effect was seen when a ratio of 100:1 was used. Therefore, to determine the effect of HATMSC2-MVs on the secretion profile of the ES-2 and OAW-42 cell lines, only the ratio of 100:1 was used. The secretion profile was evaluated using a human cytokine antibody array (Figure 8a). Most of the 120 cytokines and trophic factors identified in this analysis affect cancer cells either by promoting cancer growth or through their anti-tumor properties. For the ES-2 cells treated with HATMSC2-MVs, among cancer-promoting

cytokines and trophic factors, a decrease was observed for angiogenesis-related cytokines, such as growth related oncogene-alpha (GRO-alpha) (by 53%), angiopoietin 2 (by 10%), VEGF (by 44%), and VEGFD (by 8%), and for the pro-angiogenic and pro-inflammatory cytokines IL-6 (by 15%), IL-8 (by 36%), MIP-1α (by 7%), and MIP-1β (by 8%). The levels of apoptosis-related TRAIL-R3 and TRAIL-R4 also decreased (by 10% and 14%, respectively). However, an increase was observed in the levels of the pro-inflammatory cytokines IL-1α (by 18%), IL-1β (by 21%), MCP-1 (by 43%), MIG (by 28%), TNFα (by 13%), IL-13 (by 6%), eotaxin (by 16%), and eotaxin-2 (by 21%), and growth factors bFGF (by 9%), EGF (by 33%), and HGF (by 21%). On the other hand, we observed an increase in the levels of several anti-cancer cytokines, such as IL-1 receptor antagonist (IL-1ra) (by 42%), IL-2 by (21%), IL-2 receptor alpha chain (IL-2Ra) (by 13%), IL-12 (by 6% and 10% for the p40 and p70 subunits, respectively), IL-15 (by 34%), and IFN-γ (by 43%). Nevertheless, the overall number of expressed cytokines in the ES-2 cells was 92; however, the expression of a majority of these cells differed before and after the HATMSC2-MV treatment (Figure 8b).

For the OAW-42 cells, the overall number of expressed cytokines increased from 58 in the control group to 87 after the MV treatment. However, most of these cytokines did not show a major difference in expression between the control and test groups. Among the tumor-promoting cytokines, we observed a decrease in the levels of the pro-angiogenic and pro-inflammatory cytokines GRO-alpha (by 192%), VEGF (by 34%), IL-6 (by 176%), IL-8 (by 204%), and RANTES (by 16%), and an increase in other cytokines, such as eotaxin-2 (by 8%), eotaxin-3 (by 6%), IL-1β (by 24%), MIG (by 18%), TNFα (by 36%), TGF-beta1 (by 21%), and -beta3 (by 34%), bFGF (by 15%), TRAIL-R3 (by 11%), and TRAIL-R4 (by 15%). An increase in the levels of anti-cancer cytokines was similar as observed for the ES-2 cells. All data were presented as a heat map (Figure 8b); selected cytokines which exhibited the largest differences between the treated cells and the control group were additionally shown on a column graph (Figure 8c).

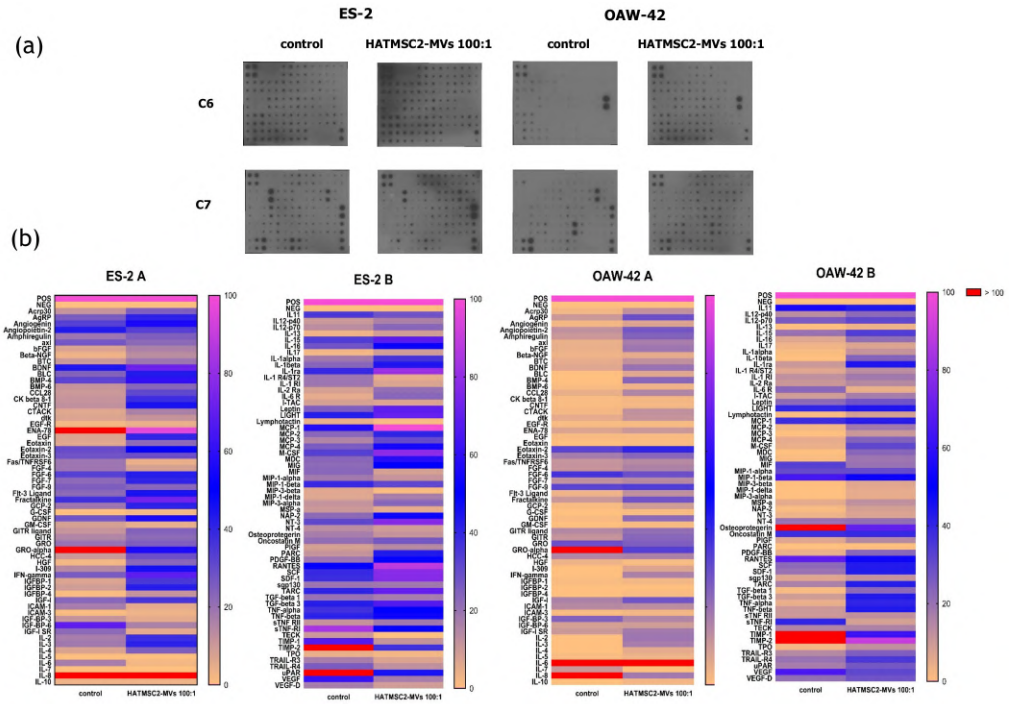

Figure 8. *Cont.*

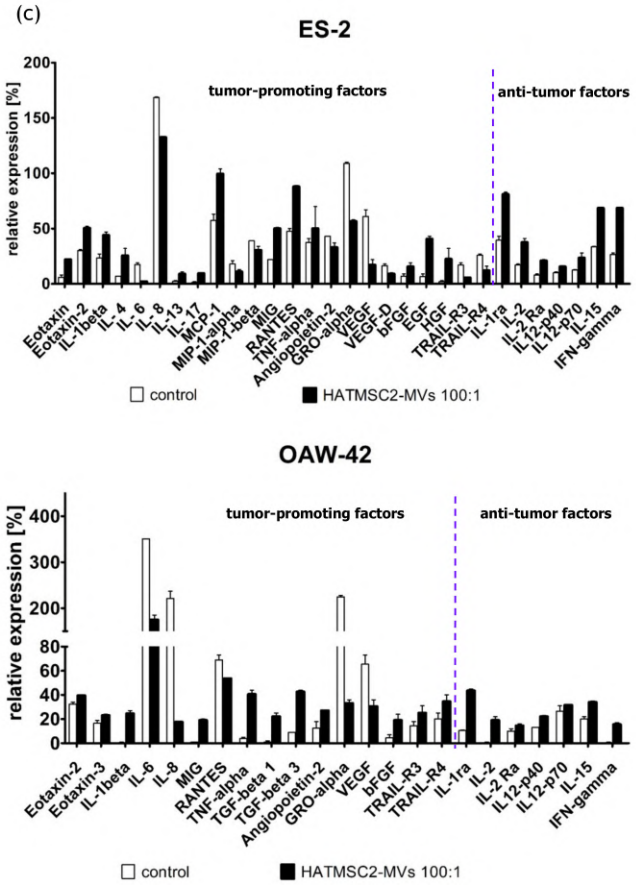

Figure 8. Effect of HATMSC2-MVs on the secretion profiles of ovarian cancer cell lines. (**a**) Scans of representative antibody arrays for ES-2 and OAW-42 supernatants. Untreated cells served as a control. The signal intensity for each antibody spot is proportional to the relative concentration of the antigen in the sample. (**b**) Heat map of cytokine levels for the ES-2 and OAW-42 supernatants; magenta and yellow indicate higher and lower expression limits, respectively. Outstanding values (above 100% of positive control) are depicted in red. Data are normalized to the internal positive control spots, which are consistent between the arrays and represent 100%. The data represent the mean from a duplicate assessment. (**c**) Column graph representing selected proteins (equal to or above 10% of the positive control). The data are presented as mean ± SEM values from a duplicate assessment. HATMSC2-MVs—microvesicles derived from immortalized human mesenchymal stem cells of adipose tissue origin.

3. Discussion

The paracrine activity of cells via EVs is an important link in cell-to-cell communication. Recent research has shown that EVs derived from MSCs play an important role in tumor microenvironment. Tumor cells secrete EVs to reprogram the mesenchymal stem cells present in the tumor microenvironment. The reprogrammed MSCs release exosomes that affect other cells in the tumor niche, such as fibroblasts, endothelial cells, and immune cells, inducing their pro-tumorigenic activity [17]. However, the effect of MVs derived from outside the tumor microenvironment, e.g., from the MSCs of adipose tissue origin, on cancer cells is not well understood and still debatable. The purpose of this study was to analyze the biological behavior of two histologically different ovarian cancer cell lines, ES-2 and OAW-42, in response to HATMSC2-MV treatment. In this study, we investigated whether MVs derived from human immortalized MSCs of adipose tissue origin may represent a new form of supportive therapy in ovarian cancer treatment. Flow cytometry and microscopic analysis confirmed the internalization of HATMSC2-MVs into target cells. Moreover, in all functional experiments, we used untouched MVs, but not the MVs lysate tested by different research

groups [14]. We showed that treatment with HATMSC2-MVs gradually decreased the proliferation of ES-2 and OAW-42 cells, depending on the dose; however, a significant effect was observed on day 3, only for the OAW-42 cell line, when the highest ratio of HATMSC2-MVs of 100:1 (100 MVs per cell) was used. Similar results were obtained by Reza et al. [14], who reported an anti-proliferative and pro-apoptotic effect of ATMSC exosomes on ovarian cancer cells. The main mechanism involved in the action of the exosomes was the transfer of different miRNAs into the recipient cells. However, Reza et al. used protease or RNase-digested exosomes. The anti-proliferative activity of MVs derived from BM-MSCs was also confirmed in vitro on the SKOV3 cell line and in vivo through an intra-tumor injection of MVs into an established tumor generated by a subcutaneous injection of these cells into SCID mice [18]. On the other hand, Dong et al. [19] showed that EVs derived from MSCs isolated from the umbilical cord increased the proliferation of lung adenocarcinoma cells by transporting miR-410 to target cells.

Further experiments involving an analysis of cell cycle progression and cell death processes, such as apoptosis and necrosis, confirmed that HATMSC2-MV treatment affected cancer cell viability. The cell cycle analysis showed that treatment with HATMSC2-MVs, at the ratio of 100:1, significantly increased the percentage of cells of both cell lines in the sub-G1 phase compared to control; however, the increase of OAW-42 cells in the sub-G1 phase was significantly higher compared to the ES-2 cell line. The increased number of cells in the sub-G1 phase suggests that both ovarian cancer cell lines underwent cell death via apoptosis. A similar pro-apoptotic effect of the bioactive factors derived from MSCs isolated from human Wharton's jelly and applied in the form of a conditioned medium or Wharton's jelly-MSCs lysate was observed in a study on the OVCAR3 and SCOV3 ovarian cancer cell lines, confirming the anti-cancer properties of the MSC secretome [20]. The pro-apoptotic effect of HATMSC2-MVs on the examined ovarian cancer cell lines was also confirmed through flow cytometry analysis of cell death processes, distinguishing between apoptosis and necrosis. When HATMSC2-MVs were cultured with ovarian cancer cell lines at the ratio of 100:1, we observed a significant increase in the percentage of early and late apoptotic cells for the ES-2 cells, whereas in the OAW-42 cells, a substantial increase was observed for late apoptotic cells. Moreover, in both cells lines, HATMSC2-MVs significantly increased the percentage of necrotic cells. These results suggest that HATMSC2-MVs at a ratio of 100:1 induce mechanisms governing ovarian cancer cell death via both apoptosis and necrosis. Studies on the anti-cancer properties of the MSC secretome report that co-culture of MSCs of different tissue origin with ovarian cancer cell lines increases apoptosis with varying effects [21]. Interestingly, the percentage of apoptotic cells was higher when the supernatant derived from AT-MSCs was applied compared to the supernatants derived from BM-MSCs and UC-MSCs [21].

Additionally, we assessed the secretion profile of ovarian cancer cell lines and the effect of HATMSC2-MVs on the presence of the produced cytokines and trophic factors with different functions; one set of bioactive factors is known to promote cancer cells growth and metastasis, and the second set of cytokines is associated with anti-tumor properties. The differences in the secretion profiles of the examined ovarian cancer cell lines correlated with the histological type of the tumor. ES-2 cells were derived from clear cell carcinoma, with a good prognosis for the patient when diagnosed at an early stage of the disease and poor survival when diagnosed at an advanced stage, because this type of ovarian cancer is often more resistant to chemotherapy than serous cystadenocarcinoma, represented by the OAW-42 cell line [22]. The presence of cancer-promoting cytokines and chemokines, such as IL-6, IL-8, GRO-alpha, MIP-1α, MIP-1β, angiopoetin-2, and VEGF, which are associated with tumor growth, metastatic properties, and a poor prognosis, was detected in the supernatants collected from both ES-2 cells and OAW-42 cells. The application of HATMSC2-MVs resulted in a substantial decrease in IL-6, IL-8, GRO-alpha, and VEGF secretion in both cell lines. IL-8 is a pleiotropic chemokine with a dual function, which acts as a chemoattractant for neutrophils, inducing innate immune responses, whereas in the ovarian cancer environment, it contributes to the pro-survival activity of tumor cells and resistance to chemotherapy. A high production of IL-8 correlates with faster proliferation and increases the potential of angiogenesis, adhesion, and invasion of platinum sensitive (PEA1 and PEO14)

and platinum resistant (PEA2 and PEO23) cell lines [23]. Browne et al. demonstrated a significant increase in the expression of IL-8 in specimens of the serous type of ovarian cancer compared to clear cancer ovarian carcinoma tissue [24]. The HATMSC2-MVs markedly inhibit IL-8 production in both examined cell lines in vitro. This effect can be used as a potential supportive therapy for ovarian cancer treatment. IL-6 was present in the OAW-42 culture supernatant at a very high level, in contrast to the ES-2 cells. It is well known that IL-6 plays a crucial role in the stimulation of inflammatory cytokine production, tumor angiogenesis, cell proliferation, and tumor macrophage infiltration [25]. A high production of IL-6 by ovarian cancer cells contributes to tumor progression and correlates with a poor prognosis [26]. The HATMSC2-MVs inhibit the activity of IL-6, and in conjunction with a decreased level of IL-8, may exert suppressive effects on the ovarian cancer cell line. GRO-alpha and VEGF were produced by ES-2 and OAW-42 cells; however, the GRO-alpha level markedly exceeded the VEGF level. Both growth factors, GRO-alpha and VEGF, are important for tumor growth and metastasis, especially in terms of supporting cancer angiogenesis. The diverse production of cytokines and growth factors by ovarian cancer cells is associated with the biological activity of cancer cells and may affect tumor progression, as reported in a study performed simultaneously on a set of 120 cytokines in ovarian cancer ascites [25]. Our study determined that HATMSC2-MVs substantially reduced the secretion of GRO-alpha and VEGF in both cell lines. Numerous growth factors and cytokines, including those assessed in our study, such as IL-6, IL-8, MCP-1, RANTES, GRO-alpha, and VEGF, are involved in promoting tumor growth and ovarian cancer cell aggressiveness. Therefore, characterizing cytokine secretion may provide information on the functional profile of cancer cells. This may help to create targeted therapy for ovarian cancer, in which angiogenesis is inhibited by a blockage of NF-κB, suppressing VEGF and IL-8 activity [27], or by targeting CXCR2, the key receptor for the GRO-alpha and IL-8 chemokine activity [28]. RANTES (CCL5) level decreased only in OAW-42 cells after the HATMSC2-MVs treatment. RANTES is involved in trafficking immune cells into the inflammation site and acts as a co-activator of T cells promoting the polarization of the immune response towards the Th1 profile. In the ovarian cancer microenvironment, RANTES acts through paracrine or autocrine signaling to promote tumor cell migration, invasion, and metastasis [29]. In contrast, MCP-1 was detected in supernatants collected from ES-2 cells, and its level increased after the HATMSC2-MV treatment. The main function of MCP-1 in the tumor microenvironment is to attract tumor-associated monocytes (TAMs) [30]. Research performed by Furukawa et al. [30] demonstrated that the MCP-1 chemokine promoted the invasion and adhesion of the ovarian cancer cell line SKOV3, contributing to the progression of tumors. Tumor necrosis factor-related apoptosis-inducing ligand (TRAIL)-R3 and –R4 are known as the negative regulators of TRAIL-mediated apoptosis in cancer cells [31–33]. The internalization of HATMSC2-MVs by the examined cell lines exerts a different effect on ovarian cancer cells, and decrease the level of TRAIL-R3 and TRAIL-R4 in ES-2 cells and increase their level in OAW-42 cell lines. The downregulation of TRAIL-R3 and TRAIL-R4 is associated with an increased level of early apoptotic cells in the ES-2 cell line treated with the 100:1 ratio. A very recent study, performed on a murine xenograft model, documented that the EVs isolated from the TRAIL expressing cell line 293T in combination with cyclin-dependent kinase inhibitor (dinaciclib) successfully inhibited the growth of human lung cancer cell lines NCI-H727 and A549 and the human breast adenocarcinoma cell line MDAMB231 by inducing apoptosis [34].

The HATMSC2-MVs used in this study affect both histologically different cell lines, the ES-2 cells and the OAW-42 cells, by increasing the production of tumor-suppressive cytokines, such as IL-1ra, IL-2, IL-2Ra, IL-12-p40, IL12-p70, IL-15, and IFN-γ. Studies that used bioactive factors released to the culture medium from Wharton's jelly MSCs led to a similar inhibition of the proliferation of the ovarian cancer cell line OVCAR3 through a decreased expression of oncogenic cytokines and growth factors and an increased expression of anti-tumor related cytokines [35]. The anti-inflammatory properties of IL-1ra, a naturally occurring inhibitor to IL-1, contribute to tumor growth inhibition by competitive binding to IL-1 receptors blocking cancer-promoting activity of IL-1 [36]. The anti-proliferative effect of ovarian cancer cell lines can be also supported by an increased production of IFN-γ following the exposure of

cells to HATMSC2-MVs, as documented in both examined cell lines. It has been reported that IFN-α and IFN-γ, applied in combination with IL-4 fused to Pseudomonas exotoxin, inhibit tumor growth in an experimental mouse model of human ovarian cancer. The anti-tumor effect was accomplished by the activation of the IFN signaling pathways and the subsequent activation of molecules inducing apoptotic cell death [37]. Characterization of a wide range of tumor-promoting factors and anti-tumor cytokines after ovarian cancer cell expose to HATMSC2-MVs provides information on how they affect the production of functional cytokines and shed light on the mechanism altering the behavior of ovarian cancer cells in response to MV treatment.

Consequently, we characterized the ovarian cancer cell lines ES-2 and OAW-42 for the presence of CSC and MSC markers. The results showed that the ES-2 and OAW-42 cells were positive for CD44 and negative for CD133, and that the application of HATMSC2-MVs had no effect on the expression of these markers. Similar results were reported by Tudrej et al., who showed that CD44 expression was higher for ES-2 cells compared to OAW-42 cell lines [38]. They found a small subpopulation of ES-2 cells positive for the CD133 marker expression (around 0.2%). However, we did not observe any CD133 positive cells in our study. To our best knowledge, the expression of specific MSC markers on ovarian cancer cell lines has been studied in the form of a single MSC marker as a potential therapeutic target [39–42], whereas a complete analysis of MSC markers has been performed in a limited number of studies concerning the biological activity of ovarian cancer cell lines [21]. Our results revealed that both ES-2 and OAW-42 cells were strongly positive for CD73, and that HATMSC2-MVs had no impact on CD73 expression. CD73, also known as cell surface nucleotidase, is an immunosuppressive enzyme involved in tumor progression and metastasis, and its expression is associated with a poor prognosis for high-grade serous ovarian cancer [42]. The functional inhibition of CD73 via either a chemical compound or a neutralizing antibody reduced the tumorigenesis of primary high-grade serous epithelial ovarian cancer cells [41]. In contrast, CD90 was present on a limited population of both examined cell lines, and co-culture of ES-2 and OAW-42 cells with HATMSC2-MVs at a ratio of 1:10 did not increase the expression of this marker. It was reported previously that the overexpression of CD90 inhibited the sphere-forming ability of SKOV3 cell lines and increased cell apoptosis. These studies also suggest that CD90 may decrease cell growth through a downregulation of the expression of other CSC markers, including CD133 and CD24 [40]. Interestingly, the CD105 molecule was detected only on poorly-differentiated ES-2 cells, but not on the better-differentiated OAW-42 cells. This finding confirmed the mesenchymal phenotype of ES-2 cells, which is associated with increased aggressiveness and metastatic potential. The HATMSC2-MVs have no marked impact on CD105 expression in either of the cell lines. Studies on the biological role of CD105 in ovarian cancer revealed that high CD105, CD44, or CD106 expression was associated with drug resistance, an advanced stage of the disease, poor differentiation, and high rate of cancer relapse [43]. The downregulation of CD105 expression with a clinically relevant CD105-neutralizing mAb (TRC105) inhibited high-grade serous cancer metastasis, reduced ascites, and hampered the growth of abdominal tumor nodules in animal models of ovarian cancer [39].

A systematic review, introducing the impact of experimental anti-tumor cellular therapies involving MSCs of different human tissue origin, also highlights the possibility to use MSC secretome, in the form of a conditioned medium or EVs, as a cell-free therapy to inhibit cancer growth [44]. Thus, MVs may serve as a carrier for the delivery of therapeutic agents to target cells. A modification of primary MSCs for the secretion of inhibitory growth factors and pro-apoptotic factors may be employed to prepare the MVs carrying the pro-apoptotic signal and transport them to target ovarian cancer cells. Thus, MVs may be applied as a supportive therapy to enhance the therapeutic effect of chemotherapy, especially for multidrug resistant cancers.

In conclusion, we confirmed an effective transfer of HATMSC2-MVs into target ovarian cancer cells, which affected the biological behavior of these cells. Our results revealed that HATMSC2-MVs inhibit tumor cell proliferation in the two histologically distinct ovarian cancer cell lines via different pathways, apoptosis and/or necrosis. This phenomenon, with high likelihood, is related to the

secretion of the different anti-tumor factors by the ES-2 (representing poorly differentiated ovarian clear cell carcinoma), and OAW-42 (representing ovarian cystadenocarcinoma) cell lines treated with HATMSC2-MVs. However, further studies are needed to determine the possible mechanisms involved in HATMSC2-MV-mediated effect on target cells, as well as to validate their anti-tumorigenic potential with respect to cancer cells isolated from human tissues. Therefore, understanding the mechanisms involved in the bilateral interaction between the MVs and ovarian cancer cells may be help to design new treatment modalities for an effective anti-tumor cell-free therapy.

4. Materials and Methods

4.1. Cell Culture

The ES-2 cell line was purchased from ATCC (American Type Culture Collection, Manassas, VA, USA) (catalog number: CRL-1978™). The cells were cultured in the DMEM and OptiMEM GlutaMax media, mixed in equal proportions. The DMEM medium was supplemented with 10% FBS (Gibco, Thermo Scientific, Carlsbad, CA, USA), a 1% penicillin/streptomycin solution (Gibco, Thermo Scientific, Carlsbad, CA, USA) and L-glutamine (Gibco, Thermo Scientific, Carlsbad, CA, USA). The OptiMEM GlutaMax medium was supplemented with 3% FBS (Gibco, Thermo Scientific, Carlsbad, CA, USA) and a 1% penicillin/streptomycin solution (Gibco, Thermo Scientific, Carlsbad, CA, USA).

The OAW-42 cell line was purchased from ECACC (European Collection of Authenticated Cell Cultures, Salisbury, United Kingdom) (catalog number: 85073102). The cells were cultured in the same media conditions, mixed in equal proportions, and additionally supplemented with a 10 µg/mL insulin solution (Sigma-Aldrich, St. Louis, MO, USA).

All cells were cultured in standard conditions (21% O_2, 5% CO_2, 95% humidity, 37 °C temperature). Upon reaching 70–80% confluence, the cells were harvested with a 0.05% trypsin/0.02% EDTA (*w/v*) solution (IIET, Wroclaw, Poland) and seeded onto new culture flasks.

The human mesenchymal stem cell line HATMSC2 was established in our laboratory using the hTERT and pSV402 plasmids, as described in a previous study [16].

4.2. MV Isolation Using Sequential Centrifugation

MVs were isolated according to the well-established protocol developed in our laboratory [45] based on the procedure introduced in the previous study [46]. HATMSC2 cells were cultured in multi-layer cell culture flasks (Nunc TripleFlasks, Thermo Scientific, Carlsbad, CA, USA) using DMEM + 10% FBS until they reached 75% confluence. Next, the cells were cultured in serum-free media in hypoxic conditions (1% O_2) for 48 h to enhance the release of MVs. The conditioned media collected from the HATMSC2 cultures were mixed to obtain a homogenous starting material before the isolation of MVs. In the next step, the conditioned media were centrifuged at 300× *g* for 10 min at 4 °C, and at 2000× *g* for 10 min at 4 °C, in order to remove cellular debris and apoptotic bodies. Subsequently, the supernatants were subjected to double centrifugation at 12,000× *g* for 30 min at 4 °C using a Sorvall LYNX 6000 ultracentrifuge (Thermo Scientific, Carlsbad, CA, USA) with an intermediate washing step in PBS (IIET, Wroclaw, Poland). The obtained MV pellets were resuspended in 150 µL of PBS and stored at −80 °C.

4.3. Analysis of MVs

The size distribution of MVs was measured with DLS (Malvern Zetasizer, Malvern, UK). The measurement was performed for 2 min at 25 °C. PBS was used to disperse the samples. Moreover, to confirm the size of the MVs, the samples were analyzed using transmission electron microscopy (TEM). The PBS-suspended MVs were placed on a carbon-coated copper grid (400 mesh) and incubated for 1 min, and the excess liquid was removed with filter paper. Next, the samples were stained with 2% uranyl acetate, dried, and examined with a transmission electron microscope (JEOL, Peabody, MA, USA) at 80 kV. The number of MVs was calculated using a BD Fortessa Flow Cytometer (BD Biosciences,

San Jose, CA, USA) and fluorescent counting beads (CountBright™ Absolute Counting Beads for flow cytometry, Thermo Scientific, Carlsbad, CA, USA). Prior to analysis, 10 µL of the MV sample was diluted in PBS to a final volume of 300 µL, after which 50 µL of counting beads were added. The threshold for the forward scatter (FSC) was set at 200. To determine the number of MVs in the samples, 5000 counting beads were collected using a BD Fortessa Flow Cytometer (BD Biosciences, San Jose, CA, USA). The data were analyzed using the BD FACSDiva Software (BD Biosciences, San Jose, CA, USA). The number of MVs was calculated according to the CountBright™ Absolute Counting Beads manufacturer's instructions, using the ratio of MV events and the number of counting bead events. The protein concentration of MVs was determined with a Bradford assay (Thermo Scientific, Carlsbad, CA, USA) according to the vendor's instructions. The MV samples or the BSA standard were briefly incubated with the Bradford reagent for 5 min on a 96-well plate. The absorbance was measured with a Synergy H4 plate reader (Biotek, Winooski, VT, USA) at 595 nm.

4.4. Flow Cytometry Analysis of HATMSC2 Cells and HATMSC2-MVs

HATMSC2 cells were detached using the trypsin/EDTA solution and incubated with PE-conjugated antibodies specific for the human CD73 (clone AD2), CD90 (clone 5E10), CD105 (clone 266), HLA ABC (clone G46-2.6), HLA DR (clone G46-6) (BD Biosciences, San Jose, CA, USA), and FITC-conjugated CD45 antibody (clone 2D1) (BD Biosciences, San Jose, CA, USA) and with the appropriate isotype controls (BD Biosciences, San Jose, CA, USA) for 30 min at 4 °C. Afterwards, the labeled cells were washed with PBS (IIET, Wroclaw, Poland) and analyzed using a FACSCalibur flow cytometer (BD Biosciences, San Jose, CA, USA). The obtained data were processed using the CellQuest software (BD Biosciences, San Jose, CA, USA). The histograms were created using Flowing Software 2. The surface markers of the MVs were analyzed using a BD Fortessa Flow Cytometer (BD Biosciences, San Jose, CA, USA) after staining with specific fluorophore-conjugated antibodies. MVs suspended in PBS were incubated with PE-conjugated antibodies specific for human CD73, CD90, and CD105, HLA ABC, HLA DR, and FITC-conjugated antibody for CD45 and with the appropriate isotype controls for 30 min at 4 °C. The percentage of positive MVs was calculated using the BD FACSDiva Software (BD Biosciences, San Jose, CA, USA).

4.5. Internalization of MVs

ES-2 and OAW-42 cells were seeded into a Lab-Tek II Chambered # 1.5 Coverglass system (Nalge Nunc International, Naperville, IL, USA) at a density of 15×10^3 cells per chamber. Fluorescence staining of the MVs was performed, as established in our recent study [45]. After washing with PBS, the MVs were resuspended in the DMEM + 10% FBS and OptiMEM GlutaMax + 3% FBS media (mixed in equal proportions), and added to the cells at a ratio of 5:1 (5 MVs per cell) and 10:1 (10 MVs per cell). The cells were incubated with MVs for 24 h and washed twice with PBS prior to imaging. The internalization of the MVs into target cells was immediately analyzed at 37 °C using an Axio Observer inverted microscope equipped with a dry 63x objective (Zeiss, Gottingen, Germany). The labeled MVs were detected using an EGFP Filter set. Thirty Z-sections with a 0.6-µm interval were recorded simultaneously in the brightfield and fluorescence channel. Optical orthogonal sectioning was performed in order to visualize the internalization of the MVs. Images were obtained and processed using the Zen Blue Software (Zeiss, Gottingen, Germany). A similar analysis of EV internalization using fluorescence microscopy was previously described by Adamiak et. al. [47]. After 24 h of incubation with MVs, the cells were washed once with PBS, detached using the trypsin/EDTA solution, washed once more with PBS, and analyzed using flow cytometry with FACSCalibur (BD Biosciences, San Jose, CA, USA). The cells were detected using the FL1 channel (480 nm). The histograms were created using Flowing Software 2 (Perttu Terho, Turku Centre for Biotechnology, Finland).

4.6. Proliferation Activity

The proliferation activity of ES-2 and OAW-42 treated with HATMSC2-MVs was measured using the MTT assay. The cells were seeded on a 96-well plate at a concentration of 2 x 10^3 cells/well in the DMEM + 10% FBS and OptiMEM GlutaMax + 3% FBS media (mixed in equal proportions); MVs at a ratio of 1:1 (1 MV per cell), 5:1 (5 MVs per cell), 10:1 (10 MVs per cell), and 100:1 (100 MVs per cell) were added to the cells. ES-2 and OAW-42 cells without MVs were used as a control. After 4 h, 24 h, 48 h, and 72 h, the absorbance of the formazan dye produced by living cells was measured using a Wallac 1420 Victor2 Microplate Reader (Perkin Elmer, Waltham, MA, USA) at 570 nm. After 72 h of co-incubation with HATMSC2-MVs, the ovarian cancer cells were stained using Calcein AM (Thermo Fisher, Carlsbad, USA). 100 µL of Calcein AM (1 µM solution) were added to each well. The cells were incubated for 15 min at room temperature. Images were obtained using an Axio Observer inverted microscope equipped with a dry 10x objective (Zeiss, Gottingen, Germany). The labeled cells were detected using an Alexa Fluor 488 Filter set. The images were processed with the Zen Blue software (Zeiss, Gottingen, Germany).

4.7. Cell Cycle Analysis

The cell cycle analysis was performed based on previously published method [20,48]. The cells were seeded on 24-well plates at a concentration of 12 × 10^3 in the DMEM + 10% FBS and OptiMEM GlutaMax + 3% FBS media (mixed in equal proportions). MVs at a ratio of 1:1 (1 MV per cell), 5:1 (5 MVs per cell), 10:1 (10 MVs per cell), and 100:1 (100 MVs per cell) were added to the cells. ES-2 and OAW-42 cells without MVs were used as a control. After 72 h, the cells were detached using the trypsin/EDTA solution; the conditioned media were also collected and mixed with the respective cell suspension samples. The samples were centrifuged at 1400 rpm for 4 min at 4 °C. After the supernatant was removed, the cells were resuspended in ice-cold 70% ethanol and incubated for 30 min on ice at 4 °C. Afterwards, PBS Ca^{2+} Mg^{2+} + 2.5% FBS was added to the cells, and the samples were centrifuged at 1400 rpm for 5 min. This step was repeated twice. The cells were then resuspended in a solution of propidium iodide in PBS (50 µg/mL) and RNase (20 µg/mL) and incubated overnight at 4 °C. The cells were analyzed using a FACSCalibur flow cytometer (BD Biosciences, San Jose, CA, USA). The obtained data were analyzed using Flowing Software 2 (Perttu Terho, Turku Centre for Biotechnology, Finland).

4.8. Cell Viability and Apoptosis Analysis Using Flow Cytometry

In order to determine the effect of HATMSC2-MVs on the viability of the cells, an Annexin V Apoptosis Detection Kit (Thermo Scientific, Carlsbad, CA, USA) was used. ES-2 and OAW-42 cells were seeded in a 24-well plate at a density of 25 × 10^3 in the DMEM + 10% FBS and OptiMEM GlutaMax + 3% FBS media (mixed in equal proportions). Before the analysis, the cells were treated with MVs at a ratio of 1:1 (1 MV per cell), 5:1 (5 MVs per cell), 10:1 (10 MVs per cell), and 100:1 (100 MVs per cell) for 72 h. ES-2 and OAW-42 cells without MVs were used as a negative control. After incubation with MVs, the cells were stained with Annexin V and propidium iodide according to the manufacturer's recommendations. The cells were analyzed for live (Annexin V negative and propidium iodide negative), early apoptotic (Annexin V positive and propidium iodide negative), late apoptotic (Annexin V positive and propidium iodide positive), and necrotic cells (Annexin V negative and propidium iodide positive) using a FACSCalibur flow cytometer (BD Biosciences, San Jose, CA, USA). The analysis was performed using Flowing Software 2 (Perttu Terho, Turku Centre for Biotechnology, Finland).

4.9. Flow Cytometry Analysis of Ovarian Cancer Cell Lines

In order to determine the effect of HATMSC2-MVs on the phenotype of ovarian cancer cell lines, flow cytometry analysis was performed. ES-2 and OAW-42 cells were treated for 72 h with MVs at a ratio of 10:1. ES-2 and OAW-42 cells were seeded in a 6-well plate at a density of 6 x 10^4 per well

in the DMEM + 10% FBS and OptiMEM GlutaMax + 3% FBS media (mixed in equal proportions). MVs were added to the cells at a ratio of 10:1. ES-2 and OAW-42 cells without MVs were used as a control. After 72 h, the cells were washed with PBS, and the culture medium was replaced with DMEM without FBS. Following a subsequent 24 h of culture in DMEM without FBS, the cells were detached using the trypsin/EDTA solution and incubated with PE-conjugated antibodies specific for the human CD34 (clone 8G12), CD44 (clone 515), CD133 (clone W6B3C1), CD73 (clone AD2), CD90 (clone 5E10), and CD105 (clone 266) molecules and the PerCP-Cy5.5—SSEA4 antibody (clone MC813-70) (all from BD Biosciences, San Jose, CA, USA) and with the appropriate isotype controls (BD Biosciences, San Jose, CA, USA) for 30 min at 4 °C. Afterwards, the labeled cells were washed with PBS (IIET, Wroclaw, Poland) and analyzed using a FACSCalibur flow cytometer (BD Biosciences, San Jose, CA, USA). The obtained data were processed using the CellQuest software (BD Biosciences, San Jose, CA, USA). The histograms were created using Flowing Software 2 (Perttu Terho, Turku Centre for Biotechnology, Finland).

4.10. Secretion Profiles of Ovarian Cancer Cell Lines

In order to determine the effect of HATMSC2-MVs on the secretion profiles of ovarian cancer cell lines, a C-Series Human Cytokine Antibody Array C1000 (RayBio®, Norcross, GA, USA) was used. ES-2 and OAW-42 cells were seeded in a 6-well plate at a density of 6×10^4 per well in the DMEM + 10% FBS and OptiMEM GlutaMax + 3% FBS media (mixed in equal proportions). MVs were added to the cells at a ratio of 100:1. The ES-2 and OAW-42 cells without MVs were used as a control. After 72 h, the cells were washed with PBS, and the culture medium was replaced with DMEM without FBS. Following the subsequent 24 h of culture in DMEM without FBS, the conditioned medium was collected and centrifuged for 10 min at 300× *g* to remove cellular debris, and the cells were used for flow cytometry analysis (see 4.9. Briefly, 2 mL of blocking buffer were applied onto the membrane and incubated for 30 min at room temperature. Next, 2 mL of the supernatant collected from the control and treated cells were incubated with the membrane overnight at 4 °C. Following a series of washes, a biotinylated antibody cocktail was applied onto the membrane and incubated for 2 h at room temperature. Unbound antibodies were removed with a series of washes, and the membrane was placed in HRP-streptavidin and incubated for 2 h at room temperature. Following a third series of washes, chemiluminescence was detected, and the bound proteins were visualized using an X-ray film. Signal intensities were compared using the ImageJ software (MosaicJ, Philippe Thevenaz): relative differences in the expression levels of each analyzed sample were measured and normalized to the intensities of the positive control using the Protein Array Analyzer plugin. The obtained data were analyzed automatically using the Microsoft® Excel-based Analysis Software Tool for Human Cytokine Antibody Array C1000. The results were calculated as a percentage of expression, with positive control set to 100% and negative control set to 0% (relative expression). The threshold was set to 10%. All results equal to or above 10% were considered as real expression.

4.11. Statistical Analysis

All statistical analyses were performed using GraphPad Prism version 7 (GraphPad Software Inc., San Diego, CA, USA). The data were compared using the one-way ANOVA test with Dunnett's multiple comparison. All results are presented as mean ± SEM values.

Author Contributions: Conceptualization, A.K. (Aleksandra Klimczak) and A.S.; methodology, A.S., A.B.-P., A.K. (Agnieszka Krawczenko), M.P., O.D. and A.K. (Aleksandra Klimczak); formal analysis, A.S., A.B.-P. and A.K. (Aleksandra Klimczak); investigation, A.S., A.B.-P., A.K. (Agnieszka Krawczenko) and O.D.; data curation, A.S., A.B.-P. and A.K. (Aleksandra Klimczak); visualization, A.S. and O.D.; supervision, A.K. (Aleksandra Klimczak); funding acquisition, A.K. (Aleksandra Klimczak); writing—original draft preparation, A.S. and A.B.-P.; writing—review and editing, A.K. (Aleksandra Klimczak). All authors have read and agreed to the published version of the manuscript.

Funding: This research was funded with the internal funds of the Hirszfeld Institute of Immunology and Experimental Therapy PAS in Poland. No. 501-20.

Acknowledgments: The authors are grateful to Sylwia Nowak and Krzysztof Pawlik from the Hirszfeld Institute of Immunology and Experimental Therapy, Polish Academy of Sciences, for their support in analyzing the MVs using transmission electron microscopy.

Conflicts of Interest: The authors declare no conflict of interest.

Abbreviations

ATMSC	Adipose tissue-derived mesenchymal stem cell
BM-MSC	Bone marrow -derived mesenchymal stem cell
CSC	Cancer stem cells
DMEM	Dulbecco's modified Eagle's medium
EGF	Epidermal growth factor
FBS	Fetal bovine serum
FGF	Fibroblast growth factor
FITC	Fluorescein isothiocyanate
GRO	Growth- regulated oncogene, CXCL1 chemokine
HATMSC	Human adipose tissue mesenchymal stem cell line
IL	Interleukin
MCP-1	Macrophage chemoattractant protein-1, CCL2 chemokine
MVs	Microvesicles
MTT	(3-(4,5-Dimetylthiazol-2-yl)-2,5-Diphenyltetrazolium Bromide
PE	Phycoerythrin
RANTES	Regulated on Activation, Normal T Cell Expressed and Secreted, CCL5 chemokine
SSEA4	Stage Specific Embryonic Antigen 4
UC-MSC	Umbilical cord -derived mesenchymal stem cell
VEGF	Vascular endothelial growth factor

References

1. Al-Alem, L.F.; Pandya, U.M.; Baker, A.T.; Bellio, C.; Zarrella, B.D.; Clark, J.; DiGloria, C.M.; Rueda, B.R. Ovarian cancer stem cells: What progress have we made? *Int. J. Biochem. Cell Biol.* **2019**, *107*, 92–103. [CrossRef] [PubMed]
2. Cortez, A.J.; Tudrej, P.; Kujawa, K.A.; Lisowska, K.M. Advances in ovarian cancer therapy. *Cancer Chemother. Pharmacol.* **2018**, *81*, 17–38. [CrossRef] [PubMed]
3. Bregenzer, M.E.; Horst, E.N.; Mehta, P.; Novak, C.M.; Repetto, T.; Mehta, G. The Role of Cancer Stem Cells and Mechanical Forces in Ovarian Cancer Metastasis. *Cancers* **2019**, *11*, 1008. [CrossRef] [PubMed]
4. Keating, A. Mesenchymal stromal cells. *Curr. Opin. Hematol.* **2006**, *13*, 419–425. [CrossRef] [PubMed]
5. Klimczak, A.; Kozlowska, U. Mesenchymal Stromal Cells and Tissue-Specific Progenitor Cells: Their Role in Tissue Homeostasis. *Stem Cells Int.* **2016**, *2016*, 4285215. [CrossRef] [PubMed]
6. Kozlowska, U.; Krawczenko, A.; Futoma, K.; Jurek, T.; Rorat, M.; Patrzalek, D.; Klimczak, A. Similarities and differences between mesenchymal stem/progenitor cells derived from various human tissues. *World J. Stem Cells* **2019**, *11*, 347–374. [CrossRef]
7. Hass, R.; Kasper, C.; Bohm, S.; Jacobs, R. Different populations and sources of human mesenchymal stem cells (MSC): A comparison of adult and neonatal tissue-derived MSC. *Cell Commun. Signal.* **2011**, *9*, 12. [CrossRef]
8. Varderidou-Minasian, S.; Lorenowicz, M.J. Mesenchymal stromal/stem cell-derived extracellular vesicles in tissue repair: Challenges and opportunities. *Theranostics* **2020**, *10*, 5979–5997. [CrossRef]
9. Camussi, G.; Deregibus, M.C.; Bruno, S.; Cantaluppi, V.; Biancone, L. Exosomes/microvesicles as a mechanism of cell-to-cell communication. *Kidney Int.* **2010**, *78*, 838–848. [CrossRef]
10. Nawaz, M.; Fatima, F.; Vallabhaneni, K.C.; Penfornis, P.; Valadi, H.; Ekstrom, K.; Kholia, S.; Whitt, J.D.; Fernandes, J.D.; Pochampally, R.; et al. Extracellular Vesicles: Evolving Factors in Stem Cell Biology. *Stem Cells Int.* **2016**, *2016*, 1073140. [CrossRef]
11. Bobis-Wozowicz, S.; Kmiotek, K.; Sekula, M.; Kedracka-Krok, S.; Kamycka, E.; Adamiak, M.; Jankowska, U.; Madetko-Talowska, A.; Sarna, M.; Bik-Multanowski, M.; et al. Human Induced Pluripotent Stem Cell-Derived Microvesicles Transmit RNAs and Proteins to Recipient Mature Heart Cells Modulating Cell Fate and Behavior. *Stem Cells* **2015**, *33*, 2748–2761. [CrossRef] [PubMed]

12. Albini, A.; Sporn, M.B. The tumour microenvironment as a target for chemoprevention. *Nat. Rev. Cancer* **2007**, *7*, 139–147. [CrossRef] [PubMed]
13. Du, T.; Ju, G.; Wu, S.; Cheng, Z.; Cheng, J.; Zou, X.; Zhang, G.; Miao, S.; Liu, G.; Zhu, Y. Microvesicles derived from human Wharton's jelly mesenchymal stem cells promote human renal cancer cell growth and aggressiveness through induction of hepatocyte growth factor. *PLoS ONE* **2014**, *9*, e96836. [CrossRef] [PubMed]
14. Reza, A.; Choi, Y.J.; Yasuda, H.; Kim, J.H. Human adipose mesenchymal stem cell-derived exosomal-miRNAs are critical factors for inducing anti-proliferation signalling to A2780 and SKOV-3 ovarian cancer cells. *Sci. Rep.* **2016**, *6*, 38498. [CrossRef]
15. Lindoso, R.S.; Collino, F.; Vieyra, A. Extracellular vesicles as regulators of tumor fate: Crosstalk among cancer stem cells, tumor cells and mesenchymal stem cells. *Stem Cell Investig.* **2017**, *4*, 75. [CrossRef]
16. Kraskiewicz, H.; Paprocka, M.; Bielawska-Pohl, A.; Krawczenko, A.; Panek, K.; Kaczynska, J.; Szyposzynska, A.; Psurski, M.; Kuropka, P.; Klimczak, A. Can supernatant from immortalized adipose tissue MSC replace cell therapy? An in vitro study in chronic wounds model. *Stem Cell Res. Ther.* **2020**, *11*, 29. [CrossRef]
17. Whiteside, T.L. Exosome and mesenchymal stem cell cross-talk in the tumor microenvironment. *Semin. Immunol.* **2018**, *35*, 69–79. [CrossRef]
18. Bruno, S.; Collino, F.; Deregibus, M.C.; Grange, C.; Tetta, C.; Camussi, G. Microvesicles derived from human bone marrow mesenchymal stem cells inhibit tumor growth. *Stem Cells Dev.* **2013**, *22*, 758–771. [CrossRef]
19. Dong, L.; Pu, Y.; Zhang, L.; Qi, Q.; Xu, L.; Li, W.; Wei, C.; Wang, X.; Zhou, S.; Zhu, J.; et al. Human umbilical cord mesenchymal stem cell-derived extracellular vesicles promote lung adenocarcinoma growth by transferring miR-410. *Cell Death Dis.* **2018**, *9*, 218. [CrossRef]
20. Kalamegam, G.; Sait, K.H.W.; Ahmed, F.; Kadam, R.; Pushparaj, P.N.; Anfinan, N.; Rasool, M.; Jamal, M.S.; Abu-Elmagd, M.; Al-Qahtani, M. Human Wharton's Jelly Stem Cell (hWJSC) Extracts Inhibit Ovarian Cancer Cell Lines OVCAR3 and SKOV3 in vitro by Inducing Cell Cycle Arrest and Apoptosis. *Front. Oncol.* **2018**, *8*, 592. [CrossRef]
21. Khalil, C.; Moussa, M.; Azar, A.; Tawk, J.; Habbouche, J.; Salameh, R.; Ibrahim, A.; Alaaeddine, N. Anti-proliferative effects of mesenchymal stem cells (MSCs) derived from multiple sources on ovarian cancer cell lines: An in-vitro experimental study. *J. Ovarian Res.* **2019**, *12*, 70. [CrossRef] [PubMed]
22. Lisio, M.A.; Fu, L.; Goyeneche, A.; Gao, Z.H.; Telleria, C. High-Grade Serous Ovarian Cancer: Basic Sciences, Clinical and Therapeutic Standpoints. *Int. J. Mol. Sci.* **2019**, *20*, 952. [CrossRef] [PubMed]
23. Stronach, E.A.; Cunnea, P.; Turner, C.; Guney, T.; Aiyappa, R.; Jeyapalan, S.; de Sousa, C.H.; Browne, A.; Magdy, N.; Studd, J.B.; et al. The role of interleukin-8 (IL-8) and IL-8 receptors in platinum response in high grade serous ovarian carcinoma. *Oncotarget* **2015**, *6*, 31593–31603. [CrossRef]
24. Browne, A.; Sriraksa, R.; Guney, T.; Rama, N.; Van Noorden, S.; Curry, E.; Gabra, H.; Stronach, E.; El-Bahrawy, M. Differential expression of IL-8 and IL-8 receptors in benign, borderline and malignant ovarian epithelial tumours. *Cytokine* **2013**, *64*, 413–421. [CrossRef] [PubMed]
25. Matte, I.; Lane, D.; Laplante, C.; Rancourt, C.; Piche, A. Profiling of cytokines in human epithelial ovarian cancer ascites. *Am. J. Cancer Res.* **2012**, *2*, 566–580. [PubMed]
26. Coward, J.; Kulbe, H.; Chakravarty, P.; Leader, D.; Vassileva, V.; Leinster, D.A.; Thompson, R.; Schioppa, T.; Nemeth, J.; Vermeulen, J.; et al. Interleukin-6 as a therapeutic target in human ovarian cancer. *Clin. Cancer Res.* **2011**, *17*, 6083–6096. [CrossRef]
27. Huang, S.; Robinson, J.B.; Deguzman, A.; Bucana, C.D.; Fidler, I.J. Blockade of nuclear factor-kappaB signaling inhibits angiogenesis and tumorigenicity of human ovarian cancer cells by suppressing expression of vascular endothelial growth factor and interleukin 8. *Cancer Res.* **2000**, *60*, 5334–5339.
28. Yung, M.M.; Tang, H.W.; Cai, P.C.; Leung, T.H.; Ngu, S.F.; Chan, K.K.; Xu, D.; Yang, H.; Ngan, H.Y.; Chan, D.W. GRO-alpha and IL-8 enhance ovarian cancer metastatic potential via the CXCR2-mediated TAK1/NFkappaB signaling cascade. *Theranostics* **2018**, *8*, 1270–1285. [CrossRef]
29. Long, H.; Xie, R.; Xiang, T.; Zhao, Z.; Lin, S.; Liang, Z.; Chen, Z.; Zhu, B. Autocrine CCL5 signaling promotes invasion and migration of CD133+ ovarian cancer stem-like cells via NF-kappaB-mediated MMP-9 upregulation. *Stem Cells* **2012**, *30*, 2309–2319. [CrossRef]

30. Furukawa, S.; Soeda, S.; Kiko, Y.; Suzuki, O.; Hashimoto, Y.; Watanabe, T.; Nishiyama, H.; Tasaki, K.; Hojo, H.; Abe, M.; et al. MCP-1 promotes invasion and adhesion of human ovarian cancer cells. *Anticancer Res.* **2013**, *33*, 4785–4790.
31. Heilmann, T.; Vondung, F.; Borzikowsky, C.; Szymczak, S.; Kruger, S.; Alkatout, I.; Wenners, A.; Bauer, M.; Klapper, W.; Rocken, C.; et al. Heterogeneous intracellular TRAIL-receptor distribution predicts poor outcome in breast cancer patients. *J. Mol. Med.* **2019**, *97*, 1155–1167. [CrossRef] [PubMed]
32. Abdollahi, T. Potential for TRAIL as a therapeutic agent in ovarian cancer. *Vitam. Horm.* **2004**, *67*, 347–364. [PubMed]
33. Braga Lda, C.; Alvares da Silva Ramos, A.P.; Traiman, P.; Silva, L.M.; Lopes da Silva-Filho, A. TRAIL-R3-related apoptosis: Epigenetic and expression analyses in women with ovarian neoplasia. *Gynecol. Oncol.* **2012**, *126*, 268–273. [CrossRef] [PubMed]
34. Ke, C.; Hou, H.; Li, J.; Su, K.; Huang, C.; Lin, Y.; Lu, Z.; Du, Z.; Tan, W.; Yuan, Z. Extracellular Vesicle Delivery of TRAIL Eradicates Resistant Tumor Growth in Combination with CDK Inhibition by Dinaciclib. *Cancers* **2020**, *12*, 1157. [CrossRef]
35. Kalamegam, G.; Sait, K.H.W.; Anfinan, N.; Kadam, R.; Ahmed, F.; Rasool, M.; Naseer, M.I.; Pushparaj, P.N.; Al-Qahtani, M. Cytokines secreted by human Wharton's jelly stem cells inhibit the proliferation of ovarian cancer (OVCAR3) cells in vitro. *Oncol. Lett.* **2019**, *17*, 4521–4531. [CrossRef]
36. Lewis, A.M.; Varghese, S.; Xu, H.; Alexander, H.R. Interleukin-1 and cancer progression: The emerging role of interleukin-1 receptor antagonist as a novel therapeutic agent in cancer treatment. *J. Transl. Med.* **2006**, *4*, 48. [CrossRef]
37. Green, D.S.; Husain, S.R.; Johnson, C.L.; Sato, Y.; Han, J.; Joshi, B.; Hewitt, S.M.; Puri, R.K.; Zoon, K.C. Combination immunotherapy with IL-4 Pseudomonas exotoxin and IFN-alpha and IFN-gamma mediate antitumor effects in vitro and in a mouse model of human ovarian cancer. *Immunotherapy* **2019**, *11*, 483–496. [CrossRef]
38. Tudrej, P.; Olbryt, M.; Zembala-Nozynska, E.; Kujawa, K.A.; Cortez, A.J.; Fiszer-Kierzkowska, A.; Piglowski, W.; Nikiel, B.; Glowala-Kosinska, M.; Bartkowska-Chrobok, A.; et al. Establishment and Characterization of the Novel High-Grade Serous Ovarian Cancer Cell Line OVPA8. *Int. J. Mol. Sci.* **2018**, *19*, 2080. [CrossRef]
39. Bai, S.; Zhu, W.; Coffman, L.; Vlad, A.; Schwartz, L.E.; Elishaev, E.; Drapkin, R.; Buckanovich, R.J. CD105 Is Expressed in Ovarian Cancer Precursor Lesions and Is Required for Metastasis to the Ovary. *Cancers* **2019**, *11*, 1710. [CrossRef]
40. Chen, W.C.; Hsu, H.P.; Li, C.Y.; Yang, Y.J.; Hung, Y.H.; Cho, C.Y.; Wang, C.Y.; Weng, T.Y.; Lai, M.D. Cancer stem cell marker CD90 inhibits ovarian cancer formation via beta3 integrin. *Int. J. Oncol.* **2016**, *49*, 1881–1889. [CrossRef]
41. Lupia, M.; Angiolini, F.; Bertalot, G.; Freddi, S.; Sachsenmeier, K.F.; Chisci, E.; Kutryb-Zajac, B.; Confalonieri, S.; Smolenski, R.T.; Giovannoni, R.; et al. CD73 Regulates Stemness and Epithelial-Mesenchymal Transition in Ovarian Cancer-Initiating Cells. *Stem Cell Rep.* **2018**, *10*, 1412–1425. [CrossRef] [PubMed]
42. Turcotte, M.; Spring, K.; Pommey, S.; Chouinard, G.; Cousineau, I.; George, J.; Chen, G.M.; Gendoo, D.M.; Haibe-Kains, B.; Karn, T.; et al. CD73 is associated with poor prognosis in high-grade serous ovarian cancer. *Cancer Res.* **2015**, *75*, 4494–4503. [CrossRef] [PubMed]
43. Zhang, J.; Yuan, B.; Zhang, H.; Li, H. Human epithelial ovarian cancer cells expressing CD105, CD44 and CD106 surface markers exhibit increased invasive capacity and drug resistance. *Oncol. Lett.* **2019**, *17*, 5351–5360. [CrossRef] [PubMed]
44. Christodoulou, I.; Goulielmaki, M.; Devetzi, M.; Panagiotidis, M.; Koliakos, G.; Zoumpourlis, V. Mesenchymal stem cells in preclinical cancer cytotherapy: A systematic review. *Stem Cell Res. Ther.* **2018**, *9*, 336. [CrossRef] [PubMed]
45. Krawczenko, A.; Bielawska-Pohl, A.; Paprocka, M.; Kraskiewicz, H.; Szyposzynska, A.; Wojdat, E.; Klimczak, A. Microvesicles from Human Immortalized Cell Lines of Endothelial Progenitor Cells and Mesenchymal Stem/Stromal Cells of Adipose Tissue Origin as Carriers of Bioactive Factors Facilitating Angiogenesis. *Stem Cells Int.* **2020**, *2020*, 1289380. [CrossRef] [PubMed]
46. Witwer, K.W.; Buzas, E.I.; Bemis, L.T.; Bora, A.; Lasser, C.; Lotvall, J.; Nolte-'t Hoen, E.N.; Piper, M.G.; Sivaraman, S.; Skog, J.; et al. Standardization of sample collection, isolation and analysis methods in extracellular vesicle research. *J. Extracell. Vesicles* **2013**, *2*. [CrossRef]

47. Adamiak, M.; Cheng, G.; Bobis-Wozowicz, S.; Zhao, L.; Kedracka-Krok, S.; Samanta, A.; Karnas, E.; Xuan, Y.T.; Skupien-Rabian, B.; Chen, X.; et al. Induced Pluripotent Stem Cell (iPSC)-Derived Extracellular Vesicles Are Safer and More Effective for Cardiac Repair Than iPSCs. *Circ. Res.* **2018**, *122*, 296–309. [CrossRef]
48. Matuszyk, J.; Cebrat, M.; Kalas, W.; Strzadala, L. HA1004, an inhibitor of serine/threonine protein kinases, restores the sensitivity of thymic lymphomas to Ca^{2+}-mediated apoptosis through a protein kinase A-independent mechanism. *Int. Immunopharmacol.* **2002**, *2*, 435–442. [CrossRef]

International Journal of
Molecular Sciences

MDPI

Article

Mesenchymal Stem Cell Microvesicles from Adipose Tissue: Unraveling Their Impact on Primary Ovarian Cancer Cells and Their Therapeutic Opportunities

Agnieszka Szyposzynska [1], Aleksandra Bielawska-Pohl [1], Marek Murawski [2], Rafal Sozanski [2], Grzegorz Chodaczek [3] and Aleksandra Klimczak [1,*]

[1] Laboratory of Biology of Stem and Neoplastic Cells, Hirszfeld Institute of Immunology and Experimental Therapy, Polish Academy of Sciences, 53-114 Wroclaw, Poland; agnieszka.szyposzynska@hirszfeld.pl (A.S.); aleksandra.bielawska-pohl@hirszfeld.pl (A.B.-P.)
[2] 1st Department of Gynecology and Obstetrics, Wroclaw Medical University, 50-599 Wroclaw, Poland; marek.murawski@umw.edu.pl (M.M.); rafal.sozanski@umw.edu.pl (R.S.)
[3] Bioimaging Laboratory, Łukasiewicz Research Network-PORT Polish Center for Technology Development, 54-066 Wroclaw, Poland; grzegorz.chodaczek@port.lukasiewicz.gov.pl
* Correspondence: aleksandra.klimczak@hirszfeld.pl

Abstract: Mesenchymal stem cells (MSCs) and their derivatives can be promising tools in oncology including ovarian cancer treatment. This study aimed to determine the effect of HATMSC2-MVs (microvesicles derived from human immortalized mesenchymal stem cells of adipose tissue origin) on the fate and behavior of primary ovarian cancer cells. Human primary ovarian cancer (OvCa) cells were isolated from two sources: post-operative tissue of ovarian cancer and ascitic fluid. The phenotype of cells was characterized using flow cytometry, real-time RT-PCR, and immunofluorescence staining. The effect of HATMSC2-MVs on the biological activity of primary cells was analyzed in 2D (proliferation, migration, and cell survival) and 3D (cell survival) models. We demonstrated that HATMSC2-MVs internalized into primary ovarian cancer cells decrease the metabolic activity and induce the cancer cell death and are leading to decreased migratory activity of tumor cells. The results suggests that the anti-cancer effect of HATMSC2-MVs, with high probability, is contributed by the delivery of molecules that induce cell cycle arrest and apoptosis (p21, tumor suppressor p53, executor caspase 3) and proapoptotic regulators (bad, BIM, Fas, FasL, p27, TRAIL-R1, TRAIL-R2), and their presence has been confirmed by apoptotic protein antibody array. In this study, we demonstrate the ability to inhibit primary OvCa cells growth and apoptosis induction after exposure of OvCa cells on HATMSC2-MVs treatment; however, further studies are needed to clarify their anticancer activities.

Keywords: ovarian cancer; primary ovarian cancer cells; mesenchymal stem cells; extracellular vesicles; MSC-microvesicles

Citation: Szyposzynska, A.; Bielawska-Pohl, A.; Murawski, M.; Sozanski, R.; Chodaczek, G.; Klimczak, A. Mesenchymal Stem Cell Microvesicles from Adipose Tissue: Unraveling Their Impact on Primary Ovarian Cancer Cells and Their Therapeutic Opportunities. *Int. J. Mol. Sci.* **2023**, *24*, 15862. https://doi.org/10.3390/ijms242115862

Academic Editor: Maria Grazia Cifone

Received: 7 October 2023
Revised: 29 October 2023
Accepted: 30 October 2023
Published: 1 November 2023

1. Introduction

Ovarian cancer (OvCa) is the global seventh most common cancer in women and eighth most common cause of death from cancer in women worldwide (International Agency for Research on Cancer, World Health Organization [1]. OvCa includes a heterogeneous group of malignancies that differ in etiology, cell of origin, phenotype, pathological grade, risk factors, prognosis, response to therapy, and numerous other characteristics [2]. Depending on the cellular origin, OvCa are divided into epithelial and non-epithelial subtypes. Epithelial cancers are most common, account for about 90% of OvCa, and are classified by tumor cell histology as: serous (52%), endometroid (10%), mucinous (6%), clear cell carcinoma (6%), and other miscellaneous and more rare subtypes [2]. Based on clinicopathologic features, epithelial carcinomas are classified into two subtypes: Type I, unilateral, considered as low-grade with good prognosis of survival, and Type II representing high-grade malignancies, characterized by involvement of both ovaries, aggressive

behavior, and low rate of survival. The most often diagnosed type of epithelial OvCa is ovarian serous carcinoma; 90% of serous subtypes are classified as high grade, and only 10% are present as low grade. Another type of OvCa is ovarian mucinous carcinoma which consists of benign and malignant cells, and clear cell carcinoma with low proliferative activity [3]. A relatively rare cancer is ovarian cystadenofibroma, which contains two types of cancer cells: epithelial and fibroblast stromal cells [3].

About 5% of patients with OvCa die, and the mortality is associated with advanced stage of tumor due to the postponed examination of diseases and inaccessibility of screening tests. Moreover, at the beginning of the disease's development, none of the signs are observed and the patients are diagnosed at the advanced stages usually with metastasis to distant organs. The choice of OvCa treatment method depends on several factors including classification of cancer, current stage, and the patient's condition and genetic background. The widely used method is chemotherapy followed by surgery or neoadjuvant therapy after surgery [4]. Immunotherapy using a combination of anti-angiogenic drugs, inhibitors of signaling pathways, or vaccines with modified T cells are used in clinical trials of OvCa; however, these approaches are still under experimental procedures [3,5].

Current conventional cancer therapies target cancer cells that are abnormally proliferating; however, these strategies are not fully effective due to the presence of cancer stem cells (CSCs) showing specific biological behavior including high resistance to radio-/chemotherapy and slower proliferation rate that leads to the treatment failure. CSCs represent a rare population of cells in tumors, typically less than one percent. CSCs have similar properties to normal stem cells such as self-renewal, the potential for differentiation, slow proliferation, and activity of aldehyde dehydrogenase 1 (ALDH1) [6]. Moreover, CSCs have features that make them aggressive and resistant to widely used drugs in cancer treatment—especially the ability to migrate from tumor stroma to surrounding tissues, escape from the activity of the immune system, and resistance to pro-apoptotic signals. OvCa stem cells are characterized by the presence of characteristic markers CD133, CD44, CD117 (c-kit), and the activity of ALDH1 [4]. CD133 (Prominin-1) is a glycoprotein involved in different processes such as cellular metabolism, autophagy, and apoptosis. CD133-positive cells in the tumor niche are chemo- and radio-resistant and have higher tumorigenic potential and potential to metastasize compared to cancer cells [7]. Overexpression of CD44 (hyaluronic acid-binding glycoprotein) is observed in different types of tumors [8]. CD117 is a tyrosine kinase receptor that plays a crucial role in signaling pathways responsible for cell proliferation, survival, and migration [9]. ALDH1 is responsible for the oxidation of intracellular aldehydes and directly related to the survival and chemoresistance of CSCs [10,11].

Cancer cells in tumor parenchyma do not exist as self-sustained entities and need for survival a non-neoplastic microenvironment, comprised of a heterogeneous network of different types of cellular and extracellular components including: tumor vasculature, inflammatory cells, tumor-associated fibroblasts, extracellular matrix, and mesenchymal stem/stromal cells [12]. In tumor niches, the most important types of cell-to-cell communication are direct contact between cells, presence of gap junctions, secretion of soluble factors, and release of extracellular vesicles (EVs). Thus, inhibition of the biological activity of cancer cells, including CSCs, would be a promising and beneficial approach in cancer therapy, and one of them is the idea of using cytotherapy with native or modified mesenchymal stem/stromal cells (MSCs) [12].

Mesenchymal stem/stromal cells (MSCs) represent a heterogeneous population of multipotent cells that are present in different adult tissues and contribute to organ homeostasis. Isolated MSCs play an important role in regenerative medicine due to their increased proliferative activity and survival, anti-inflammatory potential, and modulation of the immune system [13]. Moreover, MSCs also release various bioactive molecules in the form of soluble factors, EVs, exosomes, and microvesicles (MVs), which act in the tissue microenvironment as mediators of cell-to-cell communication by exerting paracrine effects [14,15]. It is well

documented that MSCs are recruited to the tumor site, and the tropism of MSCs to tumors has been used as the basis of cancer cytotherapy [12].

Different research reported conflicted results related to the anti-tumorigenic or pro-tumorigenic activity of MSCs and their derivatives in OvCa in vitro and in vivo [16–18]. The co-injection of umbilical cord-derived MSC (UC-MSC) with SKOV-3 (human ovarian adenocarcinoma) cells into NOD/SCID mice leads to an increase in tumor growth compared to SKOV-3 cells injections alone [18]. On the other hand, UC-MSC leads to a reduction in the survival rate of co-cultured ovarian carcinoma cells (CAOV3) [17]. Anti-proliferative and anti-tumor activity of MVs produced by bone marrow-derived MSCs (BM-MSCs) on SKOV3 cell line and in the SCID mice model was reported [16]. It was documented that the biological/therapeutic effect of MSCs in cancer therapy depends on the tissue origin of MSCs, the application of native or genetically modified MSCs, and also on the histological type of OvCa [19,20].

Importantly, MSCs are used in clinical trials not only for OvCa treatment but also in other types of solid tumors. In the completed first stage of the clinical trial (NCT02530047), MSCs isolated from healthy male donors overexpressing interferon β were used for the treatment of advanced epithelial OvCa. The administration of MSCs once a week was performed by intraperitoneal infusion. However, the results are still being analyzed and have not yet been published.

Our recent studies showed that MVs isolated from MSCs of human adipose-tissue origin (HATMSC-MVs) induce apoptosis in the OvCa cell lines OAW-42 and ES-2 [21]. Based on our experience that the transfer of HATMSC-MVs into OvCa cell lines results in inhibition of cells proliferation and apoptosis induction [21], we decided to explore this biological phenomenon on post-operative primary OvCa cells. This study aims to determine the effect of HATMSC-MVs on the biological activity of primary ovarian tumor cells, derived from post-operative tissue of OvCa (post-op. of OvCa) and ascitic fluid, in 2D and 3D models.

2. Results

2.1. Characteristics of Primary Ovarian Cancer Cells

Primary OvCa cells isolated from the post-op. tumor and/or ascitic fluid of 16 patients were characterized for MSCs phenotype (CD73, CD90, CD105), CSCs markers (CD24, CD44, CD133), and hematopoietic stem and progenitor marker (CD34) and leukocyte common antigen (CD45). Evaluation of pluripotency-related markers (Oct4, Sox2, Nanog) and proto-oncogenic transcripts (p53, p21, c-myc) has been performed to assess biological features of examined OvCa cells.

2.1.1. Phenotype of Primary Ovarian Cancer Cells

Flow cytometry analysis for the expression of MSCs markers for OvCa cells of post-op. high-grade serous OvCa (N = 9) revealed that CD73 expression is present on a subpopulation of cells ranging from 2.0% to 90.0% with a median value 82.0%. Similarly, CD90 was detected on cancer cells from 9.0% to 100.0% of the population with a median value of 80.0%, whereas CD105 was present from 4.0% to 85.0% of cancer cells population with a median value of 32.0%. Cancer stem cells markers represented by CD133 expression were present in a broad range from 0.0% to 46.0% with a median value of 0.5%; CD44 from 20.0% to 100.0% (median value 91.0%); and cells with CD24 expression were present from 0.0% to 16.0% (median value 7.0%). Cells expressing hematopoietic stem and progenitor marker CD34 (median value 0.5%) and leukocyte common antigen CD45 (median value 10.0%) were represented occasionally (Figure 1a). The median value of the subpopulation of cells expressing MSCs markers, isolated from corresponding to cancer tissue ascitic fluid (N = 9), was assessed for: CD73 (50.0%), CD90 (78.0%), and CD105 (22.0%). The fraction of cells with CSCs phenotype was represented by CD133 (median 2.0%), CD44 (median 78.0%), and CD24 (median 3.0%) (Figure 1a).

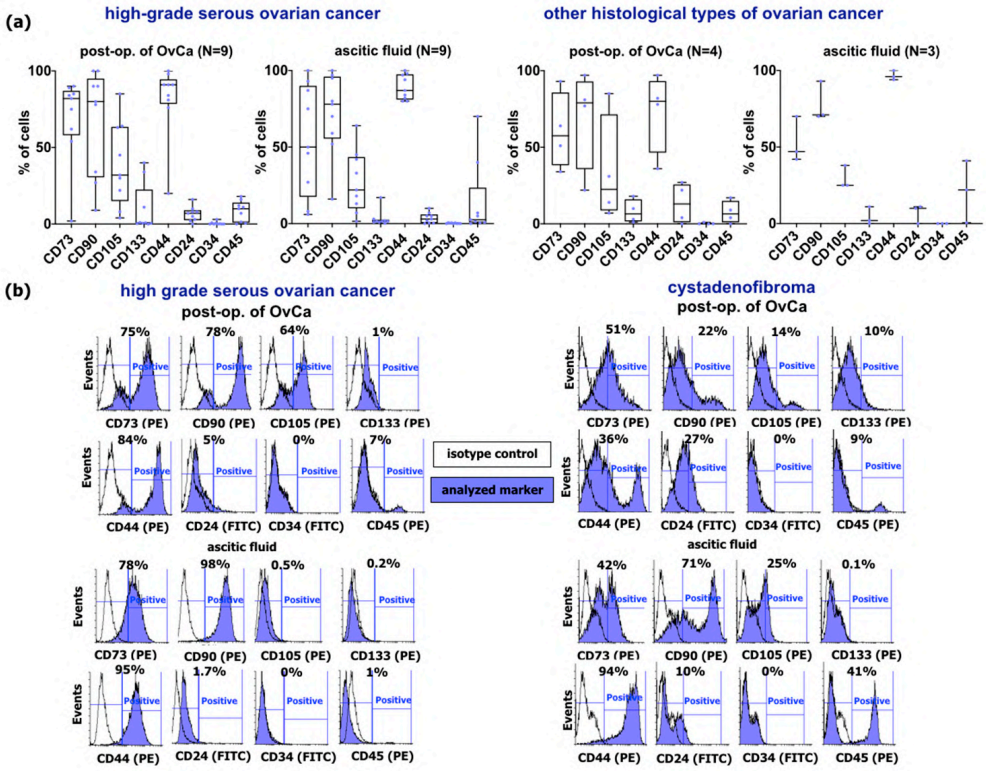

Figure 1. Characteristics of primary OvCa cells from post-op. of OvCa and ascitic fluid. (**a**) Box and whiskers plots show the expression of selected markers by cells from all patients. Cells were stained with selected antibodies conjugated with fluorochromes. Blue dots represent cells from each analyzed patient. Whiskers show minimal and maximal values for each marker. Lines represent the median. The left panel shows plots for cells from high-grade serous OvCa, and the right panel shows plots for cells from other histological types of OvCa. (**b**) Representative histograms of flow cytometry analysis of high-grade serous OvCa (**left** panel) and cystadenofibroma (**right** panel) of OvCa cells from post-operative tumor and ascitic fluid. Blue-filled histograms correspond to cells labeled with defined antibodies, and empty histograms represent the isotype controls. Abbreviations: post-op. of OvCa-post-operative tissue of ovarian cancer.

The analysis of membrane markers performed for cells derived from other histological types of OvCa (N = 4) revealed the subpopulation of CD73-positive cells ranging from 34.0% and 93.0% with a median value of 57.5%. CD105 was detected in a broad range of cells from 7.0% to 85.0% with a median value of 22.5%. The cells isolated from post-op. tissues of other histological types of OvCa also expressed CSCs such as CD133, CD44, and CD24. CD133 expression was present in a subpopulation of cancer cells from 1.1% to 18.0% with a median value of 6.5%; CD44 from 36.0% to 97.0% (median value 80.0%); and cells with CD24 expression consist of 0.0% to 16.0% (median value 7.0%) of the whole population of isolated cancer cells. Moreover, a small fraction of cells was positive for hematopoietic marker CD45 (median value 6.5%), and all isolated cells were negative for CD34.

For cells derived from corresponding to cancer tissue ascitic fluid (N = 3), the positive population of cells with MSCs phenotype CD73, CD90, and CD105 was detected. The median values of positive cancer cells for CD73, CD90, and CD105 were 47.0%, 71.0%, and 25.0% respectively. Importantly, the positive populations for CSCs markers such as CD133, CD44, and CD24 were determined in the whole population of cancer cells. The highest median value was observed for the CD44 marker (96.0%). The median for CD133 and CD24 was up to 10.0% (2.0% and 10.0%, respectively). Moreover, isolated cells were negative for hematopoietic marker CD34; however, a fraction of cells was positive for CD45 (median value 22.0%) (Figure 1a).

Flow cytometry analysis of high-grade serous OvCa and cystadenofibroma, classified in this study to other histological types of OvCa, are illustrated on representative histograms (Figure 1b).

2.1.2. mRNA Expression for Pluripotency-Related, Protooncogenic, and CSCs Markers

The real-time RT-PCR was performed for the expression of pluripotency-related transcripts (*Oct4*, *Sox2*), protooncogenic transcripts (wild-type *p53*, *p21*, *c-myc*), and *CD133* marker on cells derived from 14 patients (Figures 2 and 3).

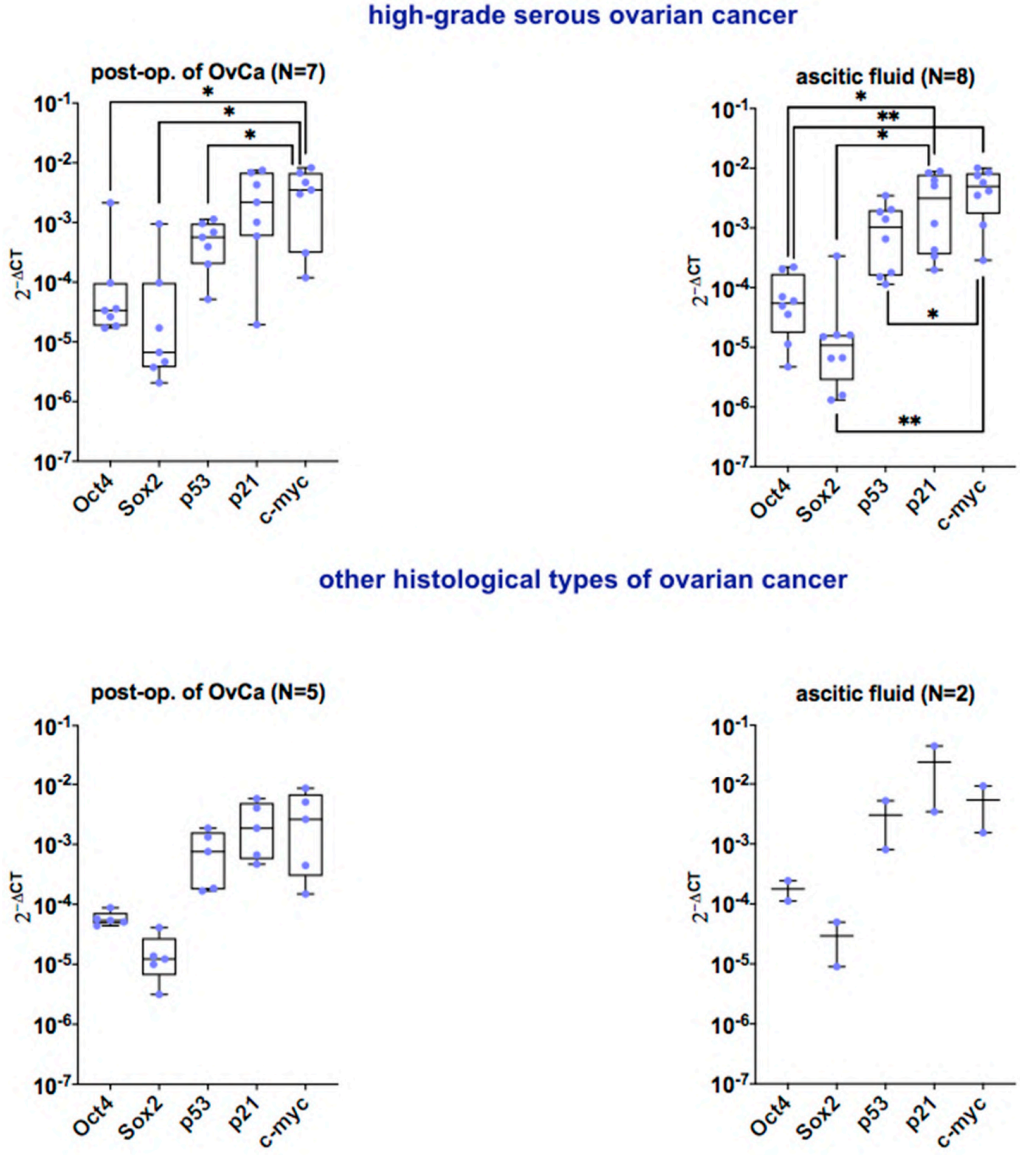

Figure 2. Characteristics of primary OvCa cells from post-op. of OvCa and ascitic fluid. Box and whiskers plots show $2^{-\Delta CT}$ of selected mRNA transcripts in cells from all patients. Blue dots represent cells from each analyzed patient. Box and whiskers plots show minimal and maximal values for each transcript. Lines represent the median. The upper panel shows plots for cells from high-grade serous OvCa, and the lower panel shows plots for cells from other histological types of OvCa. ** $p < 0.01$ and * $p < 0.05$ calculated vs. each marker by one-way ANOVA. For other histological types of ovarian cancer, there were not significant differences between markers. Abbreviations: post-op. of OvCa-post-operative tissue of ovarian cancer.

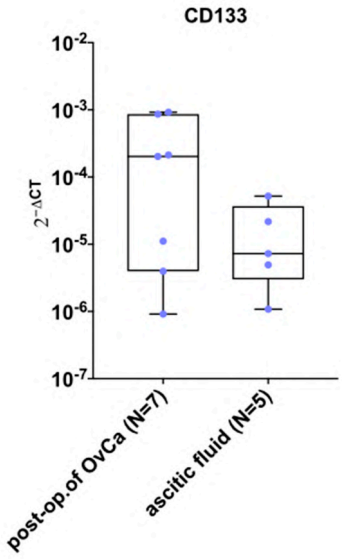

Figure 3. Characteristics of primary OvCa cells from post-op. tissues of OvCa and ascitic fluid. Box and whiskers plot shows expression of CD133 marker by cells from all patients. Blue dots represent cells from each analyzed patient. Whiskers show minimal and maximal values for CD133 marker. Lines represent the median. Abbreviations: post-op. of OvCa-post-operative tissue of ovarian cancer.

The mRNA gene expression for pluripotency markers *Oct4* and *Sox2* in cells was detected (median of $2^{-\Delta CT}$ was 3.35×10^{-5}, and 6.66×10^{-6}, respectively). Moreover, the expression of protooncogenic transcripts wild-type *p53*, *p21*, and *c-myc* was present (median of $2^{-\Delta CT}$ was 5.64×10^{-4}, 2.18×10^{-3}, and 3.51×10^{-3}, respectively). For cells from ascitic fluid of high-grade serous OvCa (N = 8), the expression of *Oct4* and *Sox2* was also observed (median of $2^{-\Delta CT}$ was 5.47×10^{-5} and 1.07×10^{-5}, respectively). The level of protooncogenic markers *p53*, *p21*, and *c-myc* was determined (median of $2^{-\Delta CT}$ was 1.03×10^{-3}, 3.13×10^{-3}, and 4.94×10^{-3}, respectively) (Figure 2).

The same analysis was performed for cells derived from other histological types of OvCa. For cells derived from post-op. tumor of OvCa (N = 5) the expression of pluripotency-related markers *Oct4* and *Sox2* was detected (median of $2^{-\Delta CT}$ was 5.38×10^{-5} and 1.22×10^{-5}, respectively). Also, the proto-oncogenic transcripts *p53*, *p21*, and *c-myc* were determined (median of $2^{-\Delta CT}$ was 7.57×10^{-4}, 1.86×10^{-3}, and 2.62×10^{-3}, respectively). For cells from ascitic fluid (N = 2), the expression of *Oct4* and *Sox2* was also present (median of $2^{-\Delta CT}$ was 1.78×10^{-4} and 2.93×10^{-5}, respectively). Moreover, the expression of proto-oncogenic markers *p53*, *p21*, and *c-myc* was determined at (median of $2^{-\Delta CT}$ was 3.02×10^{-3}, 2.41×10^{-2}, and 5.39×10^{-3}, respectively) (Figure 2).

The mRNA expression of the *CD133* marker was determined in the cells derived from post-op. of OvCa (N = 8) and ascitic fluid (N = 9) from 11 patients. For cells from post-op. tissue of OvCa (N = 7), a median value for $2^{-\Delta CT}$ of *CD133* was 2.02×10^{-4}, while for cells from ascitic fluid (N = 5) was 7.25×10^{-6} (Figure 3). For cells from tumor tissue (N = 2) and ascitic fluid (N = 3), the *CD133* expression was not detectable.

2.1.3. Expression of Membrane Markers and Transcription Factors

Immunofluorescence staining was performed on cells derived from 13 patients for the presence of cancer-associated fibroblasts (CAFs) markers (fibroblasts activation protein—FAP, platelet-derived growth factor receptor alpha—PDGFRα), epithelial to mesenchymal transition (EMT) marker (Snail, vimentin), CSCs markers (ALDH1, c-kit), pluripotency-related markers (Oct4, Sox2, Nanog). Moreover, the cytoskeleton organization including F-actin (actin filaments) and vimentin (intermediate filaments) was analyzed.

For high-grade serous OvCa, the cells from post-op. tumor and ascitic fluid were positive for CD44, and weak expression of CAFs (PDGFRα, FAP) was observed. The cells

were also positive for pluripotency-related markers (Oct4, Sox2, Nanog) and CSCs markers including ALDH1 and c-kit. The expression of F-actin showed the different organization of the cytoskeleton and the presence of filopodia (reach in F-actin) and the stress fibers along the cells. Moreover, the cells expressed vimentin localized around the cell nuclei. For cystadenofibroma, the cells from post-op. tissue and ascitic fluid were positive for CD44, Oct4, Sox2, Nanog, ALDH1, and c-kit. The cells also expressed F-actin and vimentin. Additionally, as cells from high-grade serous OvCa, cystadenofibroma occasionally present weak expression of CAFs markers (PDGFRα, FAP) (Figure 4).

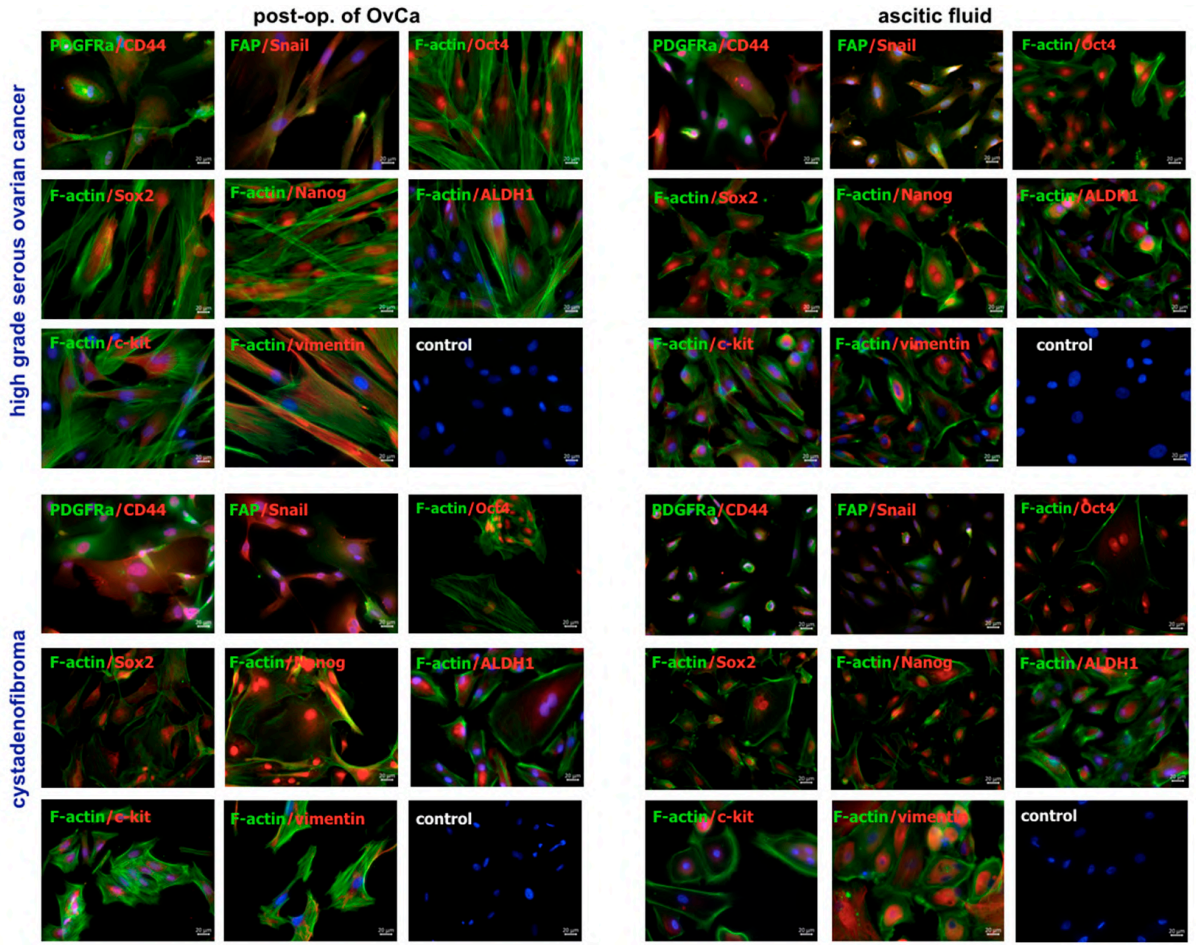

Figure 4. Characteristics of primary OvCa cells from post-op. of OvCa and ascitic fluid. The top panel shows cells from high-grade serous OvCa, bottom panel shows cells from cystadenofibroma. Fluorescence microscopy images: cell nuclei stained with DAPI (blue), selected markers stained with Alexa Fluor 488 (green) or Alexa Fluor 647 (red), F-actin stained with Alexa Fluor 488 phalloidin (green), bars represent 20 μm. Abbreviations: post-op. of OvCa—post-operative tissue of ovarian cancer.

2.2. Internalization of HATMSC2-MVs into Primary Ovarian Cancer Cells

Prior functional tests' internalization of HATMSC2-MVs into primary OvCa cells has been assessed. Internalization of far-red (DiD)-labeled HATMSC2-MVs into green (PDGFRα)-labeled primary OvCa cells after 24 h of co-culture was analyzed using confocal microscopy imaging. DiD-positive HATMSC2-MVs were present in the nuclei and cytoplasm of primary OvCa cells (Figure 5, right and left image). The image on the left shows a full cell volume (in green) with several DiD-labelled vesicles (in red). The right image demonstrates a single vertical section of the same cell proving cytoplasmic presence of the DiD-positive vesicle.

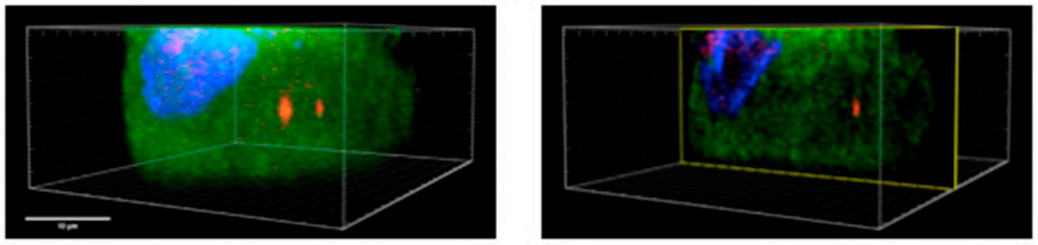

Figure 5. Confocal microscopy imaging of HATMSC2-MVs internalization into primary OvCa cells. Cells treated with HATMSC2-MVs at the ratio 100:1 for 24 h (cell nuclei stained with DAPI in blue, cytoplasmic expression of PDGFRα stained with Alexa Fluor 488 in green, HATMSC2-MVs stained with DiD in red). Bar represents 10 µm. HATMSC2-MVs—microvesicles derived from immortalized human mesenchymal stem cells of adipose tissue origin.

2.3. Effect of HATMSC2-MVs on the Metabolic Activity of Primary Ovarian Cancer Cells

The effect of HATMSC2-MVs on OvCa of metabolic activity, reflecting the proliferation, was determined by MTT assay. The decreased metabolic activity of OvCa cells treated with HATMSC2-MVs at the ratio 100:1 (100 HATMSC2-MVs: 1 OvCa cell) was observed. The untreated cells served as a control. For cells from post-op. tumor of high-grade serous OvCa (N = 9), the median value of relative absorbance at 570 nm on day 0 and day 3 was (0.97 and 0.62, respectively, $p < 0.01$), while for cells from ascitic fluid (N = 8), the median value on day 0 and day 3 was (0.99 and 0.40, respectively, $p < 0.001$). Similar results were observed for cells derived from other histological types of OvCa. For cells from post-op tissue N = 5, the median value on day 0 and day 3 was (0.90 and 0.32, respectively, $p < 0.001$), and for cells from ascitic fluid N = 4, the median on day 0 and day 3 was (0.98 and 0.32, respectively, $p < 0.001$) (Figure 6).

2.4. Effect of HATMSC2-MVs on the Migration Activity of Primary Ovarian Cancer Cells

The migration activity of OvCa cells was assessed using a scratch test. The cells were treated with HATMSC2-MVs at a ratio of 5:1 (5 HATMSC2-MVs: 1 OvCa cell), and the dynamic of scratch closure was evaluated at four time-points up to 28 h (Figure 7a,b). HATMSC2-MVs decreased migratory activity of OvCa cells isolated from post-op. tumor of high-grade serous OvCa as confirmed by the median value of relative wound closure assessed for 0.88 (estimated relative to control untreated cells), while for cells from ascitic fluid, the median was at the control level and revealed 1.06. In contrast, HATMSC2-MVs do not exert inhibitory effect on migration of OvCa cells derived from other histological types of OvCa. For cells from post-op tissue, the median value of relative wound closure was 0.99, while for cells isolated from ascitic fluid, the median was 1.16 (Figure 7c). Representative images from microscopic imaging are presented in Figure 7a,b.

2.5. Effect of HATMSC2-MVs on the Fate of Primary Ovarian Cancer Cells—Survival and Apoptosis

Immunofluorescence staining of OvCa cells allows assessment of live cells stained with Syto 9 (green), dead cells stained with propidium iodide (red), and HATMSC2-MVs stained with DiD (violet). The images acquired by confocal microscopy were processed, and live to dead channel ratio was calculated with Fiji/ImageJ software version 1.54f. For cells from post-op. tumor of high-grade serous OvCa, treated with HATMSC2-MVs, the median value of the relative live/dead ratio was 0.95, while for cells from ascitic fluid, the median value revealed 1.06 (at the control level). Increased live/dead ratio was observed for cells derived from other histological types of OvCa exposed for HATMSC2-MVs. For cells from post-op tissue, the median value was calculated for 1.29, while for cells from ascitic fluid, the median value revealed 1.22 (Figure 8a). Representative images from confocal microscopy are presented in (Figure 8b,c).

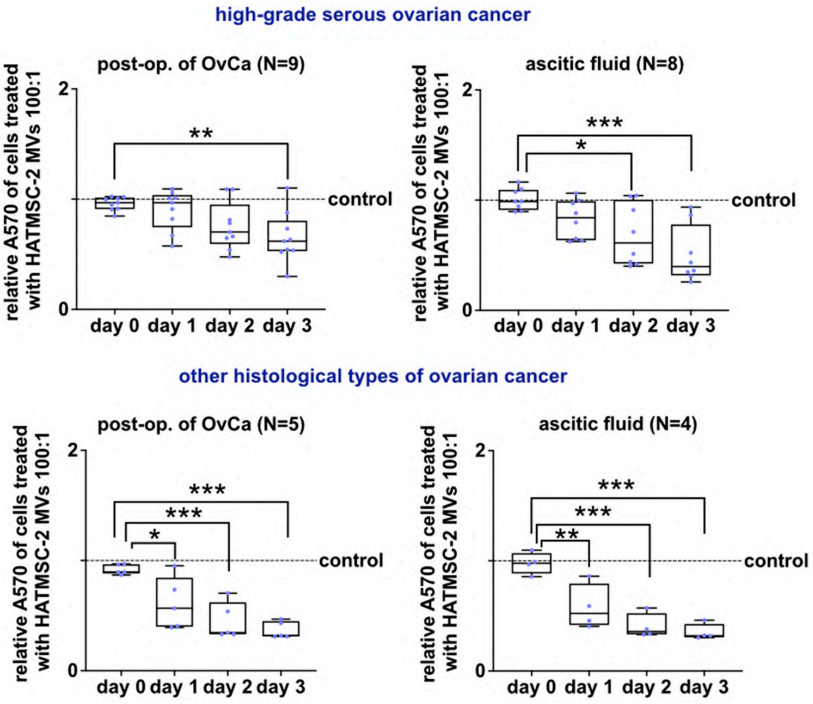

Figure 6. Effect of HATMSC2-MVs on the metabolic activity of primary OvCa cells from post-op. tissue and ascitic fluid. Metabolic activity of primary OvCa cells cultured in standard conditions was assessed using an MTT assay on days 0, 1, 2, and 3 following treatment with HATMSC2-MVs at a ratio of 100:1. Untreated cells without MVs served as a control. Box and whiskers plots show the relative absorbance of cells from all patients treated with HATMSC2-MVs. Blue dots represent cells from each analyzed patient. Whiskers show minimal and maximal values of analyzed cells. Lines represent the median. The top panel shows plots for cells from high-grade serous OvCa, and the bottom panel shows plots for cells from other histological types of OvCa. *** $p < 0.001$, ** $p < 0.01$, * $p < 0.05$ calculated vs. day 0 by one-way ANOVA. Abbreviations: post-op. of OvCa—post-operative tissue of ovarian cancer; HATMSC2-MVs—microvesicles derived from immortalized human mesenchymal stem cells of adipose tissue origin.

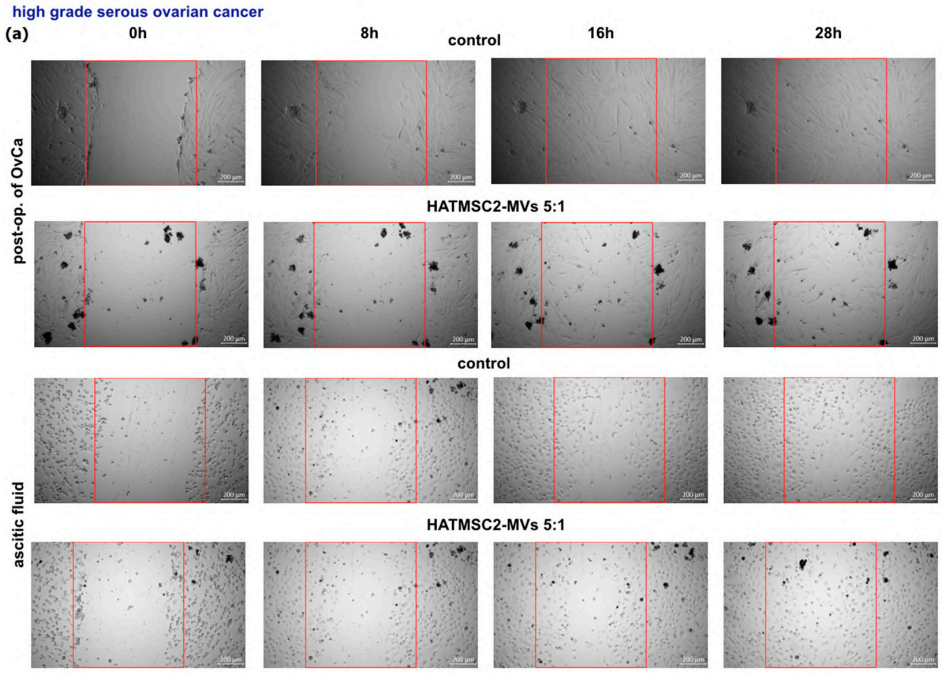

Figure 7. *Cont.*

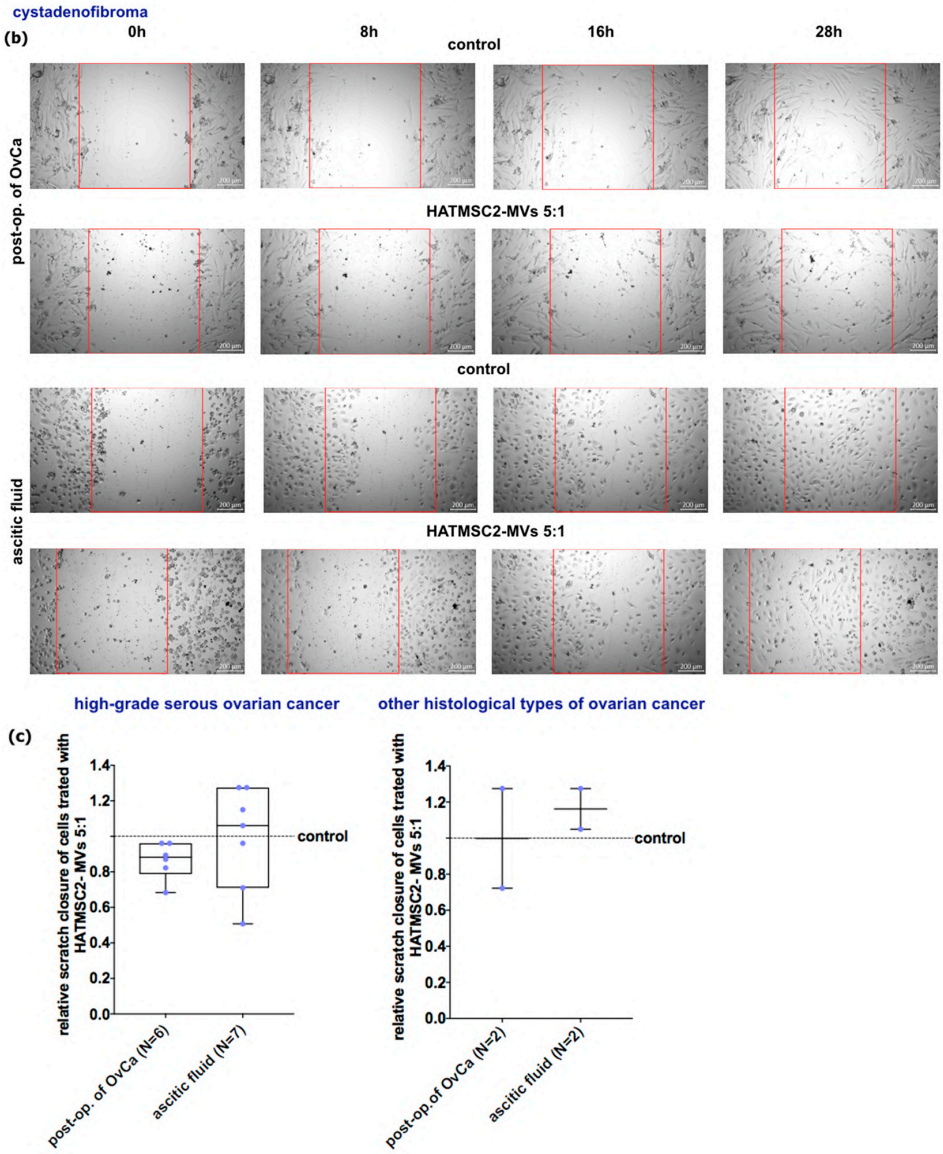

Figure 7. Effect of HATMSC2-MVs on the migration activity of primary OvCa cells from post-op tissues and ascitic fluid. Migration activity of primary OvCa cells cultured in standard conditions was measured using a scratch test following treatment with HATMSC2-MVs at a ratio of 5:1. Untreated cells without MVs served as a control. (**a**) Representative images of scratch closure (measured between the red lines) by cells from patients of high-grade serous OvCa on 0 h, 8 h, 16 h, and 28 h. The top panel shows control and HATMSC2-MVs treated cells from post-op. tumor of OvCa, and the bottom panel shows cells from ascitic fluid. Bars represent 200 µm. (**b**) Representative images of cells from patients with cystadenofibroma on 0 h, 8 h, 16 h, and 28 h. The top panel shows control and HATMSC2-MVs-treated cells from post-operative tumor of OvCa, and the bottom panel shows cells from ascitic fluid. Bars represent 200 µm. (**c**) Box and whiskers plots show relative scratch closure for cells from all samples treated with HATMSC2-MVs. Blue dots represent cells from each analyzed patient. Whiskers show minimal and maximal values for each cell type. Lines represent the median. The left plot shows values for cells from high-grade serous OvCa, and the right plot shows values for cells from other histological types of OvCa. Abbreviations: post-op. of OvCa—post-operative tissue of ovarian cancer. HATMSC2-MVs—microvesicles derived from immortalized human mesenchymal stem cells of adipose tissue origin.

The cell death process was assessed by apoptosis/necrosis assay. The cancer cell survival following treatment with HATMSC2-MVs at the ratio 100:1 was analyzed on cells derived from 12 patients (16 samples) using the flow cytometry method (Figure 9a,b).

The results showed that the percentage of alive cells after treatment with HATMSC2-MVs increased compared to control (median 67.27% vs. 52.00%) in cancer cells derived from two patients (two post-op. of OvCa). Moreover, the percentage of early apoptotic cells (median 16.38% vs. 21.35%) and late apoptotic cells (median 9.87% vs. 18.61%) following treatment decreased compared to untreated cells. The treatment with HATMSC2-MVs also decreased the percentage of necrotic cells compared to the control (median 6.5% vs. 8.03%).

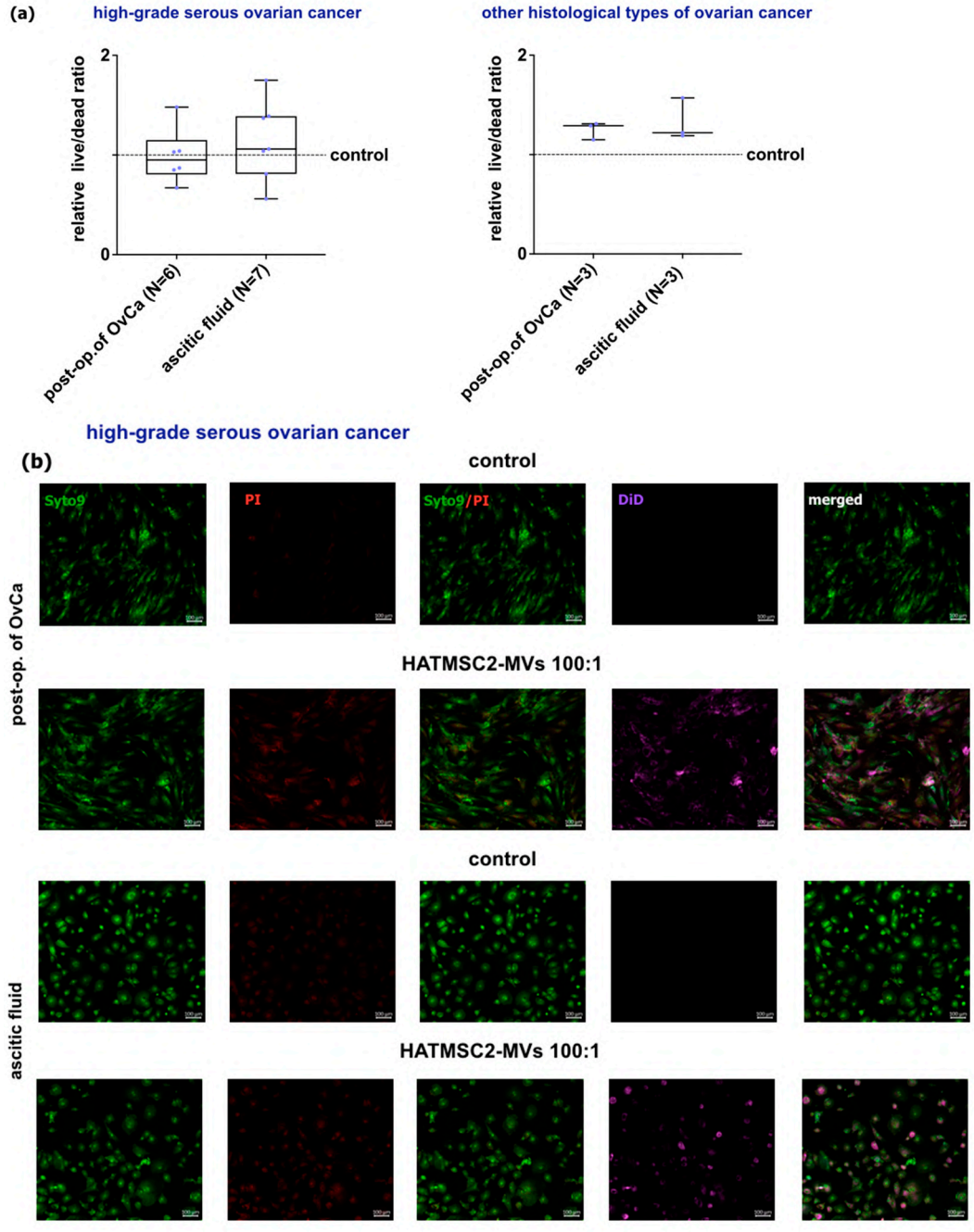

Figure 8. *Cont.*

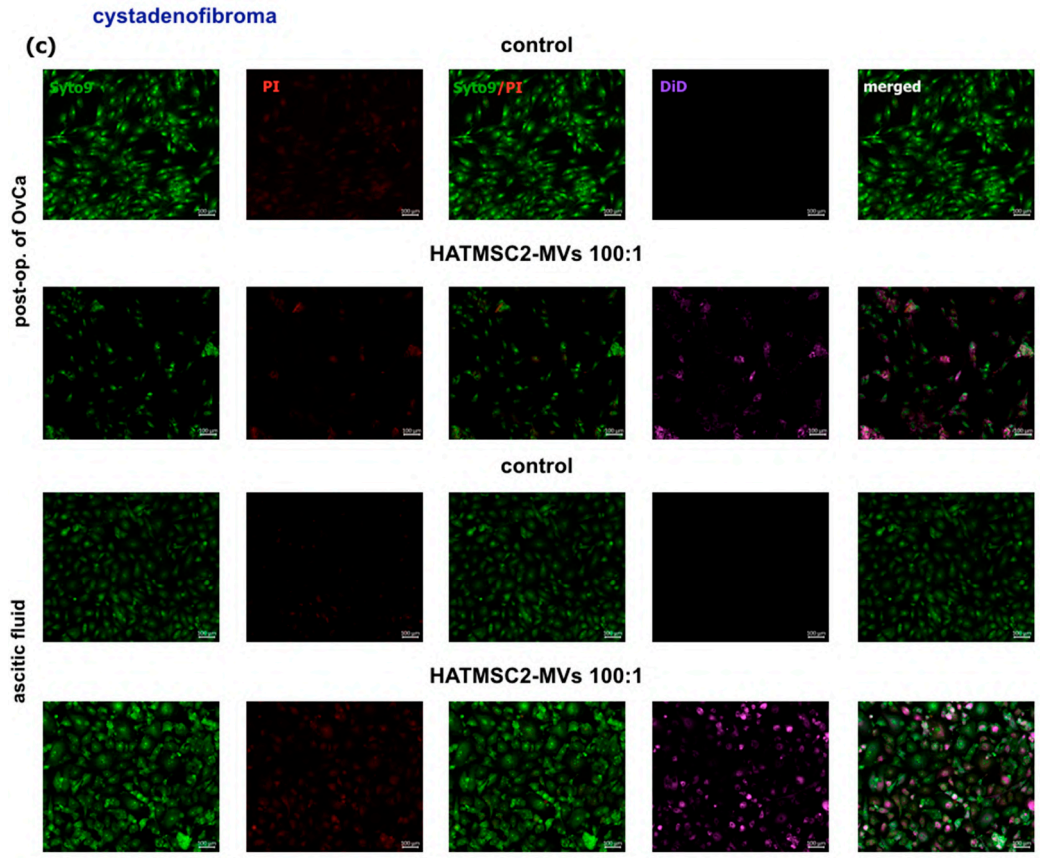

Figure 8. Effect of HATMSC2-MVs on the survival of primary OvCa cells from post-op tissues and ascitic fluid. Survival of cells following treatment with HATMSC2-MVs at a ratio of 100:1 was assessed by confocal microscopy imaging. Untreated cells without MVs served as a control. Live cells stained with Syto 9 (green), dead cells stained with propidium iodide (red), HAT-MSC2-MVs stained with DiD (violet). (**a**) Box and whiskers plots show relative ratio of live to dead channel. Whiskers show minimal and maximal values for each cell type. Lines represent the median. Blue dots represent cells from each analyzed patient. (**b**) Representative confocal microscopy images of cells from high-grade serous OvCa. The top panel shows control and HATMSC2-MVs-treated cells from post-op tumor of OvCa, and the bottom panel shows cells from ascitic fluid. Bars represent 100 µm. (**c**) Representative confocal microscopy images of cells from cystadenofibroma. The top panel shows control and HATMSC2-MVs-treated cells from post-operative OvCa, and the bottom panel shows cells from ascitic fluid. Bars represent 100 µm. Abbreviation: post-op. of OvCa—post-operative tissue of ovarian cancer. HATMSC2-MVs—microvesicles derived from immortalized human mesenchymal stem cells of adipose tissue origin.

The percentage of alive cells did not change compared to untreated control (median 67.27% vs. 67.63%) for five samples (two ascitic fluid and three post-op., five patients). Furthermore, the percentage of early apoptotic cells increased in treated group vs. control (median 2.97% vs. 0.95%). In the treated group, the percentage of late apoptotic cells (median 2.88% vs. 5.57%) and necrotic cells (median 16.75% vs. 21.74%) decreased compared to control.

Importantly, for nine samples (six ascitic fluid and three post-op. of OvCa, seven patients) treated with HATMSC2-MVs, the decrease of percentage of alive cells (median 50.94% vs. 76.25%; $p < 0.01$) was observed. In this group, the median value of early apoptotic cells was assessed for 3.52% vs. 4.56% in the control cells; however, the range of early apoptotic cells in this HATMSC2-MVs-treated group was assessed from 0.2% to 41.45%. The increase of proportion of late apoptotic cells (median 14.98% vs. 8.5%) was observed. Apart from apoptotic pathway, the treatment of cells with HATMSC2-MVs leads

to increase of the percentage of necrotic cells compared to untreated cells (median 21.27% vs. 12.20%).

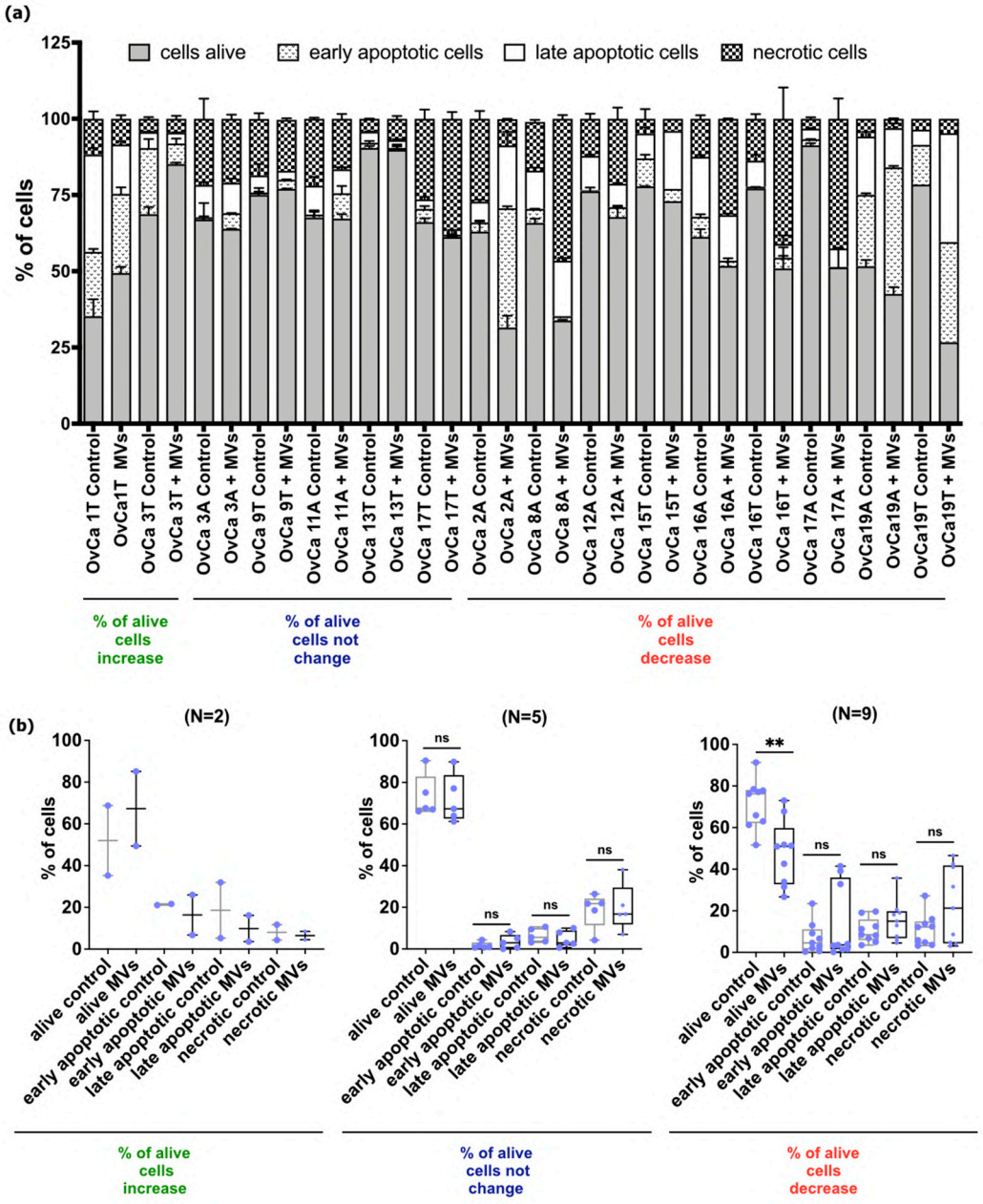

Figure 9. Effect of HATMSC2-MVs on the survival of primary OvCa cells isolated from post-op. tissues of OvCa and ascitic fluid. Survival of cells following treatment with HATMSC2-MVs at a ratio of 100:1 was assessed by flow cytometry. Untreated cells without MVs served as a control. (**a**) Quantification of cell viability after treatment with HATMSC2-MVs for 72 h was determined by the presence of apoptotic and necrotic cells via the double-staining of cells with propidium iodide and Annexin V. The percentages of alive, early apoptotic, late apoptotic, and necrotic cells were determined using Flowing Software 2. (**b**) Box and whiskers plots show percentage of alive cells, early apoptotic, late apoptotic, and necrotic cells for control cells and cells treated with HATMSC2-MVs. Blue dots represent cells from each analyzed patient. Whiskers show minimal and maximal values for each cell type. Lines represent the median. Untreated cells served as a control. ** $p < 0.01$ calculated vs. each respective control by Mann–Whitney test. Abbreviations: A—ascitic fluid, T—ovarian tumor tissue, MVs—microvesicles derived from immortalized human mesenchymal stem cells of adipose tissue origin, ns—not significant.

2.6. Characteristics of 3D Model of Primary Ovarian Cancer—Spheroids

To assess the effectiveness of the proposed HATMSC2-MVs therapy in a tumor, a 3D model of primary OvCa cells isolated from the tumor and ascitic fluid has been created. OvCa spheroids were characterized by their size and CSCs phenotype. The spheroids were formed from post-op OvCa cells (N = 9), the diameter ranging from 223 µm to 741 µm (a median value 462 µm). For spheroids derived from ascitic fluid cells (N = 9) the diameter was higher compared to spheroids from post-op OvCa cells and was ranging from 345 µm to 1301 µm with a median value of 538 µm (Figure 10a,b). Created spheroids assessed for CSCs markers revealed expression of CD44, CD133, and CD24. Spheroids formed from cells isolated from post-op tissues of OvCa contained a population of CD44 cells ranging from 10.0 to 33% with median value 24%, CD133 (range from 1.0% to 17.0%, median 3.0%), and CD24 (range from 1.0% to 16.0%, median 8.0%). While for cells from ascitic fluid, the range and median were as follows: for CD44 were (6.0–70.0%, median 27.0%), CD133 (1.0–22.0%, median 10.0%), and CD24 (0.5–41.0%, median 5.0%) (Figure 10c).

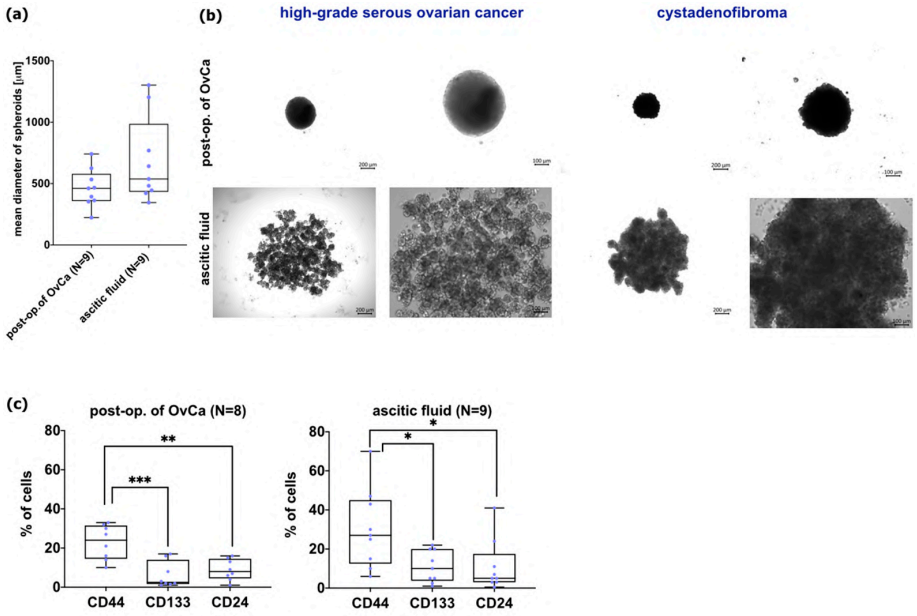

Figure 10. Characteristics of primary OvCa spheroids derived from post-op tissues of OvCa and ascitic fluid. (**a**) Box and whiskers plot shows the mean diameter of spheroids. Blue dots represent spheroids derived from one patient. Whiskers show minimal and maximal values for spheroid of each patient. Lines represent the median. (**b**) Representative images of spheroids. The left panel shows spheroids from high-grade serous OvCa cells, and the right panel shows representative images of spheroids cells from cystadenofibroma. Bars represent 200 µm and 100 µm. (**c**) Box and whiskers plots show the expression of selected CSCs markers on cells formed spheroids. Cells were stained with selected antibodies conjugated with fluorochromes. Blue dots represent cells from each analyzed patient. Whiskers show minimal and maximal values for each marker. Lines represent the median. *** $p < 0.001$, ** $p < 0.01$, * $p < 0.05$ calculated vs. each marker by one-way ANOVA. Abbreviations: post-op of OvCa—post-operative ovarian cancer.

2.7. Effect of HATMSC2-MVs on the Survival of Primary Ovarian Cancer Spheroids

Identification of the impact of HATMSC2-MVs on primary cancer cells in a 3D model of OvCa will allow development of the study on efficient therapeutic strategy. Live/dead assay was applied to assess the inhibitory effect of HATMSC2-MVs on OvCa. Untreated spheroids served as a control. For spheroids from post-op tumor of high-grade serous OvCa, the median value of the relative live/dead ratio calculated to the control spheroids was 0.85, while for spheroids from ascitic fluid, the median value was 1.02 compared to the control. Different results were obtained for spheroids derived from other histological types of OvCa. For spheroids from post-op. tumor, the median value was 1.33, while for spheroids from ascitic fluid, the median was 0.85 (Figure 11a). Representative images from confocal microscopy are presented in (Figure 11b).

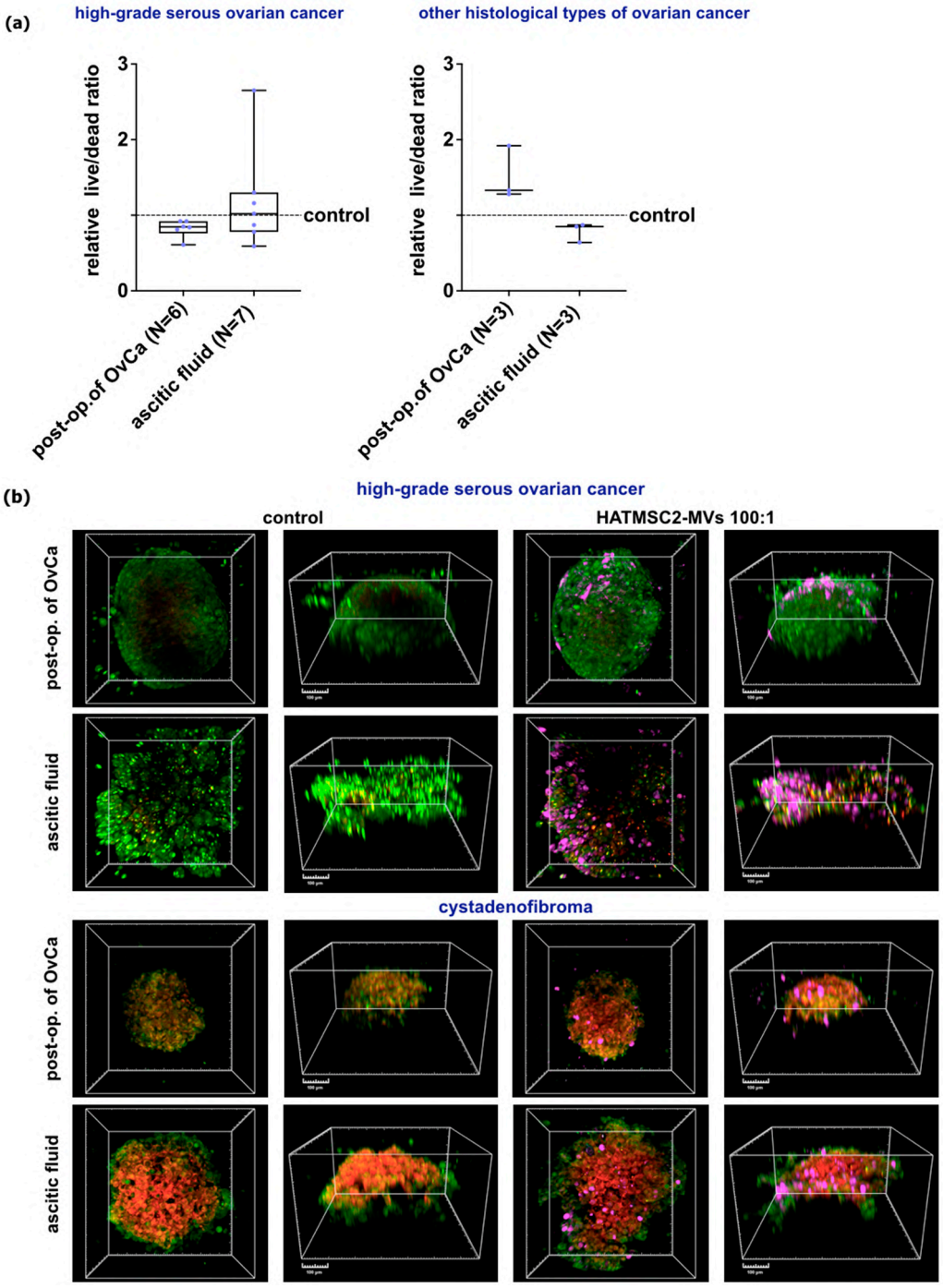

Figure 11. Effect of HATMSC2-MVs on the survival of primary OvCa spheroids. Effect of HATMSC2-MVs on the survival of primary OvCa spheroids derived from post-op. tumor and ascitic fluid. Survival of cells test following treatment with HATMSC2-MVs at a ratio of 100:1 was assessed by confocal microscopy imaging. Untreated cells without MVs served as a control. (**a**) Box and whiskers plots show relative ratio of live to dead channel. Blue dots represent cells from each analyzed patient. Whiskers show minimal and maximal values for each spheroid. Lines represent the median. (**b**) Representative confocal microscopy images of spheroids from high-grade serous OvCa and from cystadenofibroma. Live cells stained with Syto 9 (green), dead cells stained with propidium iodide (red), HATMSC2-MVs stained with DiD (violet). Bars represent 100 μm. The top panel shows control and treated spheroids from high-grade serous OvCa and the bottom panel shows spheroids from cystadenofibroma. Abbreviations: post-op. of OvCa-post-operative ovarian cancer; HATMSC2-MVs—microvesicles derived from immortalized human mesenchymal stem cells of adipose tissue origin.

2.8. Analysis of Bioactive Factors of HATMSC2-MVs Involved in Apoptosis Pathway

The content of HATMSC2-MVs was analyzed for the presence of bioactive factors that regulate apoptosis by using the Membrane-Based Protein Array. The heat-map revealed differences in the expression of analyzed factors between HATMSC2-MVs and parental cells HATMSC2. HATMSC2 cells expressed all analyzed bioactive factors (43 analytes) while HATMSC2-MVs do not express bax protein (Figure 12). In HATMSC2-MVs 15 pro-apoptotic factors (bad, BID, BIM, caspase 3, cytochrome c, Fas, FasL, HTRA, IGFBP-3, IGFBP-5, p27, p53, SMAC, TRAIL-R1, and TRAIL-R2) were detected at a higher level compared to parental HATMSC2 cells (Figure 12b,c). Only CD40, as a pro-apoptotic factor, was detected at a higher level in HATMSC2 cells. On the other hand, the HATMSC2-MVs contained 12 anti-apoptotic cytokines (bcl-2, bcl-w, HSP60, HSP70, IGF-I, IGF-II, IGFBP-6, livin, p21, TRAIL-R3, TRAIL-R4, and XIAP) at a higher level compared to HATMSC2 cells.

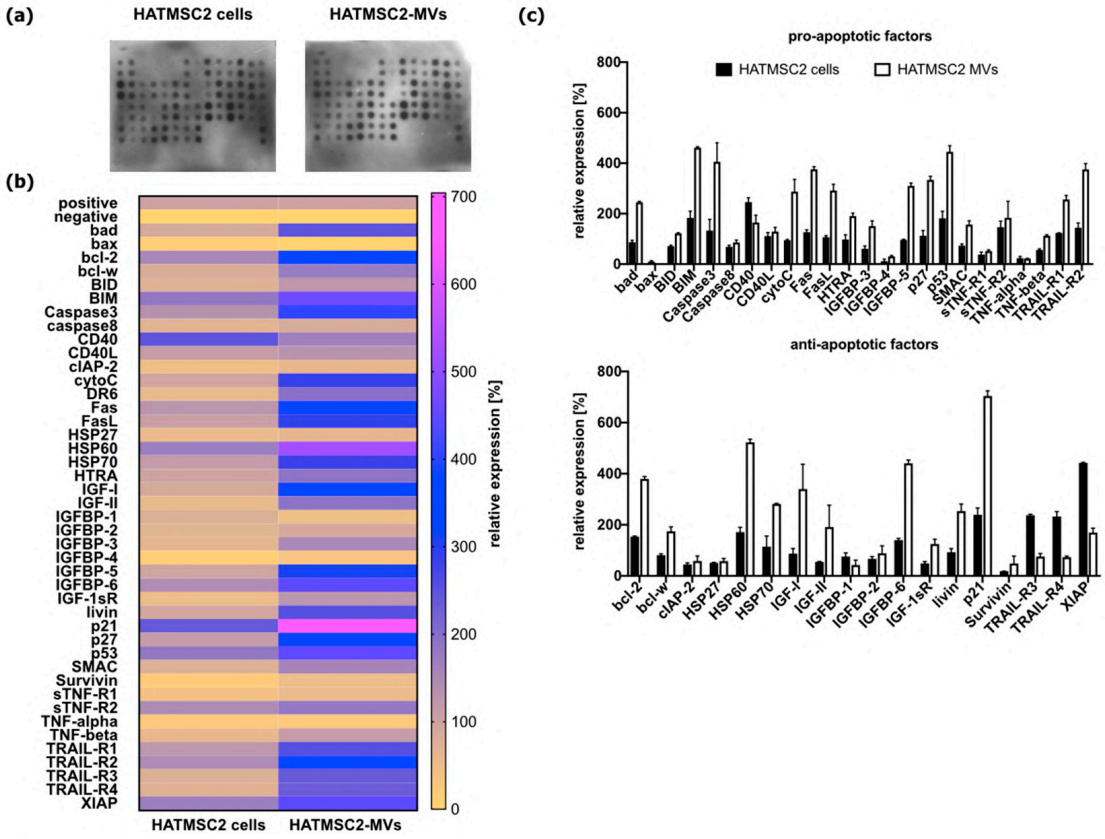

Figure 12. Composition of bioactive factors of the HATMSC2 cells and the HATMSC2—MVs. (**a**) Scans of representative protein arrays. The signal intensity for each antibody spot is proportional to the relative concentration of the protein in the sample. (**b**) Heat map of protein levels for the HATMSC2 cells and the HATMSC2-MVs; the magenta and yellow indicate higher and lower expression limits, respectively. Outstanding values (above 100% of positive control) are depicted in blue and magenta. Data are normalized to the internal positive control spots, which are consistent between the arrays and represent 100%. (**c**) Column graph representing bioactive factors and molecules regulating apoptosis. The data are presented as mean ± SEM values from a duplicate assessment. Abbreviations: HATMSC2-MVs—microvesicles derived from immortalized human mesenchymal stem cells of adipose tissue origin.

3. Discussion

Over the years, the important role of extracellular vesicles (EVs) as one of the mechanisms of cell-to-cell communication has been extensively studied [22]. EVs are secreted by all normal cells, cancer cells, and apoptotic cells [23]. The bioactive cargo of EVs consists of

cytoplasmic proteins (including enzymes and transcription factors), membrane adhesive molecules, lipids, and nucleic acids (including mRNA and regulatory miRNA). There are different types of EVs interaction with target cells leading to different biological effects, including: (i) direct activation of the target cell surface receptor after binding of the ligand derived from EVs, (ii) transfer of receptors present on the surface of EVs to the recipient cell, and (iii) functional modifications in target cells as a result from the interaction of specific miRNA or proteins transferred in vesicles with cellular effectors present in target cells [22].

There is an increasing interest in the study of MCs and their derivative EVs as new therapeutic options in several research fields including anticancer therapy, due to their role in different biological processes, including cell proliferation, apoptosis, angiogenesis, inflammation, and immune response. The biological potential of EVs is based on the biomolecular cargo transported inside these particles. However, not only composition of bioactive factors of EVs but also EVs from the same source of parental MSC can have opposite effect depending on the type of tumor cells [24,25].

A recent study by our research group confirmed that MVs derived from human immortalized MSC of adipose tissue origin (HATMSC2) affect the biological activity of two human ovarian cancer cell lines ES-2 (representing poorly differentiated ovarian clear cell carcinoma) and OAW-42 (representing ovarian cystadenocarcinoma) [17]. We demonstrated that HATMSC2-MVs treatment decreases the proliferation activity of ovarian cancer cells and induces cell death via apoptosis and/or necrosis pathway in MVs dose-dependent manner. These antitumoral effects are possibly associated with changes in the secretion profile of ovarian cancer cells, especially higher production of anti-tumor cytokines (IL-1ra, IL-2Ra, IL-12-p40, IL-12-p70, and IFN-γ) and decreased level of cancer-promoting cytokines (IL-6, IL-8, GRO-alpha, angiopoetin-2, and VEGF) after HATMSC2-MVs treatment [17].

These results encouraged us to assess the influence of HATMSC2-MVs on the biological activity of primary OvCa cells isolated from two sources, post-op. tissue and ascitic fluid. To the best of our knowledge, this is the first study where the effect of cell-free therapy, by using HATMSC2-MVs, has been assessed on primary OvCa cells. Before HATMSC2-MVs application, we characterized primary OvCa cells for the immunophenotype of MSCs and CSCs markers. All analyzed cancer cells express similar MSCs markers CD73, CD90, CD105; however, their pattern of expression is different between analyzed primary OvCa cells. Our previous study revealed that application of HATMSC2-MVs on ovarian cancer cell lines OAW-42 and ES-2 had no effect on the expression of CD73, CD90, and CD105 antigens strongly expressed on both cell lines [21]. However, biological features of the examined primary OvCa cells, characterized by high expression of MSCs markers such as CD73 and CD105, involved in tumor progression and metastasis, can serve as a therapeutic target for specific neutralizing antibodies inhibiting ovarian cancer growth and metastasis [26,27].

CSCs constitute a specific population of cancer cells and are known as cells resistant to chemotherapy and apoptosis [4,28]. Ovarian CSCs, characterized here by CD24, CD44, CD133 expression, were detected in the majority of analyzed OvCa samples; all of them express CD44 and CD133, but CD24 was not detected in 4 out of 25 analyzed samples (from tumor and ascitic fluid). CD133 is widely used for CSCs isolation in different solid tumors. In the case of ovarian cancer tumors, it has been reported that elevated levels of CD44- and CD133-positive cells were associated with chemotherapy-resistant patients and were present in metastatic and recurrent tumors (reviewed in [4]). This is in line with different reports that CSCs markers are not specific for all ovarian cancers, but their expression can predict tumor aggressiveness [29,30]. In this study, we confirmed the presence of OvCa cells with the same phenotype as tumor cells in the corresponding ascitic fluid that can be helpful in diagnosis and therapeutic approach design before surgical procedures.

Evaluation of pluripotency-related markers (Oct4, Sox2, Nanog) and proto-oncogenic transcripts (*p53*, *p21*, *c-myc*) has been performed to assess biological feature of examined OvCa cells. Oct4, Sox2, and Nanog are known as transcription factors involved in maintaining pluripotency and self-renewal [31]. Oct4 plays a role in the regulation of several signaling pathways in CSCs such as Hedgehog, Wnt, Notch, PI3K/Akt, and JAK/STAT [32].

In our study, we confirmed the expression of Oct4, Sox2, and Nanog in primary OvCa cells from both sources, ascitic fluid and post-op. tissue, by RT-PCR and/or immunofluorescence staining. Enhanced expression of Oct4, Sox2, and/or Nanog are characteristic for primary OvCa tumors, and their expression enhances chemoresistance and potential of tumor relapse [31]. Oct4, Sox2, and Nanog can be a target for cancer treatment. The knockdown of Oct4 led to the inhibition of proliferation activity, migration activity, and invasiveness of two ovarian cancer cell lines A2780 and SKOV-3, and inhibited the tumor growth and metastasis in a mouse model [33]. High expression of Sox2 is related to poor prognosis of cancer treatment. It was demonstrated that higher expression of Sox2 was detected by immunostaining in metastasis specimens compared to primary tumor [34]. The silencing of Sox2 caused decreased spheroids formation by SKOV3 and HO8910 cells and expression of EMT and stem cell-related genes, and similarly to Oct4 leads to inhibition of proliferation and migration of cells [35]. In ovarian cancer, Nanog affects cell migration and invasiveness. For the survival of patients with ovarian serous carcinoma, positive Nanog expression was lower compared to patients with negative Nanog. Thus, Nanog can be used as a predictive marker of ovarian cancer patients' survival [36]. Our studies showed overexpression of the proto-oncogene *c-myc* in the examined OvCa cells. *c-myc* regulates the expression of genes involved in cell proliferation, differentiation, apoptosis, and stem cell renewal. These properties are attractive as a therapeutic target in many tumors including OvCa. In high-grade serous OvCa, the overexpression of *c-myc* is associated with resistance to platinum-based therapy and decreased overall survival. Targeting *c-myc* by siRNA-mediated *c-myc* silencing of cisplatin-resistant A2780 OvCa cell line decreased cell proliferation and survival and inhibited cell-cycle progression [37].

In our study, the immunophenotype of primary OvCa cells has been expanded to include the expression of factors related to markers for CAFs (FAP, PDGFRα), epithelial to mesenchymal transition (EMT) markers, Snail and vimentin, and CSCs markers (ALDH1, c-kit). FAP and PDGFRα are known as cancer-associated fibroblasts markers [38]. In our study, the FAP and PDGFRα revealed weak expression or were undetected and this suggests that CAFs were poorly represented in the population of primary OvCa cells. One of the key biomarkers of EMT is vimentin, a type III intermediate filament that is normally expressed in mesenchymal cells but is upregulated during cancer metastasis. [39]. Vimentin intermediate filaments modulate Snail, which is a main transcription factor involved in EMT [39]. The inhibition of Snail via miR-137 and miR-34a leads to the inhibition of the production of Snail on transcription and protein levels and decreases the invasiveness and spheroids formation in ES-2 and SKOV-3 cell lines [40]. The presence of ALDH-1-positive cells in ovarian cancer patients leads to poor prognosis of survival [41]. The silencing of ALDH-1 leads to inhibition of tumor growth in mouse models. Increased expression of c-kit (CD117) in ovarian cancer is involved in chemoresistance. Phenotypic diversity in ovarian cancer tumors is challenging for therapeutic approaches, especially when different phenotypes of CSCs are presented and targeting therapy for one molecule will be ineffective.

In this study, we propose cell-free therapy with HATMSC2-MVs, which can be applied as a supportive biotherapy procedure in OvCa treatment. Our results revealed that the application of HATMSC2-MVs treatment on primary OvCa cells leads to a decrease in the metabolic activity of OvCa cells and apoptosis induction. The difference in metabolic activity of treated high-grade serous OvCa cells from both sources such as tumor and ascitic fluid, compared to the control untreated cells, is the most visible on day 3, while for the cells from the other histological types of ovarian cancer on day 2. Decrease of OvCa cells proliferation after exposure to HATMSC2-MVs leads to decreased migratory activity of OvCa cells isolated from post-op. tumor as confirmed in a scratch test. This phenomenon suggests that HATMSC2-MVs content may inhibit aggressiveness and invasion of OvCa cells and thus play a role as regulator of tumor progression.

In a previous study, we demonstrated that HATMSC2-MVs treatments are involved in the regulation of cell cycle and apoptosis induction of the ovarian cancer cell lines OAW-42

and ES-2 [21]. In the present study, we confirmed that HATMSC2-MVs promote apoptosis and contribute to necrosis in the majority of tested primary OvCa cells, and this may lead to tumor attenuation. To date, the knowledge about the exact mechanisms of MSC secretome-mediated effects on cancer cells is limited; however, data so far suggest complex regulation involving antagonistic effects [42].

To determine a bioactive cargo of HATMSC2-MVs that can induce cell death, we analyzed the proteins content involved in apoptosis signaling by using the RayBio® Human Apoptosis Antibody Array. Our results showed that the HATMSC2-MVs contain several pro-apoptotic proteins (including bad, BIM, caspase 3, Fas, FasL, IGFBP-5, p27, p53, TRAIL-R1, and TRAIL-R2) and anti-apoptotic factors (including bcl-2, HSP-60, IGF-I, IGFBP-6, p21, TRAIL-R3, and TRAIL-R4) at a higher level compared to HATMSC2 cells. In this study, HATMSC2-MVs serve as an apoptotic signal delivery system into cancer cells as confirmed by internalization of HATMSC2-MVs into primary OvCa cells by confocal microscopy imaging. HATMSC2-MVs-internalized OvCa cells release pro-apoptotic and anti-apoptotic molecules, and their activity depends on many factors influencing apoptotic signal induction or repression that may have a variety of outcomes depending on the molecular or transcriptional context.

Tumor necrosis factor (TNF)-related apoptosis-inducing ligand (TRAIL) belongs to the TNF family and is capable of inducing apoptosis in cancer cells while sparing normal cells. In cancer cells, TRAIL exerts its apoptotic effects through activation of caspase 8, which triggers apoptosis cascade by binding to the death receptors TRAIL-R1 and TRAIL-R2 on target cancer cells [43]. Research performed by Shamili et al. [44] showed that the exosomes derived from genetically modified MSCs to express TRAIL can delay the tumor growth and cause the decrease of tumor volume in a melanoma mouse model [44]. Moreover, the expression of TRAIL in MSCs can be induced via X-ray radiation [45]. Studies on MSC-derived EVs, as potential drug delivery vehicles, showed that TRAIL-transduced MSCs secrete EVs expressing surface TRAIL molecules that are efficiently induced apoptosis in different 11 cancer cell lines but they are not cytotoxic for normal cells [46]. Our study confirmed that MVs from immortalized HATMSC2 cell lines express the death receptors TRAIL-R1 and TRAIL-R2, which contribute to apoptosis induction. TRAIL also functions in the form of a soluble ligand and can trigger p53-independent apoptosis. A recent study demonstrated that genetically engineered umbilical cord MSCs by using recombinant TRAIL (rhTRAIL) have been designed to continuously express and secrete soluble TRAIL (MSC-sTRAIL) as a potential therapeutic approach for treatment of hematologic disorder B-cell acute lymphocytic leukemia (B-ALL). Studies performed in vitro and in vivo on the mouse B-ALL model revealed that MSC-sTRAIL can inhibit B-ALL cell proliferation by initiating apoptosis via the caspase cascade-mediated pathway and mitochondrial-mediated pathway [47].

Our study revealed upregulated expression of proapoptotic caspase 3 in HATMSC2-MVs compared to parental cells. Earlier studies on the antitumor effect of MSCs of bone marrow origin on mouse hepatoma cells documented that MSCs could induce inhibitory effects on tumor cells via upregulation of mRNA expression of cell cycle negative regulator p21 and pro-apoptotic protease caspase 3, leading to apoptotic death of cancer cells [48]. In the present study, we demonstrated that HATMSC2-MVs contain high levels of proapoptotic caspase 3 and high levels of cell cycle negative regulator p21. The p21 represent cyclin-dependent kinase inhibitor and is a major player in cell cycle control [49]. The suppressor function of p21 against cancer cells is associated with the ability of p21 to inhibit cell proliferation through the inhibition of CDK2 activity and cell growth arrest at G0/G1 phase. However, a number of oncogenes inhibit the activity of p21 to promote cell growth and tumorigenesis. As reported, p21 also functions as an inhibitor of apoptosis, thus p21 repression may have an antitumor effect by sensitization of cancer cells to apoptosis by anticancer drugs [49]. The differential effects of p21 on cell cycle arrest and apoptosis are also account by the activity of caspase 3, which specifically cleavage p21 during the DNA damage-induced apoptosis of cancer cells [50]. These studies showed that

caspase-3-mediated cleavage and repression of the p21 protein may change cancer cells from growth arrest to undergoing apoptosis. Based on these observations we suggest that HATMSC2-MVs cargo, where both pro-apoptotic caspase 3 and anti-apoptotic p21 were upregulated, can influence OvCa cells' apoptosis or growth arrest after internalization into OvCa because the cleaved p21 could not arrest the cells in the G1 phase nor suppress the cells undergoing apoptosis; however, this hypothesis should be verified in further studies.

Finally, assessment of HATMSC2-MVs efficacy was performed in a 3D model of spheroids composed from primary OvCa cells. Spheroids are widely used as a 3D model to determine the cytotoxicity of newly developed drugs especially in cancer treatment. In our study, we used spheroids to determine the effect of HATMSC2-MVs on the survival of the cells in a 3D model mimicking ovarian tissue. Our model is composed from a heterogeneous population of OvCa cells including CSCs with CD133, CD44, and CD24 phenotype. The presence of CD44 is associated with metastatic and recurrence capacity of ovarian cancer and poor overall survival [4]. CSCs in OvCa expressing CD133 and CD24 are chemoresistant, and spheroids with the presence of these markers can serve as a model for therapeutic approaches in regulation of CSCs markers expression because targeting one marker alone may be not sufficient to achieve the expected anti-cancer effect [4]. Internalization of HATMSC2-MVs has been confirmed, and live/dead assay revealed a decreased ratio of alive cells in OvCa isolated from ovarian tumor tissue. The study performed by Liao et al. showed that the spheroids derived from primary ovarian cancer cells are more sensitive to cisplatin compared to cells in the 2D model due to high proliferation activity [51]. On the other hand, the spheroids derived from the MCW-OV-SL-3 (derived from endometrioid ovarian cancer) cell line are resistant to cisplatin due to increased activation of ERK and PI3K/AKT signaling pathway [52]. A recent study demonstrated that patient-derived organoids formed from cells isolated from ascitic fluid were successfully used as a reliable model for assessment of molecular mechanisms underlying platinum resistance to extend the understanding in treatment of gynecological serous carcinomas [53].

Overall, HATMSC2-EVs could exert either antiproliferative or proapoptotic effects on OvCa cells; however, different strategies to employ MSCs and their derivatives as a biotherapy in ovarian cancer are studied. Melzer et al. [54] showed that taxol-loaded microvesicles did not affect the viability of analyzed cancer cell lines including ovarian adenocarcinoma (SKOV-3). However, taxol-loaded exosomes reduced viability and proliferation activity of human ovarian adenocarcinoma similarly compared to taxol, but the concentration of taxol in the exosomes was lower [54].

Moreover, EVs released by MSCs of bone marrow or adipose tissue origin exhibit suppressive effects on ovarian cancer cell lines. Anti-proliferative and anti-tumor activity of MVs produced by BM-MSCs on the SKOV3 cell line as well as in an SCID mice model was reported [16]. In the animals, the presence of necrotic areas in the tumor section was confirmed by histological analysis [16]. Similar results were observed by Wang et al. [55]. Extracellular vesicles derived from MSC decreased proliferation, migration, and invasiveness of ES-2 and ovarian adenocarcinoma (CAOV-3) cell lines. Moreover, this group discovered that in patients with OvCa, miR-18a-5p is down-regulated and associated with poor prognosis of survival. Thus, the application of EVs with overexpression of miR-18a-5p caused an increase in cisplatin sensitivity of analyzed ovarian cancer cell lines.

One of the mechanisms of EVs' action is non-coding RNAs, principally miRNAs. The study performed by Reza et al. [56] reported that miRNAs delivered in AT-MSCs derived exosomes are responsible for inducing particular cell signaling pathways in target ovarian cancer cells. The co-incubation of proteinases digested exosomes with epithelial ovarian cancer cells A2780 and SKOV3 cells leads to a reduction of cancer cell viability, colony formation ability, and induction of apoptosis. Most of the miRNAs detected in AT-MSCs-derived exosomes were mainly responsible for catalytic activity, channel regulatory activity, and metabolic and cellular processes.

Despite numerous analyses, we note that the presented studies have some limitations. In these studies, we performed a broad characterization of the phenotypic and molecular profiles of primary OvCa cells; however, an attempt to correlate them with the response toHATMSC2-MVs treatment did not yield significant results. This is probably due to the heterogeneous population of primary ovarian cancer cells that expressed analyzed markers at different levels and with diverse numbers of samples in each group. For this reason, it would be beneficial to perform further experiments on OvCa cells derived from greater numbers of patients. Another limitation is the need to better determine the biological cargo of HATMSC2-MVs. Further research, especially the whole proteomic analysis of HATMSC2-MVs by liquid chromatography mass spectrometry (LC-MS) and transcriptomic analysis by next-generating sequencing (NGS), could be useful to allow for identification and quantification of both unknown and known bioactive compounds of HATMSC2-MVs. Moreover, it would be important to examine which bioactive factors caring by HATMSC2-MVs are critical for the determination of ovarian cancer sensitivity. Neutralizing antibodies or siRNA for some factors of interest would be preferred for these studies. However, despite these limitations, the present study adds a novel observation for HATMSC2-MVs biological characteristics and their potential ability to inhibit primary OvCa cells growth and apoptosis induction; however, further studies are needed to clarify their anti-cancer activities.

4. Materials and Methods

4.1. Isolation and Characterization of Human Primary Ovarian Cancer Cells

The primary ovarian tumor cells were isolated from two sources: human postoperative tissue of OvCa and ascitic fluid (16 patients), according to the permission from the Bioethics Committee at the Medical University of Wroclaw (No. KB-489/2020). Procedures were performed at the Department of Gynecology and Obstetrics, Wroclaw Medical University. Characteristics of patients are presented in Table 1.

Table 1. Characteristics of patients.

No.	Patient ID	Patient's Age	OvCa Materials Collection		Histological Type
			Post-Op. Tumor (T)	Ascitic Fluid (A)	
1	OvCa1	56	1T	NA	Ovarian clear cell carcinoma
2	OvCa2	60	NA	2A	Ovarian clear cell carcinoma
3	OvCa3	70	3T	3A	High-grade serous ovarian cancer
4	OvCa 6	66	6T	NA	High-grade serous ovarian cancer
5	OvCa 7	54	NA	7A	High-grade serous ovarian cancer
6	OvCa 8	65	8T	8A	Cystadenofibroma
7	OvCa 9	82	9T	9T	High-grade serous ovarian cancer
8	OvCa10	59	10T	NA	Mucinous ovarian cancer
9	OvCa11	53	11T	11A	Mucinous ovarian cancer
10	OvCa12	52	12T	12A	High-grade serous ovarian cancer
11	OvCa13	75	13T	13A	High-grade serous ovarian cancer
12	OvCa14	69	14T	NA	Malignant mixed Mullerian tumor called carcinosarcoma
13	OvCa15	54	15T	15A	High-grade serous ovarian cancer
14	OvCa16	72	16T	16A	High-grade serous ovarian cancer
15	OvCa17	64	17A	17T	High-grade serous ovarian cancer
16	OvCa19	70	19A	19T	High-grade serous ovarian cancer

Abbreviations: NA—not applicable.

In our study, 62.7% of OvCa was high-grade serous ovarian cancer (10 patients). Six patients were classified to other histological types of OvCa (37.5%). That group consists of ovarian clear cell carcinoma (N = 2), cystadenofibroma (N = 1), mucinous ovarian cancer (N = 2), and malignant mixed Mullerian tumor (MMMT), also called a carcinosarcoma (N = 1). Tumor cells were isolated using Tumor Dissociation Kit Human (Milteni Biotec,

Bergisch Gladbach, Germany) according to the manufacturer's instructions. Briefly, the tissues were cut into small pieces and then transferred into a gentleMACS Tube dedicated to gentleMACS Dissociator (Milteni Biotec, Bergisch Gladbach, Germany) containing the mixture of Enzyme A, H, and R. Next, the tissues were proceeded in triple steps by mechanical and enzymatic digestion using the gentleMACS Dissociator. Between the digestion steps, the samples were incubated for 30 min at 37 °C with mixing three times. Finally, samples were transferred into a 70 µm cell strainer. Cell suspensions were centrifuged at 300× *g* for 7 min, and then the cells were resuspended in medium. The cells were cultured in the DMEM (IIET, Wroclaw, Poland) and OptiMEM GlutaMax media (Thermo Fisher Scientific, Carlsbad, CA, USA), mixed in equal proportions. The DMEM medium was supplemented with 10% FBS (Thermo Fisher Scientific, Carlsbad, CA, USA), a 1% penicillin/streptomycin solution (Thermo Fisher Scientific, Carlsbad, CA, USA), and 1% L-glutamine (Thermo Fisher Scientific, Carlsbad, CA, USA). The OptiMEM GlutaMax medium was supplemented with 3% FBS and a 1% penicillin/streptomycin solution. Tumor cells from the ascitic fluid were isolated according to the protocol described by [57]. Briefly, the ascitic fluid was centrifuged at 1000× *g* for 10 min. The obtained cells were washed twice in PBS (IIET, Wroclaw, Poland) and finally resuspended in culture medium. The cells were cultured in the DMEM supplemented with 10% FBS, a 1% penicillin/streptomycin solution, and 1% L-glutamine.

4.2. The Characterization of Human Primary Ovarian Cancer Cells

4.2.1. Analysis of Membrane Markers by Flow Cytometry

The characterization of primary OvCa cells included flow cytometry analysis of the expression of MSCs markers (CD73, CD90, CD105), CSCs markers (CD44, CD24, CD133), hematopoietic stem and progenitor marker (CD34), and leukocyte common antigen (CD45).

For flow cytometry analysis, the primary ovarian tumor cells were detached from cell culture flasks using the Tryple Select (Thermo Fisher Scientific, Carlsbad, CA, USA) solution. Afterward, the cells were incubated at 4 °C for 30 min with PE-conjugated antibodies for the human CD73, CD90, CD105, CD44, CD45, CD133 (BD Biosciences, San Jose, CA, USA), and FITC-conjugated CD24, CD34 antibody (BD Biosciences, San Jose, CA, USA), and with the corresponding isotype controls (BD Biosciences, San Jose, CA, USA). Then, the PBS (IIET, Wroclaw, Poland) was utilized for cell washing. The BD LSRFortessa flow cytometer (BD Biosciences, San Jose, CA, USA) was used to analyze the labeled cells. The data were acquired using the CellQuest software version 5.1 (BD Biosciences, San Jose, CA, USA). The histograms were prepared using Flowing Software 2 (Perttu Terho, Turku Centre for Biotechnology, Turku, Finland).

4.2.2. Analysis of Transcripts by Real Time RT-PCR

The genetic analysis of cells by real-time RT-PCR were used to determine the level of transcripts involved in the maintenance of pluripotency (Oct4, Sox2), pro-oncogenic transcripts (p53, p21, and c-myc), and CD133. RNA isolation was performed using a NucleoSpin® RNA Kit (Macherey-Nagel, Düren, Germany), then the reverse transcription PCR was performed according to the manufacturer's instruction of RevertAid First Strand cDNA Synthesis Kit (Thermo Fisher Scientific, Weston, FL, USA). The level of transcripts was determined using the real-time PCR method with the TaqMan Master Mix (Thermo Fisher Scientific, Weston, FL, USA) and specific TaqMan probes: Sox2 (Hs01053049), Oct4 (Hs00999632), p53 (Hs00153349), c-myc (Hs00153408), CD133 (Hs01009250), and GAPDH (Hs03929097) (Thermo Fisher Scientific, Weston, FL, USA). Quantification of mRNA content was performed on the ViiA 7 Real-Time PCR System (Applied Biosystems, Foster City, CA, USA). The calculation of results was performed using the ΔCt method [58], and the GADPH gene was applied as reference.

4.2.3. Analysis of Membrane Markers and Transcription Factors by Fluorescence Microscopy Imaging

Immunofluorescence staining of the cells for microscopic imaging included the following markers: CD44, F-actin, vimentin, cancer stem cells markers (ALDH1, c-kit (CD117)) cancer-associated fibroblasts markers (PDGFRα, FAP), epithelial to mesenchymal-transition markers (Snail, vimentin), and pluripotency-related markers (Oct4, Sox2, Nanog). The cells were fixed with 4% PFA (Merc, Kenilworth, NJ, USA) (15 min in room temperature (RT)) and permeabilized with 0.1% Triton X100 (Avantor Performance Materials Poland, Gliwice, Poland) (15 min in RT). Then, the unspecific binding of antibodies was blocked using 1% BSA (Symbios, Gdansk, Poland) (40 min incubation, RT). Selected primary antibodies were applied for 1 h (RT) or overnight incubation (4 °C) (Supplementary Materials Table S1). Then, the cells were labeled for 45 min (RT) with Alexa Fluor 488-conjugated goat anti-mouse IgG and/or Alexa Fluor 647-conjugated goat anti-rabbit IgG (Invitrogen, Carlsbad, CA, USA). The actin filaments were stained for 45 min (RT) with Alexa Fluor 488-conjugated phalloidin (Invitrogen, Carlsbad, CA, USA) (Supplementary Materials, Table S2), and the cell nuclei were stained for 30 min (RT) with NucBlue™ Fixed Cell ReadyProbes™ Reagent (DAPI) (Invitrogen, Carlsbad, CA, USA). Image acquisition was performed with an Axio Imager Z2 microscope (Zeiss, Gottingen, Germany) equipped with 40× (NA 0.75), dry objective using Zen 2.6 Blue edition Software (Zeiss, Gottingen, Germany). The images were processed with the Zen 2.6 Blue edition Software.

4.3. Isolation and Characterization of MVs Derived from HATMSC2 Cells

HATMSC2-MVs were isolated from conditioned media harvested from HATMSC2 cell cultures using the sequential centrifugation-based method according our well-establish method [21]. Briefly, the conditioned media were collected from HATMSC2 cells cultured for 48 h under hypoxic condition at 1% O_2 in serum-free medium DMEM supplemented with P/S and L/G. The conditioned media were centrifuged twice at 4 °C for 10 min at a speed of 300× *g* and 2000× *g*, respectively. Then, the conditioned media were centrifuged at 4 °C for 30 min at a speed of 12,000× *g* using a Sorvall LYNX 6000 ultracentrifuge (Thermo Scientific, Carlsbad, CA, USA). After, the PBS were used to resuspend MVs. The MVs were characterized according to Minimal Information for Studies of Extracellular Vesicles (MISEV) recommendation [59]. The size distribution of MVs was analyzed by DLS (Malvern Zetasizer, Malvern, UK), and the average size of MVs was assessed for 460 nm ± 60 nm (Figure S1). Moreover, the MVs were analyzed by transmission electron microscope (JEOL, Peabody, MA, USA) (Figure S1). The MVs concentration was determined using a BD Fortessa Flow Cytometer (BD Biosciences, San Jose, CA, USA) and fluorescent counting beads (Count Bright™ Absolute Counting Beads for flow cytometry, Thermo Scientific, Carlsbad, CA, USA). During sample acquisition, 5000 counting beads were collected by BD Fortessa Flow Cytometer (BD Biosciences, San Jose, CA, USA) (Figure S1). The concentration of MVs was determined using the formula included in the instructions for the CountBright™ Absolute Counting Beads, and it was assessed for 1028 MVs/µL.

4.4. Internalization of HATMSC2-MVs into Human Primary Ovarian Cancer Cells

Internalization of DiD-labelled HATMSC2-MVs into human primary OvCa cells was analyzed using a confocal microscope. Primary cells were stained in a suspension for the expression of PDGFRα. The cells were fixed with 4% PFA (15 min in RT) and permeabilized with 0.1% Triton X100 (0.1%; 15 min in RT). Then, the unspecific binding of antibodies was blocked using 1% BSA (40 min incubation, RT). Mouse anti-human PDGFRα antibody was applied for 1 h (RT). Then, the cells were labeled for 45 min (RT) with Alexa Fluor 488-conjugated goat anti-mouse IgG (Invitrogen, Carlsbad, CA, USA). The cell nuclei were stained for 30 min (RT) with NucBlue™ Fixed Cell ReadyProbes™ Reagent (DAPI) (Invitrogen, Carlsbad, CA, USA). Image acquisition was performed with a Leica SP8 MP confocal microscope (Leica Microsystems, Wetzlar, Germany) equipped with a 40× (NA 1.3) oil objective and spectral detectors using 400 nm, 488 nm, and 638 nm lasers

sequentially. The images were processed with Imaris software version x64 9.5.1 (Bitplane, Zurich, Switzerland) to visualize HATMSC2-MV presence within OvCa cells.

4.5. Assessment of HATMSC2-MVs Action on the Survival of Human Primary Ovarian Cancer Cells in 2D Culture

4.5.1. MTT Assay

The metabolic activity of cells treated with MVs at a ratio of 100:1 (100 MVs per 1 cell) was analyzed by MTT assay at a different time point (day 0, day 1, day 2, day 3). The cells were seeded in a 96-well plate at the density of 3×10^3 cells/well. The Wallac 1420 Victor2 Microplate Reader (Perkin Elmer, Waltham, MA, USA) was used to determine the absorbance of dye accumulated in cells. The absorbance was measured at 570 nm.

4.5.2. Scratch Test

Migration activity of primary OvCa cells was assessed using a scratch test. The cells were seeded in a 48-well plate at the density of 5×10^4 cells/well. When the cells were fully confluent, the scars were made with thin tips. The cells were treated with HATMSC2-MVs at a ratio of 5:1 (5 MVs per 1 cell). This ratio was selected based on our previously performed experiments where the ratios of MVs were determined. Since 100 MVs as well as 10 MVs added per 1 ovarian cell were making the visualization on the microscope impossible, the ratio of 5 MVs to 1 ovarian cell was therefore chosen.

Migration was observed at 37 °C in an incubation chamber (PeCon GmbH, Erbach, Germany) with 21% O_2, 5% CO_2 mounted on an Axio Observer inverted microscope equipped with a dry 5× (NA 0.16) objective (Zeiss, Gottingen, Germany). The movement of the cells was time-lapse recorded for 2 days at intervals of 4 h using Zen 2.6 Blue Edition Software (Zeiss, Gottingen, Germany). Wound closure was analyzed using Zen Blue Software. Relative wound closure (RWC) was calculated as previously described [60].

4.5.3. Live/Dead Assay in 2D Culture

For microscopic imaging, cells were seeded in a 96-well plate at a density of 3×10^3 cells/well. MVs were labeled with DiD dye (Thermo Fisher, Carlsbad, CA, USA) and incubated with 2D cultures for 72 h. Next, cells were stained for 30 min in RT with propidium iodide (PI) and SYTO 9 according to the manufacturer's recommendations (LIVE/DEAD kit, Thermo Fisher, Carlsbad, CA, USA), then washed with PBS and fixed with 4% PFA for 15 min. The microscopic imaging was performed using a Zeiss Cell Observer SD confocal microscope equipped with a dry 10× (NA 0.3) objective (Zeiss, Gottingen, Germany) and Rolera EM-C2 camera (QImaging, Surrey, BC, Canada). The labeled cells were detected sequentially using a 488 nm laser (SYTO 9-labelled living cells) and a 561 nm laser (PI-labelled dead or apoptotic cells), while MVs were detected with a 639 nm laser, using 520/35, 600/50, and 690/50 emission filters, respectively. Mosaics composed of 3 × 3 fields of view were recorded as volumes with a 5 µm interval in Z axis. The images were processed with Fiji/ImageJ software version 1.54f (National Institutes of Health, Bethesda, MD, USA). Background noise was removed with median filtering followed by maximum intensity projection (MIP) of acquired channels. To measure the effect of MVs on cells, a SYTO 9 to PI ratio channel was created using an image calculator function by dividing SYTO 9 pixel intensities by corresponding PI pixel intensities at the same coordinates. Next, SYTO 9 and PI MIP images were added using the image calculator function, and the obtained new image was thresholded to reveal cell bodies. The mean SYTO 9 to PI ratio in detected cells was calculated with an analyze particles function.

4.5.4. Apoptosis Assay

After incubation with MVs for 72 h (at the ratio 100 MVs to 1 ovarian cell), the Annexin V and propidium iodide was used for cells staining according to the manufacturer's instructions (eBioscience™ Annexin V Apoptosis Detection Kits, Thermo Fisher, Carlsbad, CA, USA). The analysis of four populations of cells—alive (Annexin V-negative and propidium

iodide-negative), early apoptotic (Annexin V-positive and propidium iodide-negative), late apoptotic (Annexin V-positive and propidium iodide-positive), and necrotic cells (Annexin V-negative and propidium iodide-positive)—was performed using a BD LSRFortessa flow cytometer (BD Biosciences, San Jose, CA, USA). The data analysis was performed by Flowing Software 2 (Perttu Terho, Turku Centre for Biotechnology, Turku, Finland).

4.6. Assessment of HATMSC2-MVs Action on the Survival of Human Primary Ovarian Cancer Cells in 3D Culture

4.6.1. Spheroids Formation and Flow Cytometry Analysis

For spheroids formation, cells were seeded in a dedicated 96-well plate Nunclon Sphera (Thermo Fisher, Carlsbad, CA, USA), at the density of 3×10^3 cells/well. To obtain cell suspension for flow cytometry, spheroids were enzymatically digested with Accutase Cell Detachment Solution (Corning, Manassas, VA, USA) and shaken for 10 min at 37 °C. After one washing in PBS, the cells were stained with PE-conjugated antibodies specific for the human CD44, CD133 (BD Biosciences, San Jose, CA, USA), and FITC-conjugated CD24 (BD Biosciences, San Jose, CA, USA) and with the appropriate isotype controls (BD Biosciences, San Jose, CA, USA) for 30 min at 4 °C. Afterward, the labeled cells were washed with PBS (IIET, Wroclaw, Poland) and proceeded using a BD LSRFortessa flow cytometer (BD Biosciences, San Jose, CA, USA). The analysis was performed using Flowing Software 2 (Perttu Terho, Turku Centre for Biotechnology, Turku, Finland).

4.6.2. Live/Dead Assay in 3D Culture

The effect of HATMSC2-MVs at a ratio 100:1 after 72 h of treatment on cancer cell survival in spheroids was analyzed by confocal microscopy imaging. For imaging, HATMSC2-MVs were additionally stained with DiD dye to assess the internalization of MVs into the cancer cells that formed spheroids. After incubation with HATMSC2-MVs for 72 h, the spheroids were stained with propidium iodide and Syto 9 according to the manufacturer's recommendations (Thermo Fisher, Carlsbad, CA, USA) for 1 h in RT then washed with PBS and fixed with 10% formalin for 30 min. Spheroids were visualized using a Zeiss Cell Observer SD confocal microscope equipped with a dry 10× (NA 0.3) objective (Zeiss, Gottingen, Germany) and Rolera EM-C2 camera (QImaging, Surrey, BC, Canada). The microscopic imaging and image analysis were performed as described in Section 4.5.3.

4.7. Examination of HATMSC2-MVs Content to Dissect Apoptotic Factors—Protein Membrane Analysis

The protein content of HATMSC2 cells and HATMSC2-MVs was examined using the Membrane-Based Antibody Array (RayBio® Human Apoptosis Antibody Array C1, RayBiotech, Peachtree Corners, GA, USA). Isolated MVs and cells were lysed in RIPA buffer with a protein inhibitor cocktail for 10 min on ice, sonicated for 15 min, then suspended in PBS. The BCA assay (Thermo Scientific, Carlsbad, CA, USA) was used according to the manufacturer's instructions to determine the protein concentration of HATMSC2 cells and HATMSC2-MVs. The HATMSC2 cells and HATMSC2-MVs samples were incubated with BCA working reagent for 30 min at 37 °C. The absorbance at 560 nm was measured using the Wallac 1420 Victor2 Microplate Reader (Perkin Elmer, Waltham, MA, USA). The protein concentration of HATMSC2 cells was assessed at 2238 µg/mL while for HATMSC2-MVs was 225 µg/mL. The 50 µg of lysed HATMSC2 cells and HATMSC2-MVs were incubated on a protein membrane according to the manufacturer's instructions. Briefly, 2.0 mL of blocking buffer was applied on the membrane and incubated 30 min at room temperature. Then, 1.0 mL of HATMSC2 cells and cell-derived microvesicles were incubated with a membrane overnight at 4 °C. Following a series of washes, a biotinylated antibody cocktail was applied on the membrane and incubated for 2 h at RT. The unbound antibody was removed by a series of washes, and the membrane was placed in HRP–streptavidin and incubated for 2 h at RT. Following a third series of washes, chemiluminescent detection was performed, and bound proteins were visualized using X-ray film. A comparison of signal intensities was performed using ImageJ software version 2.9.0 (MosaicJ, Philippe Thevenaz)

where relative differences in the expression levels of each analyzed sample were measured and normalized to the intensities of positive control using the Protein Array Analyzer plugin. Automatic analysis of obtained data was calculated using Microsoft® (Office 16) Excel-based Analysis Software Tool for Human Apoptosis kit. The results were calculated as a percentage of expression, where positive control was set to 100% and negative control was set to 0% (relative expression). The cutoff line was set to 5%. All results above 5% were considered real expressions.

4.8. Statistical Analysis

All graphs were prepared using GraphPad Prism version 7 (GraphPad Software Inc., San Diego, CA, USA). The statistical analysis was performed using the Mann–Whitney U test and one-way analysis of variance (ANOVA) followed by multiple comparison procedures (Dunnet's test). A significantly different value was considered when $p < 0.05$.

5. Conclusions

In this study, we demonstrate the possibility to inhibit OvCa cells growth and apoptosis induction after exposure of OvCa cells on HATMSC2-MVs treatment. MVs isolated from adipose tissue induced the ovarian cancer cell death in 2D and 3D cellular models. The Membrane-Based Protein Array revealed differences in the expression of analyzed factors between HATMSC2-MVs and parental cells HATMSC2. The present study adds novel observations for potential activity of HATMSC-MVs on primary OvCa cells. HATMSC-MVs with high probability activate the apoptosis process in the target ovarian cancer cells because they are able to release a number of pro-apoptotic factors (e.g., bad, BIM, caspase 3, p27, p53, and others), and this process does not allow for spontaneous repair of damaged cancer cells despite the simultaneous release of anti-apoptotic proteins (e.g., bcl-2, HSP-60, p21, and others) by HATMSC2-MVs. In this study, we used unmodified HATMSC2-MVs that carries bioactive factors known as factors involved in apoptosis. The results suggest that the anti-cancer effect of HATMSC2-MVs is mainly contributed by delivery of molecules that induce cell cycle arrest and apoptosis (p21, tumor suppressor p53, executor caspase 3) and proapoptotic regulators (bad, BIM, Fas, FasL, p27, TRAIL-R1, TRAIL-R2). However, to determine which bioactive factors released by HATMSC2-MVs are critical for the ovarian cancer cell sensitivity to HATMSC2-MVs, further studies by using the neutralizing antibodies or siRNA need to be performed. Moreover, modification of parental MSCs and subsequent application of their derivates in a form of MVs, EVs, or conditioned medium can enhance anti-cancer effects and may serve as a biotherapy, supporting standard procedures.

Supplementary Materials: The supporting information can be downloaded at: https://www.mdpi.com/article/10.3390/ijms242115862/s1.

Author Contributions: Conceptualization, A.K. and A.S.; methodology, A.S., A.B.-P., G.C. and A.K.; formal analysis, A.S., A.B.-P. and A.K.; investigation, A.S. and A.B.-P.; resources, M.M. and R.S.; data curation, A.S., A.B.-P. and A.K.; visualization, A.S. and G.C.; supervision, A.K.; funding acquisition, A.K.; writing—original draft preparation, A.S., A.B.-P. and A.K.; writing—review and editing, A.K. All authors have read and agreed to the published version of the manuscript.

Funding: This research received no external funding.

Institutional Review Board Statement: The study was conducted in accordance with the Declaration of Helsinki, and approved by the Bioethics Committee at the Medical University of Wroclaw (protocol No. KB- 489/2020).

Informed Consent Statement: Informed consent was obtained from all subjects involved in the study.

Data Availability Statement: All data generated or analyzed during this study are included in this article.

Acknowledgments: G.C. was supported by the National Science Centre Poland, grant no 2019/35/B/NZ6/03748.

Conflicts of Interest: The authors declare no conflict of interest.

References

1. Database, W.M. Deaths by Sex and Age Group for a Selected Country or Area and Year. Available online: https://platform.who.int/mortality/themes/theme-details/topics/indicator-groups/indicator-group-details/MDB/ovary-cancer (accessed on 6 October 2023).
2. Torre, L.A.; Trabert, B.; DeSantis, C.E.; Miller, K.D.; Samimi, G.; Runowicz, C.D.; Gaudet, M.M.; Jemal, A.; Siegel, R.L. Ovarian cancer statistics, 2018. *CA Cancer J. Clin.* **2018**, *68*, 284–296. [CrossRef] [PubMed]
3. Arora, T.; Mullangi, S.; Lekkala, M.R. Ovarian Cancer. In *StatPearls*; StatPearls Publishing: Treasure Island, FL, USA, 2023.
4. Al-Alem, L.F.; Pandya, U.M.; Baker, A.T.; Bellio, C.; Zarrella, B.D.; Clark, J.; DiGloria, C.M.; Rueda, B.R. Ovarian cancer stem cells: What progress have we made? *Int. J. Biochem. Cell Biol.* **2019**, *107*, 92–103. [CrossRef] [PubMed]
5. Cortez, A.J.; Tudrej, P.; Kujawa, K.A.; Lisowska, K.M. Advances in ovarian cancer therapy. *Cancer Chemother. Pharmacol.* **2018**, *81*, 17–38. [CrossRef] [PubMed]
6. Bregenzer, M.E.; Horst, E.N.; Mehta, P.; Novak, C.M.; Repetto, T.; Mehta, G. The Role of Cancer Stem Cells and Mechanical Forces in Ovarian Cancer Metastasis. *Cancers* **2019**, *11*, 1008. [CrossRef] [PubMed]
7. Barzegar Behrooz, A.; Syahir, A.; Ahmad, S. CD133: Beyond a cancer stem cell biomarker. *J. Drug Target.* **2019**, *27*, 257–269. [CrossRef] [PubMed]
8. Thapa, R.; Wilson, G.D. The Importance of CD44 as a Stem Cell Biomarker and Therapeutic Target in Cancer. *Stem Cells Int.* **2016**, *2016*, 2087204. [CrossRef]
9. Foster, B.M.; Zaidi, D.; Young, T.R.; Mobley, M.E.; Kerr, B.A. CD117/c-kit in Cancer Stem Cell-Mediated Progression and Therapeutic Resistance. *Biomedicines* **2018**, *6*, 31. [CrossRef]
10. Ginestier, C.; Hur, M.H.; Charafe-Jauffret, E.; Monville, F.; Dutcher, J.; Brown, M.; Jacquemier, J.; Viens, P.; Kleer, C.G.; Liu, S.; et al. ALDH1 is a marker of normal and malignant human mammary stem cells and a predictor of poor clinical outcome. *Cell Stem Cell* **2007**, *1*, 555–567. [CrossRef]
11. Clark, D.W.; Palle, K. Aldehyde dehydrogenases in cancer stem cells: Potential as therapeutic targets. *Ann. Transl. Med.* **2016**, *4*, 518. [CrossRef]
12. Christodoulou, I.; Goulielmaki, M.; Devetzi, M.; Panagiotidis, M.; Koliakos, G.; Zoumpourlis, V. Mesenchymal stem cells in preclinical cancer cytotherapy: A systematic review. *Stem Cell Res. Ther.* **2018**, *9*, 336. [CrossRef]
13. Klimczak, A.; Kozlowska, U. Mesenchymal Stromal Cells and Tissue-Specific Progenitor Cells: Their Role in Tissue Homeostasis. *Stem Cells Int.* **2016**, *2016*, 4285215. [CrossRef]
14. Tetta, C.; Ghigo, E.; Silengo, L.; Deregibus, M.C.; Camussi, G. Extracellular vesicles as an emerging mechanism of cell-to-cell communication. *Endocrine* **2013**, *44*, 11–19. [CrossRef] [PubMed]
15. Klimczak, A. Mesenchymal Stem/Progenitor Cells and Their Derivates in Tissue Regeneration. *Int. J. Mol. Sci.* **2022**, *23*, 6652. [CrossRef] [PubMed]
16. Bruno, S.; Collino, F.; Deregibus, M.C.; Grange, C.; Tetta, C.; Camussi, G. Microvesicles derived from human bone marrow mesenchymal stem cells inhibit tumor growth. *Stem Cells Dev.* **2013**, *22*, 758–771. [CrossRef] [PubMed]
17. Li, T.; Xia, M.; Gao, Y.; Chen, Y.; Xu, Y. Human umbilical cord mesenchymal stem cells: An overview of their potential in cell-based therapy. *Expert Opin. Biol. Ther.* **2015**, *15*, 1293–1306. [CrossRef]
18. Melzer, C.; von der Ohe, J.; Hass, R. MSC stimulate ovarian tumor growth during intercellular communication but reduce tumorigenicity after fusion with ovarian cancer cells. *Cell Commun. Signal.* **2018**, *16*, 67. [CrossRef] [PubMed]
19. Storti, G.; Scioli, M.G.; Kim, B.S.; Terriaca, S.; Fiorelli, E.; Orlandi, A.; Cervelli, V. Mesenchymal Stem Cells in Adipose Tissue and Extracellular Vesicles in Ovarian Cancer Patients: A Bridge toward Metastatic Diffusion or a New Therapeutic Opportunity? *Cells* **2021**, *10*, 2117. [CrossRef] [PubMed]
20. Jahani, S.; Zare, N.; Mirzaei, Y.; Arefnezhad, R.; Zarei, H.; Goleij, P.; Bagheri, N. Mesenchymal stem cells and ovarian cancer: Is there promising news? *J. Cell. Biochem.* **2023**, *124*, 1437–1448. [CrossRef]
21. Szyposzynska, A.; Bielawska-Pohl, A.; Krawczenko, A.; Doszyn, O.; Paprocka, M.; Klimczak, A. Suppression of Ovarian Cancer Cell Growth by AT-MSC Microvesicles. *Int. J. Mol. Sci.* **2020**, *21*, 9143. [CrossRef]
22. Camussi, G.; Deregibus, M.C.; Bruno, S.; Cantaluppi, V.; Biancone, L. Exosomes/microvesicles as a mechanism of cell-to-cell communication. *Kidney Int.* **2010**, *78*, 838–848. [CrossRef]
23. Nawaz, M.; Fatima, F.; Vallabhaneni, K.C.; Penfornis, P.; Valadi, H.; Ekstrom, K.; Kholia, S.; Whitt, J.D.; Fernandes, J.D.; Pochampally, R.; et al. Extracellular Vesicles: Evolving Factors in Stem Cell Biology. *Stem Cells Int.* **2016**, *2016*, 1073140. [CrossRef] [PubMed]
24. Kalamegam, G.; Sait, K.H.W.; Ahmed, F.; Kadam, R.; Pushparaj, P.N.; Anfinan, N.; Rasool, M.; Jamal, M.S.; Abu-Elmagd, M.; Al-Qahtani, M. Human Wharton's Jelly Stem Cell (hWJSC) Extracts Inhibit Ovarian Cancer Cell Lines OVCAR3 and SKOV3 in vitro by Inducing Cell Cycle Arrest and Apoptosis. *Front. Oncol.* **2018**, *8*, 592. [CrossRef] [PubMed]

25. Du, T.; Ju, G.; Wu, S.; Cheng, Z.; Cheng, J.; Zou, X.; Zhang, G.; Miao, S.; Liu, G.; Zhu, Y. Microvesicles derived from human Wharton's jelly mesenchymal stem cells promote human renal cancer cell growth and aggressiveness through induction of hepatocyte growth factor. *PLoS ONE* **2014**, *9*, e96836. [CrossRef] [PubMed]
26. Lupia, M.; Angiolini, F.; Bertalot, G.; Freddi, S.; Sachsenmeier, K.F.; Chisci, E.; Kutryb-Zajac, B.; Confalonieri, S.; Smolenski, R.T.; Giovannoni, R.; et al. CD73 Regulates Stemness and Epithelial-Mesenchymal Transition in Ovarian Cancer-Initiating Cells. *Stem Cell Rep.* **2018**, *10*, 1412–1425. [CrossRef]
27. Bai, S.; Zhu, W.; Coffman, L.; Vlad, A.; Schwartz, L.E.; Elishaev, E.; Drapkin, R.; Buckanovich, R.J. CD105 Is Expressed in Ovarian Cancer Precursor Lesions and Is Required for Metastasis to the Ovary. *Cancers* **2019**, *11*, 1710. [CrossRef]
28. Parte, S.C.; Batra, S.K.; Kakar, S.S. Characterization of stem cell and cancer stem cell populations in ovary and ovarian tumors. *J. Ovarian Res.* **2018**, *11*, 69. [CrossRef]
29. Tao, Y.; Li, H.; Huang, R.; Mo, D.; Zeng, T.; Fang, M.; Li, M. Clinicopathological and Prognostic Significance of Cancer Stem Cell Markers in Ovarian Cancer Patients: Evidence from 52 Studies. *Cell Physiol. Biochem.* **2018**, *46*, 1716–1726. [CrossRef]
30. Gu, Y.; Zhou, G.; Tang, X.; Shen, F.; Ding, J.; Hua, K. The biological roles of CD24 in ovarian cancer: Old story, but new tales. *Front. Immunol.* **2023**, *14*, 1183285. [CrossRef]
31. Robinson, M.; Gilbert, S.F.; Waters, J.A.; Lujano-Olazaba, O.; Lara, J.; Alexander, L.J.; Green, S.E.; Burkeen, G.A.; Patrus, O.; Sarwar, Z.; et al. Characterization of SOX2, OCT4 and NANOG in Ovarian Cancer Tumor-Initiating Cells. *Cancers* **2021**, *13*, 262. [CrossRef]
32. Zhang, Q.; Han, Z.; Zhu, Y.; Chen, J.; Li, W. The Role and Specific Mechanism of OCT4 in Cancer Stem Cells: A Review. *Int. J. Stem Cells* **2020**, *13*, 312–325. [CrossRef]
33. Xie, W.; Yu, J.; Yin, Y.; Zhang, X.; Zheng, X.; Wang, X. OCT4 induces EMT and promotes ovarian cancer progression by regulating the PI3K/AKT/mTOR pathway. *Front. Oncol.* **2022**, *12*, 876257. [CrossRef]
34. Wang, X.; Ji, X.; Chen, J.; Yan, D.; Zhang, Z.; Wang, Q.; Xi, X.; Feng, Y. SOX2 enhances the migration and invasion of ovarian cancer cells via Src kinase. *PLoS ONE* **2014**, *9*, e99594. [CrossRef] [PubMed]
35. Wen, Y.; Hou, Y.; Huang, Z.; Cai, J.; Wang, Z. SOX2 is required to maintain cancer stem cells in ovarian cancer. *Cancer Sci.* **2017**, *108*, 719–731. [CrossRef] [PubMed]
36. Lee, M.; Nam, E.J.; Kim, S.W.; Kim, S.; Kim, J.H.; Kim, Y.T. Prognostic impact of the cancer stem cell-related marker NANOG in ovarian serous carcinoma. *Int. J. Gynecol. Cancer* **2012**, *22*, 1489–1496. [CrossRef] [PubMed]
37. Reyes-Gonzalez, J.M.; Armaiz-Pena, G.N.; Mangala, L.S.; Valiyeva, F.; Ivan, C.; Pradeep, S.; Echevarria-Vargas, I.M.; Rivera-Reyes, A.; Sood, A.K.; Vivas-Mejia, P.E. Targeting c-MYC in Platinum-Resistant Ovarian Cancer. *Mol. Cancer Ther.* **2015**, *14*, 2260–2269. [CrossRef]
38. Nurmik, M.; Ullmann, P.; Rodriguez, F.; Haan, S.; Letellier, E. In search of definitions: Cancer-associated fibroblasts and their markers. *Int. J. Cancer* **2020**, *146*, 895–905. [CrossRef]
39. Usman, S.; Waseem, N.H.; Nguyen, T.K.N.; Mohsin, S.; Jamal, A.; Teh, M.T.; Waseem, A. Vimentin Is at the Heart of Epithelial Mesenchymal Transition (EMT) Mediated Metastasis. *Cancers* **2021**, *13*, 4985. [CrossRef]
40. Dong, P.; Xiong, Y.; Watari, H.; Hanley, S.J.; Konno, Y.; Ihira, K.; Yamada, T.; Kudo, M.; Yue, J.; Sakuragi, N. MiR-137 and miR-34a directly target Snail and inhibit EMT, invasion and sphere-forming ability of ovarian cancer cells. *J. Exp. Clin. Cancer Res.* **2016**, *35*, 132. [CrossRef]
41. Landen, C.N., Jr.; Goodman, B.; Katre, A.A.; Steg, A.D.; Nick, A.M.; Stone, R.L.; Miller, L.D.; Mejia, P.V.; Jennings, N.B.; Gershenson, D.M.; et al. Targeting aldehyde dehydrogenase cancer stem cells in ovarian cancer. *Mol. Cancer Ther.* **2010**, *9*, 3186–3199. [CrossRef]
42. Zhang, X.; Tu, H.; Yang, Y.; Fang, L.; Wu, Q.; Li, J. Mesenchymal Stem Cell-Derived Extracellular Vesicles: Roles in Tumor Growth, Progression, and Drug Resistance. *Stem Cells Int.* **2017**, *2017*, 1758139. [CrossRef]
43. Wang, S.; El-Deiry, W.S. TRAIL and apoptosis induction by TNF-family death receptors. *Oncogene* **2003**, *22*, 8628–8633. [CrossRef] [PubMed]
44. Shamili, F.H.; Bayegi, H.R.; Salmasi, Z.; Sadri, K.; Mahmoudi, M.; Kalantari, M.; Ramezani, M.; Abnous, K. Exosomes derived from TRAIL-engineered mesenchymal stem cells with effective anti-tumor activity in a mouse melanoma model. *Int. J. Pharm.* **2018**, *549*, 218–229. [CrossRef] [PubMed]
45. de Araujo Farias, V.; O'Valle, F.; Lerma, B.A.; Ruiz de Almodovar, C.; Lopez-Penalver, J.J.; Nieto, A.; Santos, A.; Fernandez, B.I.; Guerra-Librero, A.; Ruiz-Ruiz, M.C.; et al. Human mesenchymal stem cells enhance the systemic effects of radiotherapy. *Oncotarget* **2015**, *6*, 31164–31180. [CrossRef] [PubMed]
46. Yuan, Z.; Kolluri, K.K.; Gowers, K.H.; Janes, S.M. TRAIL delivery by MSC-derived extracellular vesicles is an effective anticancer therapy. *J. Extracell. Vesicles* **2017**, *6*, 1265291. [CrossRef] [PubMed]
47. Chen, F.; Zhong, X.; Dai, Q.; Li, K.; Zhang, W.; Wang, J.; Zhao, Y.; Shen, J.; Xiao, Z.; Xing, H.; et al. Human Umbilical Cord MSC Delivered-Soluble TRAIL Inhibits the Proliferation and Promotes Apoptosis of B-ALL Cell In Vitro and In Vivo. *Pharmaceuticals* **2022**, *15*, 1391. [CrossRef]
48. Lu, Y.R.; Yuan, Y.; Wang, X.J.; Wei, L.L.; Chen, Y.N.; Cong, C.; Li, S.F.; Long, D.; Tan, W.D.; Mao, Y.Q.; et al. The growth inhibitory effect of mesenchymal stem cells on tumor cells in vitro and in vivo. *Cancer Biol. Ther.* **2008**, *7*, 245–251. [CrossRef]
49. Gartel, A.L.; Radhakrishnan, S.K. Lost in transcription: p21 repression, mechanisms, and consequences. *Cancer Res.* **2005**, *65*, 3980–3985. [CrossRef]

50. Zhang, Y.; Fujita, N.; Tsuruo, T. Caspase-mediated cleavage of p21Waf1/Cip1 converts cancer cells from growth arrest to undergoing apoptosis. *Oncogene* **1999**, *18*, 1131–1138. [CrossRef]
51. Liao, J.; Qian, F.; Tchabo, N.; Mhawech-Fauceglia, P.; Beck, A.; Qian, Z.; Wang, X.; Huss, W.J.; Lele, S.B.; Morrison, C.D.; et al. Ovarian cancer spheroid cells with stem cell-like properties contribute to tumor generation, metastasis and chemotherapy resistance through hypoxia-resistant metabolism. *PLoS ONE* **2014**, *9*, e84941. [CrossRef]
52. Parashar, D.; Geethadevi, A.; Mittal, S.; McAlarnen, L.A.; George, J.; Kadamberi, I.P.; Gupta, P.; Uyar, D.S.; Hopp, E.E.; Drendel, H.; et al. Patient-Derived Ovarian Cancer Spheroids Rely on PI3K-AKT Signaling Addiction for Cancer Stemness and Chemoresistance. *Cancers* **2022**, *14*, 958. [CrossRef]
53. Arias-Diaz, A.E.; Ferreiro-Pantin, M.; Barbazan, J.; Perez-Beliz, E.; Ruiz-Banobre, J.; Casas-Arozamena, C.; Muinelo-Romay, L.; Lopez-Lopez, R.; Vilar, A.; Curiel, T.; et al. Ascites-Derived Organoids to Depict Platinum Resistance in Gynaecological Serous Carcinomas. *Int. J. Mol. Sci.* **2023**, *24*, 13208. [CrossRef]
54. Melzer, C.; Ohe, J.V.; Hass, R. Anti-Tumor Effects of Exosomes Derived from Drug-Incubated Permanently Growing Human MSC. *Int. J. Mol. Sci.* **2020**, *21*, 7311. [CrossRef]
55. Wang, X.; Jiang, L.; Liu, Q. miR-18a-5p derived from mesenchymal stem cells-extracellular vesicles inhibits ovarian cancer cell proliferation, migration, invasion, and chemotherapy resistance. *J. Transl. Med.* **2022**, *20*, 258. [CrossRef] [PubMed]
56. Reza, A.; Choi, Y.J.; Yasuda, H.; Kim, J.H. Human adipose mesenchymal stem cell-derived exosomal-miRNAs are critical factors for inducing anti-proliferation signalling to A2780 and SKOV-3 ovarian cancer cells. *Sci. Rep.* **2016**, *6*, 38498. [CrossRef]
57. Bar, J.K.; Harlozinska, A. Morphological and phenotypic characterization of a new established ovarian carcinoma cell line (OvBH-1). *Anticancer Res.* **2000**, *20*, 2975–2980. [PubMed]
58. Karabon, L.; Markiewicz, M.; Kosmaczewska, A.; Partyka, A.; Pawlak-Adamska, E.; Tomkiewicz, A.; Ciszak, L.; Jagoda, K.; Dzierzak-Mietla, M.; Kyrcz-Krzemien, S.; et al. Pretransplant donor and recipient CTLA-4 mRNA and protein levels as a prognostic marker for aGvHD in allogeneic hematopoietic stem cell transplantation. *Immunol. Lett.* **2015**, *165*, 52–59. [CrossRef] [PubMed]
59. Thery, C.; Witwer, K.W.; Aikawa, E.; Alcaraz, M.J.; Anderson, J.D.; Andriantsitohaina, R.; Antoniou, A.; Arab, T.; Archer, F.; Atkin-Smith, G.K.; et al. Minimal information for studies of extracellular vesicles 2018 (MISEV2018): A position statement of the International Society for Extracellular Vesicles and update of the MISEV2014 guidelines. *J. Extracell. Vesicles* **2018**, *7*, 1535750. [CrossRef]
60. Beyeler, J.; Schnyder, I.; Katsaros, C.; Chiquet, M. Accelerated wound closure in vitro by fibroblasts from a subgroup of cleft lip/palate patients: Role of transforming growth factor-alpha. *PLoS ONE* **2014**, *9*, e111752. [CrossRef]

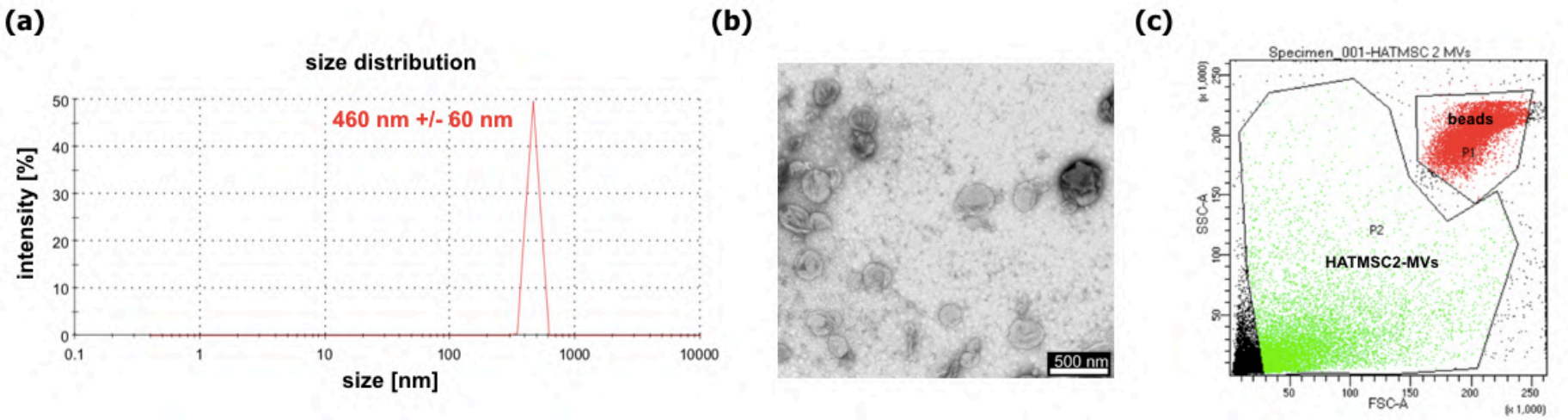

Figure S1. HATMSC2-MVs characteristics. **(a)** Representative histogram from dynamic light scattering (DLS) analysis. **(b)** Representative images from transmission electron microscopy (TEM) imaging. (c) Dot plot from flow cytometry analysis illustrating the forward scatter (FSC) versus side scatter (SSC). P1 represents counting beads, P2 represents HATMSC2-MVs. Bar represents 500 nm HATMSC2-MVs—microvesicles derived from immortalized human mesenchymal stem cells of adipose tissue origin.

Table S1. List of primary antibodies

Antigen	Host	Class of antibody	Clone	Company	Dilution	Incubation
Human PDGFRa	Mouse	Monoclonal	C-9	Santa Cruz	1:100	1h, Room Temperature (RT)
Human CD44	Rabbit	Polyclonal		Thermo Fisher Scientific	1:100	1h, RT
Human Fibroblast activation protein (FAP)	Mouse	Monoclonal	F11-24	Thermo Fisher Scientific	1:100	Overnight (O/N), 4^0C
Human Snail1	Rabbit	Polyclonal		Bio Site	1:100	O/N, 4^0C
Human Oct4	Rabbit	Polyclonal		Thermo Fisher Scientific	1:100	O/N, 4^0C
Human Sox2	Mouse	Monoclonal	20 G5	Thermo Fisher Scientific	1:100	O/N, 4^0C
Human Nanog	Rabbit	Polyclonal		Thermo Fisher Scientific	1:100	O/N, 4^0C
Human ALDH1	Rabbit	Polyclonal		Thermo Fisher Scientific	1:200	1h, RT
Human vimentin	Mouse	Monoclonal	V9	Thermo Fisher Scientific	1:100	1h, RT
Human c-kit (CD177)	Mouse	Monoclonal	K45	Thermo Fisher Scientific	1:50	O/N, 4^0C

Table S2. List of secondary antibodies

Antigen	Host	Class of antibody	Flouorophore	Company	Dilution	Incubation
F-actin		Phalloidin	Alexa Fluor 488™	Thermo Fisher Scientific	1:400	45min, RT
Mouse IgG	Goat	Polyclonal	Alexa Fluor 488™	Thermo Fisher Scientific	1:700	45min, RT
Mouse IgG	Goat	Polyclonal	Alexa Fluor 647™	Thermo Fisher Scientific	1:700	45min, RT
Rabbit IgG	Goat	Polyclonal	Alexa Fluor 647™	Thermo Fisher Scientific	1:700	45min, RT

International Journal of
Molecular Sciences

MDPI

Article

Comparative Analysis of Primary Ovarian Cancer Cells and Established Cell Lines as a New Tool for Studies on Ovarian Cancer Cell Complexity

Agnieszka Szyposzynska [1], Aleksandra Bielawska-Pohl [1], Maria Paprocka [1], Julia Bar [2], Marek Murawski [3] and Aleksandra Klimczak [1,*]

[1] Laboratory of Biology of Stem and Neoplastic Cells, Hirszfeld Institute of Immunology and Experimental Therapy, Polish Academy of Sciences, 53-114 Wroclaw, Poland; agnieszka.szyposzynska@hirszfeld.pl (A.S.); aleksandra.bielawska-pohl@hirszfeld.pl (A.B.-P.)
[2] Department of Immunopathology and Molecular Biology, Wroclaw Medical University, 50-556 Wroclaw, Poland; julia.bar@umw.edu.pl
[3] 1st Department of Gynecology and Obstetrics, Wroclaw Medical University, 50-599 Wroclaw, Poland; marek.murawski@umw.edu.pl
* Correspondence: aleksandra.klimczak@hirszfeld.pl

Abstract: Primary cancer cells reflect the genetic background and phenotype of a tumor. Immortalized cells with higher proliferation activity have an advantage over primary cells. The aim of the study was to immortalize the primary ovarian cancer (OvCa) cells using the plasmid-carrying human telomerase reverse transcriptase (hTERT) gene and compare their phenotype and biological activity with the primary cells. The primary OvCa3 A and OvCa7 A cells were isolated from the ascitic fluid of two high-grade serous ovarian cancer patients and were characterized using immunocytochemical methods, flow cytometry, real-time RT-PCR, Western blot, metabolic activity, and migratory potential. Both immortalized ovarian cancer cell lines mirrored the phenotype of primary cancer cells, albeit with modifications. The OvCa3 A hTERT cells kept the mesenchymal stem cell phenotype of CD73/CD90/CD105-positivity and were CD133-negative, whereas the cell population of OvCa7 A hTERT lost CD73 expression, but almost 90% of cells expressed the CD133 characteristic for the CSCs phenotype. Immortalized OvCa cells differed in gene expression level with respect to *Sox2* and *Oct4*, which was associated with stemness properties. The OvCa7 A hTERT cells showed higher metabolic and migratory activity and ALDH1 expression than the corresponding primary OvCa cells. Both primary and immortalized cell lines were able to form spheroids. The newly established unique immortalized cell line OvCa7 A hTERT, with the characteristic of a serous ovarian cancer malignancy feature, and with the accumulation of the p53, Pax8, and overexpression of the CD133 and CD44 molecules, may be a useful tool for research on therapeutic approaches, especially those targeting CSCs in ovarian cancer and in preclinical 2D and 3D models.

Keywords: ovarian cancer; primary cells; immortalization; cell line; cancer stem cells; CD133

Citation: Szyposzynska, A.; Bielawska-Pohl, A.; Paprocka, M.; Bar, J.; Murawski, M.; Klimczak, A. Comparative Analysis of Primary Ovarian Cancer Cells and Established Cell Lines as a New Tool for Studies on Ovarian Cancer Cell Complexity. *Int. J. Mol. Sci.* **2024**, *25*, 5384. https://doi.org/10.3390/ijms25105384

Academic Editor: Tomoyasu Sugiyama

Received: 9 April 2024
Revised: 10 May 2024
Accepted: 13 May 2024
Published: 15 May 2024

1. Introduction

Ovarian cancer is gathering increased interest among clinicians and scientists due to high mortality and poor prognosis [1]. Serous ovarian cancer, divided into low-grade and high-grade carcinoma, is one of the most frequently diagnosed ovarian epithelial carcinomas [2]. The biological behavior of high-grade serous ovarian cancer, such as rapid growth, high aggressiveness, and chemoresistance, often leads to poor prognosis for patient survival [2]; thus, new therapeutic targets for ovarian cancer treatment are needed [3]. Currently, keen attention is paid to the discovery of rapid screening tests for ovarian cancer and the development of new targeted therapies. For preclinical studies, the ideal source of primary ovarian cancer cells are cells obtained from post-operative tumors

in patients with ovarian cancer. However, such cells are not the optimal candidates for use in experimental studies due to the limited time of their biological activity in vitro. In addition to the isolation of cells from post-operative tumor tissue, ovarian cancer cells are sourced from the ascitic fluid. The ascitic fluid accumulates in the peritoneal cavity during pathological processes under excessive inflammation. The ascitic fluid, a common aspirate in patients with advanced ovarian cancer, consists of not only cancer cells, but also normal cells, such as fibroblasts, mesothelial cells, endothelial cells, immune cells, and blood cells. Moreover, the ascitic fluid contains a variety of growth factors, cytokines, chemokines, and extracellular vesicles that are involved in cell-to-cell communication [4,5].

Primary cells, including cancer cells, are a heterogeneous population of cells that consists of different types of cells isolated from tissues and organs. The primary cells reflect a phenotype, fate, and behavior resembling the cells present in the organisms they are derived from [6]. Primary cells are widely used for drug screening, determining the physiological and pathophysiological processes, or analyzing the signaling pathways present in the cells. However, the disadvantages of using primary cells in research are a limited number of obtained cells and a limited number of cell divisions. In contrast, cell lines are homogenous populations that usually consist of one type of cells. The most distinctive advantages of cell lines are unlimited cell numbers and unlimited cell division. However, cell lines may not reflect all the features that the primary cells have.

Various procedures for obtaining cell lines are used in experimental studies. One such procedure is spontaneous immortalization, which occurs during the numerous passages of primary cells (hundreds of cell passages). An example of spontaneous immortalization is the ovarian cancer OvBH-1 cell line derived from the ascitic fluid of a patient with an ovarian clear-cell adenocarcinoma [7] and a high-grade serous ovarian cancer cell line OVPA8 [8]. Another way to obtain a cell line is to immortalize the cells using vectors carrying telomerase or Simian virus 40 (SV40) genes. Telomerase is an enzyme involved in adding guanine-rich repetitive sequences, thus preventing the telomeres from shortening [9]. The cells have a limited number of cell divisions, 50–70, called the Hyflick limit, after which the cells become senescent and die [10]. Stem cells, as well as neoplastic cells, show high telomerase activity, which is why they are capable of unlimited cell division. SV40 is an oncogenic DNA virus. The SV40 gene encodes large and small tumor antigens (T antigens) responsible for regulatory function [11]. Immortalization occurs via the inhibition of retinoblastoma (Rb) and p53 genes by the SV40 large T antigen [12]. Another way to immortalize cells is to employ telomerase activity for the stabilization of telomere length. Telomerase is constitutively activated in most human cancers, but not (or expressed at very low levels) in somatic cells. Alterations in telomere length result in both the suppression and facilitation of malignant transformation by regulating genomic stability and cell lifespan [13]. Primary cells immortalized with human telomerase reverse transcriptase (hTERT) represent a breakthrough in cell biology research because they combine the in vivo nature of primary cells through the preservation of phenotypic properties with the cell lines' ability to survive continuously in vitro. Moreover, because hTERT, overexpressed in about 90% of tumors, is considered as a direct target of the Wnt/β-catenin signaling pathway, it is involved in the initiation and further progression of cancer [14].

Cancer stem cells (CSCs) are present within the heterogeneous population of cancer cells and are responsible for tumor progression, resistance to chemotherapy and cancer metastasis [15]. CSCs, in addition to the tumor-specific phenotype, are characterized by the presence of markers different from mature cancer cells. The most common marker, CD133 (a cholesterol-binding glycoprotein, prominin), is a marker of stem and progenitor cells [16] that is widely used for the isolation of CSCs from different solid tumors [17]. CD133-positive cells have been documented in ovarian cancer tissues in the context of the expression of p-p53(Ser20) and carcinoma stem cell biomarkers and in the fraction of the OvBH-1 cell line [18]. The co-expression of CD133 and other CSC markers, such as the CD44 transmembrane glycoprotein involved in cell-to-cell interactions [19], the heat-stable antigen CD24 that plays a crucial role in cell adhesion and is involved in tumor

metastasis [20], and CD117(c-kit) is observed in studies on ovarian CSCs. Ovarian CSCs play a crucial role in tumor formation and resistance to chemotherapeutics. They also lead to relapse after treatment [21].

Currently, CSCs are extensively studied as a potential target in the treatment of many cancers, including ovarian cancer. In the natural tumor microenvironment, CSCs constitute a small populations of tumor cells usually insufficient for studies on different therapeutic approaches. This study aimed to isolate and characterize primary ovarian cancer cells from the ascitic fluid of patients with high-grade serous ovarian cancer, and afterwards, to establish immortalized human ovarian cancer cell lines with a focus on tumor cells with the CSCs phenotype. The cells were immortalized using a plasmid carrying the human telomerase gene. Finally, the phenotype and functional properties of the immortalized cell lines were characterized to the corresponding primary OvCa cells.

2. Results

2.1. Characteristics of Primary Ovarian Cancer Cells and Immortalized Ovarian Cancer Cells

2.1.1. Cytomorphological Assessment

Morphological features of the primary cellular composition of the ascitic fluid collected from two patients with poorly differentiated (G3) serous ovarian carcinoma and cells after immortalization are presented in Table 1. The cells were classified according to their morphological features describing malignancy, from cells showing typical features of malignancy to cells with atypia. The primary cellular composition of the two cases consists of four cell subpopulations showing different stages of malignancy corresponding to the stage of cancer. In the first case, designated in Table 1 as type 1 cells, the cells were large, round with scant eosinophilic cytoplasm and indistinct cell borders. The nuclei showed variation in size and shape. Chromatin was dense with hyperchromasia (Figure 1a,b). The nuclear–cytoplasmic ratio was increased in a majority of cells (3:1).

Table 1. Cytomorphological features of cells from serous ovarian carcinoma before and after hTERT immortalization.

Cell Characteristics	Type of Ovarian Cell Subpopulation					
	Primary Culture				After Immortalization *	
	Type 1	**Type 2**	**Type 3**	**Type 4**	**Type 1**	**Type 4**
Cell						
Size	Large	Large	Large	Moderate	Large	Moderate
Shape	Round	Round	Round	Oval	Round	Oval
Borders	Indistinct	Indistinct	Distinct	Distinct	Distinct	Distinct
Nucleus						
Shape	Round	Round	Round	Oval	Round	Round
Localization	Central	Central	Central/atopic	Atypical	Central	Central
Hypernucleosis	+	+	–	–	+	–
Heteronucleosis	+	+	+	+	+	+
Hyperchromasia	+	–	–	–	+	+
Polynucleosis	–	–	–	–	–	–
Nucleoli	–	+	–	–	–/+	–
Cytoplasm						
Size	Moderate	Moderate	Large	Moderate	Moderate	Moderate
Staining	E	E	E	B	B	B
Vacuoles	–	single/numerous	numerous	–	–	–
N/C ratio	3:1	1:3	1:6	1:4	2:1	1:3

* After immortalization, ovarian cancer cells corresponding to type 1 and type 4 of primary cells were detected. Abbreviations: (+)—present, (−)—absent, E—Eosinophilic, B—Basophilic, N—nucleus, C—cytoplasm.

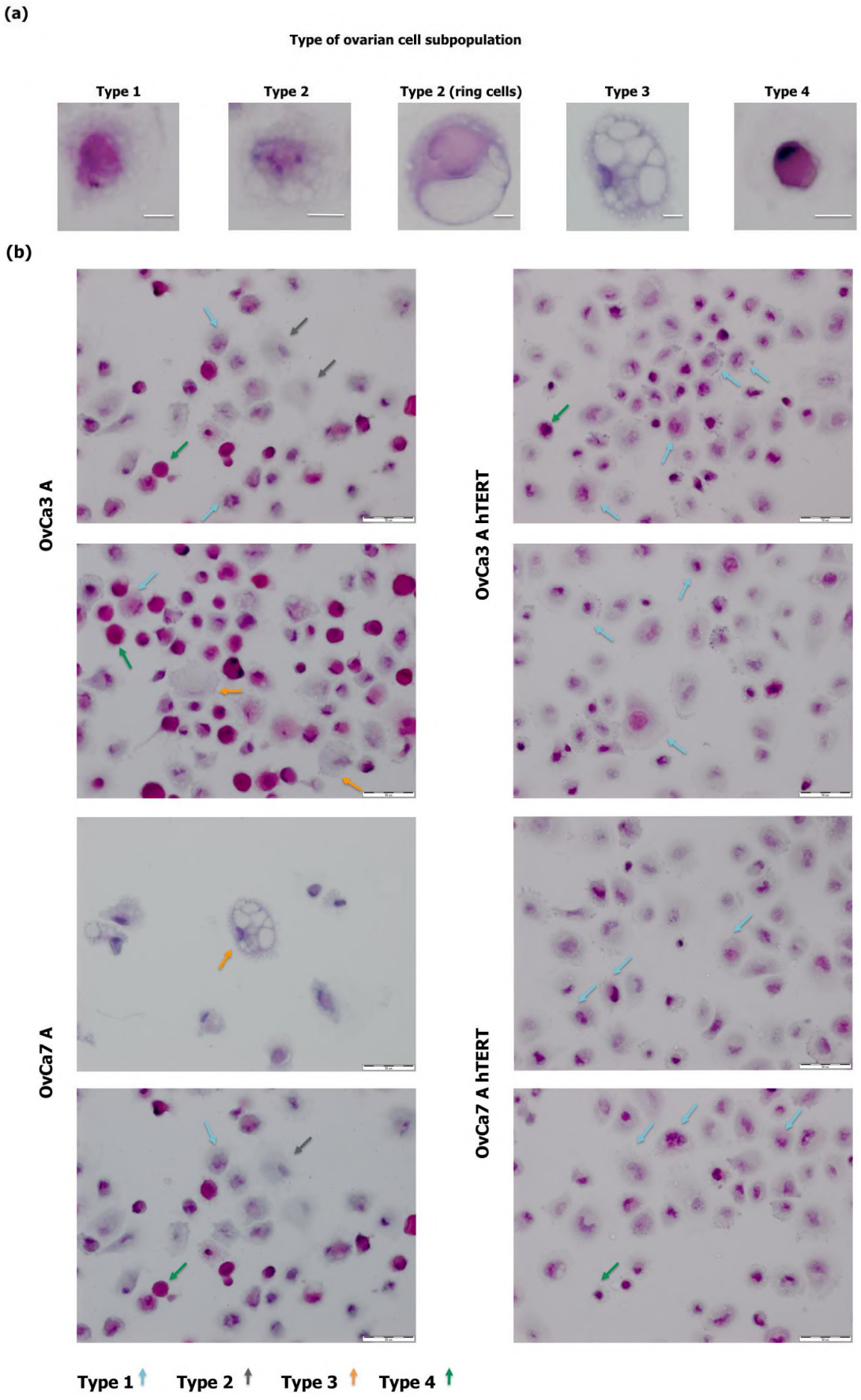

Figure 1. *Cont.*

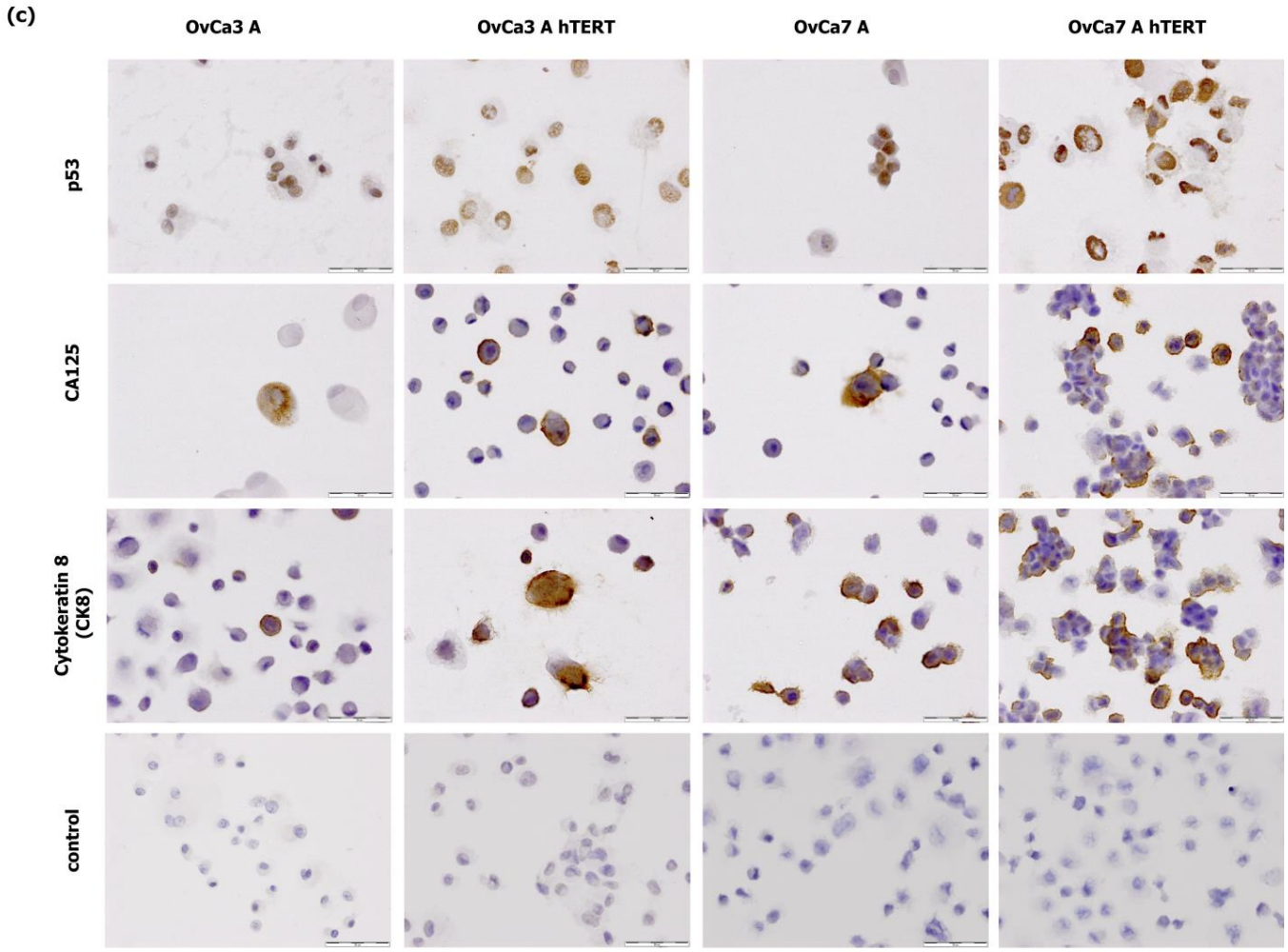

Figure 1. Characteristics of primary ovarian cancer cells and immortalized ovarian cancer cells. Representative images from H and E and immunocytochemical (ICC) staining. (**a**) Representative images of the analyzed types of cells. The bar represents 10 µm. (**b**) The left panel shows images for primary ovarian cancer cells OvCa3 A and OvCa7 A, and the right panel shows images of immortalized ovarian cancer cells OvCa3 A hTERT and OvCa7 A hTERT. The blue arrows indicate type 1 cells, gray arrows indicate type 2 cells, orange arrows indicate type 3 cells, and green arrows indicate type 4 cells. The scale bar represents 50 µm. Abbreviation: H and E—hematoxylin and eosin. (**c**) Representative images from ICC staining. The cell nuclei was stained with hematoxylin (blue), and selected markers were stained with DAB chromogen (brown). The bar represents 50 µm.

Type 2 cells were large, with indistinct borders and eosinophilic cytoplasm, and contained a single large vacuole defined as "ring cells", often observed in serous ovarian carcinoma. There were also cells with numerous vacuoles in the cytoplasm (Figure 1a,b). The nuclei were different in size and shape with nucleoli. Type 3 cells were large, with a large cytoplasm containing numerous small vacuoles. The nuclei were different in size (Figure 1a,b). Type 4 cells were medium-sized with a distinct cell border and basophilic cytoplasm (Figure 1a,b). After cell immortalization, two cell populations were classified in both analyzed cases. The first population showed typical malignant features, as found in type 1 cells before immortalization, and these cells were more homogenous than the type 1 subpopulation of primary cells. A characteristic feature of these cells were their very large nuclei (Figure 1a,b). The second type of immortalized cell subpopulations showed morphological features comparable with type 4 primary cells.

To confirm the morphological features of the cells' malignancy, the p53 immunostaining was performed on both cell lines before and after hTERT immortalization. As showed

in Figure 1c, primary cells isolated from ascitic fluid revealed a heterogeneous pattern of p53 immunostaining. Nuclear accumulation of p53 was observed in a different percentage of primary cells. After hTERT immortalization, the number of p53 immunopositive cells with strong nuclear accumulation increased from 40–50% to 90–100% of cells (Figure 1c). The origin of cells form ovarian epithelial tissue was confirmed with the expression of the CA 125 antigen and CK8. Immortalized cells showed a trend towards higher CA 125 and CK8 expression compared to primary ascitic fluid cells (Figure 1c).

2.1.2. Flow Cytometry Analysis

Flow cytometry analysis was performed to determine the expression of selected mesenchymal stem cell (MSC) markers CD73, CD90, and CD105, marker characteristics for CSCs, such as CD133, CD44, and CD24, as well as marker characteristics for hematopoietic progenitors CD34 and all nucleated hematopoietic cells CD45. The representative histograms are shown in Figure 2a,b.

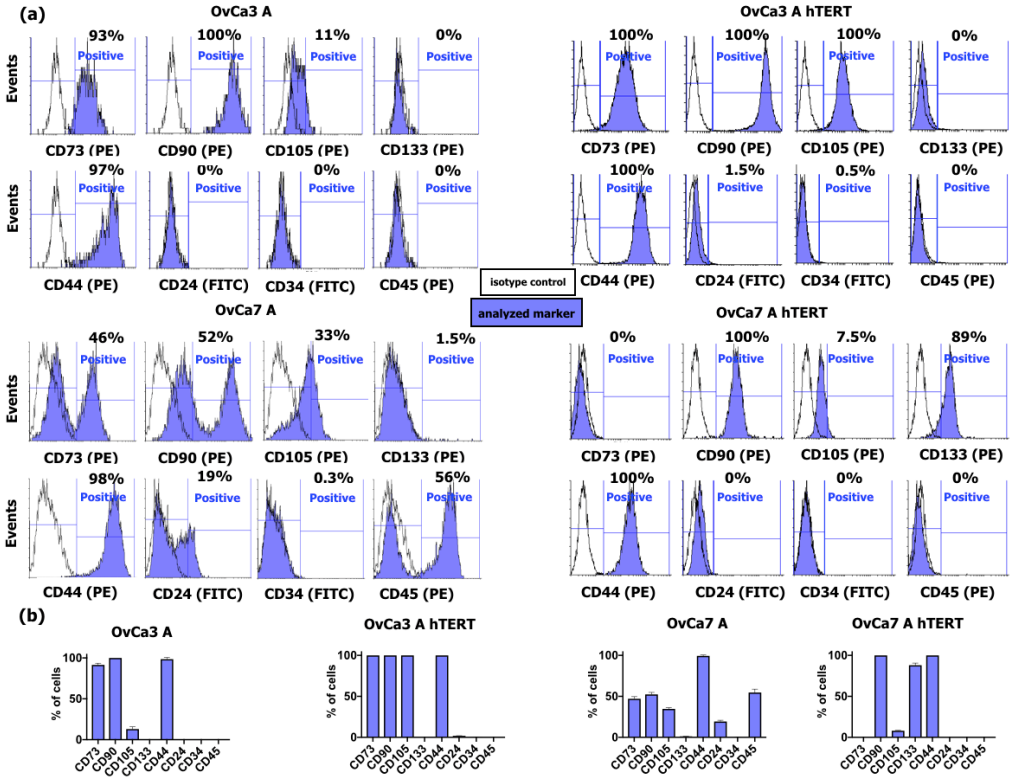

Figure 2. Characteristics of primary ovarian cancer cells and immortalized ovarian cancer cells. (**a**) Representative histograms from flow cytometry analysis. The white histograms refer to isotype controls, and the blue histograms refer to analyzed markers. The left panel shows representative histograms for primary ovarian cancer cells OvCa3 A and OvCa7 A, and the right panel shows representative histograms for immortalized ovarian cancer cells OvCa3 A hTERT and OvCa7 A hTERT. (**b**) The bar charts show the average % of cells positive for selected markers for primary cells and immortalized cells. The data represent mean ± SEM values from three independent experiments.

The primary ovarian cancer cells OvCa3 A were positive for the MSC markers CD73 (91.50% ± 1.50% of the population), CD90 (100.00% of the population), and CD105 (13.00% ± 2.00% of the population). The cells also expressed the CD44 molecule (98.50% ± 1.50% of the population). The analyzed OvCa3 A cells were negative for CSC markers CD133 and CD24 and negative for the hematopoietic markers CD34 and CD45.

In the obtained cell line OvCa3 A hTERT, the entire population of cells was positive for marker characteristics for MSC cells, such as CD73, CD90, and CD105, and for the CD44 marker (each time being 100.00% of the population). A small number of cells expressed

the CSC marker CD24 (1.75% ± 0.16% of the population). Moreover, the cells were negative for the selected CSC markers CD133 and markers characteristic for hematopoietic cells CD34 and CD45 (Figure 2a,b). A summary of the results of flow cytometry and immunofluorescence staining is presented on the heatmap (Figure S1).

The primary ovarian cancer cells OvCa7 A expressed the MSC markers CD73 (47.00% ± 1.52% of the population), CD90 (52.33% ± 1.45%), and CD105 (34.66% ± 0.88%). Importantly, 1.40% ± 0.06% of cells were positive for the CSC markers CD133, 19.33% ± 0.88% of the population expressed the CD24 molecule, and 99.30 ± 0.89% of the population were positive for CD44. The primary OvCa7 A cells were negative for CD34 and positive for CD45 (56.67% ± 3.12% of the population) (Figure 2a,b). The immortalized cells OvCa7 A hTERT did not express the CD73 marker. Only 8.00% ± 0.29% of the population expressed the CD105 marker, whereas the entire population expressed the CD90 marker (100.00% ± 0% of the population). Importantly, the cell population was positive for CD133 (88.00% ± 1.52% of the population) and CD44 (100.00% ± 0% of the population), recognized as CSC markers. However, the cells were negative for another CSC characteristic molecule, CD24. Moreover, the OvCa7 A hTERT cells were negative for the CD34 and CD45 markers (Figure 2a,b).

2.1.3. Immunofluorescence Staining and Microscopic Imaging Results

Immunofluorescence staining and microscopic imaging were used to assess the expression of selected cancer cell markers such as p53, Pax8, and cancer-associated fibroblast markers such as platelet derived growth factor receptor alpha (PDGFRα), fibroblast activation protein (FAP), pluripotency-related transcription factors Oct4, Sox2, and Nanog; and markers characteristic for ovarian CSCs, such as CD133, CD44, c-kit, and the marker of epithelial to mesenchymal transition (EMT), Snail molecule. Furthermore, the cytoskeleton of the cells was visualized using F-actin and vimentin staining.

The primary ovarian cancer cells OvCa3 A were negative for one of either the CAF markers, PDGFRα, transcription factor Sox2, and CSCs marker CD133. On the other hand, the cells were positive for the pluripotency markers Oct4 and Nanog and adhesion molecule CD44. A weak expression of the EMT marker Snail was observed. Moreover, the cells were positive for the c-kit marker, and some cells expressed the CAF marker FAP. The expression of cancer cell markers p53 and Pax8 was detected. F-actin staining visualized stress fibers across the cells. Furthermore, the presence of intermediate filaments was confirmed with vimentin staining (Figure 3).

In the immortalized OvCa3 A hTERT cells, a weak expression of the CD44 marker was observed. The cells were negative for the FAP molecule and CD133. In contrast to the primary cells, the immortalized cells were positive for all pluripotency markers: Oct4, Sox2, and Nanog. Some cells expressed PDGFRα, and a weak expression of the c-kit marker was observed. The immortalized cells strongly expressed p53 protein and Pax8. The vimentin staining visualized the intermediate filaments around cell nuclei.

As with primary ovarian cancer OvCa3 A, the OvCa7 A cells were negative for Sox2, and positive for Oct4 and Nanog. The OvCa7 A cells were positive for CD44 and Snail protein expression, but negative for the CAFs markers PDGFRα and FAP and CD133 molecule and Pax8. The expression of c-kit, nuclear accumulation of mutated p53 protein, and vimentin was also observed (Figure 3).

In the immortalized OvCa7 A hTERT cells, the nuclear expression of CD44 was observed, and the cells were positive for PDGFRα. The OvCa7 A hTERT cells were negative for FAP, and a weak expression of Snail was detected. As OvCa3 A hTERT cells, the OvCa7 A hTERT cells were positive for all the analyzed markers involved in the maintenance of pluripotency: Oct4, Sox2, and Nanog. Furthermore, the expression of c-kit, CSC marker CD133, and nuclear accumulation of mutated p53 and Pax8 was detected (Figure 3).

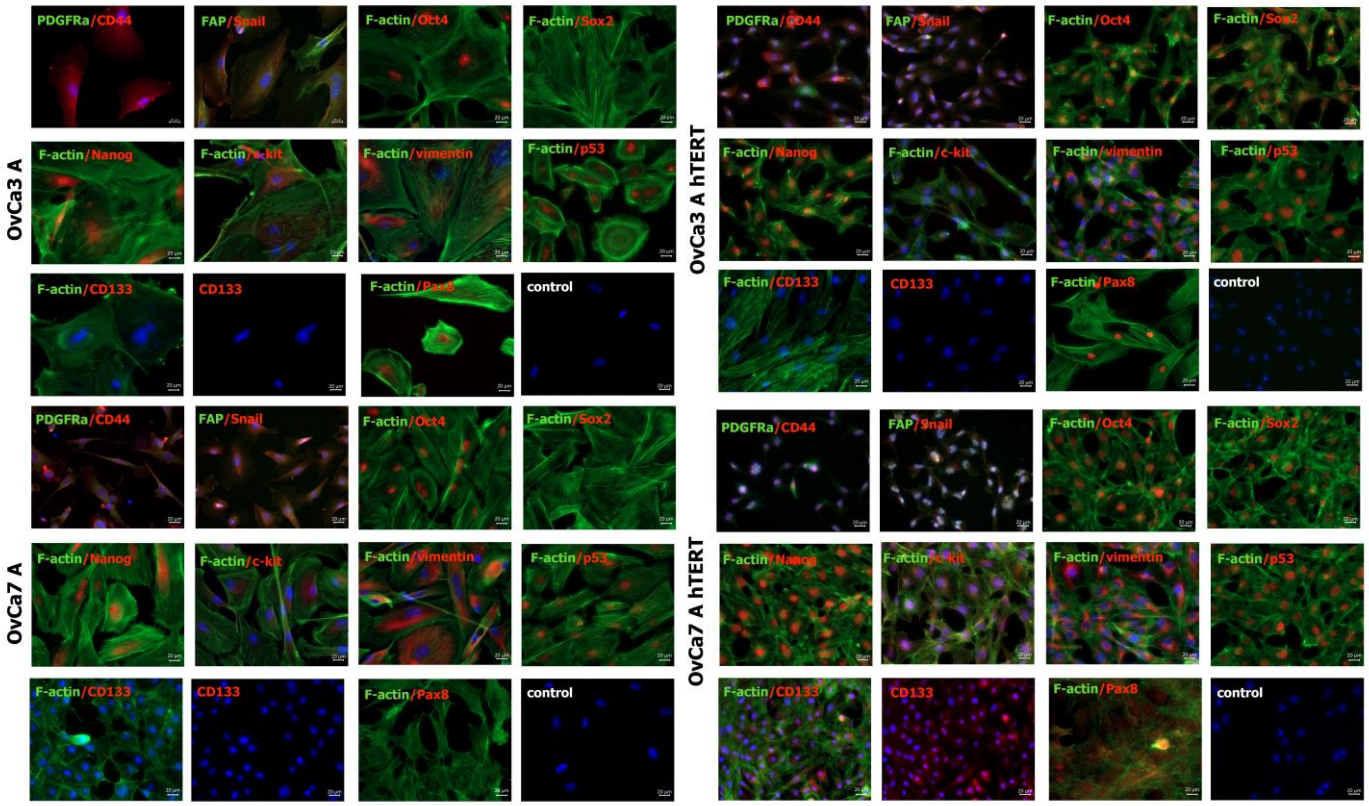

Figure 3. Characteristics of primary ovarian cancer cells and immortalized ovarian cancer cells. Representative fluorescence images. Blue color (DAPI) represents cell nuclei, green color (Alexa Fluor 488) represents selected markers or F-actin, red color (Alexa Fluor 647) represents selected markers. The scale bars represent 20 µm. The left panel shows images for the primary ovarian cancer cells OvCa3 A and OvCa7 A, and the right panel shows images for the immortalized ovarian cancer cells OvCa3 A hTERT and OvCa7 A hTERT. The immunofluorescence staining was performed in duplicate.

2.1.4. Stemness Markers, Cancer Marker Pax8 and CSC Marker CD133 in Immortalized Cell Lines

The RT-PCR was used to determine the presence of transcription factors related to the maintenance of pluripotency: *Oct4*, *Sox2*, protooncogenic molecules *p53*, *p21*, *c-myc*, and CSC marker *CD133*. Both primary cells OvCa3 A and OvCa7 A served as a control for each immortalized cell line, respectively.

In the immortalized OvCa3 A hTERT cells, *Sox2* (RQ 0.130 ± 0.070), *p21* (RQ 0.270 ± 0.001), *p53* (RQ 0.830 ± 0.064), and *c-myc* (RQ 0.869 ± 0.001) expression was downregulated compared to the primary ovarian cancer cells OvCa3 A. Only *Oct4* (RQ 3.263 ± 0.051) was overexpressed in the OvCa3 A hTERT cells (Figure 4a).

In the immortalized OvCa7 A hTERT cells, *Sox2* (RQ 3.819 ± 0.189) and *p53* (RQ 1.466 ± 0.110) expression was upregulated compared to the primary ovarian cancer cells OvCa7 A. In contrast, the expression of *Oct4* (RQ 0.188 ± 0.051), *c-myc* (RQ 0.649 ± 0.092), and *p21* (RQ 0.019 ± 0.004) in the immortalized OvCa7 A hTERT cells was downregulated (Figure 4a).

The expression of CD133 was undetermined in primary OvCa3 A and in immortalized OvCa3 A hTERT. An important observation was that the relative expression of CD133 in OvCa7 A hTERT, which was (RQ 2334 ± 922) over two thousand times higher compared to the primary OvCa7 A cells. To confirm the expression of the CD133 protein, Western blot analysis was performed in the two analyzed immortalized cell lines. The results confirmed that the cells from the OvCa3A hTERT cell line did not express the CD133 molecule, whereas the cells from OvCa7 A hTERT were strongly positive for the CD133 marker (Figures 4b and S2). Both cell lines OvCa3 A hTERT and OvCa7 A hTERT expressed

Pax8 (Figures 4c and S3). The CD133 relative expression ratio was 0.22 for OvCa7 A hTERT cells and 0.32 for HEPC-CB.1 cells. On the other hand, the Pax8 relative expression ratio was 0.93 for OvCa3 A hTERT cells, 1.10 for OvCa7 A hTERT cells, and 1.57 for OAW-42 cells, which served as the positive control (Figure 4d). These results indicated a compatibility with the findings obtained from immunofluorescence staining.

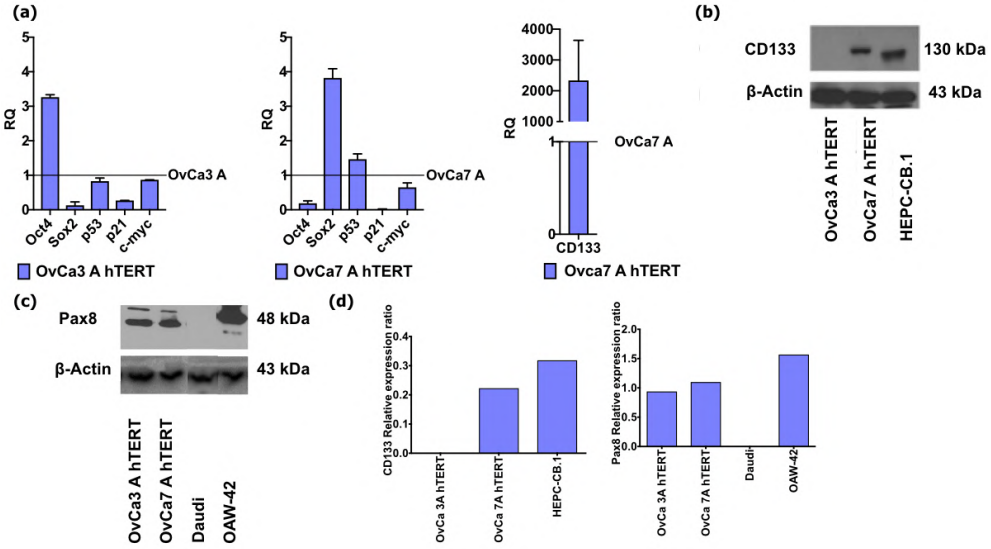

Figure 4. Characteristics of immortalized ovarian cancer cells. (**a**) The bar charts show the relative expression of the pluripotency-related markers *Oct4*, *Sox2*, protooncogenic markers *p53*, *p21*, *c-myc*, and *CD133*. The left bar chart shows the relative expression for OvCa3 A hTERT. The primary ovarian cancer cells OvCa3 A served as a control. The middle and right bar charts show the relative expression for OvCa7 A hTERT, with primary ovarian cancer cells OvCa7 A used as a control. The data represent mean ± SEM values from three independent experiments performed in duplicates. (**b**) Western blot analysis of CD133 molecule expression in immortalized ovarian cancer cell lines. CD133 and β-Actin protein levels were revealed with different sets of specific antibodies in ovarian cancer cell line extracts obtained from lysing cells with the RIPA buffer. Protein extracts from HEPC-CB.1 cells were used as a positive control. CD133—130 kDa and β-Actin—43 kDa expression. Each time, 50 µg/line of total protein was loaded. (**c**) Western blot analysis of Pax8 molecule expression in immortalized cell lines. Pax8 and β-Actin protein levels were revealed with different sets of specific antibodies in cell extracts obtained from lysing cells with the RIPA buffer. Protein extract from OAW-42 cells was used as a positive control, while protein extract from Daudi cells was used as a negative control. Pax8—48 kDa and β-Actin—43 kDa expression. Each time, 50 µg/line of total protein was loaded. The Western blot was performed in one repetition. (**d**) Densitometry analysis of CD133 and Pax8 was performed by using ImageJ software version 1.54f, and is presented as the rate of CD133 and Pax8 molecules expression to β-actin (used as an internal control). The data represent values from one experiment.

2.2. Metabolic Activity and Migration Activity of Primary Ovarian Cancer Cells and Immortalized Ovarian Cancer Cells

To determine the biological activity of primary ovarian cancer cells and immortalized ovarian cancer cells, the MTT assay and scratch test were performed. The metabolic activity of both immortalized ovarian cancer cell lines was higher compared to primary ovarian cancer cells. For the primary cells OvCa3 A and OvCa7 A, metabolic activity slowly increased and reached the highest value on day 3 (for OvCa3 A, 0.37 ± 0.01, and for OvCa7 A, 0.43 ± 0.01). For OvCa3 A hTERT, metabolic activity increased from day 1 (0.60 ± 0.03) to day 2 (1.27 ± 0.18) and was detectable at a similar level on day 3 (1.24 ± 0.02, $p < 0.001$ vs. day 0). For OvCa7 A hTERT, metabolic activity increased gradually from day 1 (0.30 ± 0.01) to day 3 and reached the highest value on day 3 (1.21 ± 0.01, $p < 0.0001$ vs. day 0) (Figure 5a).

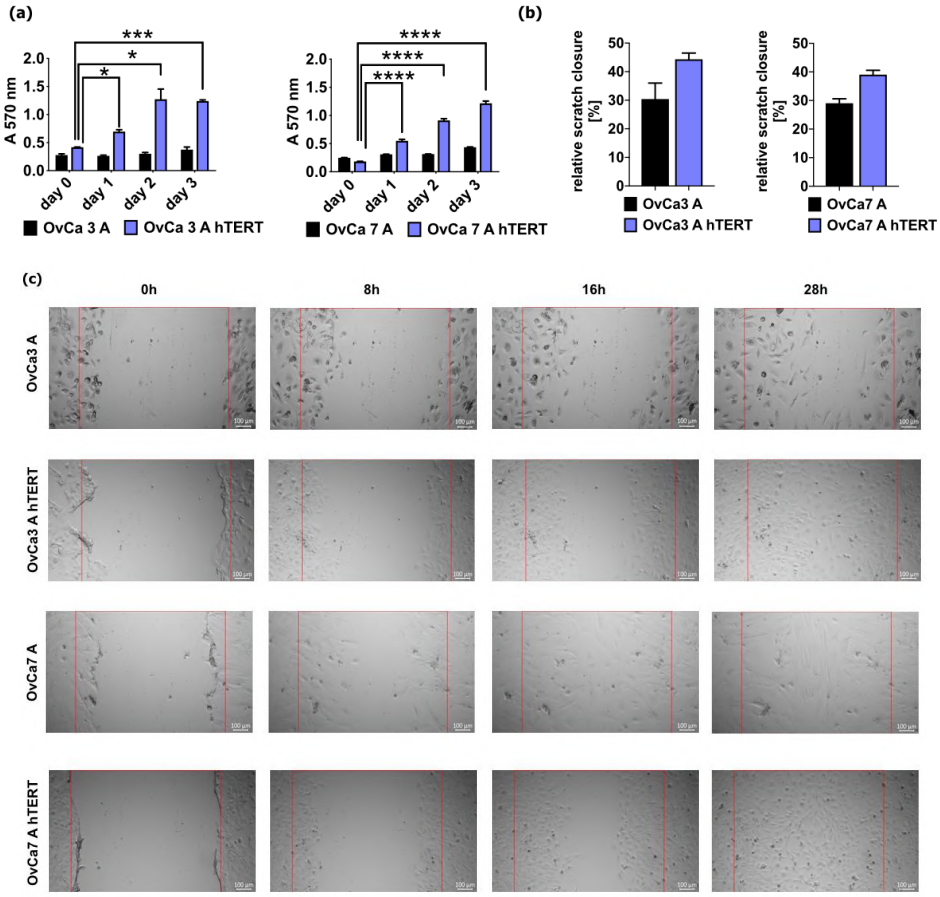

Figure 5. Metabolic activity and migration activity of primary ovarian cancer cells and immortalized ovarian cancer cells (**a**) The bar charts show absorbance at 570 nm for primary ovarian cancer cells and immortalized cancer cells at different time points. For the primary cells, the data represent mean ± SEM from experiments performed in triplicate; for immortalized cells, the data represent mean ± SEM values from three independent experiments performed in triplicate. **** $p < 0.0001$, *** $p < 0.001$, * $p < 0.05$ calculated vs. day 0 (**b**) The bar charts show relative wound closure for primary ovarian cancer cells and immortalized ovarian cancer cells. For the primary cells, the data represent mean ± SEM from experiments performed in duplicate, while for immortalized cells, the data represent mean ± SEM values from three independent experiments performed in duplicate. (**c**) Representative images of scratch closure at different time points. The top panel shows images for primary ovarian cancer cells OvCa3 A and immortalized ovarian cancer cells OvCa3 A hTERT, and the bottom panel shows images for primary ovarian cancer cells OvCa7 A and immortalized ovarian cancer cells OvCa7 A hTERT. The red lines represent scratch area. The scale bars represent 100 µm.

As with metabolic activity, the migration activity of immortalized ovarian cancer cells was higher compared to the corresponding primary ovarian cancer cells. It was shown that relative wound closure was higher for the immortalized OvCa3 A hTERT cells compared to the primary OvCA3 A cells (44.3% ± 2.1% vs. 30.4% ± 5.5%, respectively) and for the OvCa7 A hTERT cells compared to the OvCA7 A cells (39.0% ± 1.5% vs. 29.0% ± 1.6%, respectively) (Figure 5b,c).

2.3. ALDH1 Activity in Primary and Immortalized Ovarian Cancer Cells

To determine ALDH1 activity in primary and immortalized ovarian cancer cells, the colorimetric assay was performed. For primary ovarian cancer cells, the lower ALDH1 activity was observed compared to corresponding immortalized cells: for OvCa3 A (1.00 mU/mL ± 0.10 mU/mL vs. 1.92 mU/mL ± 0.01 mU/mL), and for OvCa7 A (1.33 mU/mL ± 0.10 mU/mL vs. 7.20 mU/mL ± 0.05 mU/mL), respectively. In addi-

tion, ALDH1 activity for the OvCa7 A hTERT cells was over three times higher than for the OvCa3 A hTERT cells (7.20 mU/mL ± 0.05 mU/mL vs. 1.92 mU/mL ± 0.01 mU/mL, respectively; $p < 0.0001$) (Figure 6).

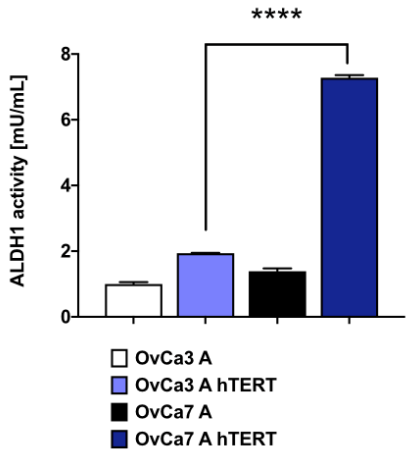

Figure 6. ALDH1 activity in immortalized ovarian cancer cells. For primary cells, the data represent mean ± SEM from duplicate, while for immortalized cells, the data represent mean ± SEM values from three independent experiments performed in duplicates. **** $p < 0.0001$ calculated vs. OvCa3 A hTERT.

2.4. Characteristics of Spheroids Derived from Primary and Immortalized Ovarian Cancer Cells

Spheroids were formed to assess the ability of primary and immortalized cells to grow in 3D conditions. The average diameter of spheroids derived from primary cells OvCa3 A and OvCa7 A was lower compared to corresponding immortalized cell lines (OvCa3 A 529.3 µm ± 6.3 µm vs. OvCa3 A hTERT 605.2 µm ± 6.3 µm, $p < 0.0001$) (OvCa7 A 458.7 µm ± 6.3 µm vs. OvCa7 A hTERT 626.3 µm ± 3.7 µm, $p < 0.0001$) (Figure 7a,b).

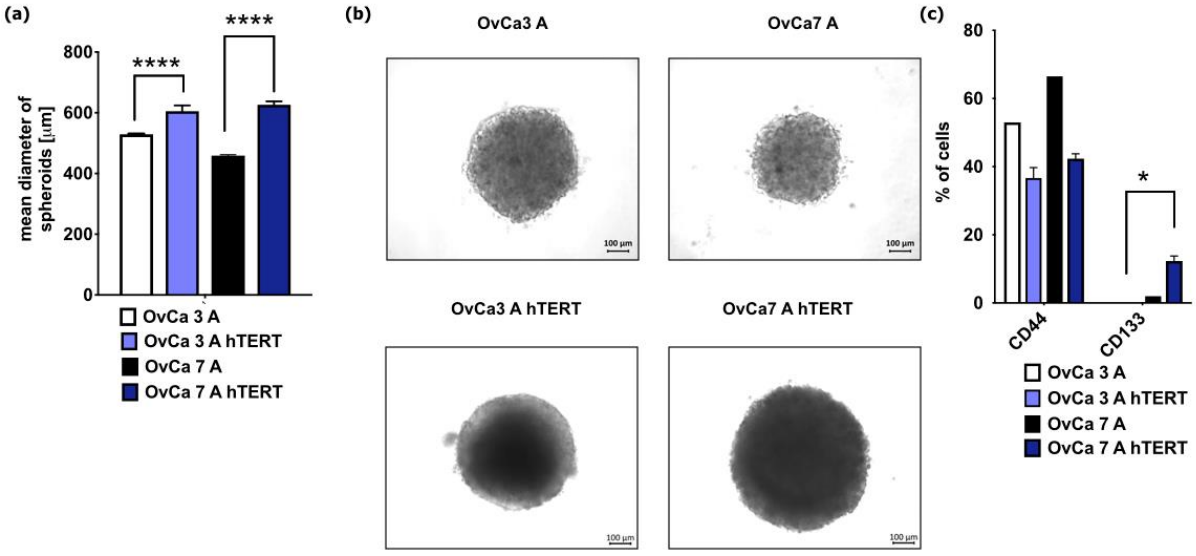

Figure 7. Characteristics of spheroids derived from immortalized ovarian cancer cells. (**a**) Mean diameter of spheroids (µm). The data represent mean ± SEM values from 10 spheroids. **** $p < 0.0001$ calculated vs. OvCa3 A hTERT or OvCa7 A hTERT. (**b**) Representative images of spheroids. The scale bars represent 100 µm. (**c**) The bar chart shows the percentage (%) of positive cells for selected markers (CD133, CD44). For primary cells, the data represent results from one experiment, while for immortalized cells, the data represent mean ± SEM values from three independent experiments. * $p < 0.05$ calculated vs. OvCa3 A hTERT.

To assess the presence of CSCs within the formed spheroids, the expression of selected markers characteristic for CSCs was determined using flow cytometry analysis after spheroid decomposition for single cells. For spheroids derived from primary OvCa3 A, there was no expression of CD133, while for spheroids from OvCa7 A, the small population of cells was positive for CD133 (2.00%). As previously shown in a 2D culture, OvCa3 A hTERT cells did not express CD133 in a 3D model, whereas for the OvCa7 A hTERT spheroids, the percentage of CD133-positive cells amounted to 12.33% ± 1.45% ($p < 0.05$). Similarly to cells in 2D model, the spheroids derived from OvCa3 A and OvCa7 A cells were positive for CD44 (53.00% vs. 66.50%, respectively). There were no differences in the expression of CD44 markers for cells derived from the OvCa3 A hTERT spheroids (36.66% ± 1.76% of the population) or the OvCa7 A hTERT spheroids (42.33% ± 1.45% of the population) (Figure 7c).

3. Discussion

Ovarian cancer of epithelial origin of the histological type of high-grade serous carcinoma is the most common malignant tumor in women with a fatal prognosis for survival due to a lack of early diagnosis and susceptibility for recurrence because of resistance to current chemotherapeutic protocols [22–24]. Extensive research on the ovarian cancer cell biology and targeted therapies focused on CSCs are necessary to develop effective treatment protocols. The advantage of using primary tumor cells from ascites or ovarian cancer tissue in CSC studies is that within heterogeneous tumor cell populations, there is a subpopulation representing CSCs responsible for tumor progression. However, there are still some difficulties, including a limited number of isolated cancer cells, short cell lifespan, and a small population of the CSCs in the heterogeneous material. In primary human cells, in which telomere-controlled senescence is the sole difficulty preventing unlimited lifespan, exogenous hTERT can be used to immortalize the cells, especially since almost 90% of cancers show overexpression of hTERT [14]. The post-operative tissue of ovarian cancer and the ascitic fluid are the main sources of primary cancer cells. Importantly, primary cancer cells can reflect the phenotype and genetic background of the tumor. However, the inter-patient heterogeneity of the cancer and the efficacy of cancer cell isolation is a great obstacle to experiment reproducibility when using samples from the primary solid tumor. Ascitic fluid is easily accessible and isolation of cancer cells is quite straightforward, but the number of cells may be insufficient for experiment repetitions and appropriate statistical analysis. Immortalization of cells using hTERT gives an opportunity to perform an appropriate number of repetitions due to the high proliferative activity of the cells. However, immortalization may affect the cell phenotype and their biological activity.

Cytomorphological analysis of primary cells from serous ovarian carcinoma before hTERT immortalization revealed four distinct subpopulations of cancer cells assessed according to the cytological criteria recommended by *Essentials of Fluid Cytology Atlas* [25]. The primary cellular composition of the ascitic fluid collected from patients with serous ovarian carcinoma showed similarities with the previously published reports, and the origin of ovarian epithelial cells was confirmed with the expression of CA 125 and CK8 [23]. After immortalization, only two cell types showed a growth advantage. The morphological characterization of the immortalized cells showed that two cell populations were established in both analyzed cases, with similar features to type 1 and 4 of primary cancer cells before immortalization. Type 1 of hTERT-immortalized cells presented typical malignant features, such as large size and round shape, central round and large nuclei, high nuclear density, and high nuclear-cytoplasmic ratio (2:1), and this subpopulation were more homogenous compared to the primary subpopulation of type 1. The second type of immortalized cells showed atypical morphological features comparable with type 4 of primary cells, with a distinct cell border and basophilic cytoplasm and inverse nuclear-cytoplasmic ratio (1:3) compared to malignant cells. These results suggest that only two cell subpopulations have the biological predispositions to growth. Based on published data, it can be assumed that only the cell clones with unique stemness features were selected during the immortalization

procedure [26,27]. This suggestion might be confirmed by the high nuclear accumulation of the p53 protein found in the majority of immortalized cells, which indicated that only malignant cells were able to survive and proliferate [7]. Strong p53 immunopositivity in immortalized cells found in the current study indicates that the selection of cells carried the TP53 gene mutation, similar to the published data on the correlation between p53 overexpression and gene mutation [28–30].

Our previous study showed that the commercially available ovarian cancer cell lines ES-2 and OAW-42 expressed the markers characteristic for the mesenchymal stem cell markers CD73 (ecto-5′-nucleotidase), CD90 (Thy-1), and CD105 (endoglin) [31]. Expression of these markers in cancer cells is associated with EMT and poor prognosis of ovarian cancer patients' survival. This study revealed that the immortalization affects the phenotype of the primary cells. For OvCa 3 A hTERT, an increased number of CD105-positive cells was observed compared to primary OvCa3 A cells, whereas for OvCa7 A hTERT, an increased number in CD90-positive cells and a decreased number in CD73- and CD105-positive cells was detected.

CD73 expression was observed on cancer-initiating cells. In high-grade serous ovarian cancer, the overexpression of the CD73 molecule with EMT markers (e.g., Snail, vimentin, or Twist1) was associated with poor prognosis of survival. Furthermore, it was shown that the expression of CD73 led to the escape of tumor cells from immune system control and induced tumor growth [24]. The silencing of CD73 expression via shRNA or using neutralizing antibodies decreased the formation of spheroids by the primary ovarian tumor cells and inhibited tumor growth in a mouse model. Moreover, the knockdown of the CD73 molecule caused a reverse from the mesenchymal to the epithelial transition phenotype of ovarian cancer cells [32]. The knockdown of the CD90 molecule in A2780 (ovarian cancer) cells decreased the proliferative activity of cells, relative cell growth (self-renewal potential), and expression of the pluripotency-related markers Nanog and Sox2. The ovarian cancer A2780 cell line, sorted for two populations with or without CD90 expression, revealed an increased proliferation activity and self-renewal in CD90-positive cells' population. In addition to the in vitro experiments in the tissue section, the expression of CD90 RNA was observed with in situ hybridization. Overall, the high expression of CD90 was associated with poor prognosis of survival in high-grade serous ovarian cancer and endometroid ovarian cancer [33]. The CD105 molecule is involved in ovarian cancer metastasis through the activation of EMT via the inhibition of NDRG1, E-cadherin [34]. The overexpression of CD105 with the co-expression of CD44 and CD106 was determined in paclitaxel-resistant ovarian cancer cell lines and primary ovarian cancer cells resistant to different chemotherapeutics. This phenotype of cells correlated with the shorter survival of ovarian cancer patients, the presence of metastasis to different organs, and fast cancer relapse [35].

In our study, the presence of the pluripotency-related markers *Oct4*, *Sox2*, and *Nanog* and the protooncogenic markers *p53*, *p21*, and *c-myc* in primary ovarian cancer cells and immortalized ovarian cancer cells was confirmed using the RT PCR and/or immunofluorescence staining. For OvCa3 A hTERT, only *Oct4* was upregulated, whereas *Sox2*, *p53*, *p21*, and *c-myc* were downregulated. Different results were obtained for OvCa 7 A hTERT, in which *Sox2* and *p53* were upregulated, and *Oct4*, *p21*, and *c-myc* were downregulated. Wang et al. showed that the immortalization of MSCs using hTERT increased the expression of the pluripotency-related markers Sox, Nanog, and Klf4 and protooncogenic myc and TP53 compared to primary cells [36]. A study conducted by Li et al. showed no significant changes in the expression of p21 in immortalized human ovarian surface epithelial cells compared to primary cells. Moreover, the immortalization did not affect the function of the p53 and pRb protein [37]. A study conducted by Samardzija et al. [38] showed that the expression of Oct4 analyzed using IHC staining was higher in the tissue samples of an increased pathological grade of serous ovarian cancer. Furthermore, the expression of Oct4 analyzed using RT-PCR was higher in cells isolated from the ascitic fluid of patients with recurrent epithelial ovarian cancer compared to patients not treated with chemotherapy.

The silencing of *Oct4* in the Hey cell lines (an invasive ovarian cancer cell line) using shRNA leads to lower proliferation activity and migration ability. Moreover, the cells became more sensitive to cisplatin. In a mouse model, an intraperitoneal injection of the knockdown Hey cells caused a reduction in tumor size and tumor aggressiveness that led to a prolonged lifespan of mice compared to Hey cells with the expression of *Oct4* [38]. A study performed by Wang et al. [39] showed that the Src kinase, which is a target of Sox2, is responsible for the different features of serous ovarian cancer cells, such as migratory activity, adhesion properties, and invasiveness. The silencing of Src kinase leads to a decreased migration in Ho8910 ovarian cancer cells and increases the adhesion of cells to different extracellular matrix proteins, such as laminin or collagen I [39]. Bareiss et al. documented that Sox2-expressing cells are more resistant to cell death the via apoptotic pathway caused by different chemotherapeutic agents or TRAIL [40]. Yun et al. [41] demonstrated that the silencing of Nanog by siRNA caused a decreased migration activity and invasiveness of two analyzed human ovarian cancer cell lines, SKOV-3 and A2780. Furthermore, the silencing of *Nanog* decreased the expression of EMT markers, such as vimentin, N-cadherin, and ZEB1, and the activation of the AMPK/mTOR signaling pathway. Overall, the results suggest that the high expression of *Nanog* and low expression of pAMPK (phosphorylated AMPK) is associated with poor prognosis of patient survival and resistance to platinum-based chemotherapy. *C-myc* is an important factor involved in different pathways, e.g., cell survival, progression of the cell cycle, and proliferation activity [42]. Moreover, *c-myc* regulates the expression of vimentin. In different types of tumors, the overexpression of *c-myc* was related to resistance to different chemotherapeutics [42]. The silencing of *c-myc* by siRNA in cisplatin-resistant A2780 cells leads to decreased cell proliferation, survival, and inhibition of cell cycle progression [42]. p53 is a tumor suppressor protein involved in the activation of proteins that play a crucial role in the repair of DNA after different types of damage. Moreover, p53 arrested the cells at the G1 checkpoint and induced apoptosis when the repair of DNA was impossible [43]. In ovarian cancer, the mutation of p53 occurs in 90% of epithelial cancers. The mutation of p53 can be used as a screening marker and prognostic marker of epithelial ovarian cancer. Furthermore, a molecule targeting the mutated p53, named PRIMA-1MET, combined with carboplatin chemotherapy is used in the II phase of clinical trials of recurrent high-grade serous ovarian cancer (NCT02098343). p21 is known as an inhibitor of cell cycle progression and proliferation [44]. The tissue section of ovarian cancer showed an overexpression of p21 [45]. The silencing of cytoplasmic p21 in cisplatin-resistant ovarian cancer cell line C13* decreased cell survival. Moreover, the inhibition of the translation of p21 into cytoplasm reduced resistance to cisplatin, in contrast to the translocation of p21 into cytoplasm. Cytoplasmic p21 may be a potential biomarker of cisplatin-resistant ovarian cancer [46]. Overall, pluripotency and proto-oncogenic markers may constitute biomarkers and potential targets for ovarian cancer treatment.

Studies on ovarian tumors also employed the expression of transcriptional factor Pax8, involved in the development of the fallopian tube epithelium and the development of Mullerian phenotype cancers (serous, clear cells, and endometroid) [47]. Pax8 is expressed in almost 90% of high-grade serous ovarian cancer and is a commonly used marker to classify ovarian serous tumors [48]. Both immortalized cell lines, OvCa3 A hTERT and OvCa7 A hTERT, express Pax8, which confirmed their epithelial origin, and is in line with similar pattern reported for OVPA8 cell line established after numerous passages [8].

EMT is a crucial process associated with cancer invasiveness and metastasis. In this process, cancer cells change their phenotype from epithelial to mesenchymal [49]. In the present study, the presence of Snail and vimentin in primary and immortalized ovarian cancer cells was detected using immunofluorescence staining. Snail, Slug, and vimentin were upregulated in cisplatin-resistant A2780 cell lines, as determined via genomic and proteomic analysis. The knockdown of Snail and Slug led to a reverse mesenchymal phenotype compared to the epithelial phenotype of cisplatin-resistant A2780 cells [50]. Vimentin, a protein of intermediate filaments, is the main important factor in the EMT marker. During EMT, cancer cells become elongated, which is associated with changes in

cytoskeleton organization mainly via vimentin. Vimentin also affects tumor angiogenesis via the activation of the NOTCH signaling pathway [51].

The CSC phenotype was assessed for primary and immortalized ovarian cancer cells based on the expression of CD133, CD24, and c-kit molecules. In the research on CSCs, CD133 is considered as a marker for the identification of CSC populations in different solid tumors, including ovarian cancer [17]. Importantly, for the immortalized OvCa7 A hTERT, an increase was observed in the percentage of CD133-positive cells to around 90%. Furthermore, the overexpression of the CD133 molecule in OvCa7 A hTERT was confirmed using the RT-PCR and Western blot. Due to the collection of the negative population for the CD133 molecule after the magnetic-activated cell sorting of OvCa3 A cells, both primary OvCa3 A and OvCa3 A hTERT were negative for CD133. The OvCa7 A cells were positive for CD24; however, the expression of CD24 was not detected after immortalization. This observation suggests that only a specific clone of the OvCa7 A cells expressing CD133 was immortalized. C-kit was detected in primary and immortalized ovarian cancer cells. Consequently, the OvCa7 A hTERT cell line may be used in further research to mimic CSC features in terms of CD133 expression, in contrast to OvCa3 A hTERT. A study conducted by Zhang et al. observed a high expression of CD133 in patients with high-grade serous ovarian cancer, diagnosed in late stages with poor prognosis of prolonged survival. Moreover, the patients did not respond to chemotherapeutic agents [52]. The spheroids derived from the SKOV-3 cells increased tumor formation and growth in a mouse model. Importantly, in the tissue section, a high expression of CD44, CD133, Ki67, and the pluripotency-related markers Oct4 and Nanog was detected. This was associated with the downregulation of the genes involved in cell adhesion and the upregulation of the genes important for the survival of cells and cell cycle progression [53]. CD24 affects the EMT via the activation of the Akt- and ERK-signaling pathways in the cisplatin-resistant ovarian cancer cell line Caov-3. The activation of EMT leads to the increased proliferation and metastatic potential of cells. Moreover, CD24 expression was observed in ovarian cancer tissue sections, and was associated with metastasis into distant lymph nodes and the peritoneal cavity [54]. A study conducted by Chau et al. [55] showed that the postulated mechanism of c-kit action is activation of the Wnt/β-catenin signaling pathway and the ATP-binding cassette transporter G2. Furthermore, a hypoxic condition can enhance the expression of the c-kit marker [55]. The silencing of the c-kit marker via siRNA leads to a decreased number of ovarian tumor-initiating cells, tumorigenic potential, and expression of CSC markers. Importantly, a clinically applied inhibitor of c-kit kinase (an Imatinib brand called Gleevec) also decreased the number of ovarian tumor-initiating cells. In our study, primary and immortalized cells were determined for the activity of ALDH1, and the ALDH1 level was found to be three times higher in the obtained CD133-positive cell line OvCa7 A hTERT compared to the CD133-negative cell line OvCa3 A hTERT. For both primary cells OvCa3 A and OvCa7A, the ALDH1 activity was lower compared to corresponding immortalized cell lines. Studies by Choi et al. revealed that double positive ALDH1 (+)/CD133 (+) ovarian cancer cells, which are highly resistant for chemotherapy, could generate a heterogeneous population of cancer cells [56]. ALDH1 activity is one of the most important features not only in normal stem cells, but also in CSCs. ALDH1 directly protects the cells from toxic aldehydes and indirectly from reactive oxygen species (ROS) [57]. The expression of ALDH1 in patients with high-grade serous ovarian cancer correlated with the resistance to platinum-based chemotherapy and poor prognosis [58]. A study performed by Kuroda [59] showed that cells with high expression of ALDH1 could be isolated from different ovarian cancer cell lines (serous ovarian cancer and clear cell carcinoma). Cells with a high expression of ALDH1 were more tumorigenic and aggressive, as shown in a mouse model [59].

Our results showed higher metabolic and migration activity of the two analyzed immortalized ovarian cancer cells OvCa3 A hTERT and OvCa7 A hTERT compared to the corresponding primary cells. The higher metabolic activity may have been related to higher proliferation activity. A study conducted by Wang et al. [36] showed that the

immortalization of MSCs using hTERT increased proliferation ability compared to primary cells. Telomerase activity is a potential biomarker of cell proliferation. The hTERT affects cell proliferation not only by preventing telomeres from shortening, but also by activating the epidermal growth factor receptor (EGFR) [60]. Research on telomerase activity in the nasopharyngeal carcinoma radioresistant cell line CNE-2R documented that the expression of stem cell-related genes (including CD133 mRNA) and the hTERT gene in radioresistant CNE-2R cells was higher than those in radiosensitive CNE-2 cells. The radioresistant cell line CNE-2R showed cancer stem cell-like characteristics (Oct4, Sox2, Nanog, Bmi1, and CD133), especially in the sorted cells that were CNE2R-CD133-positive, and, in contrast to the CNE-2R-CD133-negative cells, revealed higher proliferation activity, tumorigenesis capacity, and telomerase activity [61]. RNA sequencing performed by Liu et al. revealed that the transfection of the osteosarcoma cells U2OS and the immortalized fibroblast cells VA-13 with plasmids carrying out hTERT and mutated hTERT increased the expression of a gene involved in cell adhesion. This was also confirmed in an in vitro assay, in which the transfected cells showed increased adhesion to the ECM protein fibronectin. Moreover, increased migration and transmigration activity of U2OS cells was observed [62]. On the other hand, the silencing of hTERT via siRNA in esophageal squamous carcinoma cells decreased cell migration and invasiveness, but did not affect cell proliferation [63].

Our study revealed no differences in the size of the spheroids formed from two immortalized ovarian cancer cell lines. However, the size of the spheroids derived from the immortalized ovarian cancer cell lines was greater than that of the spheroids from primary ovarian cancer, as presented in the current and our recent study [64]. Nevertheless, differences were observed in the spheroid phenotype. For spheroids derived from OvCa3 A, as expected, there was no expression of CD133, while for OvCa7 A spheroids, the small population of cells was positive for CD133. In spheroids of OvCa7 A hTERT, a significantly higher percentage of cells expressed the CSC phenotype CD133, whereas in spheroids from OvCa3 A hTERT, CD133 cells were not detectable.

4. Materials and Methods

4.1. Isolation of Human Primary Ovarian Cancer Cells

Primary ovarian cancer cells were isolated from the ascitic fluid aspirated from two patients with permission from the Bioethics Committee at the Medical University of Wroclaw (No. KB-489/2020). Both patients suffered from high-grade serous ovarian cancer. Medical procedures were carried out at the Department of Gynecology and Obstetrics, Wroclaw Medical University in Poland. The cells were isolated from the ascitic fluid, as previously described [64]. The obtained ascitic fluid was centrifuged for 10 min 1000× *g*. The cells were washed in PBS twice. Finally, the isolated cells were resuspended in a culture medium (DMEM, Thermo Fisher Scientific, Carlsbad, CA, USA) containing 10% FBS (Thermo Fisher Scientific, Carlsbad, CA, USA), a 1% penicillin/streptomycin solution (Thermo Fisher Scientific, Carlsbad, CA, USA), and 1% L-glutamine (Thermo Fisher Scientific, Carlsbad, CA, USA), and cultured in standard conditions (37 °C, 5% CO_2).

4.2. Isolation of CD133 Positive and Negative Cells-Magnetic-Activated Cell Sorting

The cells derived from the ascitic fluid of patients with high-grade serous ovarian cancer were magnetically sorted using CD133 beads (Milteni Biotec, Bergisch Gladbach, Germany) and an MS column (Milteni Biotec, Bergisch Gladbach, Germany) according to the manufacturer's instructions. In total, 1×10^6 cells were centrifuged at 300× *g* for 10 min. After centrifugation, the cell pellet was resuspended in 40 µL of a sorting buffer (PBS with 2% BSA and 2 mM EDTA, pH = 7.2, IIET, Wroclaw, Poland). Next, 10 µL of the anti-human CD133-Biotinyled antibody was added. The cells were incubated on ice for 15 min. After incubation, the cells were washed with a sorting buffer and centrifuged at 300× *g* for 10 min. The cell pellet was resuspended in a sorting buffer with the addition of 20 µL of Anti-Biotin MicroBeads and incubated on ice for 15 min. Next, the cells were washed with a sorting buffer and centrifuged at 300× *g* for 10 min. After centrifugation,

the cell pellet was resuspended in 500 µL of a sorting buffer. Before magnetic separation, the MS column was placed in a magnetic field and activated with a sorting buffer. The cell suspension was then applied to the MS column. The flowthrough contained unlabeled cells representing a CD133-negative cell population. Subsequently, the column was washed with an appropriate volume of a sorting buffer, and the flowthrough from this step was combined with unlabeled cells. A CD133-positive population was obtained when the column was removed from the magnetic field and washed with a sorting buffer. In the final step, the negative and positive populations of isolated cells were centrifuged at 300× *g* for 10 min. Next, the cells were resuspended in a culture medium (DMEM) containing 10% FBS (Thermo Fisher Scientific, Carlsbad, CA, USA), a 1% penicillin/streptomycin solution (Thermo Fisher Scientific, Carlsbad, CA, USA), and 1% L-glutamine (Thermo Fisher Scientific, Carlsbad, CA, USA) and cultured in standard conditions (37 °C, 5% CO_2). Because the number of obtained CD133-positive cells was insufficient, the cells were not able to proliferate and could not be used in further experiments.

4.3. Immortalization of Primary Ovarian Cancer Cells

Initially, the cells derived from the patients' ascitic fluid presented a highly heterogeneous population of various cell types including cancer cells, mesothelial cells, and fibroblast-like cells. To remove fibroblasts and mesothelial cells from the primary culture, cells were detached from plastic surface after 2 min of exposure to trypsin. Cells showing a fibroblast-like morphology, but not epithelial cancer cells, were removed, and the culture medium supplemented with FBS was added to inactivate the remaining trypsin. The transfection was performed on cells with significantly higher adhesion to plastic surface with cancerous cell morphology and clustered growth. The primary ovarian cancer cells were transfected with the hTERT plasmid (pBABE-puro-hTERT, www.addgene.org) after second passage and selected with Puromycin (Merck, Kenilworth, NJ, USA). The ViaFect™ Transfection Reagent (Promega, Mannheim, Germany) was applied for transfection according to the manufacturer's protocol. A day before the transfection, the cells were seeded in a 24-well plate (2.0×10^4 cells/well) in the OptiMEM medium supplemented with GlutaMAX (Thermo Fisher Scientific, Carlsbad, CA, USA) and 3% of FBS (Thermo Fisher Scientific, Carlsbad, CA, USA). Before the transfection, the culture medium with FBS was replaced with a serum-free Opti-MEM medium. Two micrograms of DNA plasmids were mixed with 200 µL of the serum-free Opti-MEM medium and 6 µL of the ViaFect™ transfection reagent. Following 20 min of incubation at room temperature (RT), the DNA-Transfection Reagent complex was mixed with 2 mL of Opti-MEM medium, and 0.5 mL of the mixture was applied to each well of a 24-well plate. After 24 h of incubation at 37 °C, 5% CO_2, 0.5 mL of Opti-MEM medium with 3% of FBS was applied to each well and exchanged after 48 h. All transfection details are presented in our previous paper [65]. The immortalized cell lines were called OvCa3 A hTERT and OvCa7 A hTERT, as they were isolated from the ascitic fluid of patients with ovarian cancer numbers 3 and 7, respectively.

4.4. Characteristics of Primary Ovarian Cancer Cells and Immortalized Ovarian Cancer Cells

The primary cells were used for all experiments from passage 1 to passage 3, while immortalized cells were used for all experiments from passage 1 to passage 5.

4.4.1. Cytological Assessment

For cytological assessment, primary cells from passage 2 and immortalized cells from passage 2 were used. For cytospin preparation, the cells were seeded at a density of 5×10^3 cells/100 µL PBS per drop on slides. The slides were kept in 37 °C for 30 min to increase cell adhesion. Next, the specimens were fixed in cold acetone for 15 min, stained with hematoxylin and eosin, and were examined cytologically according to the standard protocol [25]. The cytospin specimens were assessed with a 40× dry objective of an Olympus microscope (BX61, Olympus, Japan) and Cell Sens Dimension version 3.2 Image Acquisition, Process Analysis Software documentation.

4.4.2. Immunocytochemical Staining (ICC)

To assess the cancerous feature of cells isolated from ascitic fluid the immunohistochemical staining for the presence of the p53 protein, CA 125 antigen and cytokeratin 8 (CK8) was performed on cytospin specimens using and the Universal Dako REAL EnVision Detection System, Peroxidase/DAB+, Rabbit/Mouse (Dako, Copenhagen, Denmark). Endogenous peroxidase reactivity was blocked with the Dako REAL Peroxidase Blocking Solution (Dako, Copenhagen, Denmark). Next, the cytospin specimens were incubated with primary antibodies (Table S1) for 60 min at RT. After washing, with 0.1 M Tris buffer, pH = 7.4 (TBS), cells were incubated with Dako REAL EnVision/HRP, Rabbit/Mouse (Dako, Copenhagen, Denmark) for 30 min at RT. The binding of the antibody was visualized using DAB (3,3 diaminobenzidine) chromogen (Dako, Copenhagen, Denmark) for four minutes at RT. The sections were counterstained with hematoxylin and mounted. The TBS buffer without primary antibodies was used as a negative control. Positive controls for each antibody were performed according to the manufacturer's recommendation. The following positive controls were used: CA125 antigen-ovarian serous adenocarcinoma tissue from patient with high serum level of CA125 antigen, cytokeratin 8 (CK8)-ovarian serous adenocarcinoma tissue, and p53 antigen-OvBH-1 cell line [7,18].

The expression of the analyzed proteins on cell cytospines was assessed semi-quantitatively, taking into account the intensity staining and the number of cells showing immunoreactivity for the p53 protein, CA 125, and CK8. The percentage of immunopositive cells was determined by counting 1000 cells in randomly selected areas using an Olympus BX51 microscope (Olympus, Tokyo, Japan). The cell specimens were assessed by cytopathologist J.B. twice, and the average value from two independent analyses was taken into account. Staining was scored as positive when more than 5% of cells showed immunoreactivity. The intensity score was based on the color of the reaction and was assessed as follows: 0 = no immunostaining, light yellow color = weak (+), medium brown color = moderate (++), and strong brown color = strong (+++).

4.4.3. Flow Cytometry Analysis

The primary ovarian cancer cells (passages 1–3) and immortalized ovarian cancer cells (passages 1–3) were analyzed using flow cytometry. After trypsinization (IIET, Wroclaw, Poland), the cells were washed with PBS and stained with the fluorochrome-conjugated anti-human PE-conjugated antibodies CD73, CD90, CD105, CD44, CD45, CD133 (BD Biosciences, San Jose, CA, USA), FITC-conjugated CD24, CD34 antibodies (BD Biosciences, San Jose, CA, USA), and isotype controls (BD Biosciences, San Jose, CA, USA) at 4 °C for 30 min. The cells were then washed with PBS (IIET, Wroclaw, Poland) and analyzed using a BD LSRFortessa flow cytometer (BD Biosciences, San Jose, CA, USA). The data were processed with Flowing Software 2 version 2.5 (Perttu Terho, Turku Centre for Biotechnology, Turku, Finland), and appropriate histograms were prepared.

4.4.4. Immunofluorescence Staining and Microscopic Imaging

The primary ovarian cancer cells (passage 2) and immortalized ovarian cancer cells (passage 2) were stained for the expression of selected markers: p53, Pax8, CD133, PDGFRα, CD44, FAP, Snail, Oct, Sox, Nanog, vimentin, c-kit, and F-actin. Before immunostaining, the cells were fixated with 4% PFA for 15 min at RT. Next, to analyze the expression of markers with nuclear localization, the cell membrane was permeabilized with 0.1% Triton X100 (Avantor Performance Materials Poland, Gliwice, Poland) for 15 min at RT. After permeabilization, the unspecific binding of antibodies was blocked with 1% BSA (Symbios, Gdansk, Poland) for 40 min at RT. Subsequently, the cells with selected primary antibodies were incubated for 1 h at RT or overnight at 4 °C (Table S1). The cells were stained with secondary antibodies Alexa Fluor 488-conjugated goat anti-mouse IgG and/or Alexa Fluor 647-conjugated goat anti-rabbit IgG (Invitrogen, Carlsbad, CA, USA) for 45 min (RT). F-actin was stained with Alexa Fluor 488-conjugated phalloidin (Invitrogen, CA, USA) for 45 min (RT) (Table S2). The NucBlue™ Fixed Cell ReadyProbes™ Reagent (DAPI) (Invitrogen,

Carlsbad, CA, USA) was used to stain the cell nuclei for 30 min (RT). Images were acquired with a 40x dry objective of an Axio Imager Z2 microscope (Zeiss, Gottingen, Germany) and Zen Blue 2.6 Software (Zeiss, Gottingen, Germany). This software was also used to process the obtained images.

4.4.5. Western Blot

Immortalized ovarian cancer cells (passage 3) were lysed in the RIPA Lysis and Extraction Buffer (Thermo Fisher Scientific, Carlsbad, CA, USA) and stored at −80 °C. In the next step, the total protein amount in the lysed samples was calculated using the BCA Protein Assay Kits (Thermo Fisher Scientific, Carlsbad, CA, USA). Each time, 50 µg of total protein was applied per line on SDS-PAGE gels. The WB analysis was performed according to the previously described method [66]. The cell extracts were loaded on SDS-PAGE and, after electrophoresis, were transferred onto an Immobilon PVDF Membrane (Merc, Kenilworth, NJ, USA). After semi-dry transfer, the membrane was blocked with a 5% solution of BLOT-QuickBlocker™ (Merc, Kenilworth, NJ, USA) for 1 h at RT. In the next step, an overnight incubation with primary antibodies against human CD133 (2F8C5 Mouse mAb, Invitrogen, Carlsbad, CA, USA), Pax8 (D2S2I Rabbit mAb, Cell Signaling Technology, Danvers, MA, USA), and β-Actin (13E5 Rabbit mAb, Cell Signaling Technology, Danvers, MA, USA) was applied at 4 °C. After washing three times with a 0.05% (*v*/*v*) Tween-20 (Thermo Fisher Scientific, Carlsbad, CA, USA) solution in PBS, the membrane was incubated with a secondary biotinylated antibody against rabbit (for β-Actin and Pax8) and mouse (for CD133) (Thermo Fisher Scientific, Carlsbad, CA, USA) for 1 h at RT. After the next washing in a 0.05% Tween-20/PBS solution, the membrane was incubated with streptavidin-HRP (Dako, Glostrup, Denmark) at RT for 1 h. The chemiluminescent reaction was developed using the ECL Western Blotting Substrate (Thermo Fisher Scientific, Carlsbad, CA, USA) and visualized on a CL-XPosure film (Thermo Fisher Scientific, Carlsbad, CA, USA). As a positive control, human HEPC-CB.1 cell lysate was used as the reference cell line positive for the CD133 molecule [67]. OAW-42 cell lysate was used as the reference cell line positive for Pax8, while Daudi cell lysate was used as the reference negative for Pax8. The densitometry analysis of CD133 and Pax8 was conducted using ImageJ software version 1.54f (National Institutes of Health, Bethesda, MD, USA). The results were presented as the ratio of CD133 and Pax8 protein expression levels to β-actin, which served as an internal control for normalization.

4.4.6. Real-Time RT-PCR

RNA from the primary ovarian cancer cells (passage 2) and immortalized ovarian cancer cells (passage 3) was isolated using the NucleoSpin® RNA Kit (Macherey-Nagel, Düren, Germany). The obtained RNA was then reverse-transcripted using the RevertAid First Strand cDNA Synthesis Kit (Thermo Fisher Scientific, Carlsbad, CA, USA). The expression of *Oct4*, *Sox2*, *p53*, *p21*, *c-myc*, and *CD133* was determined using appropriate TaqMan probes (Thermo Fisher Scientific, Carlsbad, CA, USA) and the TaqMan Master Mix (Thermo Fisher Scientific, Carlsbad, CA, USA). The reaction was performed with the ViiA 7 Real-Time PCR System (Applied Biosystems, Foster City, CA, USA). The housekeeping gene for calibration of the gene expression levels was GADPH. The results were analyzed using the $^{\Delta\Delta}$Ct method [64]. The primary ovarian cancer OvCa3 A served as a control for OvCa3 A hTERT, while OvCa7 A served as a control for OvCa7 A hTERT.

4.5. Metabolic Activity of Primary Ovarian Cancer Cells and Immortalized Ovarian Cancer Cells

An MTT assay was used to compare the metabolic activity of the primary ovarian cancer cells (passage 2) and immortalized ovarian cancer cells (passage 2 and 3). In total, 3×10^3 cells were seeded at each well in 96-well plates. Metabolic activity was analyzed at four time-points (0 days, 1 day, 2 days, and 3 days). At each time-point, 4mg/mL of the MTT solution (Merc, Kenilworth, NJ, USA) were added to cells. The metabolic active cells converted the MTT reagent into formazan dye. The formazan dye

was then dissolved in DMSO (Avantor Performance Materials Poland, Gliwice, Poland), and absorbance was read at 570 nm using a Wallac 1420 Victor2 Microplate Reader (Perkin Elmer, Waltham, MA, USA).

4.6. Migration Activity of Primary Ovarian Cancer Cells and Immortalized Ovarian Cancer Cells

The scratch test was used to compare the migration activity of primary ovarian cancer cells (passage 2) and immortalized ovarian cancer cells (passage 3). The cells were seeded onto 48-well plates at a density of 5×10^4 per well. When cells fully covered the surface of the well, the scratch with 200 µL tips was made. The migration of cells was analyzed for 48 h with an interval of 4 h using an Axio Observer Microscope (Zeiss, Gottingen, Germany) equipped with a chamber for cell incubation (PeCon GmbH, Erbach, Germany). The cells were recorded at 37 °C 5% CO_2 using a 5x dry objective (Zeiss, Gottingen, Germany). The video was acquired with Zen 2.6 Blue Edition Software (Zeiss, Gottingen, Germany). The same software was utilized for both video and image processing, as well as for measuring the scratch area in square micrometers (μm^2) at both 0 h and 28 h post-scratch. The closure of the scratch area was determined by calculating the difference in the area between 0 h (A0h) and 28 h (A28h), with a total image size of 4,764,685 μm^2. To obtain the relative scratch closure percentage, the scratch closure area in μm^2 was multiplied by 100 and then divided by the total image size in μm^2. This methodology for calculating relative scratch closure was consistent with previous descriptions, utilizing the area measurements in μm^2 instead of pixels [68].

4.7. ALDH1 Activity in Primary and Immortalized Ovarian Cancer Cells

To determine the ALDH1 activity in primary (passage 3) and immortalized ovarian cancer cells (passages 4 and 5), the Aldehyde Dehydrogenase Activity Colorimetric Assay Kit (Merc, Kenilworth, NJ, USA) was used according to the manufacturer's instructions. In total, 1×10^6 cells were resuspended in 200 µL of ice-cold ALDH Assay Buffer and centrifuged at 13,000× *g* for 10 min. Next, the 50 µL of reaction mixes (including Sample and Standards of NADH in an ALDH Assay Buffer, ALDH Substrate Mix, and Acetaldehyde) were prepared and added into a 96-well plate. The plate was then incubated for 5 min at RT while protected from light. The initial absorbance at 450 nm was measured using a Wallac 1420 Victor2 Microplate Reader (Perkin Elmer, Waltham, MA, USA). The measurement of absorbance continued until the value of the most active sample was higher than the value of the highest standard. The activity of ALDH1 (mU/mL) was calculated according to the formulas from the Aldehyde Dehydrogenase Activity Colorimetric Assay Kit (Merc, Kenilworth, NJ, USA) guidelines.

4.8. 3D Cell Culture

Spheroids were formed at a dedicated 96-well plate Nunclon (Thermo Fisher Scientific, Carlsbad, CA, USA). At 96-well plates, the primary (passage 3) and immortalized ovarian cancer cells (passages 4 and 5) were seeded at a density of 1×10^4 cells per well. The spheroids were formed for 2 days. Microscopic imaging of spheroids was performed using an Axio Observer Microscope (Zeiss, Gottingen, Germany) equipped with dry 10 × objectives. Images were acquired with the Zen 2.6 Blue Edition Software (Zeiss, Gottingen, Germany). This software was also used for image processing and calculation of spheroid diameters. Moreover, the spheroids were used for flow cytometric analysis for the expression of CD133 and CD44 markers. The spheroids were decomposed into single cells in a solution of the Accutase Cell Detachment Solution (Corning, Manassas, VA, USA) and shaken in a water bath (Thermo Fisher Scientific, Carlsbad, CA, USA) at 37 °C for 10 min. Subsequently, the cells were washed with PBS and stained with PE-conjugated anti-human antibodies CD44, CD133 (BD Biosciences, San Jose, CA, USA), and with the isotype controls (BD Biosciences, San Jose, CA, USA) at 4 °C for 30 min. The cells were then washed with PBS (IIET, Wroclaw, Poland) and analyzed using a BD LSRFortessa flow cytometer (BD Biosciences, San Jose, CA, USA). The data were processed with Flowing

Software 2 version 2.5 (Perttu Terho, Turku Centre for Biotechnology, Turku, Finland), and appropriate histograms were prepared.

4.9. Statistical Analysis

Data analysis and preparation of graphs were performed using the GraphPad Prism version 7 (GraphPad Software Inc., San Diego, CA, USA). Statistical analysis was performed using a *t*-test.

5. Conclusions

In conclusion, we showed that primary ovarian cancer cells from the ascitic fluid may be successfully immortalized using plasmids carrying the hTERT gene. hTERT-immortalized ovarian cancer cells created in this study offer the advantage of being able to explore the "normal" characteristics of primary human cancer cells without the limitation of their lifespan. The obtained cells should be particularly useful to the study of the functional processes that are normally different during cancer development, such as cell cycle controls, adherence, motility, and regulation of gene expression, as well as their response to therapeutic strategies. This study shows that the immortalized ovarian cancer cells had higher proliferation activity than primary ovarian cancer cells. In general, both immortalized ovarian cancer cell lines reflected the phenotype of primary cancer cells, albeit with modifications. OvCa3 A hTERT kept the mesenchymal stem cell phenotype CD73+, CD90+, and CD105+, and was CD133-negative, whereas the cell population of OvCa7 A hTERT lost CD73 expression, but a majority of cells (almost 90%) expressed the CD133 characteristic for the CSCs phenotype. Furthermore, immortalized cells differed in gene expression level with respect to *Sox2* and *Oct4*, which was associated with stemness properties. The newly established unique immortalized cell line OvCa7 A hTERT with a characteristic of serous ovarian cancer malignancy feature, with the accumulation of the p53 and Pax8, and the overexpression of the CD133 and CD44 molecules, may be a useful tool in preclinical research on therapeutic approaches, especially those targeting the CSCs of ovarian cancer.

Supplementary Materials: The following supporting information can be downloaded at: https://www.mdpi.com/article/10.3390/ijms25105384/s1.

Author Contributions: Conceptualization, A.K., and A.S.; methodology, A.S., A.B.-P., M.P., J.B., M.M., and A.K.; formal analysis, A.S., A.B.-P., and A.K.; investigation, A.S., A.B.-P., and J.B.; data curation, A.S., A.B.-P., and A.K.; visualization, A.S., and J.B.; supervision, A.K.; funding acquisition, A.K.; writing—original draft preparation, A.S., A.B.-P., and A.K.; writing—review and editing, A.K. All authors have read and agreed to the published version of the manuscript.

Funding: This research received no external funding.

Institutional Review Board Statement: The study was conducted in accordance with the Declaration of Helsinki, and approved by the Bioethics Committee at the Medical University of Wroclaw (protocol No. KB-489/2020).

Informed Consent Statement: Informed consent was obtained from all subjects involved in the study.

Data Availability Statement: All data generated or analyzed during this study are included in this article.

Acknowledgments: The authors are grateful to Piotr Grelewski, from the Department of Immunopathology and Molecular Biology, Wroclaw Medical University, for technical support.

Conflicts of Interest: The authors declare no conflicts of interest.

References

1. Chandra, A.; Pius, C.; Nabeel, M.; Nair, M.; Vishwanatha, J.K.; Ahmad, S.; Basha, R. Ovarian cancer: Current status and strategies for improving therapeutic outcomes. *Cancer Med.* **2019**, *8*, 7018–7031. [CrossRef] [PubMed]
2. Arora, T.M.S.; Lekkala, M.R. Ovarian Cancer. In *StatPearls*; StatPearls Publishing: Treasure Island, FL, USA, 2023. Available online: https://www.ncbi.nlm.nih.gov/books/NBK567760/ (accessed on 15 January 2024).
3. Fantone, S.; Piani, F.; Olivieri, F.; Rippo, M.R.; Sirico, A.; Di Simone, N.; Marzioni, D.; Tossetta, G. Role of SLC7A11/xCT in Ovarian Cancer. *Int. J. Mol. Sci.* **2024**, *25*, 587. [CrossRef] [PubMed]
4. Bortot, B.; Apollonio, M.; Rampazzo, E.; Valle, F.; Brucale, M.; Ridolfi, A.; Ura, B.; Addobbati, R.; Di Lorenzo, G.; Romano, F.; et al. Small extracellular vesicles from malignant ascites of patients with advanced ovarian cancer provide insights into the dynamics of the extracellular matrix. *Mol. Oncol.* **2021**, *15*, 3596–3614. [CrossRef] [PubMed]
5. Nunes, M.; Ricardo, S. Chemoresistance in Ovarian Cancer: The Role of Malignant Ascites. In *Ovarian Cancer*; Lele, S., Ed.; Exon Publications: Brisbane, Australia, 2022.
6. Li, Z. *Comprehensive Biotechnology*, 3rd ed.; Elsevier: Amsterdam, The Netherlands, 2019.
7. Bar, J.K.; Harlozinska, A. Morphological and phenotypic characterization of a new established ovarian carcinoma cell line (OvBH-1). *Anticancer Res.* **2000**, *20*, 2975–2980. [PubMed]
8. Tudrej, P.; Olbryt, M.; Zembala-Nozynska, E.; Kujawa, K.A.; Cortez, A.J.; Fiszer-Kierzkowska, A.; Piglowski, W.; Nikiel, B.; Glowala-Kosinska, M.; Bartkowska-Chrobok, A.; et al. Establishment and Characterization of the Novel High-Grade Serous Ovarian Cancer Cell Line OVPA8. *Int. J. Mol. Sci.* **2018**, *19*, 2080. [CrossRef] [PubMed]
9. Zvereva, M.I.; Shcherbakova, D.M.; Dontsova, O.A. Telomerase: Structure, functions, and activity regulation. *Biochemistry* **2010**, *75*, 1563–1583. [CrossRef]
10. Shay, J.W.; Wright, W.E. Hayflick, his limit, and cellular ageing. *Nat. Rev. Mol. Cell Biol.* **2000**, *1*, 72–76. [CrossRef]
11. Sullivan, C.S.; Pipas, J.M. T antigens of simian virus 40: Molecular chaperones for viral replication and tumorigenesis. *Microbiol. Mol. Biol. Rev.* **2002**, *66*, 179–202. [CrossRef]
12. Bryan, T.M.; Reddel, R.R. SV40-induced immortalization of human cells. *Crit. Rev. Oncog.* **1994**, *5*, 331–357. [CrossRef]
13. Blasco, M.A.; Hahn, W.C. Evolving views of telomerase and cancer. *Trends Cell Biol.* **2003**, *13*, 289–294. [CrossRef]
14. Zhang, Y.; Toh, L.; Lau, P.; Wang, X. Human telomerase reverse transcriptase (hTERT) is a novel target of the Wnt/beta-catenin pathway in human cancer. *J. Biol. Chem.* **2012**, *287*, 32494–32511. [CrossRef] [PubMed]
15. Al-Alem, L.F.; Pandya, U.M.; Baker, A.T.; Bellio, C.; Zarrella, B.D.; Clark, J.; DiGloria, C.M.; Rueda, B.R. Ovarian cancer stem cells: What progress have we made? *Int. J. Biochem. Cell Biol.* **2019**, *107*, 92–103. [CrossRef] [PubMed]
16. Karbanova, J.; Missol-Kolka, E.; Fonseca, A.V.; Lorra, C.; Janich, P.; Hollerova, H.; Jaszai, J.; Ehrmann, J.; Kolar, Z.; Liebers, C.; et al. The stem cell marker CD133 (Prominin-1) is expressed in various human glandular epithelia. *J. Histochem. Cytochem.* **2008**, *56*, 977–993. [CrossRef] [PubMed]
17. Glumac, P.M.; LeBeau, A.M. The role of CD133 in cancer: A concise review. *Clin. Transl. Med.* **2018**, *7*, 18. [CrossRef] [PubMed]
18. Bar, J.; Grelewski, P.; Deszcz, I.; Noga, L.; Hirnle, L.; Lis-Nawara, A. Association between p53 protein phosphorylated at serine 20 expression and ovarian carcinoma stem cells phenotype: Correlation with clinicopathological parameters of ovarian cancer. *Neoplasma* **2019**, *66*, 801–809. [CrossRef] [PubMed]
19. Ponta, H.; Sherman, L.; Herrlich, P.A. CD44: From adhesion molecules to signalling regulators. *Nat. Rev. Mol. Cell Biol.* **2003**, *4*, 33–45. [CrossRef] [PubMed]
20. Kristiansen, G.; Sammar, M.; Altevogt, P. Tumour biological aspects of CD24, a mucin-like adhesion molecule. *J. Mol. Histol.* **2004**, *35*, 255–262. [CrossRef] [PubMed]
21. Kenda Suster, N.; Virant-Klun, I. Presence and role of stem cells in ovarian cancer. *World J. Stem Cells* **2019**, *11*, 383–397. [CrossRef] [PubMed]
22. Feng, L.Y.; Yan, B.B.; Huang, Y.Z.; Li, L. Abnormal methylation characteristics predict chemoresistance and poor prognosis in advanced high-grade serous ovarian cancer. *Clin. Epigenet.* **2021**, *13*, 141. [CrossRef]
23. Harlozinska, A.; Bar, J.K.; Richter, R.; Cislo, M. Comparison of cellular phenotypes in tumor cyst and ascitic fluid from ovarian serous carcinoma. *Acta Cytol.* **1992**, *36*, 869–874.
24. Turcotte, M.; Spring, K.; Pommey, S.; Chouinard, G.; Cousineau, I.; George, J.; Chen, G.M.; Gendoo, D.M.; Haibe-Kains, B.; Karn, T.; et al. CD73 is associated with poor prognosis in high-grade serous ovarian cancer. *Cancer Res.* **2015**, *75*, 4494–4503. [CrossRef] [PubMed]
25. Nguyen, G.-K. *Essentials of Fluid Cytology*, 1st ed.; The University of British Columbia: Vancouver, BC, Canada, 2009.
26. Ma, H.; Tian, T.; Cui, Z. Targeting ovarian cancer stem cells: A new way out. *Stem Cell Res. Ther.* **2023**, *14*, 28. [CrossRef]
27. Nowicki, A.; Kulus, M.; Wieczorkiewicz, M.; Pienkowski, W.; Stefanska, K.; Skupin-Mrugalska, P.; Bryl, R.; Mozdziak, P.; Kempisty, B.; Piotrowska-Kempisty, H. Ovarian Cancer and Cancer Stem Cells-Cellular and Molecular Characteristics, Signaling Pathways, and Usefulness as a Diagnostic Tool in Medicine and Oncology. *Cancers* **2021**, *13*, 4178. [CrossRef] [PubMed]
28. Antoun, S.; Atallah, D.; Tahtouh, R.; Alaaeddine, N.; Moubarak, M.; Khaddage, A.; Ayoub, E.N.; Chahine, G.; Hilal, G. Different TP53 mutants in p53 overexpressed epithelial ovarian carcinoma can be associated both with altered and unaltered glycolytic and apoptotic profiles. *Cancer Cell Int.* **2018**, *18*, 14. [CrossRef] [PubMed]
29. DiCioccio, R.A.; Werness, B.A.; Peng, R.; Allen, H.J.; Piver, M.S. Correlation of TP53 mutations and p53 expression in ovarian tumors. *Cancer Genet. Cytogenet.* **1998**, *105*, 93–102. [CrossRef] [PubMed]

30. Kim, K.M.; Ahn, A.R.; Park, H.S.; Jang, K.Y.; Moon, W.S.; Kang, M.J.; Ha, G.W.; Lee, M.R.; Chung, M.J. Clinical significance of p53 protein expression and TP53 variation status in colorectal cancer. *BMC Cancer* **2022**, *22*, 940. [CrossRef]
31. Szyposzynska, A.; Bielawska-Pohl, A.; Krawczenko, A.; Doszyn, O.; Paprocka, M.; Klimczak, A. Suppression of Ovarian Cancer Cell Growth by AT-MSC Microvesicles. *Int. J. Mol. Sci.* **2020**, *21*, 9143. [CrossRef] [PubMed]
32. Lupia, M.; Angiolini, F.; Bertalot, G.; Freddi, S.; Sachsenmeier, K.F.; Chisci, E.; Kutryb-Zajac, B.; Confalonieri, S.; Smolenski, R.T.; Giovannoni, R.; et al. CD73 Regulates Stemness and Epithelial-Mesenchymal Transition in Ovarian Cancer-Initiating Cells. *Stem Cell Rep.* **2018**, *10*, 1412–1425. [CrossRef] [PubMed]
33. Connor, E.V.; Saygin, C.; Braley, C.; Wiechert, A.C.; Karunanithi, S.; Crean-Tate, K.; Abdul-Karim, F.W.; Michener, C.M.; Rose, P.G.; Lathia, J.D.; et al. Thy-1 predicts poor prognosis and is associated with self-renewal in ovarian cancer. *J. Ovarian Res.* **2019**, *12*, 112. [CrossRef]
34. Zhang, J.; Sang, X.; Zhang, R.; Chi, J.; Bai, W. CD105 expression is associated with invasive capacity in ovarian cancer and promotes invasiveness by inhibiting NDRG1 and regulating the epithelial-mesenchymal transition. *Am. J. Transl. Res.* **2021**, *13*, 12461–12479.
35. Zhang, J.; Yuan, B.; Zhang, H.; Li, H. Human epithelial ovarian cancer cells expressing CD105, CD44 and CD106 surface markers exhibit increased invasive capacity and drug resistance. *Oncol. Lett.* **2019**, *17*, 5351–5360. [CrossRef] [PubMed]
36. Wang, Y.; Pei, Y.A.; Sun, Y.; Zhou, S.; Zhang, X.B.; Pei, M. Stem cells immortalized by hTERT perform differently from those immortalized by SV40LT in proliferation, differentiation, and reconstruction of matrix microenvironment. *Acta Biomater.* **2021**, *136*, 184–198. [CrossRef] [PubMed]
37. Li, N.F.; Broad, S.; Lu, Y.J.; Yang, J.S.; Watson, R.; Hagemann, T.; Wilbanks, G.; Jacobs, I.; Balkwill, F.; Dafou, D.; et al. Human ovarian surface epithelial cells immortalized with hTERT maintain functional pRb and p53 expression. *Cell Prolif.* **2007**, *40*, 780–794. [CrossRef] [PubMed]
38. Samardzija, C.; Luwor, R.B.; Volchek, M.; Quinn, M.A.; Findlay, J.K.; Ahmed, N. A critical role of Oct4A in mediating metastasis and disease-free survival in a mouse model of ovarian cancer. *Mol. Cancer* **2015**, *14*, 152. [CrossRef] [PubMed]
39. Wang, X.; Ji, X.; Chen, J.; Yan, D.; Zhang, Z.; Wang, Q.; Xi, X.; Feng, Y. SOX2 enhances the migration and invasion of ovarian cancer cells via Src kinase. *PLoS ONE* **2014**, *9*, e99594. [CrossRef] [PubMed]
40. Bareiss, P.M.; Paczulla, A.; Wang, H.; Schairer, R.; Wiehr, S.; Kohlhofer, U.; Rothfuss, O.C.; Fischer, A.; Perner, S.; Staebler, A.; et al. SOX2 expression associates with stem cell state in human ovarian carcinoma. *Cancer Res.* **2013**, *73*, 5544–5555. [CrossRef] [PubMed]
41. Yun, H.; Han, G.H.; Kim, J.; Chung, J.Y.; Kim, J.H.; Cho, H. NANOG regulates epithelial-mesenchymal transition via AMPK/mTOR signalling pathway in ovarian cancer SKOV-3 and A2780 cells. *J. Cell Mol. Med.* **2022**, *26*, 5277–5291. [CrossRef] [PubMed]
42. Reyes-Gonzalez, J.M.; Armaiz-Pena, G.N.; Mangala, L.S.; Valiyeva, F.; Ivan, C.; Pradeep, S.; Echevarria-Vargas, I.M.; Rivera-Reyes, A.; Sood, A.K.; Vivas-Mejia, P.E. Targeting c-MYC in Platinum-Resistant Ovarian Cancer. *Mol. Cancer Ther.* **2015**, *14*, 2260–2269. [CrossRef]
43. Zhang, Y.; Cao, L.; Nguyen, D.; Lu, H. TP53 mutations in epithelial ovarian cancer. *Transl. Cancer Res.* **2016**, *5*, 650–663. [CrossRef]
44. Harper, J.W.; Adami, G.R.; Wei, N.; Keyomarsi, K.; Elledge, S.J. The p21 Cdk-interacting protein Cip1 is a potent inhibitor of G1 cyclin-dependent kinases. *Cell* **1993**, *75*, 805–816. [CrossRef]
45. Ferrandina, G.; Stoler, A.; Fagotti, A.; Fanfani, F.; Sacco, R.; De Pasqua, A.; Mancuso, S.; Scambia, G. p21WAF1/CIP1 protein expression in primary ovarian cancer. *Int. J. Oncol.* **2000**, *17*, 1231–1235. [CrossRef] [PubMed]
46. Xia, X.; Ma, Q.; Li, X.; Ji, T.; Chen, P.; Xu, H.; Li, K.; Fang, Y.; Weng, D.; Weng, Y.; et al. Cytoplasmic p21 is a potential predictor for cisplatin sensitivity in ovarian cancer. *BMC Cancer* **2011**, *11*, 399. [CrossRef]
47. Salvi, A.; Hardy, L.R.; Heath, K.N.; Watry, S.; Pergande, M.R.; Cologna, S.M.; Burdette, J.E. PAX8 modulates the tumor microenvironment of high grade serous ovarian cancer through changes in the secretome. *Neoplasia* **2023**, *36*, 100866. [CrossRef] [PubMed]
48. Laury, A.R.; Hornick, J.L.; Perets, R.; Krane, J.F.; Corson, J.; Drapkin, R.; Hirsch, M.S. PAX8 reliably distinguishes ovarian serous tumors from malignant mesothelioma. *Am. J. Surg. Pathol.* **2010**, *34*, 627–635. [CrossRef]
49. Davidson, B.; Trope, C.G.; Reich, R. Epithelial-mesenchymal transition in ovarian carcinoma. *Front. Oncol.* **2012**, *2*, 33. [CrossRef] [PubMed]
50. Haslehurst, A.M.; Koti, M.; Dharsee, M.; Nuin, P.; Evans, K.; Geraci, J.; Childs, T.; Chen, J.; Li, J.; Weberpals, J.; et al. EMT transcription factors snail and slug directly contribute to cisplatin resistance in ovarian cancer. *BMC Cancer* **2012**, *12*, 91. [CrossRef] [PubMed]
51. Usman, S.; Waseem, N.H.; Nguyen, T.K.N.; Mohsin, S.; Jamal, A.; Teh, M.T.; Waseem, A. Vimentin Is at the Heart of Epithelial Mesenchymal Transition (EMT) Mediated Metastasis. *Cancers* **2021**, *13*, 4985. [CrossRef]
52. Zhang, J.; Guo, X.; Chang, D.Y.; Rosen, D.G.; Mercado-Uribe, I.; Liu, J. CD133 expression associated with poor prognosis in ovarian cancer. *Mod. Pathol.* **2012**, *25*, 456–464. [CrossRef]
53. Liu, C.L.; Chen, Y.J.; Fan, M.H.; Liao, Y.J.; Mao, T.L. Characteristics of CD133-Sustained Chemoresistant Cancer Stem-Like Cells in Human Ovarian Carcinoma. *Int. J. Mol. Sci.* **2020**, *21*, 6467. [CrossRef]

54. Nakamura, K.; Terai, Y.; Tanabe, A.; Ono, Y.J.; Hayashi, M.; Maeda, K.; Fujiwara, S.; Ashihara, K.; Nakamura, M.; Tanaka, Y.; et al. CD24 expression is a marker for predicting clinical outcome and regulates the epithelial-mesenchymal transition in ovarian cancer via both the Akt and ERK pathways. *Oncol. Rep.* **2017**, *37*, 3189–3200. [CrossRef]
55. Chau, W.K.; Ip, C.K.; Mak, A.S.; Lai, H.C.; Wong, A.S. c-Kit mediates chemoresistance and tumor-initiating capacity of ovarian cancer cells through activation of Wnt/beta-catenin-ATP-binding cassette G2 signaling. *Oncogene* **2013**, *32*, 2767–2781. [CrossRef] [PubMed]
56. Choi, Y.J.; Ingram, P.N.; Yang, K.; Coffman, L.; Iyengar, M.; Bai, S.; Thomas, D.G.; Yoon, E.; Buckanovich, R.J. Identifying an ovarian cancer cell hierarchy regulated by bone morphogenetic protein 2. *Proc. Natl. Acad. Sci. USA* **2015**, *112*, E6882–E6888. [CrossRef] [PubMed]
57. Zanoni, M.; Bravaccini, S.; Fabbri, F.; Arienti, C. Emerging Roles of Aldehyde Dehydrogenase Isoforms in Anti-cancer Therapy Resistance. *Front. Med.* **2022**, *9*, 795762. [CrossRef] [PubMed]
58. Roy, M.; Connor, J.; Al-Niaimi, A.; Rose, S.L.; Mahajan, A. Aldehyde dehydrogenase 1A1 (ALDH1A1) expression by immunohistochemistry is associated with chemo-refractoriness in patients with high-grade ovarian serous carcinoma. *Hum. Pathol.* **2018**, *73*, 1–6. [CrossRef] [PubMed]
59. Kuroda, T.; Hirohashi, Y.; Torigoe, T.; Yasuda, K.; Takahashi, A.; Asanuma, H.; Morita, R.; Mariya, T.; Asano, T.; Mizuuchi, M.; et al. ALDH1-high ovarian cancer stem-like cells can be isolated from serous and clear cell adenocarcinoma cells, and ALDH1 high expression is associated with poor prognosis. *PLoS ONE* **2013**, *8*, e65158. [CrossRef] [PubMed]
60. Smith, L.L.; Coller, H.A.; Roberts, J.M. Telomerase modulates expression of growth-controlling genes and enhances cell proliferation. *Nat. Cell Biol.* **2003**, *5*, 474–479. [CrossRef] [PubMed]
61. Chen, K.H.; Guo, Y.; Li, L.; Qu, S.; Zhao, W.; Lu, Q.T.; Mo, Q.Y.; Yu, B.B.; Zhou, L.; Lin, G.X.; et al. Cancer stem cell-like characteristics and telomerase activity of the nasopharyngeal carcinoma radioresistant cell line CNE-2R. *Cancer Med.* **2018**, *7*, 4755–4764. [CrossRef] [PubMed]
62. Liu, H.; Liu, Q.; Ge, Y.; Zhao, Q.; Zheng, X.; Zhao, Y. hTERT promotes cell adhesion and migration independent of telomerase activity. *Sci. Rep.* **2016**, *6*, 22886. [CrossRef]
63. Li, J.; Dong, G.; Song, J.; Tan, G.; Wu, X. Telomerase inhibition decreases esophageal squamous carcinoma cell migration and invasion. *Oncol. Lett.* **2020**, *20*, 2870–2880. [CrossRef]
64. Szyposzynska, A.; Bielawska-Pohl, A.; Murawski, M.; Sozanski, R.; Chodaczek, G.; Klimczak, A. Mesenchymal Stem Cell Microvesicles from Adipose Tissue: Unraveling Their Impact on Primary Ovarian Cancer Cells and Their Therapeutic Opportunities. *Int. J. Mol. Sci.* **2023**, *24*, 15862. [CrossRef]
65. Kraskiewicz, H.; Paprocka, M.; Bielawska-Pohl, A.; Krawczenko, A.; Panek, K.; Kaczynska, J.; Szyposzynska, A.; Psurski, M.; Kuropka, P.; Klimczak, A. Can supernatant from immortalized adipose tissue MSC replace cell therapy? An in vitro study in chronic wounds model. *Stem Cell Res. Ther.* **2020**, *11*, 29. [CrossRef] [PubMed]
66. Krawczenko, A.; Bielawska-Pohl, A.; Wojtowicz, K.; Jura, R.; Paprocka, M.; Wojdat, E.; Kozlowska, U.; Klimczak, A.; Grillon, C.; Kieda, C.; et al. Expression and activity of multidrug resistance proteins in mature endothelial cells and their precursors: A challenging correlation. *PLoS ONE* **2017**, *12*, e0172371. [CrossRef] [PubMed]
67. Paprocka, M.; Krawczenko, A.; Dus, D.; Kantor, A.; Carreau, A.; Grillon, C.; Kieda, C. CD133 positive progenitor endothelial cell lines from human cord blood. *Cytom. A* **2011**, *79*, 594–602. [CrossRef]
68. Beyeler, J.; Schnyder, I.; Katsaros, C.; Chiquet, M. Accelerated wound closure in vitro by fibroblasts from a subgroup of cleft lip/palate patients: Role of transforming growth factor-alpha. *PLoS ONE* **2014**, *9*, e111752. [CrossRef] [PubMed]

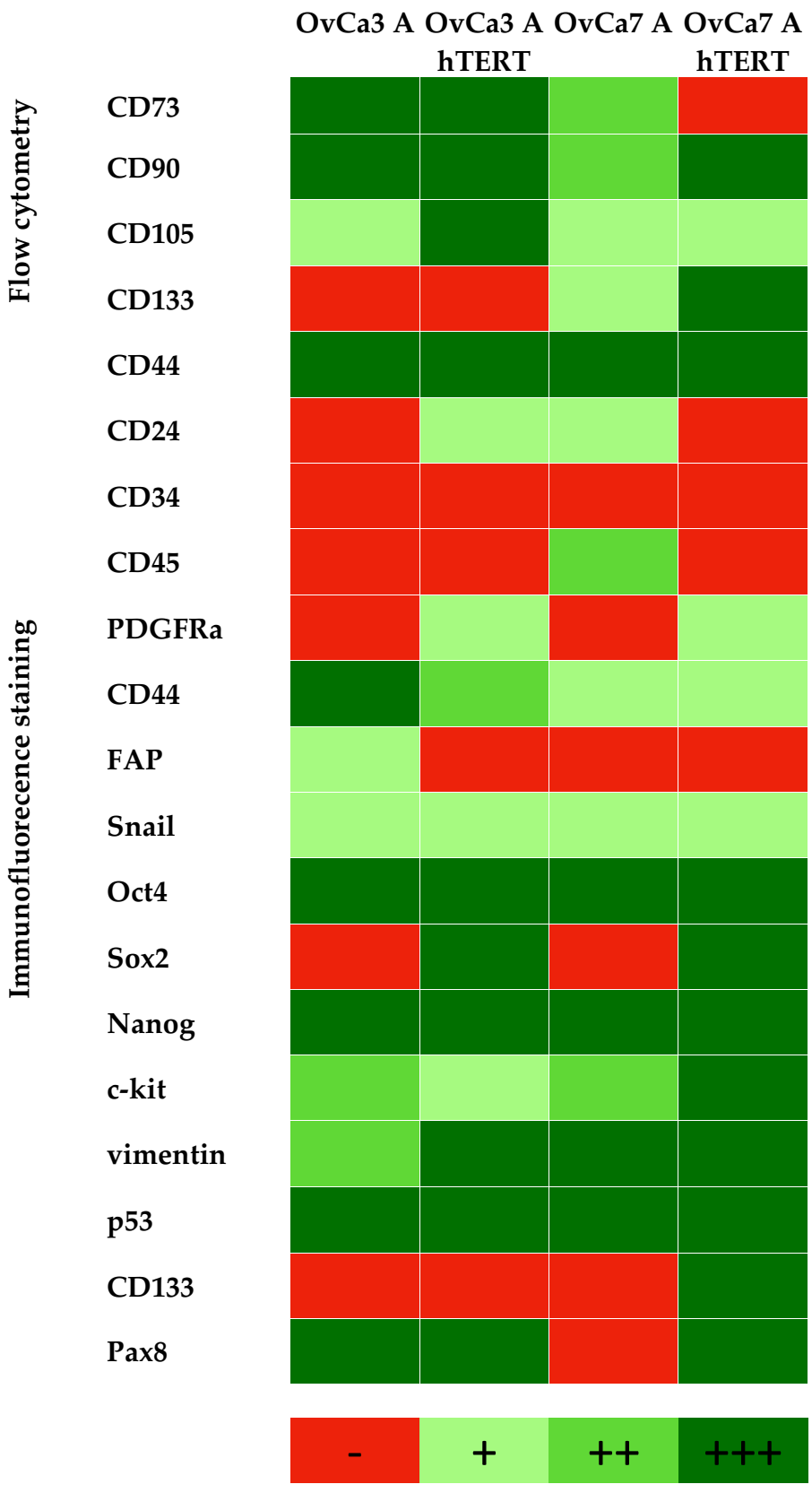

Figure S1. Heat map summarizing the phenotype characteristics of ovarian cancer cells before and after hTERT immortalization by using flow cytometry and immunofluorescence

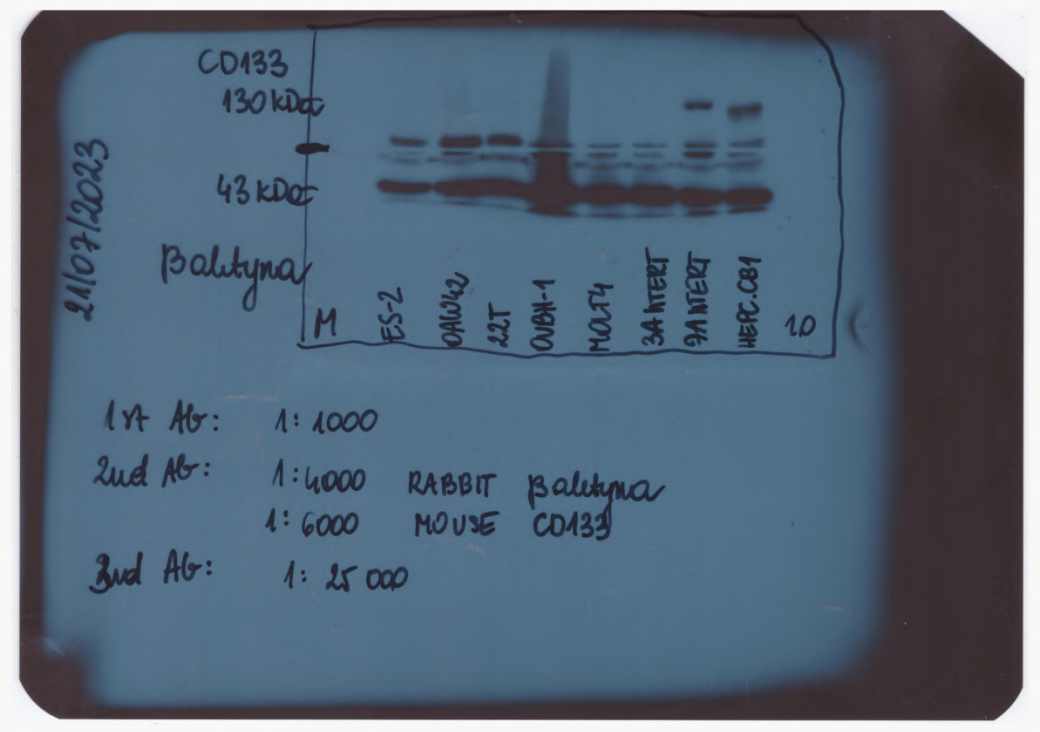

Figure S2. Western blot analysis of CD133 molecule expression in immortalized ovarian cancer cell lines. CD133 and β-Actin protein levels were revealed with different sets of specific antibodies in cell extracts obtained from lysing cells with RIPA buffer. Protein extracts from HEPC-CB.1 cells were used as a positive control CD133 – 130 kDa and β-Actin – 43 kDa expression. Each time 50 μg/line of total protein was loaded.

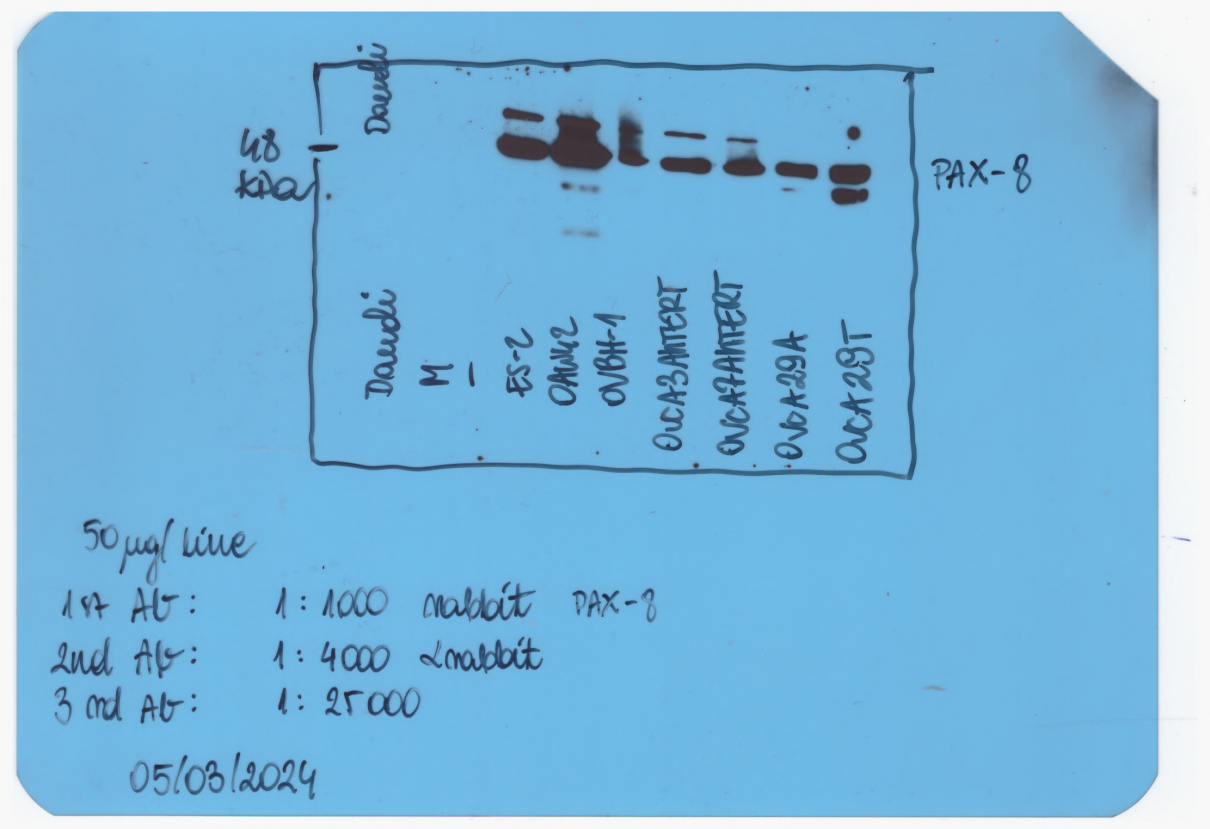

Figure S3. Western blot analysis of Pax8 molecule expression in immortalized cell lines. Pax8 and β-Actin protein levels were revealed with different sets of specific antibodies in cell extracts obtained from lysing cells with RIPA buffer. Protein extract from OAW-42 cells was used as a positive control, while protein extract from Daudi cells was used as a negative control. Pax8 –48 kDa and β-Actin – 43 kDa expression. Each time 50 µg/line of total protein was loaded.

Table S1. List of primary antibodies

Antigen	Host	Class of antibody	Clone	Company	Dilution	Incubation
Human PDGFRa	Mouse	Monoclonal	C-9	Santa Cruz	1:100	1h, Room Temperature (RT)
Human CD44	Rabbit	Polyclonal		Thermo Fisher Scientific	1:100	1h, RT
Human Fibroblast activation protein (FAP)	Mouse	Monoclonal	F11-24	Thermo Fisher Scientific	1:100	Overnight (O/N), 4^0C
Human Snail1	Rabbit	Polyclonal		Bio Site	1:100	O/N, 4^0C
Human Oct4	Rabbit	Polyclonal		Thermo Fisher Scientific	1:100	O/N, 4^0C
Human Sox2	Mouse	Monoclonal	20 G5	Thermo Fisher Scientific	1:100	O/N, 4^0C
Human Nanog	Rabbit	Polyclonal		Thermo Fisher Scientific	1:100	O/N, 4^0C
Human vimentin	Mouse	Monoclonal	V9	Thermo Fisher Scientific	1:100	1h, RT
Human c-kit (CD177)	Mouse	Monoclonal	K45	Thermo Fisher Scientific	1:50	O/N, 4^0C
Human p53	Mouse	Monoclonal	DO-7	Dako	1:50	1h, RT
Human CD133	Mouse	Monoclonal	2F8C5	Thermo Fisher Scientific	1:100	O/N, 4^0C
Human Pax8	Rabbit	Monoclonal	D2S2I	Cell Sygnaling Technology	1:100	1h, RT
Human CA125	Mouse	Monoclonal	185 1	Leica Biosystem	1:100	1h, RT
Human Cytokeratin 8	Mouse	Monoclonal	TS1	Novocastra	1:100	1h, RT

Table S2. List of secondary antibodies

Antigen	Host	Class of antibody	Flouorophore	Company	Dilution	Incubation
F-actin		Phalloidin	Alexa Fluor 488™	Thermo Fisher Scientific	1:400	45min, RT
Mouse IgG	Goat	Polyclonal	Alexa Fluor 488™	Thermo Fisher Scientific	1:700	45min, RT
Mouse IgG	Goat	Polyclonal	Alexa Fluor 647™	Thermo Fisher Scientific	1:700	45min, RT
Rabbit IgG	Goat	Polyclonal	Alexa Fluor 647™	Thermo Fisher Scientific	1:700	45min, RT

Wnioski

1. HATMSC2-MVs hamują proliferację komórek raka jajnika linii OAW-42 oraz prowadzą do śmierci komórek obu linii raka jajnika ES-2 i OAW-42 na drodze apoptozy i/lub nekrozy. Internalizacja HATMSC2-MVs do komórek ES-2 i OAW-42 związana była ze wzrostem wydzielania przez komórki nowotworowe czynników hamujących wzrost nowotworów (w tym IL-2, IL-15, IFN-γ).
2. Pierwotne komórki raka jajnika z tkanki pooperacyjnej i płynu puchlinowego były heterogenną populacją pod względem analizowanych markerów: MSCs (CD73, CD90, CD105), CSCs (CD24, CD44, CD133, ALDH1, c-kit), CAFs (PDGFRa, FAP), EMT (Snail, wimentyna) i odpowiedzialnych za utrzymanie pluripotencji (Oct4, Sox2, Nanog). HATMSC2-MVs spowodowały spadek aktywności metabolicznej pierwotnych komórek raka jajnika oraz indukowały śmierć pierwotnych komórek raka jajnika w modelu 2D i 3D, co z dużym prawdopodobieństwem było związane ze zwiększoną ekspresją czynników proapoptotycznych transportowanych przez HATMSC2-MVs (w tym bad, BID, BIM, kaspaza 3, cytochrom c, TRAIL-R1 i TRAIL-R2).
3. Wykazano, że plazmid niosący gen hTERT może być wykorzystany do unieśmiertelnienia pierwotnych komórek raka jajnika przy zachowaniu fenotypu komórek pierwotnych. Unieśmiertelnione komórki raka jajnika OvCa3 A hTERT i OvCa7 A hTERT wykazywały wyższą aktywność metaboliczną, migracyjną i ALDH1 w porównaniu do komórek pierwotnych. Otrzymana linia komórkowa OvCa7 A hTERT o fenotypie CD133+, CD44+ z ekspresją markerów Pax8 i p53 może stanowić obiecujące narzędzie w badaniach na biologią CSCs oraz nad nowymi terapiami nakierowanymi na CSCs.